SYNTHESIS AND CHARACTERIZATION OF RED LIGHT EMITTING MATERIALS FOR ORGANIC LIGHT EMITTING DIODES

Teadkait Kaewpuang

A Thesis Submitted in Partial Fulfillment of the Requirements for the

Degree of Doctor of Philosophy in Chemistry

Suranaree University of Technology

Academic Year 2018

การสังเคราะห์และการพิสูจน์เอกลักษณ์วัสดุสารเปล่งแสงสีแดง เพื่อใช้ในอุปกรณ์ไดโอดเปล่งแสงอินทรีย์

นายเทอดเกียรติ แก้วพวง

มหาวิทยาลัยเทคโนโลยีสุรนารี

วิทยานิพนธ์นี้เป็นส่วนหนึ่งของการศึกษาตามหลักสูตรปริญญาวิทยาศาสตรดุษฎีบัณฑิต

สาขาวิชาเคมี

มหาวิทยาลัยเทคโนโลยีสุรนารี

ปีการศึกษา 2561

SYNTHESIS AND CHARACTERIZATION OF RED LIGHT EMITTING MATERIALS FOR ORGANIC LIGHT EMITTIING DIODES

Suranaree University of Technology has approved this thesis submitted in partial fulfillment of the requirements for the Degree of Doctor of Philosophy.

Thesis Examining Committee

(Prof. Dr. James R. Ketudat-Cairns)
Chairperson

(Asst. Prof. Dr. Thanaporn Manyum)
Member (Thesis Advisor)

(Prof. Dr. Vinich Promarak)
Member (Thesis Co-Advisor)

(Asst. Prof. Dr. Chanokporn Phaosiri)
Member

(Asst. Prof. Dr. Tinnagon Kaewin)
Member

(Asst. Prof. Dr. Anyanee Kamkaew)
Member

(Assoc. Prof. Dr. Chatchai Jothityangkoon)
Vice Rector for Academic Affairs and Quality Assurance

(Prof. Dr. Santi Maensiri)
Dean of Institute of Science

มหาวิทยาลัยเทคโนโลยีสุรนารี

เทอดเกียรติ แก้วพวง : การสังเคราะห์และการพิสูจน์เอกลักษณ์วัสดุสารเปล่งแสงสีแดงเพื่อใช้ในอุปกรณ์ไดโอดเปล่งแสงอินทรีย์ (SYNTHESIS AND CHARACTERIZATION OF RED LIGHT EMITTING MATERIALS FOR ORGANIC LIGHT EMITTIING DIODES) อาจารย์ที่ปรึกษา : ผู้ช่วยศาสตราจารย์ ดร.ธนพร แม่นยำ, 220 หน้า.

จุดมุ่งหมายของวิทยานิพนธ์นี้เพื่อพัฒนาวัสดุสารเปล่งแสงสีแดงสำหรับใช้งานด้านออปโตอิเล็กทรอนิกส์ ซึ่งเป็นที่สนใจอย่างมากทั้งในด้านอุตสาหกรรมและด้านวิชาการ โดยงานวิทยานิพนธ์นี้ได้มุ่งเน้นการออกแบบและการสังเคราะห์วัสดุสารเปล่งแสงสีแดงสำหรับอุปกรณ์ไดโอดเปล่งแสงอินทรีย์ (OLEDs) สิ่งหนึ่งที่ดึงดูดใจในการพัฒนาด้านเทคโนโลยีของอุปกรณ์อินทรีย์อิเล็กทรอนิกส์ คือ ชั้นที่แอกทีฟ ซึ่งสามารถลดอุณหภูมิให้ต่ำลงโดยการใช้เทคนิคของชั้นของเหลว ซึ่งสามารถสร้างสารอินทรีย์ที่ใช้ในกึ่งตัวนำที่เหมาะสมราคาน้อย ประยุกต์ใช้งานกับพื้นผิวอิเล็กทรอนิกส์ที่มีความยืดหยุ่นที่ขนาดใหญ่ การออกแบบโครงสร้างวัสดุอินทรีย์ชนิดใหม่ที่มีความสามารถทางไฟฟ้า โครงสร้างที่มีคุณสมบัติทางปฏิกิริยาเคมีที่ดี ที่ใช้งานสำหรับอุปกรณ์อิเล็กทรอนิกส์และออปโตอิเล็กทรอนิกส์ได้วิจัยและศึกษาอย่างกว้างขวาง

ดังนั้นวิทยานิพนธ์นี้จึงมีการพัฒนาทางด้านการสังเคราะห์และศึกษาคุณสมบัติทางกายภาพและทางเคมีของวัสดุอินทรีย์ชนิดใหม่สำหรับการประยุกต์ใช้ในไดโอดเรืองแสงอินทรีย์ (OLEDs)

วัตถุประสงค์ของวิทยานิพนธ์นี้แบ่งของเป็น 3 วัตถุประสงค์ คือ (1) เพื่อการสังเคราะห์วัสดุอินทรีย์ชนิดใหม่ที่มีโครงสร้างเป็น donor-π-Accepter-π-donor (D-π-A-π-D) โดยมีส่วนสำคัญ 3 ส่วนคือ ส่วนที่หนึ่งเป็นส่วนแกนกลางของโครงสร้างใช้โมเลกุลของ bezothidiazole (BT) difluoro-bezothidiazole (BT-2F) dithiophenebezothidiazole (BT1T4) napthobezothidiazole (NapBT) antracenedione (Ant) diTPA-antracenedione (Ant-2TPA) thioxanthenonedioxide (TOX) thioxanthenonedioxide-TPA (TOX-TPA) และ *p*-triazene ส่วนที่สองคือ π ทำหน้าที่เป็นสะพานเชื่อมให้อิเล็กตรอนเคลื่อนที่ผ่านจากตัวให้ กับ ตัวรับ จะใช้ oligothiophene หรือ diCarbazole และส่วนที่สามคือตัวรับ ทำหน้าที่ดึงอิเล็กตรอน ซึ่งโครงสร้างประกอบไปด้วยตัวให้ เป็นส่วนที่ทำหน้าที่ให้อิเล็กตรอนแก่โมเลกุลจะใช้ triphenylamine และ carbazole โดยกลุ่มของ oligothiophene มีความเสถียรทางความร้อนที่สูงและมีโครงสร้างที่แบนราบ นอกจากนั้นกลุ่มของ triphenylamine และ carbazole ความสามารถในการให้อิเล็กตรอนที่ดีและมีโครงสร้างที่แบนราบ และกลุ่มของ alkyl เพิ่มความสามารถในการละลายของโมเลกุลในสารละลายต่าง ๆ (2) เพื่อทำการยืนยันโครงสร้างที่ทำการสังเคราะห์และศึกษาคุณสมบัติทางไฟฟ้า คุณสมบัติทางแสง คุณสมบัติทาง

ไฟฟ้าเคมี และคุณสมบัติทางความร้อน ของโมเลกุลเป้าหมายและ (3) เพื่อศึกษาทางศักย์ไฟฟ้าเมื่อนำไปประยุกต์ใช้สำหรับอุปกรณ์ไดโอดเรืองแสง (OLEDs)

มหาวิทยาลัยเทคโนโลยีสุรนารี

สาขาวิชาเคมี
ปีการศึกษา 2561

ลายมือชื่อนักศึกษา_____
ลายมือชื่ออาจารย์ที่ปรึกษา_____
ลายมือชื่ออาจารย์ที่ปรึกษาร่วม_____

TEADKAIT KAEWPUANG : SYNTHESIS AND CHARACTERIZATION OF RED LIGHT EMITTING MATERIALS FOR ORGANIC LIGHT EMITTIING DIODES. THESIS ADVISOR : ASST. PROF. THANAPORN MANYUM, Ph.D. 220 PP.

BENZOTHIADIAZOLE, DONOR-П-ACCEPTOR, HOLE-TRANSPORT, DEEP RED EMITTERS, ORGANIC LIGHT EMITTING DIODE

The aim of this thesis is to develop the red light emitting materials for optoelectronic applications which have attracted a lot of interest both in industries and academics. The work focused on the designs and syntheses of the red light emitting materials for organic light emitting diodes (OLEDs). One of the main technological attractions of organic electronics is that the active layers can be deposited at low temperatures by liquid phase techniques. This makes organic semiconductors ideal candidates for low-cost, large-area electronic applications on flexible substrates. The design of novel photo and electro-active organic materials and their structures, reactions, properties, functions and applications for electronic and optoelectronic devices has widely been investigated. Therefore, this thesis reports the development of the synthesis and characterization of novel organic materials for application in organic light emitting diodes (OLEDs)

The aims of this work are: (1) To synthesize a novel donor-π-acceptor-π-donor (D-π-A-π-D) materials based on benzothiadiazole (BT), difluoro-benzothidiazole (BT-2F), dithiophenebenzo-thidiazole (BT1T4), napthobenzothidiazole (NapBT), antracenedione (Ant), diTPA-antracenedione (Ant-2TPA), thioxanthenonedioxide (TOX), thioxanthenonedioxide -TPA (TOX-TPA) and *p*-triazene as core materials oligothiophene

4 or dicarbazole as the linker and triphenylamine as the donor group for using as hole-transporting layer in Alq_3-based organic light-emitting diode (OLED). The oligothiophene showed good high thermal stability and it has planar structure. The triphenylamine group showed good donor group and it has planar structure. The alkyl group is introduced on oligothiophene to increase the solubility. (2) To characterize and study the electronic, photophysical, electrochemical and thermal properties of the target molecules. (3) To investigate their potential applications as emitters for OLED devices.

มหาวิทยาลัยเทคโนโลยีสุรนารี

School of Chemistry

Academic Year 2018

Student's Signature_____

Advisor's Signature_____

Co-Advisor's Signature_____

ACKNOWLEDGEMENTS

I would like to express gratitude and appreciation to everyone who helps me to complete my thesis. First of all, I would like to specially thank my wonderful graduate advisor, Asst. Prof. Dr. Thanaporn Manyum and co-advisor Prof. Dr. Vinich Promarak for giving me the chance to study at Suranaree University of Technology to work partially at Vidyasirimedhi Institute of Science and Technology and to work on an interesting research topic, as well as their supports, encouragements, discussions and suggestions throughout this research.

I am also thankful to all my thesis committee members, including, Prof. Dr. James R. Ketudat-Cairns, Asst. Prof. Dr. Chanokporn Phaosiri, Asst. Prof. Dr. Tinnagon Kaewin and Asst. Prof. Dr. Anyanee Kamkaew for their helpful suggestions and criticisms during my thesis defense. I would also like to thank Asst. Prof. Dr. Taweesak Sudyoadsuk for advising me on optoelectronic devices.

I would like to acknowledge all the lecturers at the School of Chemistry for their good attitude and advices, and the staff at the Center for Scientific and Technological Equipment for their assistance and suggestion for the use of instruments.

Thanks to all of my good friends in the Organic Materials and Alternative Energy Research Laboratory Group at Vidyasirimedhi Institute of Science and Technology and in the School of Chemistry, Institute of Science, Suranaree University of Technology for their helps and the impressive atmosphere.

Finally, I would like to thank very much my family for their under standings, encouragements, motivations and inspiration raising.

Teadkait Kaewpuang

CONTENTS

Page

ABTRACT IN THAI I

ABTRACT IN ENGLISH III

ACKNOWLEDGEMNTS V

CONTENTS VII

LIST OF TABLES XIV

LIST OF FIGURES XV

LIST OF ABBREVITIONS XIV

CHAPTER

I INTRODUCTION 1

1.1 Organic Light Emitting Diode 2

1.2 Advantages and disadvantages of OLED 4

1.3 Structure of organic light emitting diode 5

1.4 Working Principle 6

1.5 Materials for emissive layer of OLEDs 7

1.6 Literature review 10

1.6.1 Red light emitting materials 10

1.6.2 Green light emitting materials 14

1.6.3 Blue light emitting materials 16

CONTENTS (Continued)

Page

II EXPERIMENTAL 19

2.1 Materials and Methods 19

2.2 Device fabrication and measurements 19

2.3 Synthesis 21

2.3.1 General method for Suzuki cross coupling reaction 21

2.3.2 General method for bromination reaction 21

2.4 Product compounds and Intermediates 22

2.4.1 4,7-dibromobenzo[c][1,2,5]thiadiazole (**BT-2Br**) 22

2.4.2 4,7-Bis(3-hexylthiophen-2-yl)-2,1,3-benzothiadiazole (**2**) 23

2.4.3 4,7-Bis(5-bromo-3-hexylthiophen-2-yl)-2,1,3-benzothiadiazole (**3**) 24

2.4.4 4,7-Bis(4,5-dibromo-3-hexylthiophen-2-yl)-2,1,3-benzothiadiazole (**4**) 25

2.4.5 4,7-Bis(4-hexylthiophen-2-yl)-2,1,3-benzothiadiazole (**5**) 26

2.4.6 4,7-Bis(4-hexyl-5-bromothiophen-2-yl)-2,1,3-benzothiadiazole (**6**) 26

2.4.7 4,7-Bis(3,5-dibromo-4-hexylthiophen-2-yl)-2,1,3-benzothiadiazole (**7**) 27

มหาวิทยาลัยเทคโนโลยีสุรนารี

CONTENTS (Continued)

Page

2.4.8 4,7-bis(3,4'-dihexyl-[2,2'-bithiophen]-5-yl)benzo[c][1,2,5] thiadiazole (**BT2T4**) 28

2.4.9 4,7-bis(3,4'-dihexyl-5'-iodo-[2,2'-bithiophen]-5-yl) benzo [c][1,2,5]thiadiazole (**BT2T4-2I**)..... 29

2.4.10 4,7-bis(3,4',4"-trihexyl-[2,2':5',2"-terthiophen]-5-yl) benzo[c][1,2,5] thiadiazole (**BT3T4**)..... 30

2.4.11 4,7-bis(3,4',4"-trihexyl-5"-iodo-[2,2':5',2"-terthiophen]-5-yl) benzo[c][1,2,5]thiadiazole (**BT3T4-2I**)..... 32

2.4.12 4,7-bis(5'-bromo-3,4'-dihexyl-[2,2'-bithiophen]-5-yl) benzo[c][1,2,5] thiadiazole (**BT2T4-2Br**) 33

2.4.13 4,7-bis(3',4,5'-tribromo-3,4'-dihexyl-[2,2'-bithiophen]-5-yl) benzo[c] [1,2,5]thiadiazole (**BT2T4-6Br**)..... 34

2.4.14 4,7- Bis(5-(9-phenyl-9H-carbazole-3-yl)-3-hexylthiophene-2-yl)- 2,1,3-benzothiadiazole (**BTZ1**)..... 35

2.4.15 4,7-Bis(4,5-bis(4-(diphenylamino(phenyl)-3-hexylthiophen-2-yl)-2,1,3-benzothiadiazole (**BTZ2**) 36

2.4.16 4,7-Bis(5-(4-(diphenylamino)phenyl)-3-hexylthiophene-2-yl)-2,1,3- benzothiadiazole (**BTZ3**) 37

2.4.17 4,7-Bis(5-(4-(diphenylamino)phenyl)-4-hexylthiophene-2-yl)-2,1,3- benzothiadiazole (**BTZ4**) 38

CONTENTS (Continued)

Page

2.4.18 4,7-Bis(5-(9-phenyl-9H-carbazole-3-yl-4-hexylthiophen-2-yl)-2,1,3- benzothiadiazole (**TBtz1**) 39

2.4.19 4,7-Bis(3,5-bis(4-(diphenylamino)phenyl)-5-hexylthiophen-2-yl-2,1,3-benzothiadiazole (**TBtz2**) 40

2.4.20 **BT2T4-6TPA** 41

2.4.21 4,7-bis(3-hexyl-5-(9-phenyl-9H-carbazol-3-yl)thiophen-2-yl) benzo[c][1,2,5] thiadiazole (**CTBtz1**) 42

2.4.22 4,7-bis(4-hexyl-5-(9-phenyl-9H-carbazol-3-yl)thiophen-2yl) benzo[c] [1,2,5] thiadiazole (**CTBtz2**) 43

2.4.23 6-bromo-3",6"-di-tert-butyl-9,9'-didodecyl-9*H*,9'*H*-3,3':6',9"-tercarbazole (**G1diC12-Br**) 44

2.4.24 3",6"-di-tert-butyl-9,9'-didodecyl-6-(4,4,5,5-tetramethyl-1,3,2-dioxaborolan-2-yl)-9*H*,9'*H*-3,3':6',9"-tercarbazole (**G1diC12-Boran**) 45

2.4.25 4,7-bis(3",6"-di-tert-butyl-9,9'-didodecyl-9*H*,9'*H*-[3,3':6',9"-tercarbazol]-6-yl) benzo[c][1,2,5]thiadiazole (**di[diC12-G1]BT**) 46

2.4.26 4,7-bis(5-(3",6"-di-tert-butyl-9,9'-didodecyl-9*H*,9'*H*-[3,3':6',9"-tercarbazol]- 6-yl)-4-hexylthiophen-2-yl)benzo [c][1,2,5]thiadiazole (**di[diC12-G1]BT1T4**) 47

CONTENTS (Continued)

Page

2.4.27 4,7-bis(3",6"-di-tert-butyl-9,9'-didodecyl-9*H*,9'*H*-[3,3':6',9"-tercarbazol]-6-yl)-5,6-difluorobenzo[c][1,2,5]thiadiazole (**di[diC12-G1]BT-2F**) 48

2.4.28 4,9-bis(3",6"-di-tert-butyl-9,9'-didodecyl-9*H*,9'*H*-[3,3':6',9"-tercarbazol]-6-yl) naphtho[2,3-c][1,2,5]thiadiazole (**di[diC12-G1]NapBT**) 49

2.4.29 2,6-bis(3",6"-di-tert-butyl-9,9'-didodecyl-9H,9'H-[3,3':6',9"-tercarbazol]-6-yl) anthracene-9,10-dione (**di[diC12-G1]Ant**) 50

2.4.30 **Tetra[diC12-G1]Ant-2TPA** 51

2.4.31 2-(3",6"-di-tert-butyl-9,9'-didodecyl-9*H*,9'*H*-[3,3':6',9"-tercarbazol]-6-yl)-9*H*-thioxanthen-9-one 10,10-dioxide (**[diC12-G1]TOX**) 52

2.4.32 2-(4-(bis(4-(3",6"-di-tert-butyl-9,9'-didodecyl-9*H*,9'*H*-[3,3':6',9"-tercarbazol]-6-yl)phenyl)amino)phenyl)-9*H*-thioxanthen-9-one10,10-dioxide **([diC12-G1]TOX-TPA)** 53

2.4.33 2,4,6-tris(4-(3",6"-di-tert-butyl-9,9'-didodecyl-9*H*,9'*H*-[3,3':6',9"-tercarbazol]-6-yl)phenyl)-1,3,5-triazine (**[tri[diC12-G1]*p*-triazene]**) 54

CONTENTS (Continued)

Page

III RESULTS AND DISCUSSION 55

3.1 Introduction 55

3.2 Synthesis and characterization trialyamines substituted bis(hexyl-thiophene-2-yl)-benzothiadiazoles as solution-processable hole-transporting red emitters for efficient non-doped electroluminescent device 58

3.2.1 Aim of the study 58

3.2.2 Results and discussion 59

3.2.2.1 Synthesis 59

3.2.2.2 Theoretical Calculation 75

3.2.2.3 Photophysical Properties 77

3.2.2.4 Thermal properties and morphology 79

3.2.2.5 Electrochemical Properties 82

3.2.2.6 Electroluminescent performances 83

3.3 High efficiency solution-processed NIR OLEDs based on sample oligosthiophene benzothiadiazoles 89

3.3.1 Aim of the study 89

3.3.2 Results and discussion 90

3.3.2.1 Synthesis 90

3.3.2.2 Photophysical Properties 99

3.3.2.3 Electroluminescent performances 103

CONTENTS (Continued)

Page

3.4 Highly fluorescent solid-state thiophene-benzothiadiazole derivatives as hole-transporting red emitters for solution processed OLEDs 104

3.4.1 Aim of the study 104

3.4.2 Results and discussion 105

3.4.2.1 Synthesis 105

3.4.2.2 Theoretical Calculation 108

3.4.2.3 Photophysical Properties 110

REFERENCES 111

APPENDIX 130

CURRICULUM VITAE 220

มหาวิทยาลัยเทคโนโลยีสุรนารี

LIST OF TABLES

Table		Page
3.1	Key physical data of the new compounds	81
3.2	Performance of devices fabricated with **BTZ4** as EL	86
3.3	Performance of devices fabricated with **BTZ1-4** as EL	87
3.4	Key physical data of the synthesized compounds	101
3.5	Electroluminescent data of solution-processed devices fabricated with **TBtz1-2** as EL	102

มหาวิทยาลัยเทคโนโลยีสุรนารี

LIST OF FIGURES

Figure **Page**

3.1 Show structure of target red-light emitting molecules (**BTZ1-4**) 59

3.2 Synthesis of (3-hexylthiophen-2-yl)-benzothiazole core **2** 60

3.3 The ^{1}H-NMR spectra in $CDCl_3$ of (3-hexylthiophen-2-yl)benzothiazole core **2** 61

3.4 Synthesis of (4-hexylthiophen-2-yl)-benzothiazole core **5** 61

3.5 The ^{1}H-NMR spectra in $CDCl_3$ of (3-hexylthiophen-2-yl)benzothiazole core **5** 62

3.6 Synthesis of compound **3** 63

3.7 The ^{1}H-NMR spectra in $CDCl_3$ of compound **3** 64

3.8 Synthesis of final product **BTZ1** 64

3.9 The ^{1}H-NMR spectra in $CDCl_3$ of **BTZ1** 65

3.10 Synthesis of compound **4** 66

3.11 The ^{1}H-NMR spectra in $CDCl_3$ of compound **4** 67

3.12 Synthesis of final product **BTZ2** 67

3.13 The ^{1}H-NMR spectra in $CDCl_3$ of final product **BTZ2** 68

3.14 Synthesis of compound **6** 69

3.15 The ^{1}H-NMR spectra in $CDCl_3$ of compound **6** 70

3.16 Synthesis of compound **7** 70

3.17 The ^{1}H-NMR spectra in $CDCl_3$ of compound **7** 71

3.18 Synthesis of final product **BTZ3** 72

LIST OF FIGURES (Continued)

Figure **Page**

3.19 The ^{1}H-NMR spectra in $CDCl_3$ of final product **BTZ3**.....73

3.20 Synthesis of final product **BTZ4** 73

3.21 The ^{1}H-NMR spectra in $CDCl_3$ of final product **BTZ4**.....74

3.22 The optimized structures with dihedral angle, HOMOs and LUMOs of **BTZ1-4** calculated by TD-DFT B3LYP/6-31G(d,p) in CH_2Cl_2 75

3.23 UV-vis absorption and PL spectra of **BTZ1-4** 78

3.24 a) CV plots measured by and b) DSC (1st heating scan (thick line) and 2nd heating scan (thin line)) and TGA traces of **BTZ1-4** 82

3.25 The optimize EL performances and the solution processed non-doped single layer OLED was fabricated with a configuration of ITO/PEDOT: PSS (40nm)/BTZ4 (60nm)/LiF (0.5nm)/AL (150nm) 84

3.26 Device structures and energy levels (relative to the vacuum energy level) of the materials.....85

3.27 a) current density-voltage-luminance (*J-V-L*) plots, b) luminance-current density-voltage (J-V) curves the fabricated OLEDs, c) current density-external quantum efficiency (EQE) plots of the fabricated OLEDs, and d) normalized EL spectra under different applied voltages 85

LIST OF FIGURES (Continued)

Figure **Page**

3.28 a) Device structures and energy levels (relative to the vacuum energy level) of the materials used, b) current density-voltage-luminance (*J*-*V*-*L*) plots, c) luminance efficiency-current density-external quantum efficiency (LE-J-EQE) plots of the fabricated OLEDs), and d) normalized EL spectra (Insert: photographs of the OLED devices) 88

3.29 AFM images of the thin film of **BTZ1**, **BTZ2**, **BTZ3** and **BTZ4** 20wt% doped in the CBP host 89

3.30 Molecular structures of oligothiophene-benzothiadiazoles **TBtz1-2** 90

3.31 Synthesis of compound **BT2T4** 91

3.32 The ^{1}H-NMR spectra in $CDCl_3$ of compound **BT2T4** 92

3.33 Synthesis of compound **BT2T4-2I** 93

3.34 The ^{1}H-NMR spectra in $CDCl_3$ of compound **BT2T4-2I** 94

3.35 Synthesis of final product **TBtz1** 94

3.36 The ^{1}H-NMR spectra in $CDCl_3$ of final product **TBtz1** 95

3.37 Synthesis of compound **BT3T4** 96

3.38 The ^{1}H-NMR spectra in $CDCl_3$ of compound **BT3T4** 97

3.39 Synthesis of compound **BT3T4-2I** 97

3.40 Synthesis of compound **BT3T4-2I** 98

3.41 Synthesis of final product **TBtz2** 99

LIST OF FIGURES (Continued)

Figure **Page**

3.42 a) UV-vis absorption and PL spectra of **TBtz1-2** in CH_2Cl_2 solution b) PL spectra and c) Transient PL spectra of thin films of neat **TBtz1-2** and 30wt% doped in CBP coated on fused silica substrates. d) AFM images of neat **TBtz1-2** and 30wt% doped in CBP spin-coated on ITO glass 100

3.43 a) Schematic energy diagram (relative to the vacuum energy level) and molecular structures of organic materials used in this study, b) Compared electroluminescence spectra, c) Current density-voltage-radiance (*J*-*V*-*R*) characteristics, and d) EQE-J characteristics of solution-processed devices I-IV fabricated with neat **TBtz1-2** and 30wt% doped in CBP as EL 103

3.44 Molecular structures of oligothiophene-benzothiadiazoles **CTBtz1-2**..... 105

3.45 Synthesis of final product **CTBtz1** 105

3.46 The ^{1}H-NMR spectra in $CDCl_3$ of final product **CTBtz1** 106

3.47 Synthesis of final product **CTBtz2** 107

3.48 The ^{1}H-NMR spectra in $CDCl_3$ of final product **CTBtz2** 108

3.49 The optimized structures with dihedral angle, HOMOs and LUMOs of **CTBtz1-2** calculated by TD-DFT B3LYP/6-31G (d,p) in CH_2Cl_2 109

3.50 UV-vis absorption and PL spectra of **CTBtz1-2** 110

LIST OF ABBREVIATIONS

AFM	=	Atomic Force Microscope
DSC	=	Differential Scanning Calorimetry
TGA	=	Thermogravimetric Analysis
FT-IR	=	Fourier Transforms Infrared
^{1}H NMR	=	Proton Nuclear Magnetic Resonance
^{13}C NMR	=	Carbon Nuclear Magnetic Resonance
MALDI-TOF	=	Matrix Assisted Laser Desorption/Ionisation Time-of-Flight Mass Spectrometry
UV-Vis	=	Ultraviolet–Visible spectrophotometry
PL	=	Photoluminescence spectroscopy
IUPAC	=	International Union of Pure and Applied Chemistry

มหาวิทยาลัยเทคโนโลยีสุรนารี

CHAPTER I

INTRODUCTION

Optoelectronics is the study and application of electronic devices that deals with converting electrical energy to light and converting light to electrical energy by way of materials called semiconductors. Consequently, these materials were used as nonconductors in the electronic industry. Since 1977, Heeger, MacDiarmid and Shirakawa have found that the conductivity of poly(acetylene) can be increased by eleven orders of magnitude when it is doped with halogens (Baude et al., 2003; Sunder et al., 2004). After that, in 2000 received The Nobel Prize in chemistry for the discovery and development of conductive polymers. Therefore, the possibility of using organic semiconducting materials for applications in optoelectronics and the semiconductor has been of great scientific and technological interest (Li et al., 2005; Wu et al., 2005; Adam et al., 1994). An important advantage of organic semiconducting materials is ease of processing, i.e. from solution with large area coverage. The possibility to use flexible substrates makes organic semiconductors ideal candidates for low cost electronic applications. During the last 15 years, rapid progress took place in the field of material developments, device, design, deposition processes and molecular modeling (Craats et al., 1999). The researcher's attention to modify and search for organic light emitting diodes (OLEDs) (Fechtenkotter et al., 1999), organic field-effect transistors (OFETs) (Funahashi and Hanna, 2000), sensors (Sirringhaus et al., 2000), organic photovoltaics (McCulloch et al., 2006), dye solar cells (DSCs) etc. Organic Solid-State Lighting

(OSSL) is an attractive technology for solid state lighting applications. Organic light-emitting devices (OLEDs) offer a number of advantages-lighter weight, performing at lower power, greater brightness, fast response time, high luminance, wide viewing angle, low operating voltage, and emission colors across the entire visible spectrum. In 2004, Bardsley et al. proposed that the desired properties for OLEDs should have a luminous efficiency of 20 lm/W for commercial applications, luminance more than 20,000 cd/m^2, quantum efficiency more than 4%, turn-on voltage lower than 6 V and lifetime more than 10,000 h (Bardsley et al., 2004). This work focused on the synthesis of red light emitting materials for organic light emitting diodes.

1.1 Organic Light Emitting Diodes

Solid state lighting is the alternative lighting achieved by an eco-friendly, energy efficient, and new light source technology, where illumination is obtained through semiconductor devices such as light-emitting diodes (LEDs), organic light-emitting diodes (OLEDs) and light emitting polymers (LEPs). OLEDs are cheaper to manufacture and more efficient than tungsten light and neon light. Therefore, organic light emitting diode is important technology for next generation full color flat panel displays and light source. It is a general light-emitting diode with an organic film as an emitting layer. Because the luminescence nature of an organic light emitting diode is from the organic luminescent materials, organic light emitting diode is a direct light source without a backlight and can display deep black level colors compared to liquid crystal display (LCD). More interestingly, it can be fabricated on a flexible substrate which can be processed with roll-to-roll techniques. Moreover, the organic light

emitting diode has wider viewing angles, higher power efficiency and faster response time than LCD, making it a promising display.

In 1960, Pope et al. at New York University developed ohmic, dark injecting electrode contacting to organic crystals. Pope's group first observed electroluminescence under vacuum on a pure single crystal of anthracene. However, this did not attract the researchers due to its ultra-high voltage and poor device performance (Burroughes et al., 1990). Also in 1965, Helfrich and Schneider of the National Research Council in Canada produced double injection recombination electroluminescence for the first time in an anthracene single crystal using hole and electron injecting electrodes (Lee et al., 2007). In 1987, the first diode device was reported at Eastman Kodak by Ching After that, Tang and Steven Van Slyke (Jin et al., 2009) improved the device performance by inserting hole transport layer (HTL), electron transport layer (ETL) and hole blocking layer (HBL) showing high efficiency. This resulted in a reduction of operating voltage and improvement in efficiency that led to the current era of OLED research and device production. In 1990, Burroughes et al. (Duan et al., 2007) proposed the concept of p-type doped hole transport layer (HTL) and n-type doped electron transport layer (ETL). These p-type semiconductor and n-type semiconductor diode (PIN diode) structure devices showed high luminance and efficiency at extremely low operating voltage. In this work, we were interested in organic light emitting devices because of their application in flat panel displays (Sano et al., 1965) and general lighting (Helfrich, W. and Schneider, 1965; Tang et al., 1987) by focusing on the synthesis of the novel organic materials can that used to be in OLEDs the study of their thermal, optical and electrochemical properties and the fabrication of the devices to study their efficiency.

1.2 Advantages and disadvantages of OLEDs

As emitting materials, polymeric/organic structures possess many advantages over inorganic ones, such as good film-forming properties, susceptibility to structure modification and so on (Tsuchiya et al., 2010; Lovinger and Rothberg, 1996; Sheats et al., 1996; Bradley, 1992). Examples are as follows:

Flexibility - An OLED can be fabricated on flexible plastic substrates important to the possible fabrication of flexible organic light-emitting diodes for other new applications.

Self-luminescence - The efficiency of OLEDs is more than that of other display technologies without the use of backlight.

Color selectivity - There are abundant organic materials which produce blue to red light.

Lightweight, compact and thin devices - OLEDs are commonly as thin, as about 100 nm.

Low cost and ease of fabrication - Roll to roll manufacturing processes such as inkjet printing and screen printing, are possible for polymer OLEDs.

High brightness and high resolution - OLEDs are very bright at low operating voltage (white OLEDs can be as bright as 150,000 cd/m^2).

Wide viewing angle - OLEDs emit lambertian reflection with viewing angle as high as 160 degrees.

Fast response - OLEDs electroluminescence decay time is lower than 1μs

However, the OLEDs also have disadvantages such as:

- While red and green OLED films have longer lifetimes (46,000 to 230,000 h), blue ones have much shorter lifetimes (14,000 h).

- Low mobility due to amorphous nature of the organic molecules. Therefore, the operating temperature cannot exceed the glass transition temperature.

- Low glass transition temperature (Tg) for small molecular devices.

- Water can easily damage OLEDs.

1.3 Structure of organic light emitting diode

A simplified OLED structure (as shown in Figure 1.1) consists of a stack of thin organic layers sandwiched between a transparent anode and a metallic cathode. The organic layers comprise a hole-injection layer (HIL), a hole-transport layer (HTL), an emissive layer (EML) and an electron-transport layer (ETL). In the structure of OLEDs, the organic layers between anode and cathode are designed to maximize the recombination process in the emissive layer, thus maximizing the light output from the OLED device. Both the electroluminescent efficiency and control of color output can be significantly enhanced by "doping" the emissive layer with a small amount of highly fluorescent molecules (Ito et al., 2006; Kim et al., 2007).

An OLED consists of the following parts:

- **Substrate** (clear plastic, glass, foil) - The substrate supports the OLED.

- **Anode** (transparent) - The anode removes electrons (generating "holes") when

a current flow through the device. Indium tin oxide is commonly used as the anode material.

- **Hole transport layer** - It transports the positively charged particles, named holes, from the anode in direction to the emissive organic layers that produce light.

Typical polymers used in PLED displays include derivatives of poly (*p*-phenylene vinylene) and polyfluorene.

- **Emissive layer** - This layer is made of organic molecules that transport electrons from the cathode; this is where light is made.

- **Electron transport layer** - This layer produces an improved charge carrier injection and the development of internal energy barriers between the organic layers.

- **Cathode** (may or may not be transparent depending on the type of OLED)- The cathode injects electrons when a current flow through the device. Metals such as aluminum and calcium are often used as the cathode.

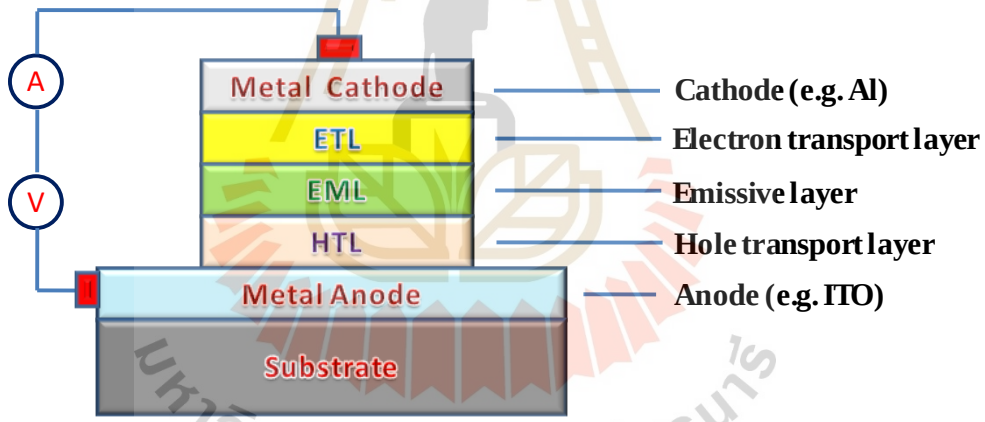

Figure 1.1 Organic light emitting diode (OLED) Structure.

1.4 Working Principle

When a voltage is applied to the electrodes, the charges start moving in the device under the influence of the electric field. Electrons leave the cathode and holes move from the anode in opposite direction. The recombination of these charges creates a

photon with a frequency given by the energy gap ($E = hv$) between the LUMO and HOMO levels of the emitting molecules (see Figure 2.2). Therefore, the electrical power applied to the electrodes is transformed into light. Different materials and dopants can be used to generate different colors and the combination of them allows building up a white light source (Lovinger and Rothberg, 1996).

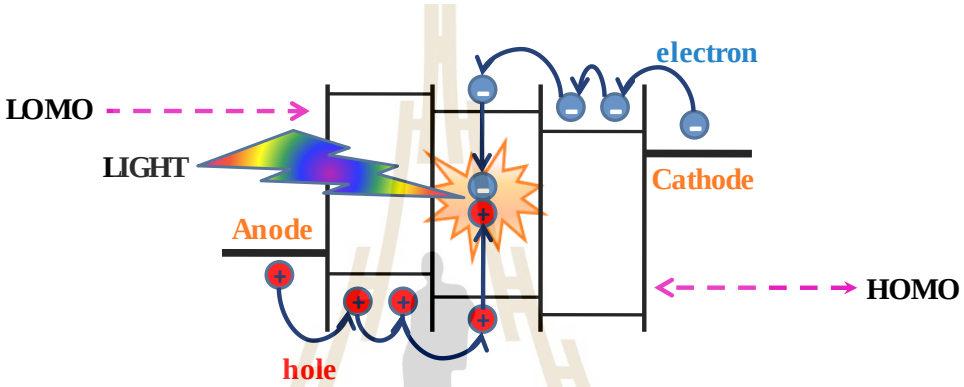

Figure 1.2 Organic light emitting diode (OLED) working principle.

1.5 Materials for the emissive layer of OLEDs

The development of new materials, particularly for achieving emission in the blue, green and red region of the spectrum for organic light-emitting devices, has been intensively investigated throughout the world. Scientists have developed a new class of materials that demonstrate exceptional promise for use as electron transport materials within an OLED device. The successful development of practical blue OLED devices would significantly impact advancement of OLED technology in both display devices and energy-efficient solid-state lighting. These materials address the critical issue of achieving high quantum efficiency (photons generated per electron injected into an OLED device) at low voltages. Devices built at Pacific Northwest National Laboratory

(PNNL) using the new materials have produced external quantum efficiencies at brightness of 800 cd/m^2 as high as 11% at only 6.3 V without using conductivity doping. One class of new OLED materials developed at PNNL is based on organic phosphine oxide compounds while another is based on organic phosphine sulfides.

In the following passage some basics on materials used in OLEDs are given (Wang et al., 2008; Kim et al., 2010; Chen et al., 2012). The colors of the emitted light can be tuned by the molecular structure of the organic emissive material (see Figure 1.3). Typical emitters for different colors can either be well-defined low molecular compounds such as DPVBI (4,40-bis(2,2-diphenylethen-1-yl)diphenyl) for blue emission, Alq_3 (tris(8-oxychinolinato)aluminum) for green emission (Lai et al., 2013), and DCM (4-(dicyanomethylene)-2-methyl-6-(*p*-dimethyl-aminostyryl)-4*H*-pyrene) for red emission, or polymers (see Figure 1.4) such as polyfluorenes (blue) (Tang and Vanslyke, 1987), PPV (poly(p-phenylenvinylene)) (green) (Tang et al., (1989), and MEH-PPV (poly[(2-(2-ethylhexyloxy)-5-methoxy-p-phenylen)vinylene]) (orange) (Chen, 2004).

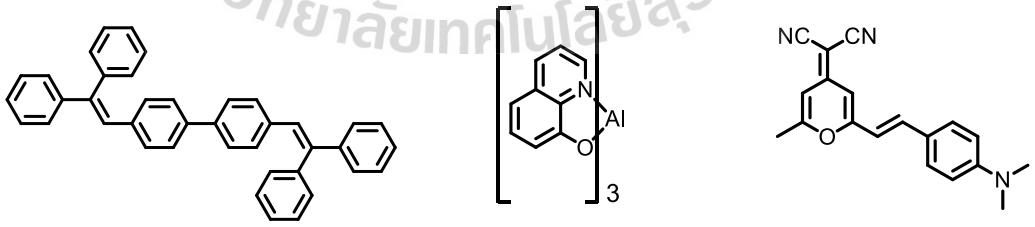

DPVBI Alq_3 DCM

Figure 1.3 Chemical structures of various emitting materials small molecules used in OLEDs.

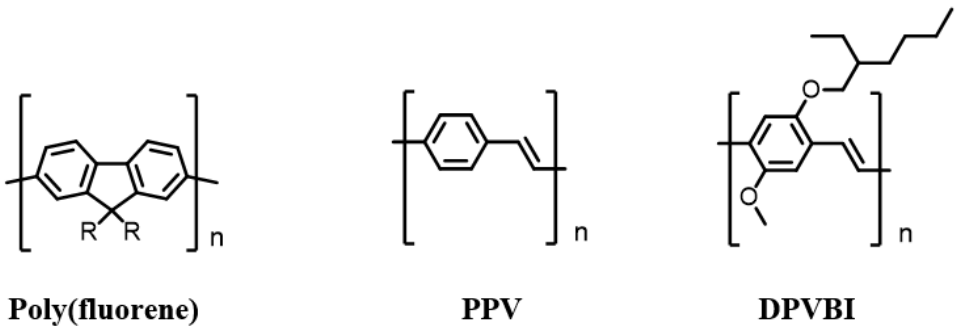

Poly(fluorene) **PPV** **DPVBI**

Figure 1.4 Chemical structures of various emitting materials polymers used in OLEDs.

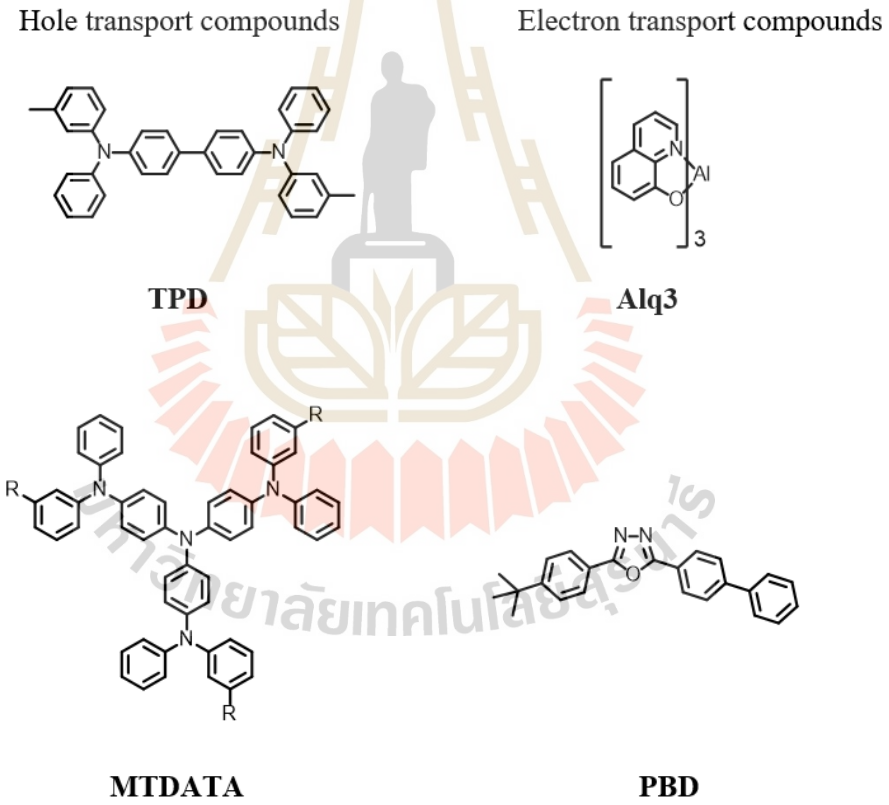

TPD **Alq3**

MTDATA **PBD**

Figure 1.5 Various hole transport and electron transport materials used in OLEDs.

Typical hole transporters are materials based on the triarylamine motive like TPD (*N*,*N*-bis(3-methylphenyl)-*N*,*N*-diphenylbenzidine) or MTDATA (m-methyltris (diphenylamine)triphenylamin), while compounds like Alq_3 and PBD (2-(4-biphenyl)-5-(4-*tert*-butylphenyl)-1,3,4-oxadiazole) (Webster et al., 1974). are able to transport electrons especially well (Figure 1.5).

1.6 Literature review

The organic light emitting diode (OLED) is a solid-state light emitting device based on organic materials. Currently, the efficiency of OLEDs is comparable to that of inorganic LEDs. Additionally, OLEDs are considered to be an alternative solid-state lighting source. Small molecule of OLEDs displays has been already commercialised in mobile phones, portable music players etc. Thus, many researchers observed and development new organic material for using larger scale OLED applications.

1.6.1 Red light emitting materials

In 2002, Ma et al. (Chen et al., 1999). synthesized a novel red luminescent material *N*,*N*-bis{4-[2-(4-dicyanomethylene-6-methyl-4*H*-pyran-2-yl)ethylene]phenyl} aniline **(BDCM)** with two (4-dicyanomethylene)-4*H*-pyranelectron-acceptor moieties and a triphenylamine electron-donor moiety for application in OLEDs. The three-layered electroluminescence device with the structure ITO/CuPc/DPPhP/BDCM/Mg: Ag has a turn-on voltage of less than 4V, which suggests that BDCM has an excellent electron injection property and show a brightness of **(BDCM)** 582 cd/m^2 at 19V.

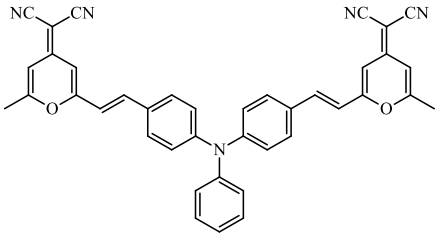

In 2013, Promarak et al. (Chen et al., 1999) synthesized a novel Bis[5-(fluoren-2-yl)thiophen-2-yl]benzo-thiadiazole end-capped with carbazole dendrons as highly efficient solution-processed non doped red emitters for organic light emitting diodes. These dendrimers show a bright-red fluorescence and can form morphologically stable amorphous thin films with shown high glass-transition temperatures at 283 °C. Simple structured solution-processed OLEDs using these materials as hole-transporting nondoped emitters and BCP as the holeblocking layer emit a stable red color around 622 - 645 nm, with high luminance efficiencies (up to 4.80 cd A^{-1} at 1.2 mA cm^{-2}) and show pure red color.

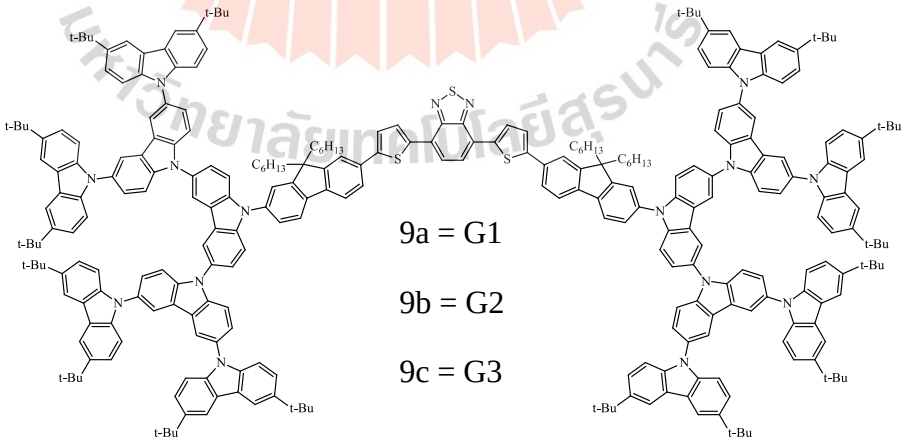

Tavgeniene et al. (Tavgeniene et al., 2017) synthesized three newly developed bipolar phenanthro[9,10-d]imidazole based derivatives are highly thermally stable

materials. The derivatives were used as hosts in red phosphorescent organic light-emitting diodes. The 2-[4-(N,Ndiphenylamino)phenyl]-1-phenylphenan thro[9,10-d]imidazole (**H3**) exhibited superior performance with peak efficiency of 15.9% (21.5 cd/A and 29.9 l m/W) and very low turn on voltage of 2.8 V. Efficiency of the device is about 35e67% higher than those of devices containing commercial host materials.

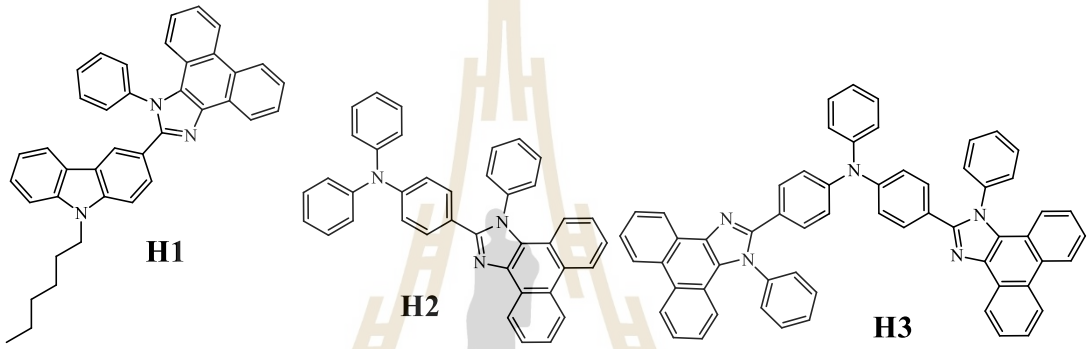

Bi et al. (Bi et al., 2015) reported Organic light-emitting molecular glasses (OEMGs). They are synthesized of nonplanar donor and branched aliphatic chain into electroluminescent emitters. The OEMGs are showed good electron-donating group. This non-doped red OLED device including the maximum electroluminescent wavelength of 640 nm, the stable luminous efficiency of 2.4 cd/A and the stable CIE 1931 coordinate of (x, y) = (0.64, 0.35) of red light in PAL

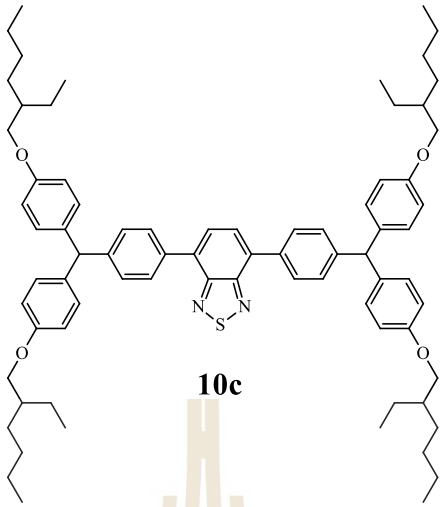

10c

system

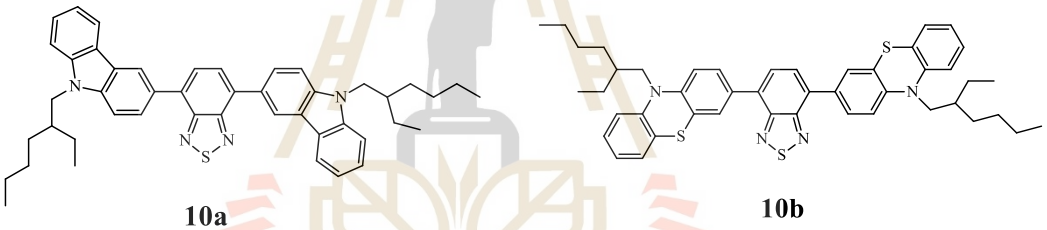

10a **10b**

In 2011, Qing et al. (Qing et al., 2011) synthesized Two novel red-emitting thieno-[3,4-b]-pyrazine-cored molecules with phenyls (TP) or polyphenyls (Müllen type dendron, DTP) as peripheral groups. They have large stokes shifts over 100 nm and more thermally stable temperature up to 458^{o}C and high glass transition temperature of 262^{o}C. The evaporated device exhibited a maximum brightness of 1753 cd m^{-2} and a luminous efficiency of 0.74 cd A^{-}. In contrary, TP failed to produce satisfied red emission in OLEDs device.

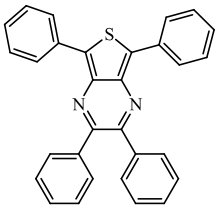

TP

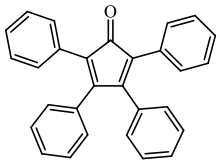

DTP

In 2017, Wang and et al. (Wang et al., 2017) synthesized bipolar compound consist of carbazole as electron donor and 4,5-diphenylimidazole as electron acceptor as good performance in applied as emitting layer for both non-doped and doped single layer OLEDs fabricated by solution processing. The single layer doped OLEDs with the bipolar compound as host achieved blue, green and red phosphorescence OLEDs with current efficiency of 0.083, 13.42, 2.58 cd A^{-1} and luminance up to 108, 17103, 1347 cd m^{-2}, respectively.

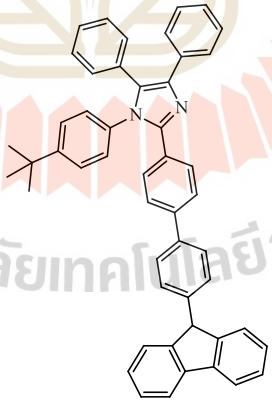

Cz-BP-DPI

1.6.2 Green light emitting marterials

Ku et al. (Chen et al., 2000) reported highly efficient non-doped green OLEDS by incorporating a novel 9,9-diarylfluorene-terminated 2,1,3-benzothiadiazole

(**DFBTA**), which exhibits an excellent solid-state photoluminescence quantum yield about 81%. The optimal device: ITO/DPAInT$_2$ /DPAInF/TCTA/DFBTA/Alq3/LiF/Al displaye **DFBTA** impressive device haracteristics, with maximum external quantum efficiency of 12.9 cd/A.

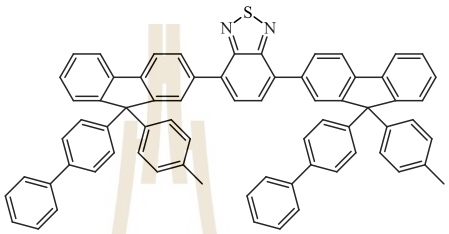

High efficiency green OLEDs were fabricated from solution processed ambipolar blends of electron and hole transport polymer hosts doped with green light emitting iridium complex sandwiched between HTL and ETL. In this research, they are used poly(norbornene) electron transport materials and poly(N-vinylcarbozole) for electron and hole transport layer. An external quantum efficiency of 13.6% and a maximum luminous efficiency of 44.6 cd/A at 1000cd/m^2 with turn on voltage of 5.9V were obtained (Chang et al., 2003).

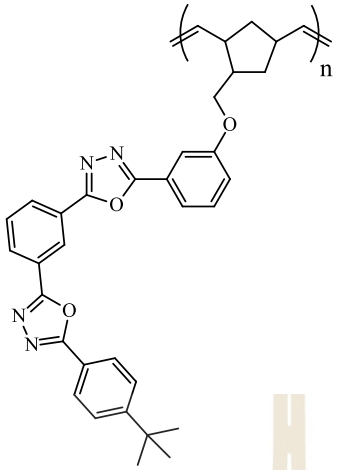

Oxadiazole polymer (OP1)

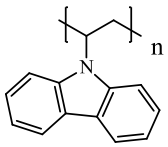

PVK

1.6.3 Blue light emitting materials

In 2019, Islam et al. (Islam et al., 2019) synthesized deep blue electroluminescent materials for organic light emitting devices (OLEDs). This a novel ambipolar meta-substituted emitter (TPA-BIPI) consist of phenanthroimidazole, benzimidazole and triphenyl-amine units for OLED devices. The TPA-BIPI as emitter gave deep-blue emission at 442 nm with CIE of (0.149, 0.105) and showed high EQE as 4.53%, with the current efficiency (CE) of 4.3 cd/A and a power efficiency (PE) of 3.7 lm/W. The TPA-BIPI showed high electroluminescence of 12,491 cd/m^{-2}

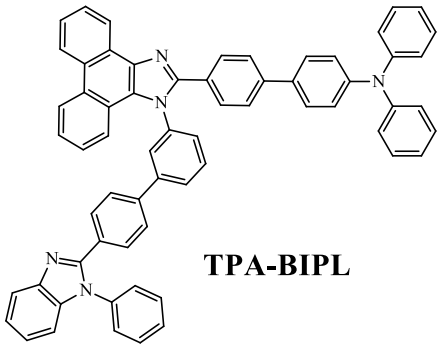

TPA-BIPL

Chen et al. (Ma et al., 2003) synthesized three anthracene derivatives featuring carbazole moieties as side groups-tert-butyl-9, 10-bis[4-(9-carbazolyl)phenyl] anthracene (Cz^9PhAnt), 2-tert-butyl-9,10-bis{4-[3,6-di-tert-butyl-(9-carbazolyl)]phenyl} anthracene (tCz^9PhAnt), and 2-tert-butyl-9,10-bis{4-[3,6-di-tert-butyl-(9-carbazolyl)] biphenyl-4-yl}anthracene ($tCz^9Ph2Ant$) for use in blue OLEDs with high glass-transition temperature of 220 °C. They exhibited strong blue emissions in solution, with high quantum efficiency of 91%.

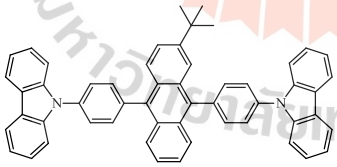

Cz^9PhAnt

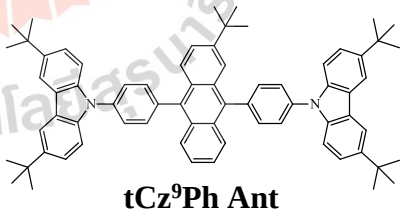

tCz^9Ph Ant

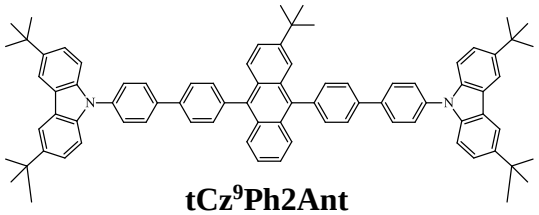

$tCz^9Ph2Ant$

In 2013, Lai et al. (Zhang et al., 2000) are synthesized bis(4,6-difluoro-phenyl-pyridinato-N, C_2^1)(picolinate)irridium (III) (Firpic) for use in blue OLEDs. They exhibited blue emission.

In 2018, Zassowski et al. (Zassowski et al., 2018) synthesized series of compounds consisting of carbazole arm and 1,3,5-triazine core linked by amino group. The exciplex-forming properties of the compound as donor, and acceptors 4,7-diphenyl-1,10-phenanthroline (Bphen) and 2,2′,2"-(1,3,5-benzenetriyl)-tris(1-phenyl-1-H-benzimidazole) (TPBi). The 3CzNC compound provides the high performance with EQE up to 6.84%

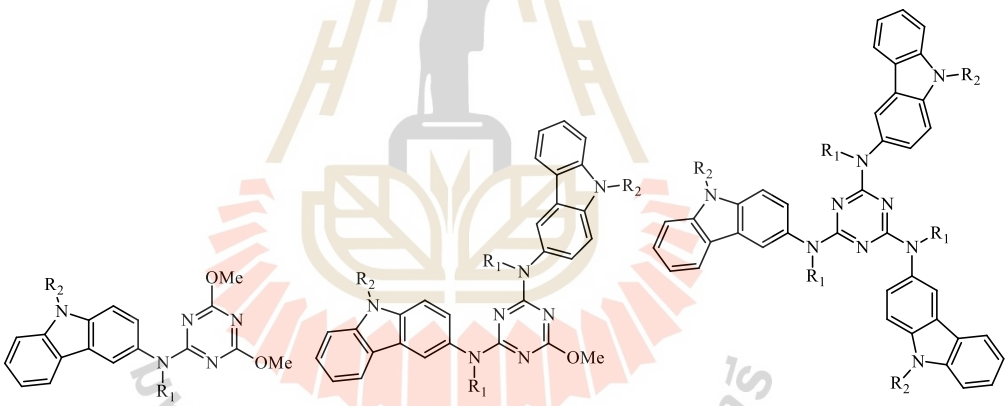

1CzNH: R_1=H R_2=C_8H_{17} **2CzNH: R_1=H R_2=C_8H_{17}** **3CzNH: R_1=H R_2=C_8H_{17}**
1CZNC: R_1=CH_3 R_2=C_2H_5 **2CZNC: R_1=CH_3 R_2=C_2H_5** **3CZNC: R_1=CH_3 R_2=C_2H_5**

In 2018, Liua and et al. (Liua et al., 2018) synthesized three dimesity borane-containing fluorophores with various π-conjugated systems attached at the 9th position of carbazole, namely, 9-(4′-bromobiphenyl-4-yl)-9H-carbazole (Cz9Ph2B), 9-(4-(5-(dimesitylboryl) thiophen-2-yl)phenyl)-9H-carbazole (Cz9ThPhB), and 9-(4-(4-(dimesitylboryl)styryl)phenyl) -9H-carbazole (Cz9SB).

CHAPTER II

EXPERIMENTAL

2.1 Materials and Methods

Measurements ^{1}H and ^{13}C spectra were recorded on a Bruker Avance III HD 600 MHz spectrometer using $CDCl_3$ as solvent in all cases. UV-Vis spectra were recorded as a dilute solution in a spectroscopic grade dichloromethane on a Perkin-Elmer Lambda 1050 spectrometer. CV measurements were carried out under inert argon atmosphere with an Autolab potentiostat PGSTAT 101 using platinum counter electrode, glassy carbon working electrode, and Ag/AgCl reference electrode in distilled dichloromethane with tetra-n-butylammonium hexafluorophosphate (n-Bu_4NPF_6) as a supporting electrode at a scan rate of 50 mV s^{-1}. High resolution MALDI-TOF mass spectra were recorded with a Bruker Autoflex speed mass spectrometer. X-ray diffraction (XRD) of organic semiconductor powder were measured on a Bruker New D8 Advance diffractometer. The detector was moved by 2θ steps of 0.02°. Morphologies of PDI-T and PDI-DT films were investigated using Park Systems NX-10 atomic force microscope (AFM) using true non-contact mode and NCHR cantilever. Differential scanning calorimetry (DSC) measurements were carried under nitrogen atmosphere using Perkin Elmer DSC-8500 thermal analyzer at a heating rate of 10 °C/min.

2.2 Device fabrication and measurements

OLED devices using **BTZ4** as EL with configuration ITO/PEDOT: PSS (40 nm)/ BTZ6 (60 nm)/ETL/LiF (0.5 nm): Al (150 nm) and **BTZ1-4** as EL with configuration of ITO/PEDOT: PSS (40 nm)/EL (50 nm)/2,2',2"-(1,3,5-benzinetriyl)- tris(1-phenyl-1-H-benzimidazole) (TPBi) (50 nm)/ LiF (0. 5 nm): Al (150 nm) were fabricated and characterized as followed. The patterned indium tin oxide (ITO) glass substrate with a sheet resistance 12 Ω/sq. was thoroughly cleaned by successive ultrasonic treatment in Liquinox detergent, deionized water, acetone, and isopropanol and brew with nitrogen for drying. The cleaned ITO was then treated by UV ozone for 30 min before deposited the hole injection layer (HTL) layer. A 40 nm thick poly (3,4-ethylene dioxy thiophene: poly(4-styrene sulfonate) (PEDOT: PSS, CLEVIOSTM P VP Al 4083) hole injection layer was spin-coated on top of UV ozone treated ITO from a 1.2 wt% aqueous dispersion at a spin speed of 5000 rpm for 30 s and dried at 120 °C for 15 min. Thin films of **BTZ1-4** EL were deposited on top of PEDOT: PSS layer by spin-coating toluene solution of **BTZ1-4** (2% w/v) at a spin speed of 2000 rpm for 30 second to get a 50 - 60 nm thick. The 2,9-dimethyl-4,7-diphenyl-1,10-phenanthroline (BCP), tris(8-hydroxy-quinoline)aluminum (Alq3), 2,2',2"-(1,3,5-benzinetriyl)-tris(1-phenyl-1-H-benzimidazole) (TPBi), 3-(biphenyl-4-yl)-5-(4-tert-butylphenyl)-4-phenyl-4H-1,2,4-triazole (TAZ) or 1,3,5-tri (m-pyridin-3-ylphenyl)benzene (TmPyPB) electron transport layers (ETL) were deposited at the evaporation rate of 1 Å/s from low temperature evaporator sources in Kurt J. Lasker mini SPECTROS 100 thin film deposition system under a base pressure of $5x10^{-7}$ mbar. The film thickness was monitored by quartz oscillator thickness sensor. A 0.5 nm thick LiF and a 150 nm thick aluminium layers were the subsequently deposited through a shadow mask on the top

of ETL film without braking vacuum to form an active diode area of 4 mm^2. Current density-voltage-luminescence (*J-V-L*) characteristics were measured simultaneous using a Keithley 2400 source meter and a Hamamatsu Photonics PMA-12 multi-channel analyser. The absolute external quantum efficiency (EQE) of OLED devices was obtained by Hamamatsu Photonics C9920-12 External Quantum Efficiency Measurement System utilizing an integrating sphere. All the measurements were performed under ambient atmosphere at room temperature.

2.3 Synthesis

2.3.1 General method for Suzuki cross coupling reaction

A mixture of aryl bromide (1.71 mmol), aryl borolane/ aryl boronic acid, $Pd(PPh_3)_4$ (0.05 mmol) and 2 M Na_2CO_3 (15 ml) in THF (30 ml) was degassed with N_2 for 10 min. The mixture was stirred at reflux under N_2 for 24 h. After cooling, water (50 ml) was added, and the mixture was extracted with CH_2Cl_2 (3 x 50 ml). The combined organic phase was washed with water (50 ml), brine solution (50 ml), dried over anhydrous Na_2SO_4 and filtered. The solvent was removed to dryness and the crude product was purified by column chromatography on silica gel eluting with a mixture of CH_2Cl_2/hexane.

2.3.2 General method for bromination reaction

To a solution of the bis(hexylthiophenyl)-benzothiadiazoles (0.39 mmol) in THF (20 ml) was added with NBS in small portions. After completion, water was added and the mixture was extracted with CH_2Cl_2 (3 x 50 ml). The combined organic phase was washed with water (50 ml), brine solution (50 ml), dried over anhydrous Na_2SO_4 and

filtered. The solvent was removed to dryness and the crude product was purified by column chromatography on silica gel eluting with a mixture of CH_2Cl_2/hexane.

2.4 Product compounds and Intermediates

2.4.1 4,7-dibromobenzo[c][1,2,5]thiadiazole (BT-2Br)

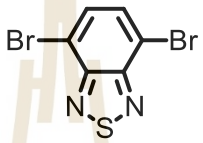

A dry 250 ml round-bottomed flask with a magnetic stirring bar. In the flask was placed benzo[c][1,2,5]thiadiazole (4.26 g, 31.29 mmol) and HBr (50 ml). Then Br_2 (mixture between bromine in HBr) was added dropwise at reflux for 2 h. The reaction was cooled to room temperature and separated. The aqueous solution was extracted thrice with dichloromethane (3 x 50 ml) and the combined organic layers with aqueous sodium thiosulfate solution until red color of bromine disappeared. After that were added $NaHCO_3$ solution to be neutral and dried over anhydrous Na_2SO_3, filtered and the solvent was removed under reduced pressure. The finally was purified by column chromatography on silica gel eluting with a mixture of CH_2Cl_2/hexane gave **BT-2Br** (8.36 g, 91 %) as white solid; m.p. 169 - 170 °C; ^{1}H-NMR (500 MHz, $CDCl_3$) 7.73 (s, 2H). ^{13}C-NMR (125 MHz, $CDCl_3$) $\boldsymbol{\delta}$ = 132.37, 113.92; (APCI): clacd. for $C_6H_2Br_2N_2S$ 293.8285; found: 294.8294 (M^{+1}).

2.4.2 4,7-Bis(3-hexylthiophen-2-yl)-2,1,3-benzothiadiazole (2)

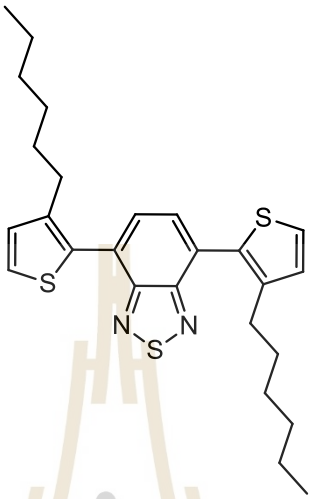

Compound **2** was prepared from Suzuki coupling reaction of **1** (0.50 g, 1.71 mmol) and 3-hexylthiophene-2-yl-4,4,5,5-tetramethyl-1,3,2-dioxaborolane (1.06 g, 3.61 mmol) and obtained as orange solids (0.78 g, 97%); m.p. 87 - 88 °C; ^{1}H-NMR (600 MHz, $CDCl_3$) $\boldsymbol{\delta}$ = 7.65 (s, 2H), 7.44 (d, J = 5.4 Hz, 2H), 7.11 (d, J = 5.4 Hz, 2H), 2.67 (t, J = 7.8 Hz, 4H), 1.65 - 1.60 (m, 4H), 1.26 - 1.18 (m, 12H), 0.81(t, J = 6.6 Hz, 6H); ^{13}C-NMR (150 MHz, $CDCl_3$) $\boldsymbol{\delta}$ = 153.28, 140.68, 131.18, 128.88, 128.20, 126.48, 124.82, 30.53, 29.64, 28.33, 28.07, 21.49, 12.99; MALDI-TOF clacd. for $C_{26}H_{32}N_2S_3$: 468.1728, found: 468.1335.

2.4.3 4,7-Bis(5-bromo-3-hexylthiophen-2-yl)-2,1,3-benzothiadiazole (3)

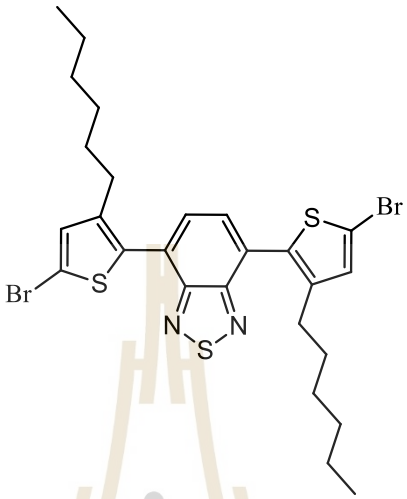

Compound **3** was prepared from bromination of **2** (0.18 g, 0.39 mmol) with NBS (0.15 g, 0.81 mmol) and obtained as orange solids (0.23 g, 95%); m.p. 90 - 91 °C; ^{1}H-NMR (600 MHz, $CDCl_3$) $\boldsymbol{\delta}$ = 7.06 (s, 2H), 7.05 (s, 2H), 2.60 (t, *J* = 7.8 Hz, 4H), 1.60 - 1.58 (m, 4H), 1.25 - 1.24 (m, 12H), 0.89 - 0.80 (m, 6H); ^{13}C-NMR (150 MHz, $CDCl_3$) $\boldsymbol{\delta}$ = 153.95, 142.46, 133.57, 132.01, 129.71, 126.66, 113.20, 31.94, 31.52, 30.50, 29.72, 29.42, 29.38, 29.03, 22.71, 22.51, 14.12, 14.01; MALDI- TOF clacd. for $C_{26}H_{30}Br_2N_2S_3$: 625.9917, found: 626.1159.

2.4.4 4,7-Bis(4,5-dibromo-3-hexylthiophen-2-yl)-2,1,3-benzothiadiazole (4)

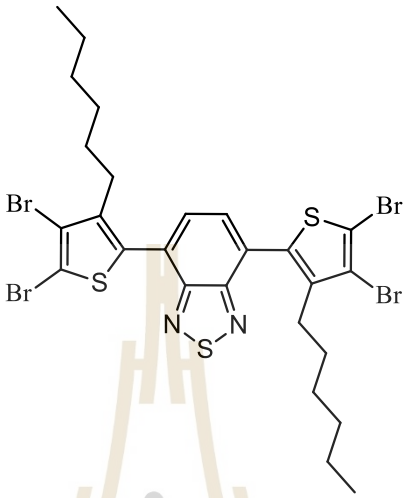

Compound **4** was prepared from bromination of **3** (0.23 g, 0.38 mmol) with NBS (0.26 g, 1.47 mmol) and obtained as orange solids (0.21 g, 73%); m.p. 97 -98 °C; ^{1}H-NMR (600 MHz, $CDCl_3$) $\boldsymbol{\delta}$ = 7.64 (s, 2H), 2.69 (t, J = 7.8 Hz, 4H), 1.53 - 1.26 (m, 16H), 0.88 - 0.77 (m, 6H); ^{13}C-NMR (150 MHz, $CDCl_3$) $\boldsymbol{\delta}$ = 153.93, 153.80, 153.75, 142.62, 142.45, 140.90, 138.72, 133.55, 133.20, 132.05, 132.00, 130.03, 129.86, 129.55, 127.03, 126.64, 117.66, 113.19, 112.51, 31.50, 31.24, 30.48, 29.70, 29.40, 29.34, 29.01, 28.95, 22.49, 22.45, 14.00, 13.96; APCI clacd. for $C_{26}H_{28}Br_4N_2S_3$: 783.8107, found: 784.8135 (M^{+1}).

2.4.5 4,7-Bis(4-hexylthiophen-2-yl)-2,1,3-benzothiadiazole (5)

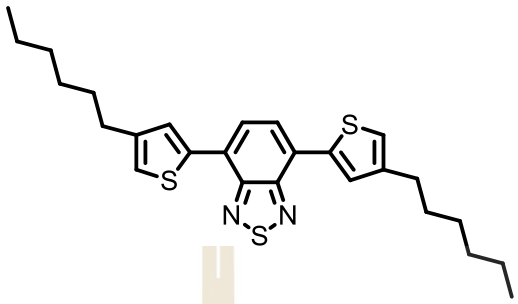

Compound **5** was prepared from Suzuki coupling reaction of **1** (0.70 g, 2.38 mmol) and 4-hexylthiophen-2-yl-4,4,5,5-tetramethyl-1,3,2-dioxaborolane (1.47g, 5.00 mmol) and obtained as orange solids (1.04 g, 93%); m.p. 93 - 94 °C; ^{1}H-NMR (500 MHz, $CDCl_3$) $\boldsymbol{\delta}$ = 7.97 (s, 2H), 7.82 (s, 2H), 7.038 (s, 2H), 2.69 (t, *J* = 7.5 Hz, 4H), 1.73 - 1.67 (m, 4H), 1.40 - 1.32 (m, 12H), 0.90 (t, *J* = 6.5 Hz, 6H); ^{13}C-NMR (125 MHz, $CDCl_3$) $\boldsymbol{\delta}$ = 152.65, 144.37, 139.01, 132.26, 129.62, 129.00, 126.03, 125.59, 125.54, 122.07, 121.53, 31.71, 30.67, 30.61, 30. 49, 29.06, 22.64, 14.12; MALDI- TOF clacd. for $C_{26}H_{32}N_2S_3$: 468.1728, found: 468.1920.

มหาวิทยาลัยเทคโนโลยีสุรนารี

2.4.6 4,7-Bis(4-hexyl-5-bromothiophen-2-yl)-2,1,3-benzothiadiazole (6)

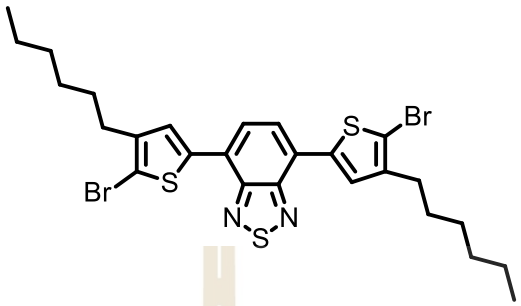

Compound **6** was prepared from bromination of **5** (1.00 g, 1.39 mmol) with NBS (0.65 g, 2.91 mmol) and obtained as orange-red solids (1.51g, 98%); m.p. 98 - 99 °C; ^{1}H-NMR (500 MHz, $CDCl_3$) $\boldsymbol{\delta}$ = 7.75 (s, 2H), 7.70 (s, 2H), 2.61 (t, J = 8 Hz, 4H), 1.67 - 1.64 (m, 4H), 1.55 (s, 6H), 1.42 - 1.33 (m, 14H), 0.90 (t, J = 6.5 Hz, 6H); ^{13}C-NMR (125 MHz, $CDCl_3$) $\boldsymbol{\delta}$ = 152.25, 148.27, 143.61, 127.75, 125.44, 125.04, 32.25, 31.67, 30.06, 29.71, 28.96, 22.63, 14.12; MALDI-TOF clacd. for $C_{26}H_{30}I_2N_2S_3$: 719.9660, found: 719.9730.

2.4.7 4,7-Bis(3,5-dibromo-4-hexylthiophen-2-yl)-2,1,3-benzothiadiazole (7)

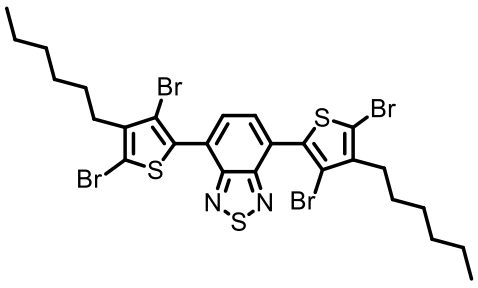

Compound **7** was prepared from bromination of **6** (0.29 g, 0.59 mmol) with NBS (0.42 g, 2.39 mmol) and obtained as orange solids (0.22 g, 78%); m.p. 97 -98 °C; ^{1}H-NMR (600 MHz, $CDCl_3$) $\boldsymbol{\delta}$ = 8.06 (s, 2H), 2.75 (t, *J* = 9.6 Hz, 4H), 1.63 - 1.58 (m, 4H), 1.45 - 1.44 (m, 4H), 1.42 (s, 8H), 1.37 - 1.34 (m, 6H); ^{13}C-NMR (150 MHz, $CDCl_3$) $\boldsymbol{\delta}$ = 153.24, 150.06, 141.75, 132.84, 129.87, 125.97, 112.20, 111.53, 31.95, 31.59, 30.40, 29.68, 29.38, 28.67, 22.71, 22.65, 14.12; MALDI-TOF clacd. for $C_{26}H_{28}Br_4N_2S_3$: 783.8107, found: 783.8642.

2.4.8 4, 7-bis(3,4'-dihexyl-[2,2'-bithiophen]-5-yl)benzo[c][1,2,5] thiadiazole (BT2T4)

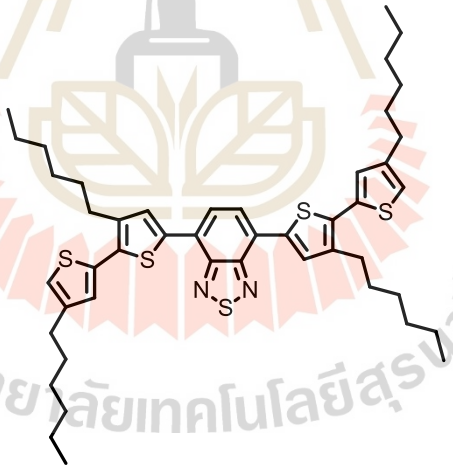

To mixture of 4,7-bis(4-hexyl-5-iodothiophen-2-yl)benzo[c][1,2,5]thiadiazole (0.33 g, 0.45 mmol), 4-hexylthiophen-2-yl-4,4,5,5-tetramethyl-1,3,2-dioxaborolane (0.28 g, 0.95 mmol), $Pd(PPh_3)_4$ (0.02 g, 0.02 mmol) and 2 M Na_2CO_3 (15 ml) in THF (30 ml) was degassed with N_2 for 10 min. The mixture was stirred at reflux under N_2 for 24 h. After cooling, water (50 ml) was added, and the mixture was extracted with

dichloromethane (3 x 50 ml). The combined organic phase was washed with water (50 ml), brine solution (50 ml), dried with anhydrous Na_2SO_4 and filtered. The solvent was removed to dryness and the crude product was purified by column chromatography on silica gel eluting with a mixture of CH_2Cl_2/hexane gave red solid (**BT2T4**) (0.30g, 83%); m. p. 94 - 95 °C; ^{1}H-NMR (600 MHz, $CDCl_3$) $\boldsymbol{\delta}$ = 7.95 (s, 2H), 7.78 (s, 2H), 7.07 (s, 2H), 6.93 (s, 2H), 2.83 (t = 7.8 Hz, 4H) 2.63 (t, *J* = 7.8 Hz, 4H), 1.76-1.71 (m, 4H), 1.69-1.64 (m, 4H), 1.44-1.41 (m, 4H), 1.39-1.33 (m, 20H); ^{13}C-NMR (150 MHz, $CDCl_3$) $\boldsymbol{\delta}$ = 152.57, 144.38, 143.75, 140.23, 136.61, 135.70, 132.89, 130.59, 129.01, 127.39, 125.50, 125.44, 125.14, 121.56, 120.27, 31.71, 30.61, 30.53, 30.43, 29.53, 29.33, 29.04, 28.06, 22.67, 22.64, 14.11 ppm. (MALDI-TOF): clacd. for $C_{46}H_{60}N_2S_5$: 800.3360 found: 800.3821.

2.4.9 4,7-bis(3,4'-dihexyl-5'-iodo-[2,2'-bithiophen]-5-yl)benzo[c][1,2,5]thiadiazole (BT2T4-2I)

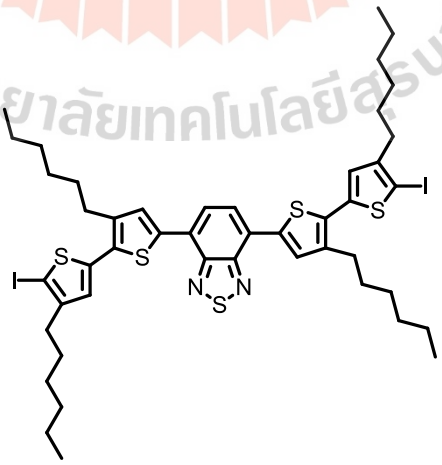

To dissolve of 4,7-bis(3,4'-dihexyl-[2,2'-bithiophen]-5-yl)benzo[c][1,2,5]thiadiazole (0.23 g, 0.28 mmol) with mixture solvent between CH_3COOH/ $CHCl_3$ (1:1). After that NIS (0.13 g, 0.59 mmol) was slowly added. When reaction completed, the reaction mixture was poured into water and extracted with dichloromethane (3 x 50 ml). The combined organic phase was washed with water (50ml), brine solution (50 ml), dried with anhydrous Na_2CO_3, filtered and the solvent was removed in vacuum. The crude product was purified by column chromatography on silica gel eluting with a mixture of CH_2Cl_2/hexane gave red solid (**BT2T4-2I**) (0.25 g, 84%); m.p. 89 - 90 °C; ^{1}H-NMR (500 MHz, $CDCl_3$) $\boldsymbol{\delta}$ = 7.94 (s, 2H), 7.81 (s, 2H), 6.88 (s, 2H), 2.79 (t = 7.5 Hz, 4H) 2.56 (t, *J* = 8.0 Hz, 4H), 1.73-1.70 (m, 4H), 1.63-1.60 (m, 12H), 1.44-1.32 (m, 26H), 0.92 - 89 (m, 14H); ^{13}C-NMR (125 MHz, $CDCl_3$) $\boldsymbol{\delta}$ = 152.54, 147.74, 140.78, 140.60, 137.04, 132.08, 130.51, 126.60, 125.45, 125.27, 32.38, 31.69, 31.67, 30.61, 29.99, 29.72, 29.53, 29.28, 28.95, 22.66, 22.63, 14.13 ppm (MALDI-TOF): clacd. for $C_{46}H_{58}I_2N_2S_5$: 1052.1293.

2.4.10 4,7-bis(3,4',4''-trihexyl-[2,2':5',2''-terthiophen]-5-yl) benzo[c][1,2,5] thiadiazole (BT3T4)

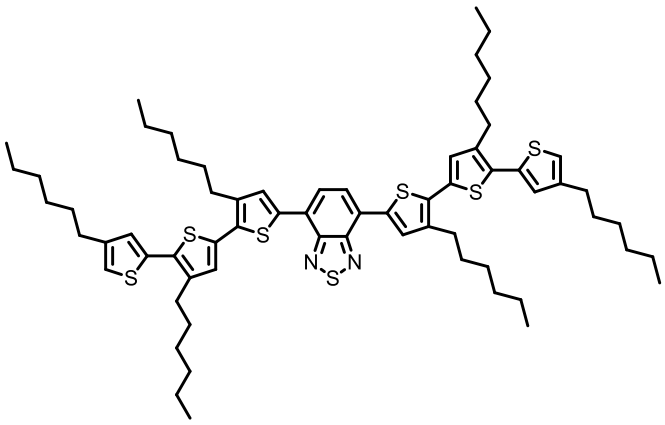

To mixture of 4,7-bis(3,4'-dihexyl-5'-iodo-[2,2'-bithiophen]-5-yl)benzo[c] [1,2,5] thiadiazole (0.18 g, 0.17 mmol), 4-hexylthiophen-2-yl-4,4,5,5-tetramethyl-1,3,2-dioxaborolane (0.11 g, 0.36 mmol), $Pd(PPh_3)_4$ (0.01 g, 0.01 mmol), and 2 M Na_2CO_3 (15 ml) in THF (30 ml) was degassed with N_2 for 10 min. The mixture was stirred at reflux under N_2 for 24 h. After cooling, water (50 ml) was added, and the mixture was extracted with dichloromethane (3 x 50 ml). The combined organic phase was washed with water (50 ml), brine solution (50 ml), dried with anhydrous Na_2SO_4 and filtered. The solvent was removed to dryness and the crude product was purified by column chromatography on silica gel eluting with a mixture of CH_2Cl_2/hexane gave as red-purple solid (**BT3T4**) (0.14 g, 73%); m.p. 97 - 98 °C; ^{1}H-NMR (600 MHz, $CDCl_3$) $\boldsymbol{\delta}$ = 7.98 (s, 2H), 7.83 (s, 2H), 7.07 (s, 2H), 6.99 (s, 2H), 6.91 (s, 2H), 2.87 (t, *J* = 7.8 Hz, 4H), 2.77 (t, *J* = 7.8 Hz, 4H), 2.62 (t, *J* = 7.8 Hz, 4H), 1.77 - 1.73 (m, 4H), 1.70 - 1.62 (m, 8H), 1.47 - 1.32 (m, 38H), 0.90 (s, 18H); ^{13}C-NMR (150 MHz, $CDCl_3$) $\boldsymbol{\delta}$ = 152.61, 143.71, 140.42, 139.72, 136.67, 135.50, 133.64, 132.57, 131.34, 130.75, 128.77, 127.24, 125.46, 125.20, 120.10, 31.69, 31.62, 30.58, 30.56, 30.41, 29.65, 29.31, 29.26, 29.01, 22.65, 22.63, 22.62, 14.11, 14.08 ppm. (MALDI-TOF): clacd. for $C_{66}H_{88}N_2S_7$: 1132.4992 found: 1132.5853.

มหาวิทยาลัยเทคโนโลยีสุรนารี

2.4.11 4,7-bis(3,4',4''-trihexyl-5''-iodo- [2,2':5',2''-terthiophen]-5-yl)benzo [c][1,2,5]thiadiazole (BT3T4-2I)

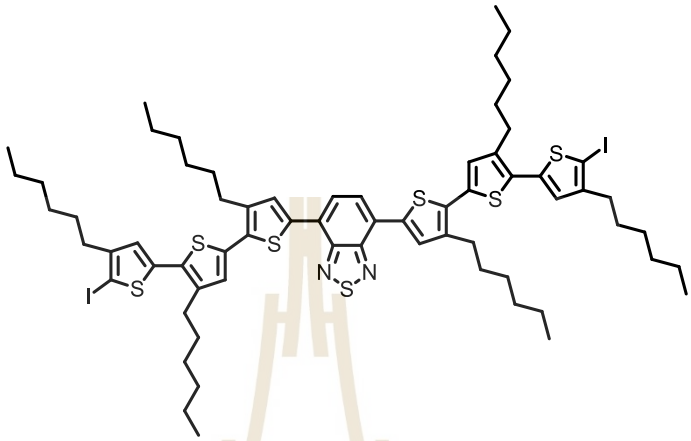

To dissolve of 4,7-bis(3,4',4"-trihexyl-[2,2':5',2"-terthiophen]-5-yl)benzo[c][1,2,5] thiadiazole (0.14 g, 1.26 mmol) with mixture solvent between $CH_3COOH/CHCl_3$ (1:1). After that NIS (0.06 g, 0.26 mmol) was slowly added. When reaction completed, the reaction mixture was poured into water and extracted with dichloromethane (3 x 50 ml). The combined organic phase was washed with water (50 mL), brine solution (50 ml), dried with anhydrous Na_2CO_3, filtered and the solvent was removed in vacuum. The crude product was purified by column chromatography on silica gel eluting with a mixture of CH_2Cl_2/hexane gave purple solid (**BT3T4-2I**) (0.12 g, 71%); m.p. 88 - 89 °C; ^{1}H-NMR (600 MHz, $CDCl_3$) $\boldsymbol{\delta}$ = 7.97 (s, 2H), 7.82 (s, 2H), 7.06 (s, 2H), 6.80 (s, 2H), 2.86 (t, *J* = 7.8 Hz, 4H), 2.73 (t, *J* = 7.8 Hz, 4H), 2.55 (t, *J* = 7.8 Hz, 4H), 1.75-1.74 (m, 4H), 1.67 - 1.66 (m, 4H), 1.62 - 1.60 (m, 4H), 1.53 (s, 8H), 1.47 - 1.33 (m, 48H), 0.91 (m, 18H); ^{13}C-NMR (150 MHz, $CDCl_3$) $\boldsymbol{\delta}$ = 152.59, 143.70, 140.40, 139.70, 136.67, 135.51, 133.65, 132.56, 131.33, 130.74, 128.74, 127.23, 125.43, 125.17, 120.08, 31.69,

30.58, 30.55, 30.51, 30.40, 29.66, 29.31, 29.26, 29.02, 22.66, 22.63, 22.62, 14.11, 14.08 ppm. (MALDI-TOF): clacd. for $C_{66}H_{86}I_2N_2S_7$: 1384.2925 found: 1384.4622.

2.4.12 4,7-bis(5'-bromo-3,4'-dihexyl-[2,2'-bithiophen]-5-yl)benzo[c][1,2,5] thiadiazole (BT2T4-2Br)

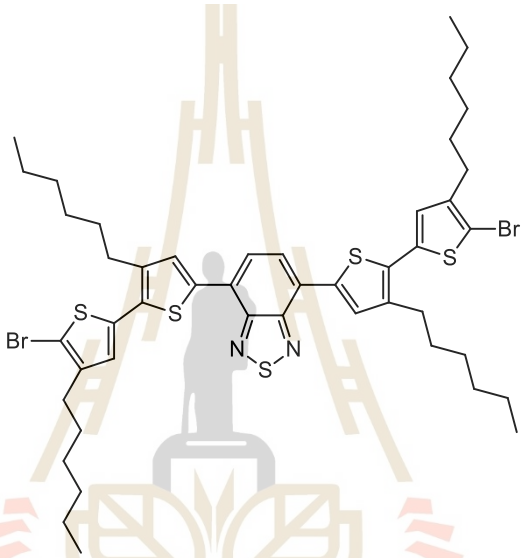

To dissolve of 4,7-bis(3,4'-dihexyl-[2,2'-bithiophen]-5-yl)benzo[c][1,2,5]thiadiazole (0.15 g, 0.19 mmol) in THF (20 ml). After that NBS (0.07 g, 0.39 mmol) was slowly added. When reaction completed, the reaction mixture was poured into water and extracted with dichloromethane (3 x 50 ml). The combined organic phase was washed with water (50ml), brine solution (50 ml), dried with anhydrous Na_2CO_3, filtered and the solvent was removed in vacuum. The crude product was purified by column chromatography on silica gel eluting with a mixture of CH_2Cl_2/hexane gave orange solid (**BT2T4-2Br**) (0.17 g, 96%); m. p. 136 - 137 °C; ^{1}H-NMR (600 MHz, $CDCl_3$) $\boldsymbol{\delta}$ = 7.94 (s, 2H), 7.80 (s, 8H), 6.92 (, 2H), 2.79 (t, *J* = 7.8 Hz, 4H), 2.58 (t, *J* = 7.8 Hz, 4H),

1.72 (t, *J* = 7.8 Hz, 4H), 1.63 (t, *J* = 7.2 Hz, 4H), 1.43-1.25 (m, 28H), 0.91 (s, 12H); ^{13}C-NMR (150 MHz, $CDCl_3$) ***δ*** = 152.55, 142.59, 140.74, 137.05, 135.51, 131.97, 130.53, 126.89, 125.48, 125.26, 109.01, 31.68, 31.65, 30.62, 29.68, 29.59, 29.50, 29.28, 28.94, 22.65, 22.62, 14.10 ppm. (MALDI-TOF): clacd. for $C_{46}H_{58}Br_2N_2S_5$: 958.1550 found: 958.2459.

2.2.13 4,7-bis(3',4,5'-tribromo-3,4'-dihexyl-[2,2'-bithiophen]-5-yl)benzo[c] [1,2,5]thiadiazole (BT2T4-6Br)

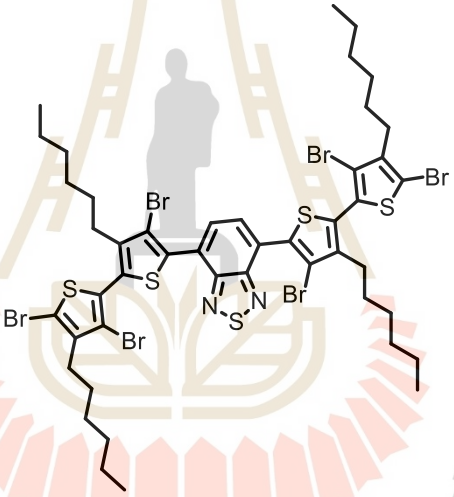

To dissolve of 4,7-bis(5'-bromo-3,4'-dihexyl-[2,2'-bithiophen]-5-yl)benzo[c] [1,2,5]thiadiazole (0.11 g, 0.12 mmol) with mixture between $CH_3COOH/CHCl_3$ ((1:1) 30 ml). After that NBS (0.16 g, 0.92 mmol) was slowly added. When reaction completed, the reaction mixture was poured into water and extracted with dichloromethane (3 x 50 ml). The combined organic phase was washed with water (50 ml), brine solution (50 ml), dried with anhydrous Na_2CO_3, filtered and the solvent was removed in vacuum. The crude product was purified by column chromatography

on silica gel eluting with a mixture of CH_2Cl_2/hexane gave orange solid (**BT2T4-6Br**) (0.09 g, 65%); m. p. 138 - 139 ° C; ^{1}H-NMR (600 MHz, $CDCl_3$) $\boldsymbol{\delta}$ = 8.13 (s, 2H), 2.70 (s, 8H), 1.54-1.26 (m, 20H), 0.88 (q, *J* = 4.2 Hz, 24H); ^{13}C-NMR (150 MHz, $CDCl_3$) $\boldsymbol{\delta}$ = 152.55, 142.59, 140.74, 137.05, 135.51, 131.97, 130.53, 126.89, 125.48, 125.26, 109.01, 31.68, 31.65, 30.62, 29.68, 29.59, 29.50, 29.28, 28.94, 22.65, 22.62, 14.10 ppm. (MALDI-TOF): clacd. for $C_{46}H_{54}Br_6N_2S_5$: 1273.7929 found: 1273.6308.

2.4.14 4,7-Bis(5-(9-phenyl-9H-carbazole-3-yl)-3-hexylthiophene-2-yl)-2,1, 3-benzothiadiazole (BTZ1)

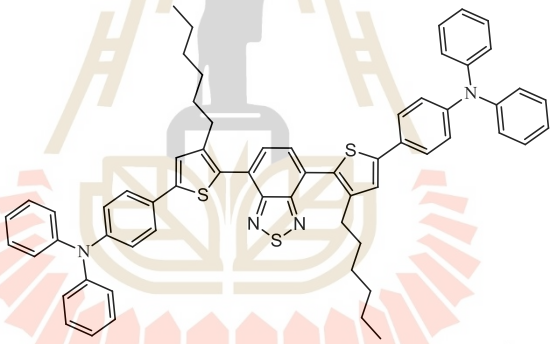

BTZ1 was prepared from Suzuki coupling reaction of **3** (0.14 g, 0.19 mmol) and (4-(diphenylamino)phenyl)boronic acid (0.12 g, 0.39 mmol), and obtained after recrystallisation from CH_2Cl_2/MeOH as dark red solids (0.13 g, 73%); m.p. 177 - 178 °C; ^{1}H-NMR (600 MHz, $CDCl_3$) $\boldsymbol{\delta}$ = 8.44 (s, 2H), 8.21 (d, *J* = 7.8 Hz, 2H), 7.75 (t, *J* = 4.2 Hz, 4H), 7.64-7.59 (m, 8H), 7.49 (t, *J* = 7.2 Hz, 2H), 7.43 (t, *J* = 4.8 Hz, 6H), 7.39 (s, 2H), 7.32 (t, *J* = 6.0 Hz, 2H), 2.76 (t, *J* = 7.8 Hz, 4H), 1.75 (t, *J* = 7.8 Hz, 4H), 1.35 (t, *J* = 7.2 Hz, 4H), 1.29-1.26 (m, 10H), 0.85 (t, *J* = 7.2 Hz, 4H); ^{13}C-NMR (150 MHz, $CDCl_3$) $\boldsymbol{\delta}$ = 154.31, 142.88, 141.44, 140.58, 137.56, 129.95, 129.66, 127.61, 127.30, 127.10,

126.69, 126.30, 124.72, 124.43, 123.88, 123.36, 120.51, 120.22, 117.68, 110.11, 110.00, 31.63, 30.76, 29.82, 29.25, 22.58, 14.06; MALDI-TOF clacd. for $C_{62}H_{54}N_4S_3$: 950.3511, found: 950.3056.

2.4.15 4,7-Bis(4,5-bis(4-(diphenylamino(phenyl)-3-hexylthiophen-2-yl)-2, 1, 3-benzothiadiazole (BTZ2)

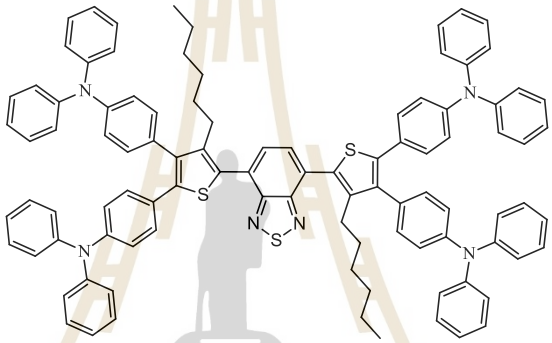

BTZ2 was prepared from Suzuki coupling reaction of **4** (0.12 g, 0.15 mmol), (4-(diphenylamino)phenyl)boronic acid (0.22 g, 0.76 mmol), and obtained after recrystallisation from CH_2Cl_2/MeOH as dark red solids (0.14g, 64%); m.p. 145 - 146 °C C; ^{1}H-NMR (600 MHz, $CDCl_3$) $\boldsymbol{\delta}$ = 7.75 (s, 2H), 7.24 (q, *J* = 7.8 Hz, 16H), 7.20 (d, *J* = 7.8 Hz, 4H), 7.15 (d, *J* = 8.4 Hz, 4H), 7.10 (d, *J* = 4.2 Hz, 20H), 7.02 (q, *J* = 7.2 Hz, 8H), 6.92 (d, *J* = 8.4 Hz, 4H), 2.62 (t, *J* = 7.2 Hz, 4H), 1.25-1.23 (m, 6H), 1.06 (t, *J* = 7.2 Hz, 4H), 1.02-0.96 (m, 8H), 0.74 (t, *J* = 7.2 Hz, 6H); ^{13}C-NMR (150 MHz, $CDCl_3$) $\boldsymbol{\delta}$ = 147.69, 146.73, 143.20, 129.22, 124.31, 123.83, 122.82, 31.59, 31.11, 29.78, 29.70, 28.99, 28.39, 22.65, 22.35, 14.11, 13.99; MALDI-TOF clacd. for $C_{98}H_{84}N_6S_3$: 1441.5953, found: 1441.4032.

2.4.16 4,7-Bis(5-(4-(diphenylamino)phenyl)-3-hexylthiophene-2-yl)-2,1,3-benzothiadiazole (BTZ3)

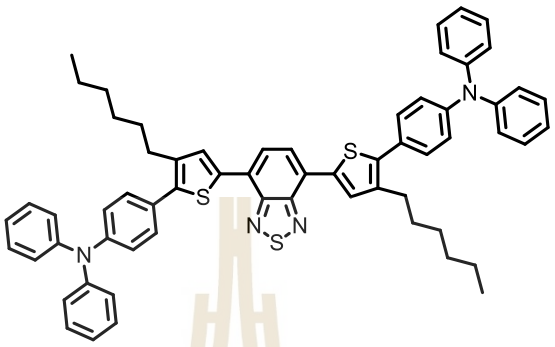

BTZ3 was prepared from Suzuki coupling reaction of **3** (0.10 g, 0.14 mmol) and (4-(diphenylamino)phenyl)boronic acid (0.08 g, 0.29 mmol), and obtained after recrystallisation from CH_2Cl_2/MeOH as dark red solids (0.11 g, 90%); m.p. 110 - 111 °C; ^{1}H-NMR (600 MHz, $CDCl_3$) $\boldsymbol{\delta}$ = 7.70 (s, 2H), 7.56 (d, *J* = 8.4 Hz, 4H), 7.32-7.28 (m, 10H), 7.16 (d, *J* = 7.8 Hz, 8H), 7.11 (d, *J* = 7.8 Hz, 4H), 7.07 (t, *J* = 7.2 Hz, 4H), 2.72 (t, *J* = 7.2 Hz, 4H), 1.70 (qq, *J* = 7.8 Hz, 4H), 1.34-1.23 (m, 12H), 0.85 (t, *J* = 6.6 Hz, 30H); ^{13}C-NMR (150 MHz, $CDCl_3$) $\boldsymbol{\delta}$ = 154.19, 147.51, 147.39, 144.45, 142.79, 129.63, 129.38, 129.32, 128.42, 127.22, 126.59, 124.98, 124.70, 124.57, 123.63, 123.13, 31.60, 30.67, 29.72, 29.16, 22.55, 14.05; MALDI-TOF clacd. for $C_{62}H_{58}N_4S_3$: 954.3824, found: 954.2314.

2.4.17 4,7-Bis(5-(4-(diphenylamino)phenyl)-4-hexylthiophene-2-yl)-2,1,3-benzothiadiazole (BTZ4)

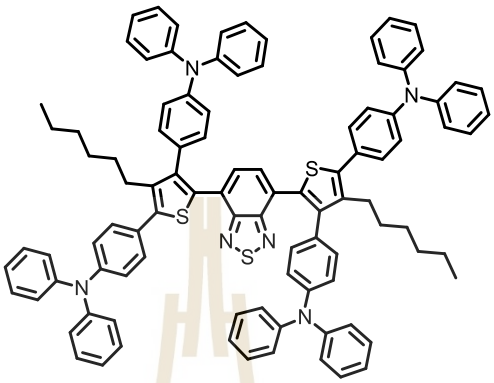

BTZ4 was prepared from Suzuki coupling reaction of **6** (0.10 g, 0.14 mmol), (4-(diphenylamino)phenyl)boronic acid (0.084 g, 0.29 mmol), and obtained after recrystallisation from CH_2Cl_2/MeOH as red solids (0.12g, 53%); m.p. 189 - 190 °C; ^{1}H-NMR (600 MHz, $CDCl_3$) $\boldsymbol{\delta}$ = 8.02 (s, 2H), 7.83 (s, 4H), 7.38 (d, *J* = 8.4 Hz, 4H), 7.29 (dd, *J* = 8.4, *J* = 0.6 Hz, 18H), 7.26 (s, 4H), 7.16 - 7.15 (m, 8H), 7.12 (d, *J* = 8.4 Hz, 4H), 7.05 (t = 7.2 Hz, 4H) 2.75 (t, *J* = 7.8 Hz, 4H), 1.73 - 1.70 (m, 4H), 1.53 (s, 8H), 1.39 (t, *J* = 7,2 Hz, 4H), 1.31 - 1.29 (m, 8H), (m, 6H); ^{13}C-NMR (150 MHz, $CDCl_3$) $\boldsymbol{\delta}$ = 152.68, 147.54, 147.27, 139.51, 139.39, 136.70, 130.31, 129.87, 129.34, 128.22, 125.63, 125.14, 124.71, 123.19, 123.06, 31.68, 31.01, 29.25, 29.02, 22.63, 14.11; MALDI-TOF clacd. for $C_{62}H_{58}N_4S_3$: 954.3824, found: 954.3505.

2.4.18 4,7-Bis(5-(9-phenyl-9H-carbazole-3-yl-4-hexylthiophen-2-yl)-2,1,3-benzothiadiazole (TBtz1)

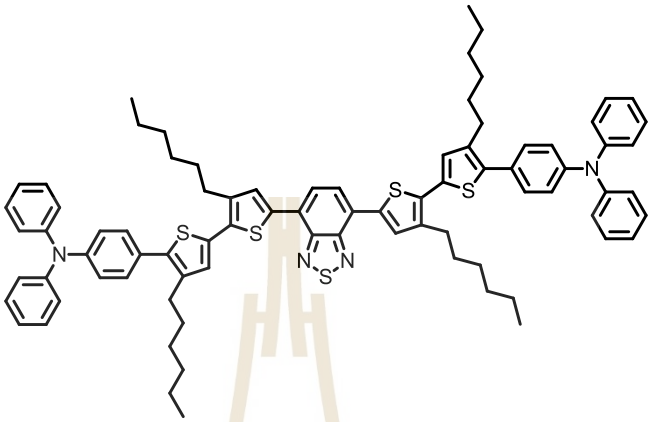

TBtz1 was prepared from Suzuki coupling reaction of **6** (0.25 g, 0.35 mmol), (4-(diphenylamino)phenyl)boronic acid (0. 21 g, 0. 73 mmol), and obtained after recrystallisation from CH_2Cl_2/MeOH as dark red solids (0.20 g, 61%); m.p. 172 - 173 °C; ^{1}H-NMR (600 MHz, $CDCl_3$) $\boldsymbol{\delta}$ = 8.29 (s, 2H), 8.18 (d, *J* = 7.2 Hz, 2H), 8.08 (s, 2H), 7.90 (s, 2H), 7.65 - 7.57 (m, 10H), 7.50 - 7.43 (m, 8H), 7.32 (q, *J* = 1.2 Hz, 2H), 2.82 (t, *J* = 7.8 Hz, 4H), 2.76 (t, *J* = 7.8 Hz, 4H), 1.39 (t, *J* = 7.2 Hz, 4H), 1.29 (t, *J* = 3.0 Hz, 8H), 0.85 (t, *J* = 6.6 Hz, 4H); ^{13}C-NMR (150 MHz, $CDCl_3$) $\boldsymbol{\delta}$ = 152.79, 141.39, 140. 64, 140. 39, 139. 45, 137. 59, 136. 88, 130. 18, 129. 95, 127. 63, 127. 52, 127. 12, 126.28, 125.77, 125.21, 123.61, 123.30, 121.15, 120.46, 120.22, 109.98, 109.78, 31.70, 31. 12, 29. 29, 29. 01, 22. 64, 14. 07; MALDI-TOF clacd. for $C_{62}H_{54}N_4S_3$: 950. 3511, found: 950.2472.

2.4.19 4,7-Bis(3,5-bis(4-(diphenylamino)phenyl)-5-hexylthiophen-2-yl- 2,1,3-benzothiadiazole (TBtz2)

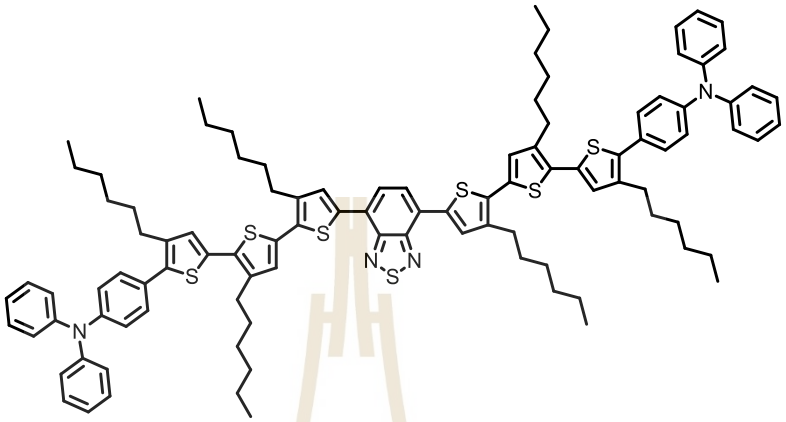

TBtz2 was prepared from Suzuki coupling reaction of **6** (0.23 g, 0.29 mmol), (4-(diphenylamino)phenyl)boronic acid (0.35 g, 1.21 mmol), and obtained after recrystallisation from CH_2Cl_2/MeOH as dark red solids (0.18 g, 43%); m.p. 139 - 140 °C; ^{1}H-NMR (600 MHz, $CDCl_3$) $\boldsymbol{\delta}$ = 7.42 (d, J = 9.0 Hz, 4H), 7.28 (t, J = 8.4 Hz, 8H), 7.20 (t, J = 8.4 Hz, 8H), 7.17 (d, J = 0.6 Hz, 4H), 7.15 (s, 6H), 7.12 (d, J = 9.0 Hz, 4H), 7.08-7.04 (m, 10H), 7.00 (d, J = 7.2 Hz, 8H), 6.97 (s, 2H), 6.95 (t, J = 4.8 Hz, 8H) 2.66 (t, J = 7.8 Hz, 4H), 1.28-1.25 (m, 4H), 1.19-1.14 (m, 4H), 1.13-1.07 (m, 8H), 0.82 (t, J = 7.8 Hz, 6H); ^{13}C-NMR (150 MHz, $CDCl_3$) $\boldsymbol{\delta}$ = 153.85, 147.65, 147.60, 147.34, 146.69, 142.41, 139.98, 138.49, 132.48, 131.78, 130.87, 130.21, 129.52, 129.35, 129.24, 128.57, 126.44, 124.73, 124.21, 123.62, 123.18, 123.04, 122.81, 31.22, 30.03, 29.10, 27.55, 22.45, 14.08; MALDI-TOF clacd. for $C_{98}H_{84}N_6S_3$: 1441.5953, found: 1441.6424.

2.4.20 BT2T4-6TPA

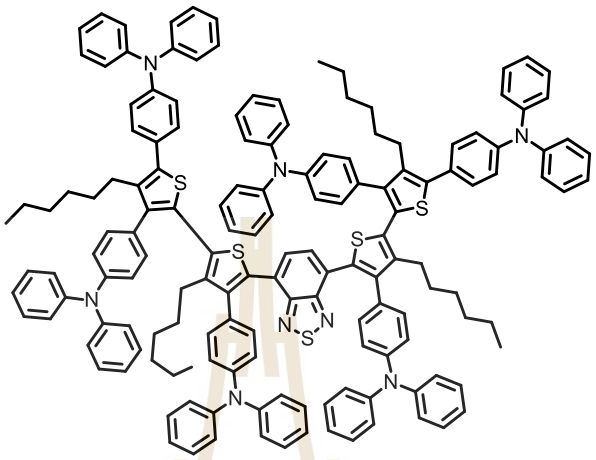

A mixture of 4,7-bis(3',4,5'-tribromo-3,4'-dihexyl-[2,2'-bithiophen]-5-yl)benzo[c] [1,2,5]thiadiazole (0.09 g, 0.08 mmol), (4-(diphenylamino)phenyl)boronic acid (0.17 g, 0.58 mmol), $Pd(PPh_3)_4$ (0.01 g, 0.01 mmol) and 2 M Na_2CO_3 (15 ml) in THF (30 ml) was degassed with N_2 for 10 min. The mixture was stirred at reflux under N_2 for 96 h. After cooling, water (50 ml) was added, and the mixture was extracted with dichloromethane (3 x 50 ml). The combined organic phase was washed with water (50 ml), brine solution (50 ml), dried with anhydrous Na_2SO_4 and filtered. The solvent was removed to dryness and the crude product was purified by column chromatography on silica gel eluting with a mixture of CH_2Cl_2/hexane gave purple solid (0.09 g, 56%); m. p. 205 - 206 °C; ^{1}H-NMR (600 MHz, $CDCl_3$) $\boldsymbol{\delta}$ = 7.39 (d, J = 9.0 Hz, 4H), 7.28 (t, J = 7.8 Hz, 8H), 7.21 - 7.10 (m, 34H), 7.07 - 7.03 (m, 16H), 6.97 - 6.90 (m, 24H), 2.67 (t, J = 7.2 Hz, 4H), 2.43 (d, J = 7.8 Hz, 4H), 1.30 - 1.25 (m, 6H), 1.19 - 1.06 (m, 30H), 0.84 - 0.78 (m, 12H); ^{13}C-NMR (150 MHz, $CDCl_3$) $\boldsymbol{\delta}$ = 146.77, 146.59, 146.21, 145.62,

130.07, 129.63, 129.13, 128.83, 128.32, 128.14, 128.12, 123.69, 123.32,123.19, 123.13, 123.01, 122.61, 122.13, 122.07, 122.03, 121.87, 121.78, 121.71, 121.60, 30.67, 30.57, 30.22, 30.20, 28.92, 28.69, 28.35, 28.21, 28.17, 28.05, 28.03, 21.67, 21.64, 21.60, 21.48, 21.43, 13.12, 13.09, 13.05 ppm. (MALDI-TOF): clacd. for $C_{154}H_{138}N_8S_5$: 2259.9682 found: 2260.0358.

2.4.21 4,7-bis(3-hexyl-5-(9-phenyl-9H-carbazol-3-yl)thiophen-2-yl)benzo[c] [1,2,5] thiadiazole (CTBtz1)

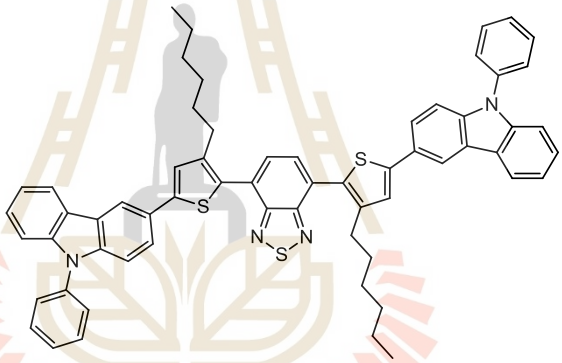

A mixture of 4,7-bis(5-bromo-3-hexylthiophen-2-yl)benzo[c][1,2,5]thiadiazole (0.14 g, 0.19 mmol), (9-phenyl-9H-carbazol-3-yl)boronic acid (0.12 g, 0.39 mmol), $Pd(PPh_3)_4$, (0.01 g, 0.01 mmol) and 2 M Na_2CO_3 (15 ml) in THF (30 ml) was degassed with N_2 for 10 min. The mixture was stirred at reflux under N_2 for 24 h. After cooling, water (50 ml) was added, and the mixture was extracted with dichloromethane (3 x 50 ml). The combined organic phase was washed with water (50 ml), brine solution (50 ml), dried with anhydrous Na_2SO_4 and filtered. The solvent was removed to dryness and the crude product was purified by column chromatography on silica gel eluting

with a mixture of CH_2Cl_2/hexane gave purple solid (**CTBtz1**) (0.13 g, 73%); m. p. 177 - 178 °C; ^{1}H-NMR (600 MHz, $CDCl_3$) $\boldsymbol{\delta}$ = 8.44 (s, 2H), 8.21 (d, *J* = 7.8 Hz, 2H), 7.75 (t, *J* = 4.2 Hz, 4H), 7.64-7.59 (m, 8H), 7.49 (t, *J* = 7.2 Hz, 2H), 7.43 (t, *J* = 4.8 Hz, 6H), 7.39 (s, 2H), 7.32 (t, *J* = 6.0 Hz, 2H), 2.76 (t, *J* = 7.8 Hz, 4H), 1.75 (t, *J* = 7.8 Hz, 4H), 1.35 (t, *J* = 7.2 Hz, 4H), 1.29-1.26 (m, 10H), 0.85 (t, *J* = 7.2 Hz, 4H); ^{13}C-NMR (150 MHz, $CDCl_3$) $\boldsymbol{\delta}$ = 154.31, 142.88, 141.44, 140.58, 137.56, 129.95, 129.66, 127.61, 127.30, 127.10, 126.69, 126.30, 124.72, 124.43, 123.88, 123.36, 120.51, 120.22, 117.68, 110.11, 110.00, 31.63, 30.76, 29.82, 29.25, 22.58, 14.06 ppm. (MALDI-TOF): clacd. for $C_{62}H_{54}N_4S_3$: 950.3511 found: 950.3056.

2.4.22 4,7-bis(4-hexyl-5-(9-phenyl-9H-carbazol-3-yl)thiophen-2yl)benzo[c] [1,2,5] thiadiazole (CTBtz2)

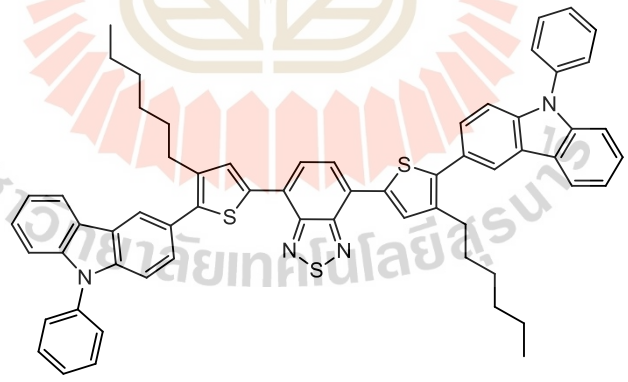

A mixture of 4,7-bis(5-bromo-4-hexylthiophen-2-yl)benzo[c][1,2,5]thiadiazole (0.25 g, 0.35 mmol), (9-phenyl-9H-carbazol-3-yl)boronic acid (0.21 g, 0.73 mmol), $Pd(PPh_3)_4$, (0.02 g, 0.02 mmol) and 2 M Na_2CO_3 (15 ml) in THF (30 ml) was degassed with N_2 for 10 min. The mixture was stirred at reflux under N_2 for 24 h. After cooling,

water (50 ml) was added, and the mixture was extracted with dichloromethane (3 x 50 ml). The combined organic phase was washed with water (50 ml), brine solution (50 ml), dried with anhydrous Na_2SO_4 and filtered. The solvent was removed to dryness and the crude product was purified by column chromatography on silica gel eluting with a mixture of CH_2Cl_2/hexane gave purple solid (**CTBtz2**) (0.20 g, 61%); m. p. 172 - 173 °C; ^{1}H-NMR (600 MHz, $CDCl_3$) $\boldsymbol{\delta}$ = 8.29 (s, 2H), 8.18 (d, *J* = 7.2 Hz, 2H), 8.08 (s, 2H), 7.90 (s, 2H), 7.65-7.57 (m, 10H), 7.50-7.43 (m, 8H), 7.32 (q, *J* = 1.2 Hz, 2H), 2.82 (t, *J* = 7.8 Hz, 4H), 1.76 (t, *J* = 7.8 Hz, 4H), 1.39 (t, *J* = 7.2 Hz, 4H), 1.29 (t, *J* = 3.0 Hz, 8H), 0.85 (t, *J* = 6.6 Hz, 4H); ^{13}C-NMR (150 MHz, $CDCl_3$) $\boldsymbol{\delta}$ = 152.79, 141.39, 140.64, 140.39, 139.45, 137.59, 136.88, 130.18, 129.95, 127.63, 127.52, 127.12, 126.28, 125.77, 125.21, 123.61, 123.30, 121.15, 120.46, 120.22, 109.98, 109.78, 31.70, 31.12, 29.29, 29.01, 22.64, 14.07 ppm. (MALDI-TOF): clacd. for $C_{62}H_{54}N_4S_3$: 950.3511 found: 950.2472.

2.4.23 6-bromo-3'',6''-di-tert-butyl-9,9'-didodecyl-9*H*,9'*H*-3,3':6',9''-tercarbazole (G1diC12-Br)

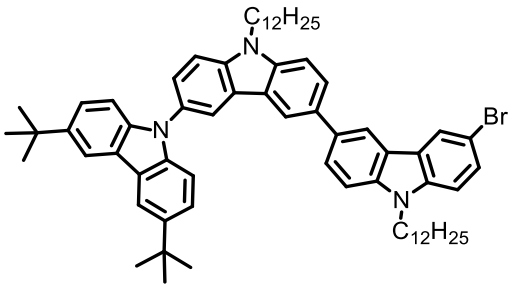

A stirred mixture of 6,6'-dibromo-9,9'-didodecyl-9*H*,9'*H*-3,3'-bicarbazole (9.08 g, 10.98 mmol), 3,6-di-*tert*-butyl-9*H*-carbazole (0.88 g, 3.14 mmol), copper iodide

(0.30 g, 1.57 mmol), potassium phosphate (1.66 g, 7.84 mmol) and *trans*-diamino-cyclohexane (0.18 g, 1.57 mmol) in toluene (100 ml) was refluxed for 24 h under N_2 atmosphere. After cooling, the reaction mixture was extracted with dichloromethane (100 x 3 ml). The combined organic phase was washed with water (50 x 3 ml), brine solution (50 x 3 ml), dried over sodium sulfate anhydrous, filtered and the solvent was removed in vacuum. The product was purified by silica gel chromatography to give (**G1diC12-Br**) as yellow viscous (1.44 g, 45%).

2.4.24 3'',6''-di-tert-butyl-9,9'-didodecyl-6-(4,4,5,5-tetramethyl-1,3,2- dioxa borolan-2-yl)- 9*H*,9'*H*-3,3':6',9''-tercarbazole (G1diC12-Boran)

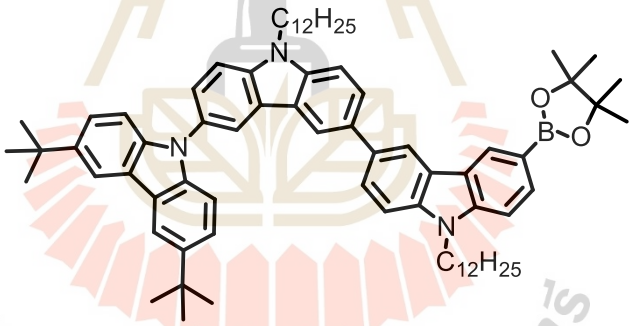

A mixture of 6-bromo-3",6"-di-tert-butyl-9,9'-didodecyl-9*H*,9'*H*-3,3':6',9"-tercarbazole (1.44 g, 1.41 mmol), 4,4,4',4',5,5,5',5'-octamethyl-2,2'-bi(1,3,2-dioxaborolane) (0.71 g, 0.32 mmol), $Pd(PPh_3)_2Cl_2$ (0.08 g, 0.11 mmol) and KOAc (0.55g, 5.63 mmol) in toluene (50 ml) was degassed with N_2 for 5 min. The mixture was stirred at reflux under N_2 for 24 h. After cooling, water (50 ml) was added, and the mixture was extracted with dichloromethane (3 x 50 ml). The combined organic phase was washed with water (50 ml), brine solution (50 ml), dried with anhydrous Na_2SO_4 and filtered. The solvent was

removed to dryness and the crude product was purified by column chromatography on silica gel eluting with a mixture of CH_2Cl_2/hexane gave white solid (**G1diC12-Boran**) (1.44g, 93%).

2.4.25 4,7-bis(3'',6''-di-tert-butyl-9,9'-didodecyl-9*H*,9'*H*-[3,3':6',9''-tercarbazol]-6-yl) benzo[c][1,2,5]thiadiazole (di[diC12-G1]BT)

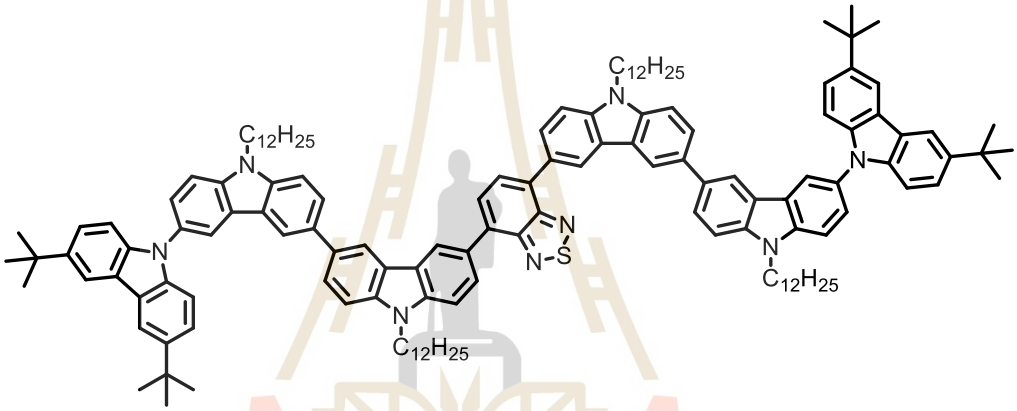

To mixture of 4,7-dibromobenzo[c][1,2,5]thiadiazole (0.06 g, 0.02 mmol), 3",6"-di-tert-butyl-9,9'-didodecyl-6-(4,4,5,5-tetramethyl-1,3,2-dioxaborolan-2-yl)-H,9'H,3':6',9"-tercarbazole (0.05 g, 0.05 mmol), $Pd(PPh_3)_4$ (0.01 g, 0.01 mmol) and 2 M Na_2CO_3 (15 ml) in THF (15 ml) was degassed with N_2 for 10 min. The mixture was stirred at reflux under N_2 for 24 h. After cooling, water (50 ml) was added, and the mixture was extracted with dichloromethane (3 x 50 ml). The combined organic phase was washed with water (50 ml), brine solution (50 ml), dried with anhydrous Na_2SO_4 and filtered. The solvent was removed to dryness and the crude product was purified by column chromatography on silica gel eluting with a mixture of CH_2Cl_2/hexane gave violet solid (**di[diC12-G1]BT**) (0.23g, 54%).

2.4.26 4,7-bis(5-(3'',6''-di-tert-butyl-9,9'-didodecyl-9*H*,9'*H*-[3,3':6',9''-tercarbazol]-6-yl)-4-hexylthiophen-2-yl)benzo[c][1,2,5]thiadiazole (di[diC12-G1]BT1T4)

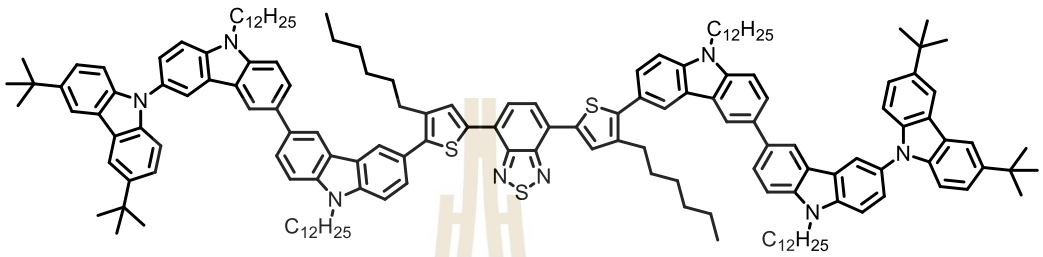

A mixture of 4,7-bis(3-hexyl-5-iodothiophen-2-yl)benzo[c][1,2,5]thiadiazole (0.11 g, 0.15 mmol), 3'',6''-di-tert-butyl-9,9'-didodecyl-6-(4,4,5,5-tetramethyl-1,3,2-dioxaborolan-2-yl)-9H,9'H-3,3':6',9''-tercarbazole (0.34 g, 0.32 mmol), $Pd(PPh_3)_4$ (0.01 g, 0.01 mmol) and 2 M Na_2CO_3 (10 ml) in THF (20 ml) was degassed with N_2 for 10 min. The mixture was stirred at reflux under N_2 for 24 h. After cooling, water (50 ml) was added, and the mixture was extracted with dichloromethane (3 x 50 ml). The combined organic phase was washed with water (50 ml), brine solution (50 ml), dried with anhydrous Na_2SO_4 and filtered. The solvent was removed to dryness and the crude product was purified by column chromatography on silica gel eluting with a mixture of CH_2Cl_2/hexane gave red solid (**di[diC12-G1]BT1T4**) (0.23g, 64%).

2.4.27 4,7-bis(3'',6''-di-tert-butyl-9,9'-didodecyl-9*H*,9'*H*-[3,3':6',9''-tercar bazol]-6-yl)- 5,6-difluorobenzo[c][1,2,5]thiadiazole (di[diC12-G1]BT-2F)

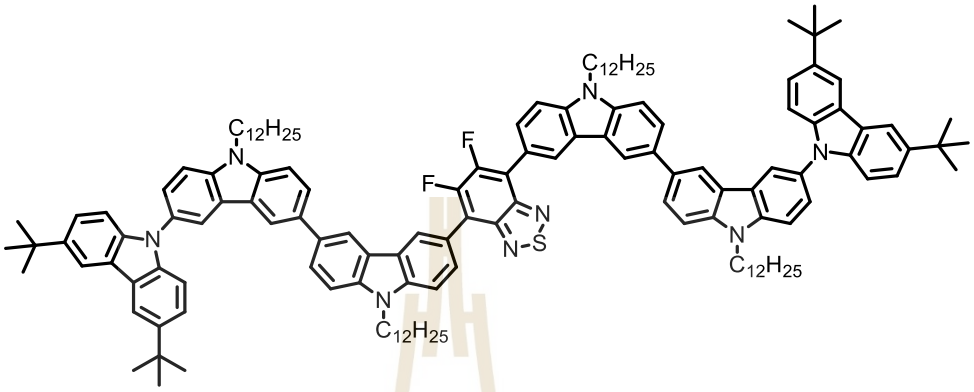

To mixture of 4,7-dibromo-5,6-difluorobenzo[c][1,2,5]thiadiazole (0.10 g, 0.30 mmol), 3'',6''-di-tert-butyl-9,9'-didodecyl-6-(4,4,5,5-tetramethyl-1,3,2-dioxaborolan-2-yl)-9*H*,9'*H*-3,3':6',9''-tercarbazole (0.68 g, 0.64 mmol), $Pd(PPh_3)_4$ (0.01 g, 0.01 mmol) and 2 M Na_2CO_3 (25 ml) in THF (25 ml) was degassed with N_2 for 10 min. The mixture was stirred at reflux under N_2 for 24 h. After cooling, water (50 ml) was added, and the mixture was extracted with dichloromethane (3 x 50 ml). The combined organic phase was washed with water (50 ml), brine solution (50 ml), dried with anhydrous Na_2SO_4 and filtered. The solvent was removed to dryness and the crude product was purified by column chromatography on silica gel eluting with a mixture of CH_2Cl_2/hexane gave red solid (**di[diC12-G1]BT-2F**) (0.19g, 30%).

2.4.28 4,9-bis(3'',6''-di-tert-butyl-9,9'-didodecyl-9*H*,9'*H*-[3,3':6',9''-tercar bazol]-6-yl) naphtho[2,3-c][1,2,5]thiadiazole (di[diC12-G1]NapBT)

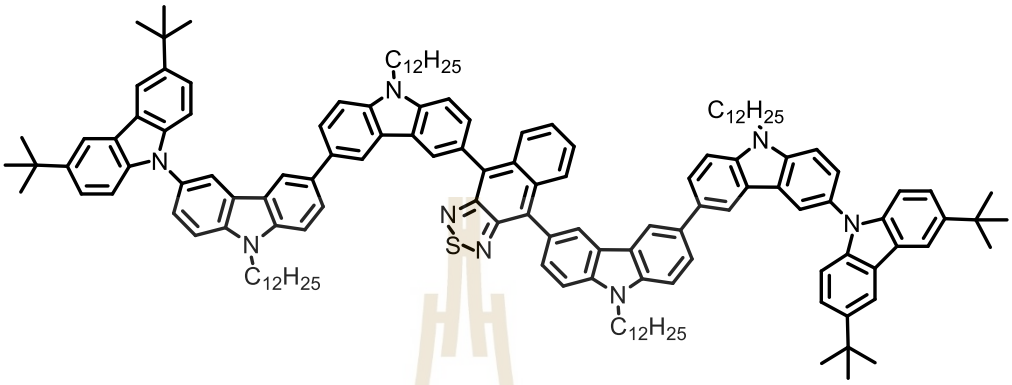

To mixture of 4,9-dibromonaphtho [2,3-c][1,2,5]thiadiazole (0.07 g, 0.20 mmol), 3'',6''- di- tert- butyl- 9,9'- didodecyl- 6- (4,4,5,5- tetramethyl- 1,3,2- dioxaborolan- 2- yl)- 9*H*,9'*H*-3,3': 6',9''-tercarbazole (0.45 g, 0.42 mmol), $Pd(PPh_3)_4$ (0.01 g, 0.01 mmol) and 2 M Na_2CO_3 (25 ml) in THF (25 ml) was degassed with N_2 for 10 min. The mixture was stirred at reflux under N_2 for 24 h. After cooling, water (50 ml) was added, and the mixture was extracted with dichloromethane (3 x 50 ml). The combined organic phase was washed with water (50 ml), brine solution (50 ml), dried with anhydrous Na_2SO_4 and filtered. The solvent was removed to dryness and the crude product was purified by column chromatography on silica gel eluting with a mixture of CH_2Cl_2/hexane gave red solid (**di[diC12-G1]NapBT**) (0.21g, 54%).

2.4.29 2,6-bis(3'',6''-di-tert-butyl-9,9'-didodecyl-9*H*,9'*H*-[3,3':6',9''-tercar bazol]- 6-yl) anthracene-9,10-dione. (di[diC12-G1]Ant)

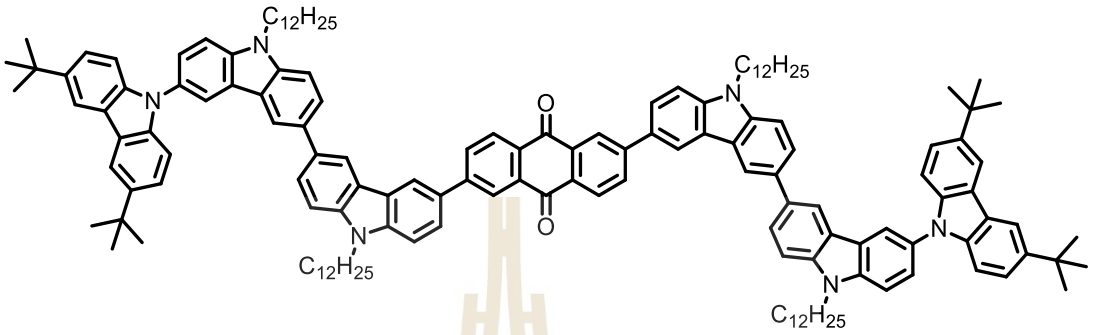

To dissolve of 2,6-dibromoanthracene-9,10-dione (0.03 g, 0.09 mmol) 3",6"-di-tert-butyl-9,9'-didodecyl-6- (4,4,5,5-tetramethyl-1,3,2-dioxaborolan-2-yl) -9*H*,9'*H*-, 3':6',9''-tercarbazole (0.20 g, 0.19 mmol), $Pd(PPh_3)_4$ (0.01 g, 0.01 mmol) and 2 M Na_2CO_3 (15 ml) in THF (20 ml) was degassed with N_2 for 10 min. The mixture was stirred at reflux under N_2 for 24 h. After cooling, water (50 ml) was added, and the mixture was extracted with dichloromethane (3 x 50 ml). The combined organic phase was washed with water (50 ml), brine solution (50 ml), dried with anhydrous Na_2SO_4 and filtered. The solvent was removed to dryness and the crude product was purified by column chromatography on silica gel eluting with a mixture of CH_2Cl_2/hexane gave orange solid (**di[diC12-G1]Ant**) (0.16g, 84%).

2.4.30 Tetra[diC12-G1]Ant-2TPA

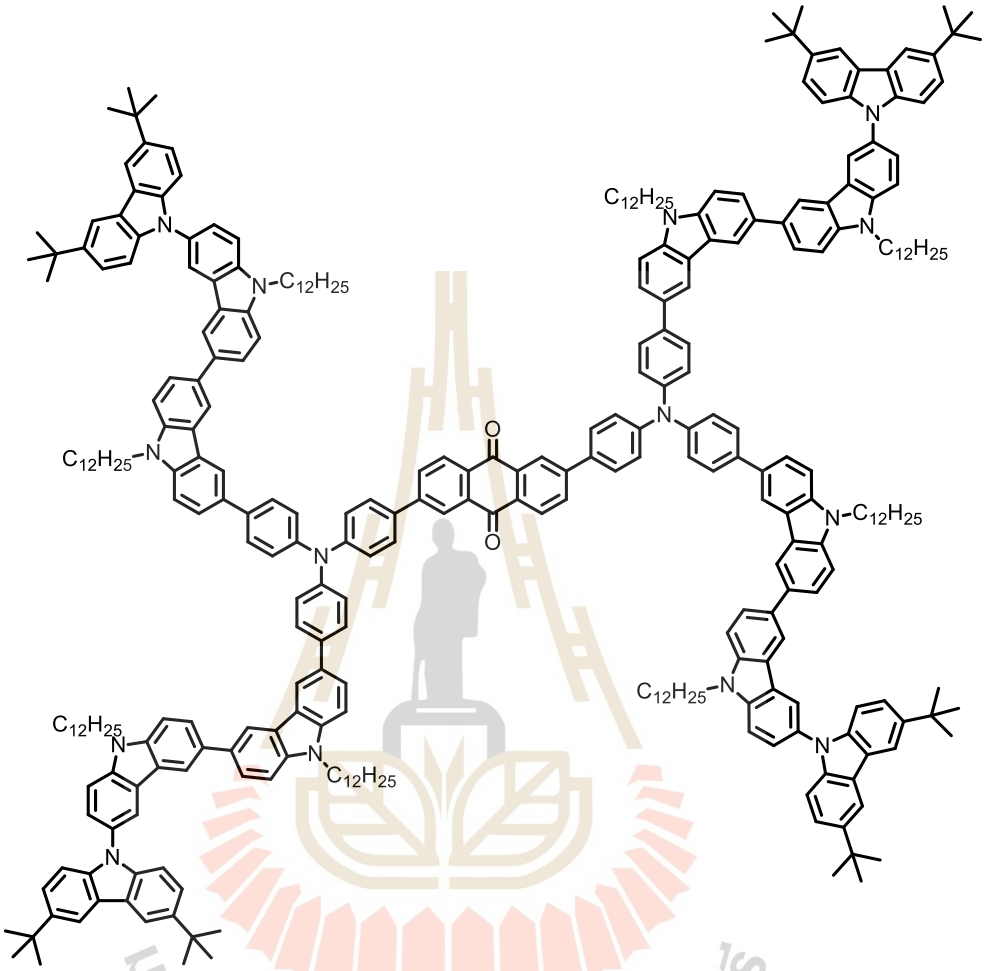

To mixture of 2,6-bis(4-(bis(4-bromophenyl)amino)phenyl)anthracene-9,10-dione (0.13 g, 0.13 mmol), 3",6"-di-tert-butyl-9,9'-didodecyl-6-(4,4,5,5-tetramethyl-1,3,2-dioxaborolan-2-yl)-9*H*,9'*H*-3,3':6',9"-tercarbazole (0.64 g, 0.59 mmol), $Pd(PPh_3)_4$ (0.01 g, 0.01 mmol) and 2 M Na_2CO_3 (25 ml) in THF (25 ml) was degassed with N_2 for 10 min. The mixture was stirred at reflux under N_2 for 24 h. After cooling, water (50 ml) was added, and the mixture was extracted with dichloromethane (3 x 50 ml). The combined organic phase was washed with water (50 ml), brine solution (50 ml), dried

with anhydrous Na_2SO_4 and filtered. The solvent was removed to dryness and the crude product was purified by column chromatography on silica gel eluting with a mixture of CH_2Cl_2/hexane gave orange solid (**tetra[diC12-G1]Ant-2TPA**) (0.24g, 41%).

2.4.31 2-(3'',6''-di-tert-butyl-9,9'-didodecyl-9*H*,9'*H*-[3,3':6',9''tercarbazol]-6-yl)-9*H*-thioxanthen-9-one 10,10-dioxide [diC12-G1]TOX

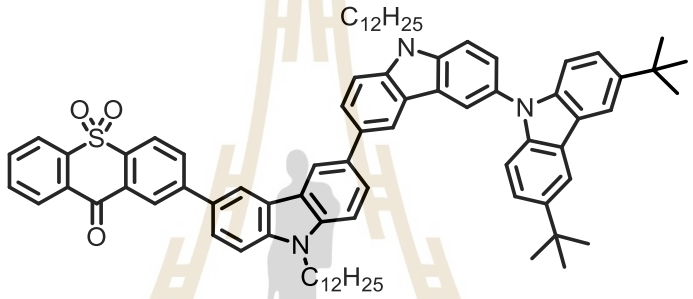

To mixture of 2-bromo-9*H*-thioxanthen-9-one 10,10-dioxide (0.12 g, 0.37 mmol), 3'',6''-di-tert-butyl-9,9'-didodecyl-6-(4,4,5,5-tetramethyl-1,3,2-dioxaborolan-2-yl)-*H*,9'*H*-3,3':6',9''-tercarbazole (0.44 g, 0.41 mmol), $Pd(PPh_3)_4$ (0.02 g, 0.02 mmol) and 2 M Na_2CO_3 (25 ml) in THF (25 ml) was degassed with N_2 for 10 min. The mixture was stirred at reflux under N_2 for 24 h. After cooling, water (50 ml) was added, and the mixture was extracted with dichloromethane (3 x 50 ml). The combined organic phase was washed with water (50 ml), brine solution (50 ml), dried with anhydrous Na_2SO_4 and filtered. The solvent was removed to dryness and the crude product was purified by column chromatography on silica gel eluting with a mixture of CH_2Cl_2/hexane gave orange solid (**diC12-G1]TOX**) (0.21g, 48%).

2.4.32 2-(4-(bis(4-(3'',6''-di-tert-butyl-9,9'-didodecyl-9*H*,9'*H*-[3,3':6',9''-tercarbazol]- 6- yl) phenyl) amino) phenyl)- 9*H*- thioxanthen- 9- one 10, 10- dioxide [diC12-G1]TOX-TPA

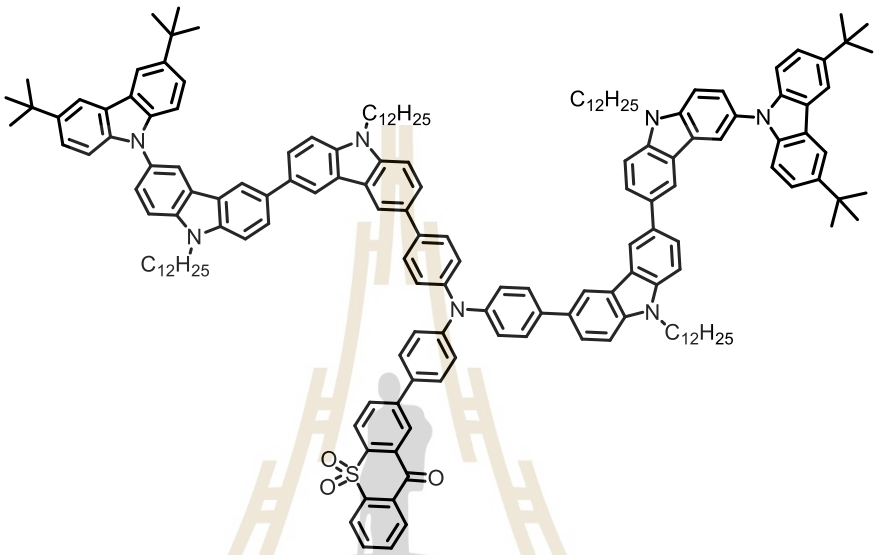

To mixture of 2-(4-(bis(4-bromophenyl)amino)phenyl)-9*H*-thioxanthen-9-one 10, 10-dioxide (0.15 g, 0.23 mmol), 3'', 6''-di-tert-butyl-9, 9'-didodecyl-6-(4, 4, 5, 5-tetramethyl-1,3,2-dioxaborolan-2-yl)-9*H*,9'*H*-3,3':6',9''-tercarbazole (0.53 g, 0.49 mmol), $Pd(PPh_3)_4$ (0.01 g, 0.01 mmol) and 2 M Na_2CO_3 (25 ml) in THF (25 ml) was degassed with N_2 for 10 min. The mixture was stirred at reflux under N_2 for 24 h. After cooling, water (50 ml) was added, and the mixture was extracted with dichloromethane (3 x 50 ml). The combined organic phase was washed with water (50 ml), brine solution (50 ml), dried with anhydrous Na_2SO_4 and filtered. The solvent was removed to dryness and the crude product was purified by column chromatography on silica gel eluting with a mixture of CH_2Cl_2/hexane gave green solid (**[diC12-G1]TOX-TPA**) (0.29g, 53%).

2.4.33 2,4,6-tris(4-(3'',6''-di-tert-butyl-9,9'-didodecyl-9*H*,9'*H*-[3,3':6',9''-tercarbazol]- 6-yl)phenyl)-1,3,5-triazine [tri[diC12-G1]*p*-triazene]

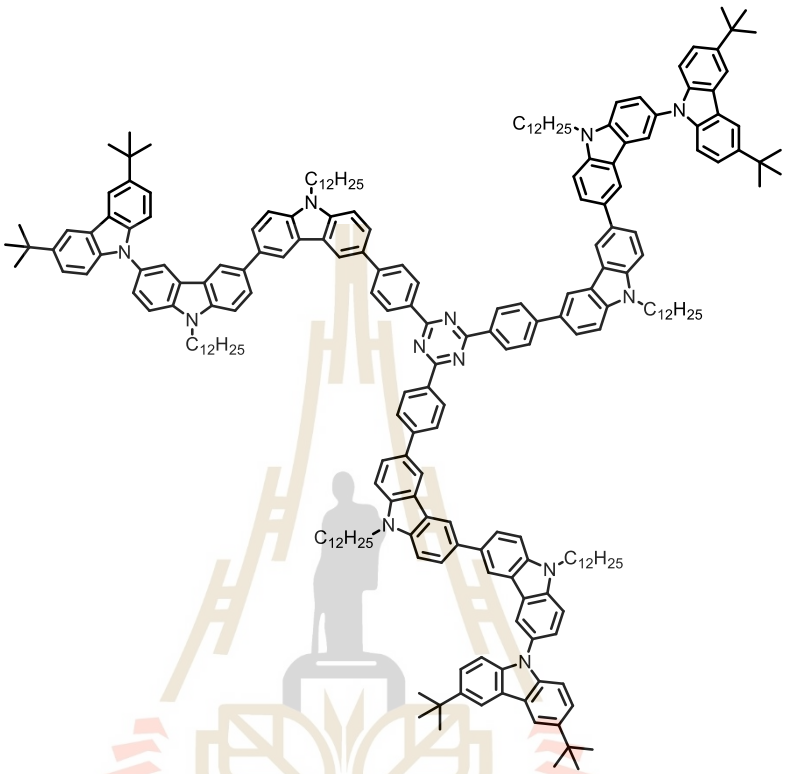

To mixture of 2,4,6-tris(4-bromophenyl)-1,3,5-triazine (0.10g, 0.18mmol), 3",6"-di-tert-butyl-9,9'-didodecyl-6-(4,4,5,5-tetramethyl-1,3,2-dioxaborolane-2-yl)-9*H*,9'*H*-3,3':6',9"-tercarbazole (0.69 g, 0.49 mmol), $Pd(PPh_3)_4$ (0.01 g, 0.01 mmol) and 2 M Na_2CO_3 (25 ml) in THF (25 ml) was degassed with N_2 for 10 min. The mixture was stirred at reflux under N_2 for 24 h. After cooling, water (50 ml) was added, and the mixture was extracted with dichloromethane (3 x 50 ml). The combined organic phase was washed with water (50 ml), brine solution (50 ml), dried with anhydrous Na_2SO_4 and filtered. The solvent was removed to dryness and the crude product was purified by column chromatography on silica gel eluting with a mixture of CH_2Cl_2/hexane gave orange solid (**[diC12-G1]TOX-TPA**) (0.29g, 53%).

CHAPTER III

RESULTS AND DISCUSSION

3.1 Introduction

The general structure of OLEDs consists of a light emissive layer sandwiched in between two metal electrodes, one of which is transparent conducting electrode. Additional layers between the cathode and the emissive layer (electrontransport layer, ETL) or between the anode and the emissive layer (hole transport layer, HTL) is used for high efficiency OLED devices. So, the pioneering works on the first organic light-emitting diodes (OLEDs) by Tang in 1987 (VanSlyke et al., 1987), OLEDs have attracted massive attentions in the scientific community due to their potential for future flat-panel displays and lighting applications (Wu et al., 2005). The past decade has seen great progress in both device fabrication techniques and materials development (Thangtong et al., 2011; Kelley et al., 2004). One of the key developments is the use of hole-transporting layers (HTL) for hole injection from the anode into the light-emitting layer providing significant improvement in the performance of the device (Tang, 1987). As a result, many new hole-transporting materials (HTM) have been developed. In particular, low-molecular weight amorphous materials have received interest as candidates for HTM due to their easy purification by vapor deposition or column chromatographic techniques, and uniformly thin films can be processed simply by coating techniques. The most commonly used amorphous hole-transporting materials

(AHTM) are triarylamine derivatives such as *N*,*N*′-diphenyl-*N*,*N*′-bis(1-naphthyl)-(1,1′-biphenyl)-4,4′-diamine (NPB) and *N*,*N*′-bis(3-methylphenyl)-*N*,*N*′-bis(phenyl) benzidine (TPD) which have excellent hole-transporting properties. However, their low thermal and morphological stability usually lead to their degradation. In order to achieve highly efficient and long lifetime devices, an AHTM with high mobility, a high glass transition temperature (T_g), a stable amorphous state and good thin film formation is desirable. To optimize all these requirements, many efforts have been devoted to the synthesis of new AHTM. Carbazole derivatives containing peripheral diarylamine, additional carbazole, bis(4-*tert*-butylphenyl)carbazole units and dipyrenyl units were also reported to exhibit good thermal and morphological stability. Recently, we synthesized a series of aromatic compounds with peripheral triphenylamine-carbazole possessing high T_g (121 - 185 °C) values and found the OLED devices based on the resulting carbazole compounds to be promising in terms of device performance and stability. Undoubtedly, it is very attractive to explore and develop new carbazole derivatives that meet the requirements as AHTM for OLEDs and which can be synthesized using simple and low-cost methods. Our design involved multiple substitution of the carbazole ring with triphenylamine moieties. With this molecular architecture, amorphous hole-transporting materials would be achieved (Kochapradist et al., 2012).

In 2011, Deng et al. (Deng et al., 2011) investigated that the TPA-containing linear D-A-D molecules with benzothiadiazole (**BT**) as acceptor unit and TPA-(4-hexyl) thiophene (**TPA-HT**) and TPA-(4-hexyl)thieno[3,2-b]thiophene (**TPA-HTT**) as donor units, **TPA-HT-BT** and **TPA-HTT-BT**, gave an overall conversion efficiency

(η) of 1.44%. The design of the molecular structure was from the following consider-anions:

(1) the D-A-D structure of the molecules is to reduce the band gap of the materials for improving the absorption;

(2) (4-hexyl)thieno[3,2-b]thiophene is introduced in **TPA-HTT-BT** for enhancing the hole mobility and improving absorption of the compounds, because fused thiophenes usually show larger pconjugation and higher hole mobility.

TPA-HT-BT and **TPA-HTT-BT** films show broad absorption band in the range of 350–700 nm, lower band gap and good thermal stability. The solution processed bulk-heterojunction OSC devices based on the blend of **TPA-HT-BT** or **TPA-HTT-BT** as donor and PC70BM as acceptor (the weight ratio of donor/acceptor is 1:3), reached 1.44% under the illumination of AM1.5 G, 100 mW/cm^2, which indicates that **TPA-HT-BT** and **TPAHTT-BT** are promising organic donor photovoltaic materials.

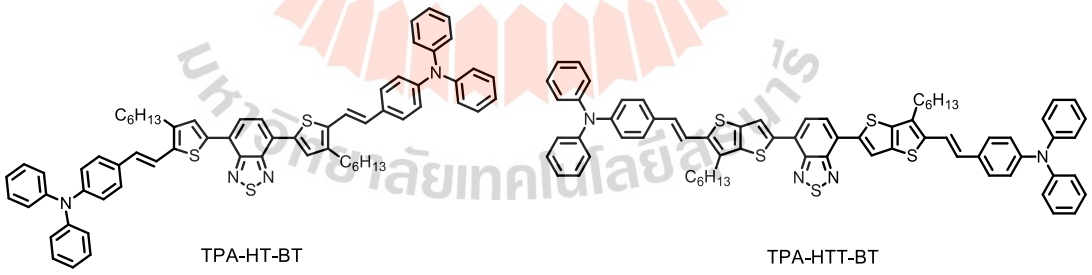

TPA-HT-BT TPA-HTT-BT

Recent studies revealed that organic multilayer structures typically enhance the performance of the devices by lowering the barrier for hole injection from the anode and by enabling control over the electron-hole recombination region, moving it from the organic/cathode interface, where the defect density is high, into the bulk. Hence, the layer deposited on the anode would generally be a good hole transport material (HTM),

providing HTL. Similarly, the organic layer in contact with the cathode would be the optimized ETL (Adachi et al., 1988; Deshpande et al., 1999; Zhang et al., 2009).

3.2 Synthesis and characterization trialyamines substituted bis (hexyl-thiophene-2-yl)-benzothiadiazoles as solution-processable hole-transporting red emitters for efficient non-doped electroluminescent device

3.2.1 Aim of the study

We accomplished the synthesis of red light emitting materials based on benzothiadiazole bearing hexylthiophene and triphenylamine end-capped for using as emitters in optoelectronic devices. Luminescence materials consist of triphenylamine moiety as the electron donor group. Here, hexylthiophene was incorporated for extened π-conjugation and good electron delocalize trough planar structure and to have better solubility for easier device fabrication. Besides of this, two hexyl groups could inevitably decrease the intermolecular interaction and approach higher emission efficiency in solid states. Therefore, the objectives of this chapter are following:

1. To designs and synthesize red-light emitting molecules (**BTZ1-4** molecules shown Figure 3.1) by a combination of Bromination, Iodination, and Suzuki cross coupling reactions.

2. To characterize the synthesized red-light emitting materials by NMR and MALDI-TOF techniques.

3. To study the photophysical, electrochemical and thermal property of the synthesized target compound by UV-Vis, fluorescent, cyclic voltammetry and thermal gravimetric analysis technique, respectively.

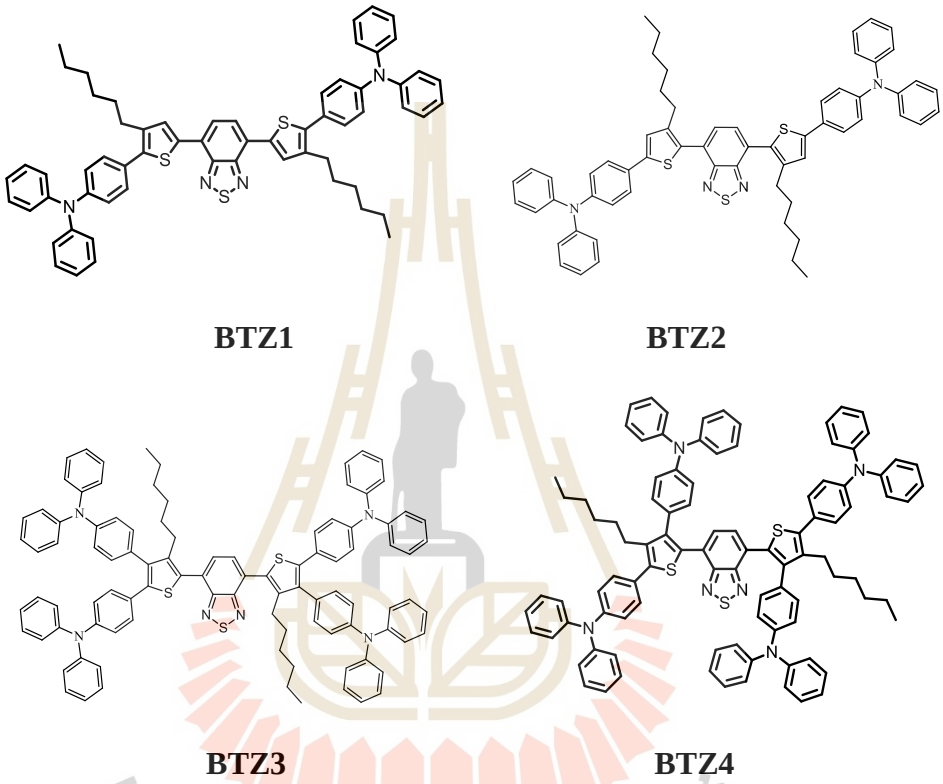

Figure 3.1 Show structure of target red-light emitting molecules (**BTZ1-4**).

3.2.2 Results and Discussion

3.2.2.1 Synthesis

The synthesis of all trialylamines substituted 4,7 bis(hexylthiophene-2-yl)-benzothidiazoles **BTZ1-4**. Firstly, the Suzuki coupling of dibromobenzothidiazoles with 3-hexylthiophene borolanes in the presence of $Pd(PPh_3)_4$ as catalyst and Na_2CO_3

as a base in THF as a solvent reflux for 24 h to give (3-hexylthiophen-2-yl)-benzothiazole core **2** as orange solids in 97% yield as outlined in Figure 3.2.

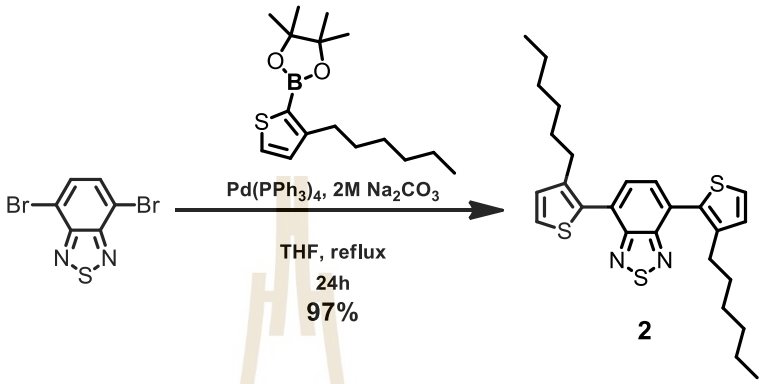

Figure 3.2 Synthesis of (3-hexylthiophen-2-yl)-benzothiazole core **2**.

The chemical structure of (3-hexylthiophen-2-yl)-benzothiazole core **2** was confirmed by ^{1}H-NMR and ^{13}C-NMR. The ^{1}H-NMR spectrum (shown in Figure 3.3) of shows high field shifted at aromatic region of the compound **2** shows a singlet signal at chemical shift 7.65 ppm (2H) assigning of 2-H proton of benzothiadiazole and a doublet signal at chemical shift 7.44 ppm (2H) assigning of 2-H proton of thiophene and low field shifted at alkyl region of the alkyl group as a triplet signal at chemical shift 2.67 ppm (4H) assigning of 4-H proton.

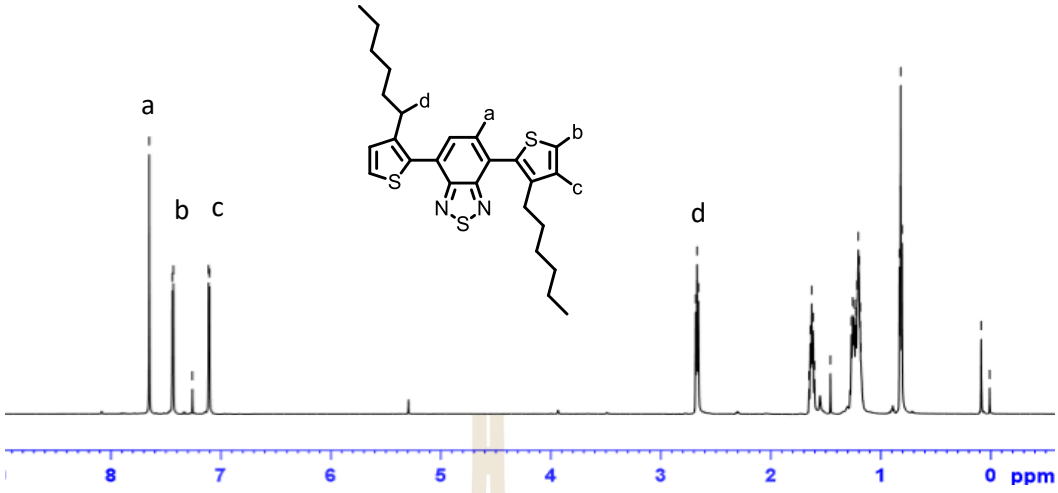

Figure 3.3 The ^{1}H-NMR spectra in $CDCl_3$ of (3-hexylthiophen-2-yl)benzothiazole core **2**.

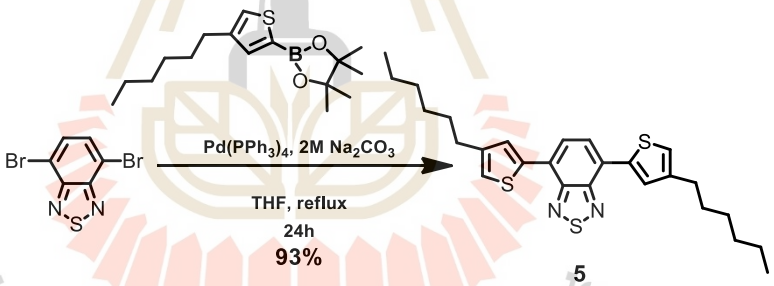

Figure 3.4 Synthesis of (4-hexylthiophen-2-yl)-benzothiazole core **5**.

The intermediate (4-hexylthiophen-2-yl)benzothiazole core **5** was accomplished by Suzuki coupling of dibromobenzothidiazoles with 4-hexylthiophene borolanes in the presence of $Pd(PPh_3)_4$ as catalyst and Na_2CO_3 as a base in THF as a solvent reflux for 24 h to give (4-hexylthiophen-2-yl)-benzothiazole core **5** as orange solids in 93% yield as shown in Figure 3.4.

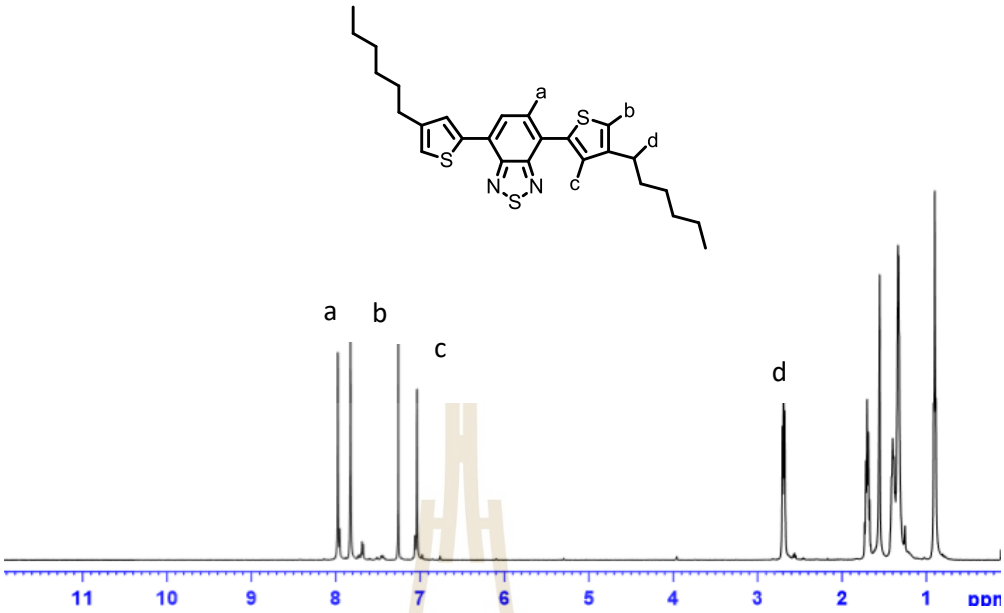

Figure 3.5 The ^{1}H-NMR spectra in $CDCl_3$ of (3-hexylthiophen-2-yl)benzothiazole core **5**.

The chemical structure of (4-hexylthiophen-2-yl)-benzothiazole core **5** was confirmed by ^{1}H-NMR and ^{13}C-NMR. The ^{1}H-NMR spectrum (shown in Figure 3.5) of shows high field shifted at aromatic region of the compound 5 shows a singlet signal at chemical shift 7.97 ppm (2H) assigning of 2-H proton of benzothiadiazole and a singlet signal at chemical shift 7.82 ppm (2H) assigning of 2-H proton of thiophene and a singlet signal at chemical shift 7.03 ppm (2H) assigning of 2-H proton of thiophene and low field shifted at alkyl region of the alkyl group as a triplet signal at chemical shift 2.69 ppm (4H) assigning of 4-H proton.

Subsequently, the intermediate compound **3** was prepared form bromination of (3-hexylthiophen-2-yl)benzothiazole core 2 with NBS in THF and obtained as orange solids 95% yield as shown in Figure 3.6.

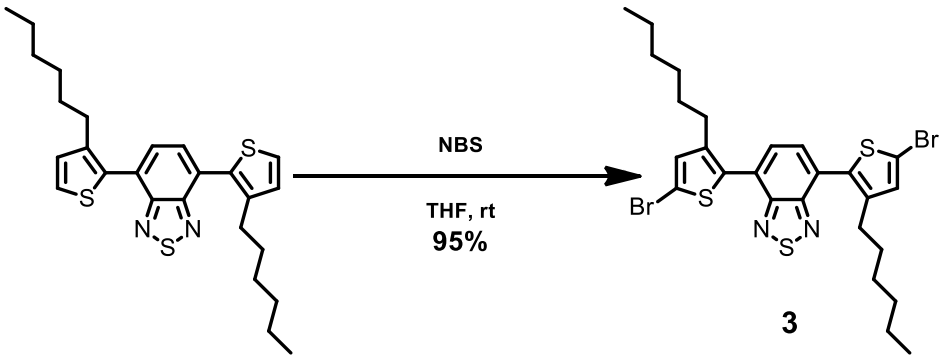

Figure 3.6 Synthesis of compound **3**.

The chemical structure of compound **3** was confirmed by ^{1}H-NMR analysis. The ^{1}H-NMR spectrum of shows high field shifted at aromatic region of the compound **3** (shown in Figure 3.7) as a singlet signal at chemical shift 7.60 ppm (2H) assigning of 2-H proton of benzothiadiazole and a singlet signal at chemical shift 7.05 ppm (2H) assigning of 2-H proton of thiophene and missing 2H-proton one peak of thiophene and low field shifted at alkyl region of the alkyl group as a triplet signal at chemical shift 2.67 ppm (4H) assigning of 4-H proton.

มหาวิทยาลัยเทคโนโลยีสุรนารี

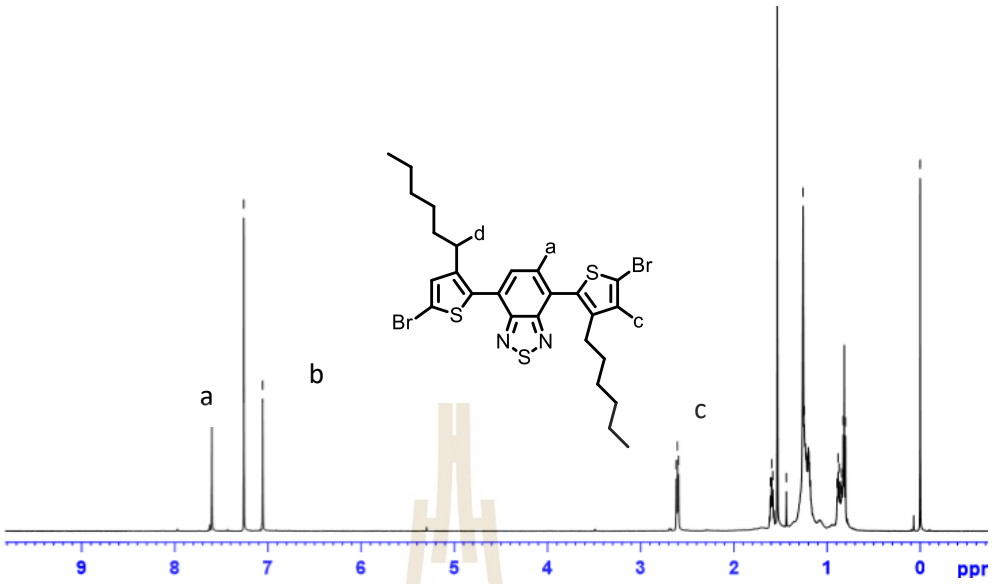

Figure 3.7 The ^{1}H-NMR spectra in $CDCl_3$ of compound **3**.

The Suzuki coupling between compound **3** with (4-(diphenylamino)phenyl) boronic acid in the presence of $Pd(PPh_3)_4$ as catalyst and Na_2CO_3 as a base in THF as a solvent reflux for 24 h to give **BTZ1** in 73% yield as shown in Figure 3.8.

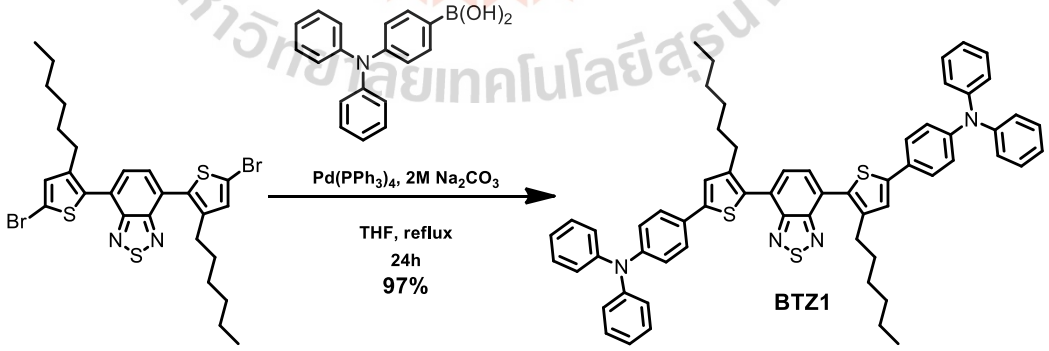

Figure 3.8 Synthesis of final product **BTZ1**.

The chemical structure of final product **BTZ1**. was confirmed by ^{1}H-NMR analysis. The ^{1}H-NMR spectrum of shows high field shifted at aromatic region of the final product **BTZ1**. (shown in Figure 3.9) as a singlet signal at chemical shift 7.60 ppm (2H) assigning of 2-H proton of benzothiadiazole and a singlet signal at chemical shift 7.05 ppm (2H) assigning of 2-H proton of thiophene and missing 2H-proton one peak of thiophene and low field shifted at alkyl region of the alkyl group as a triplet signal at chemical shift 2.67 ppm (4H) assigning of 4-H proton.

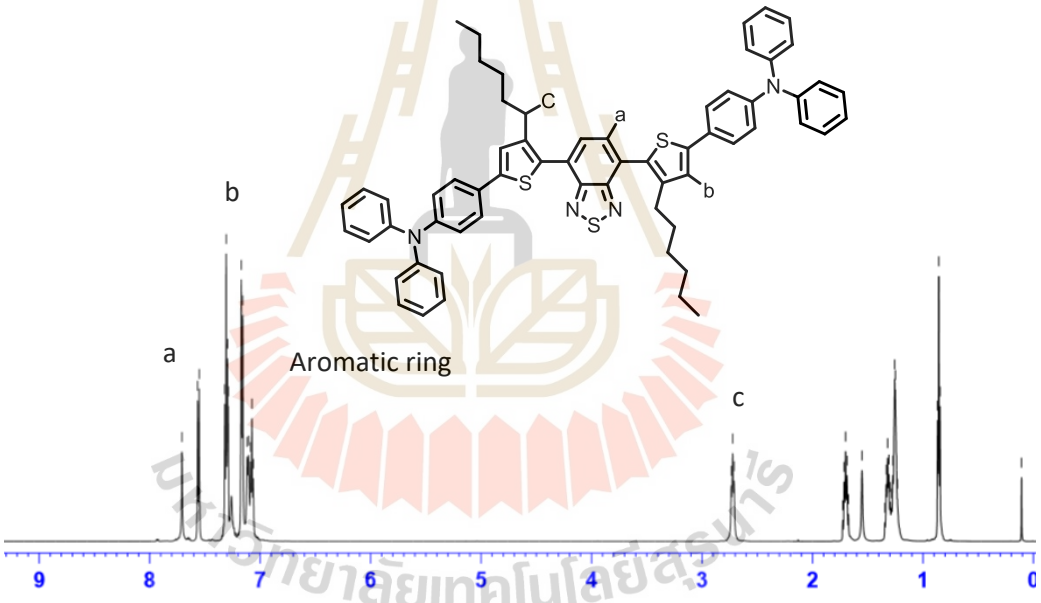

Figure 3.9 The ^{1}H-NMR spectra in $CDCl_3$ of **BTZ1**.

Subsequently, the intermediate compound **4** was prepared form bromination of compound 3 with NBS in THF and obtained as orange solids 73% yield as shown in Figure 3.10.

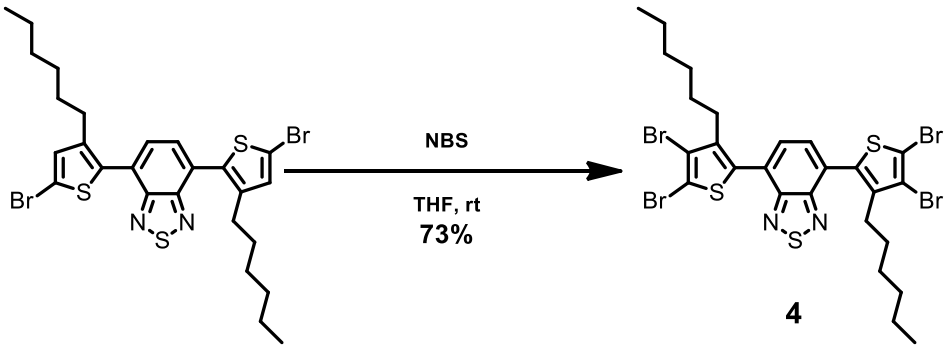

Figure 3.10 Synthesis of compound **4**.

The chemical structure of compound **4** was confirmed by ^{1}H-NMR analysis. The ^{1}H-NMR spectrum of shows one peak as high field shifted at aromatic region of the compound 4 (shown in Figure 3.11) as a singlet signal at chemical shift 7.64 ppm (2H) assigning of 2-H proton of benzothiadiazole and missing 2H-proton one peak of thiophene compare with ^{1}H-NMR spectrum of compound **3** and low field shifted at alkyl region of the alkyl group as a triplet signal at chemical shift 2.69 ppm (4H) assigning of 4-H proton.

มหาวิทยาลัยเทคโนโลยีสุรนารี

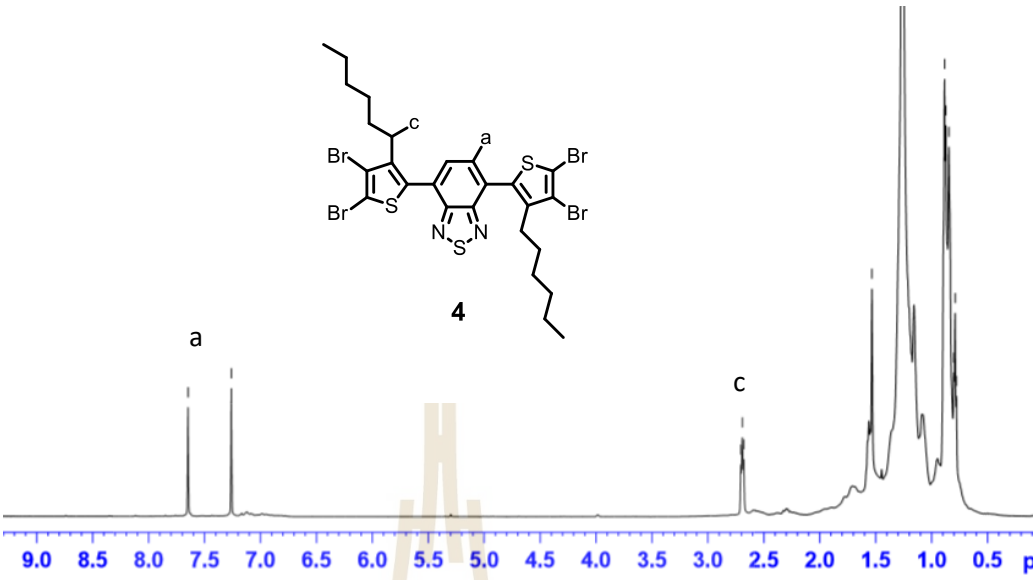

Figure 3.11 The ^{1}H-NMR spectra in $CDCl_3$ of compound **4**.

The synthesis of the final product **BTZ2** was started with compound **4** react with (4-(diphenylamino) phenyl) boronic acid in the presence of $Pd(PPh_3)_4$ as catalyst and Na_2CO_3 as a base in THF as a solvent reflux for 24 h to give dark red solids **BTZ2** in 64% yield as shown in Figure 3.12.

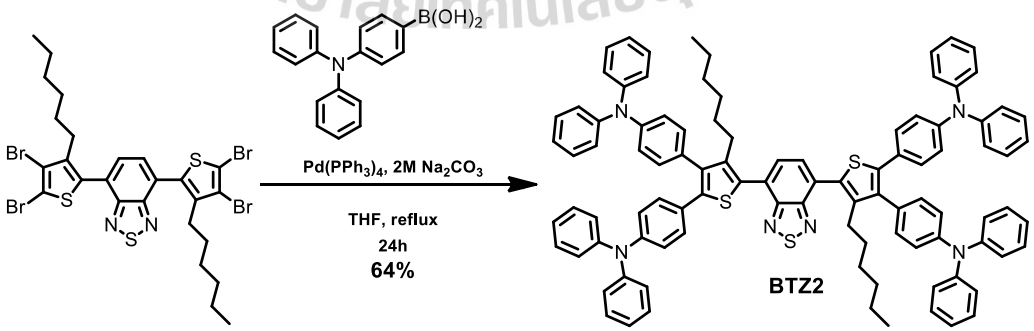

Figure 3.12 Synthesis of final product **BTZ2**.

The chemical structure of final product **BTZ2** was confirmed by ^{1}H-NMR analysis. The ^{1}H-NMR spectrum of shows high field shifted at aromatic region of the final product **BTZ2** (shown in Figure 3.13) as a singlet signal at chemical shift 7.75 ppm (2H) assigning of 2-H proton of benzothiadiazole and a quartet, doublet, singlet signal at chemical shift between 7.24 - 6.92 ppm (56H) assigning of 2-H proton of -(diphenylamino)phenyl group and low field shifted at alkyl region of the alkyl group as a triplet signal at chemical shift 2.62 ppm (4H) assigning of 4-H proton.

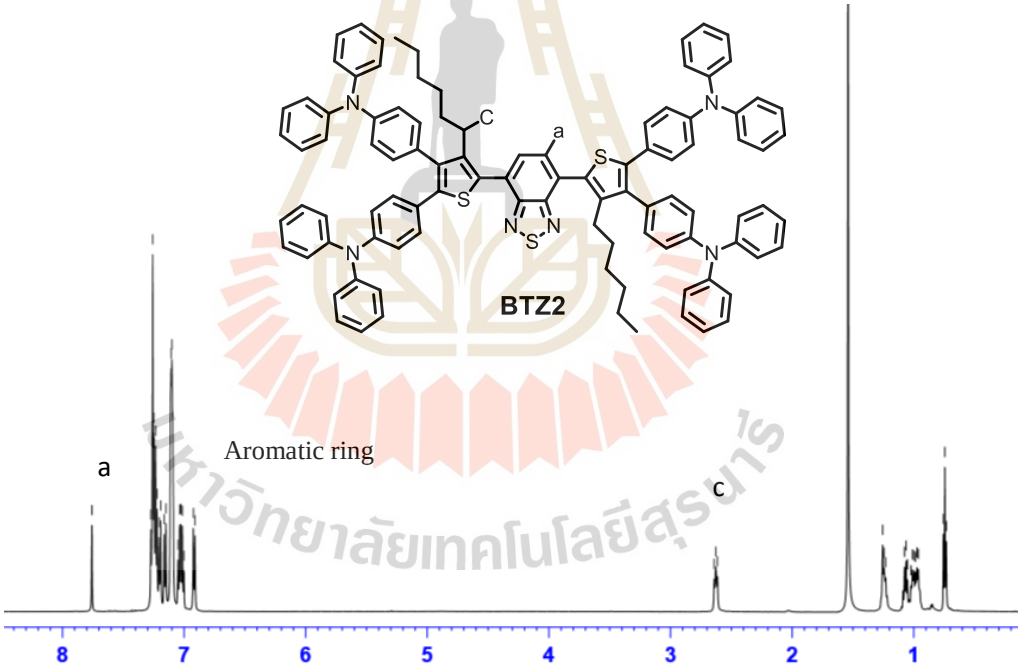

Figure 3.13 The ^{1}H-NMR spectra in $CDCl_3$ of final product **BTZ2**.

The introduction of compound **6** moiety was proceeded under bromination reaction between compound **5** and NBS in THF at room temperature to give compound **6** as orange-red solids compound **6** in 98% yield shown in Figure 3.14.

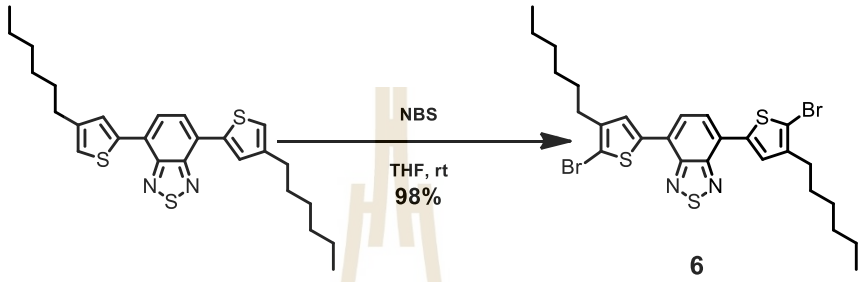

Figure 3.14 Synthesis of compound **6**.

The chemical structure of compound **6** was confirmed by ^{1}H-NMR analysis. The ^{1}H-NMR spectrum of shows high field shifted at aromatic region of the compound **6** (shown in Figure 3.15) as a singlet signal at chemical shift 7.75 ppm (2H) assigning of 2-H proton of benzothiadiazole and a singlet signal at chemical shift 7.70 ppm (2H) assigning of 2-H proton of thiophene and low field shifted at alkyl region of the alkyl group as a triplet signal at chemical shift 2.61 ppm (4H) assigning of 4-H proton.

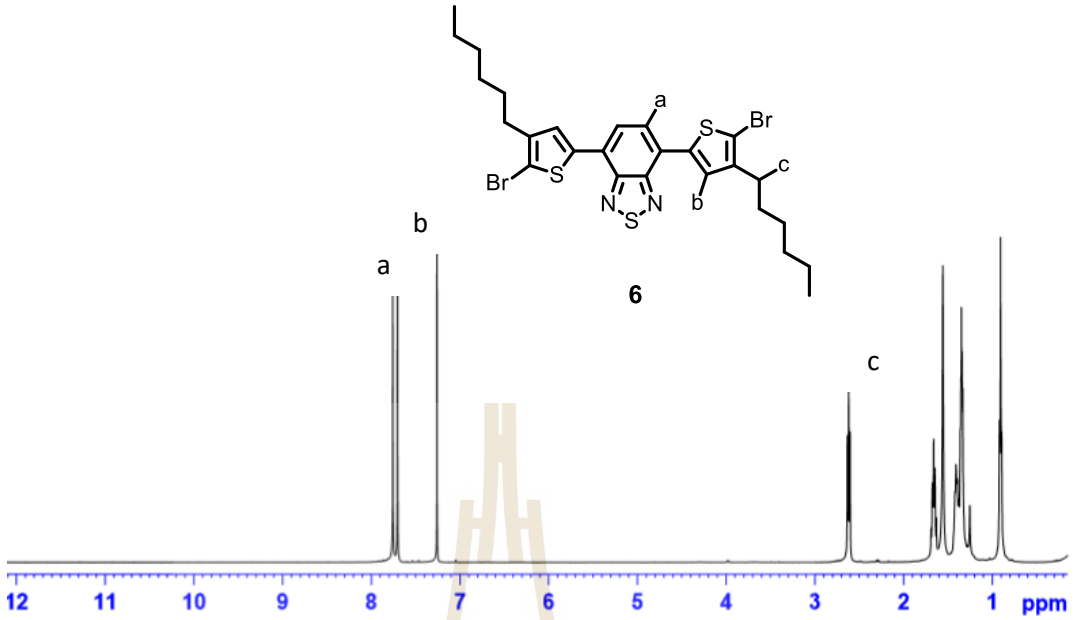

Figure 3.15 The ^{1}H-NMR spectra in $CDCl_3$ of compound **6**.

Compound **7** was prepared from bromination of compound **6** with NBS in THF at room temperature to give orange-red solids compound **7** in 78% yield shown in Figure 3.16.

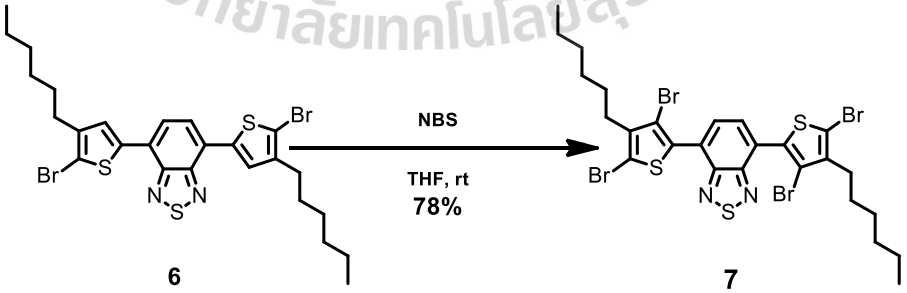

Figure 3.16 Synthesis of compound **7**.

The chemical structure of compound **7** was confirmed by ^{1}H-NMR analysis. The ^{1}H-NMR spectrum of shows one peak as high field shifted at aromatic region of the compound **7** (as shown in Figure 3.17) as a singlet signal at chemical shift 8.06 ppm (2H) assigning of 2-H proton of benzothiadiazole and missing 2H-proton one peak of thiophene compare with ^{1}H-NMR spectrum of compound **6** and low field shifted at alkyl region of the alkyl group as a triplet signal at chemical shift 2.75 ppm (4H) assigning of 4-H proton.

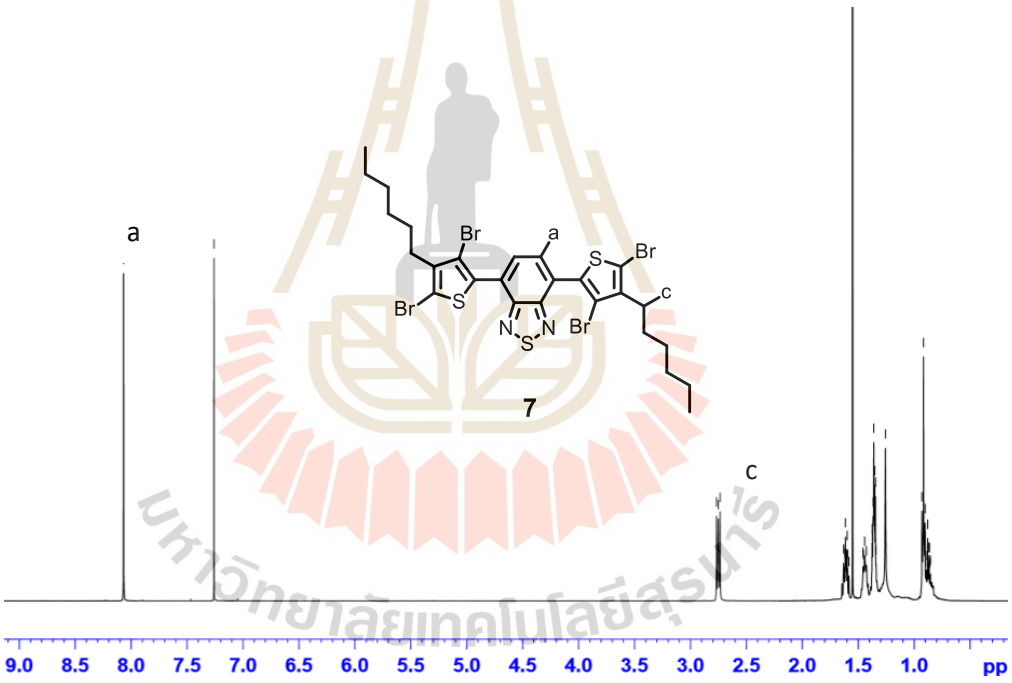

Figure 3.17 The ^{1}H-NMR spectra in $CDCl_3$ of compound **7**.

The Suzuki cross coupling between compound **6** react with (4-(diphenylamino) phenyl) boronic acid n the presence of $Pd(PPh_3)_4$ as catalyst and Na_2CO_3 as a base in THF as a solvent reflux for 24 h to give dark red solids **BTZ3** in 90% yield as shown in Figure 3.18.

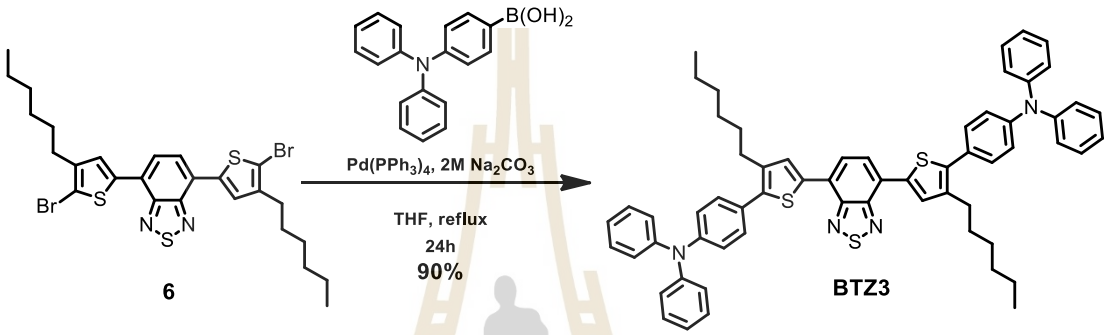

Figure 3.18 Synthesis of final product **BTZ3**.

The chemical structure of final product **BTZ3** was confirmed by ^{1}H-NMR analysis. The ^{1}H-NMR spectrum of shows high field shifted at aromatic region of the final product **BTZ3** (as shown in Figure 3.19) as a singlet signal at chemical shift 7.70 ppm (2H) assigning of 2-H proton of benzothiadiazole and a doublet signal at chemical shift 7.56 ppm (2H) assigning of 2-H proton of thiophene and multiplet signal between 7.32 - 7.07 ppm (26H) as sinning of 26-H proton of (diphenylamino)phenyl group and low field shifted at alkyl region of the alkyl group as a triplet signal at chemical shift 2.72 ppm (4H) assigning of 4-H proton.

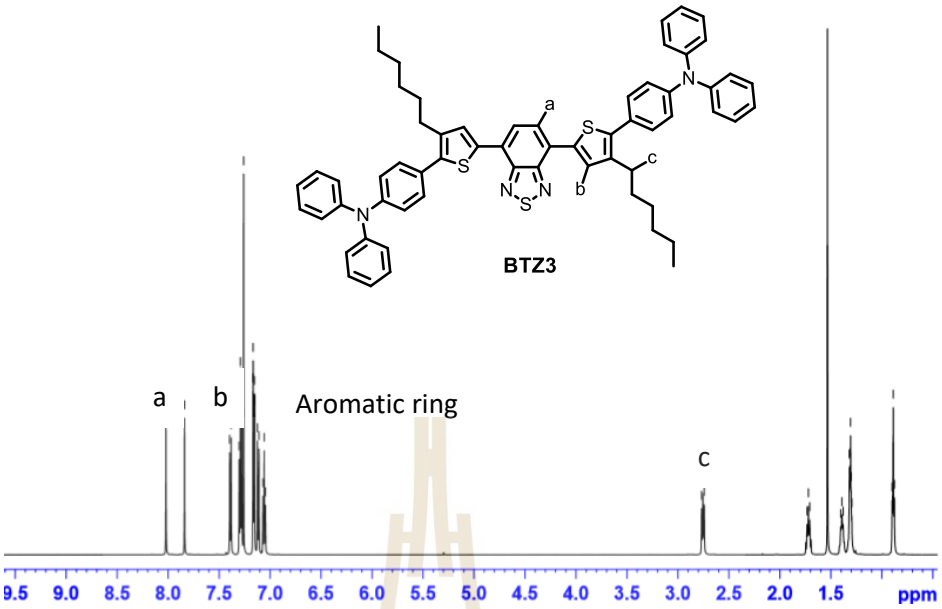

Figure 3.19 The ^{1}H-NMR spectra in $CDCl_3$ of final product **BTZ3**.

The synthesis of the final product **BTZ4** was started with compound **7** react with (4-(diphenylamino)phenyl)boronic acid in the presence of $Pd(PPh_3)_4$ as catalyst and Na_2CO_3 as a base in THF as a solvent reflux for 24 h to give red solids **BTZ4** in 53% yield as shown in Figure 3.20.

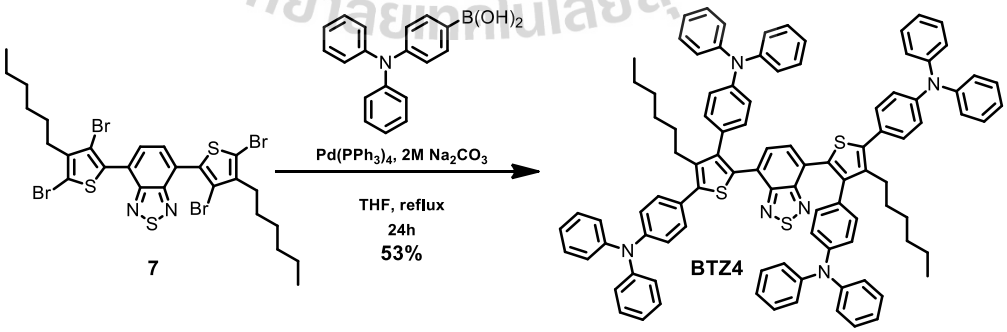

Figure 3.20 Synthesis of final product **BTZ4**.

The chemical structure of final product **BTZ4**. was confirmed by ^{1}H-NMR analysis. The ^{1}H-NMR spectrum of shows high field shifted at aromatic region of the final product **BTZ4**. (as shown in Figure 3.21) as a singlet signal at chemical shift 8.02 ppm (2H) assigning of 2-H proton of benzothiadiazole and aromatic region of (diphenylamino)phenyl group as shown single, doublet, doublet of doublet, singlet, and multiplet signal at chemical shift between 7.83 - 7.05 ppm (56H) assigning of 2-H proton of (diphenylamino)phenyl group and low field shifted at alkyl region of the alkyl group as a triplet signal at chemical shift 2.75 ppm (4H) assigning of 4-H proton.

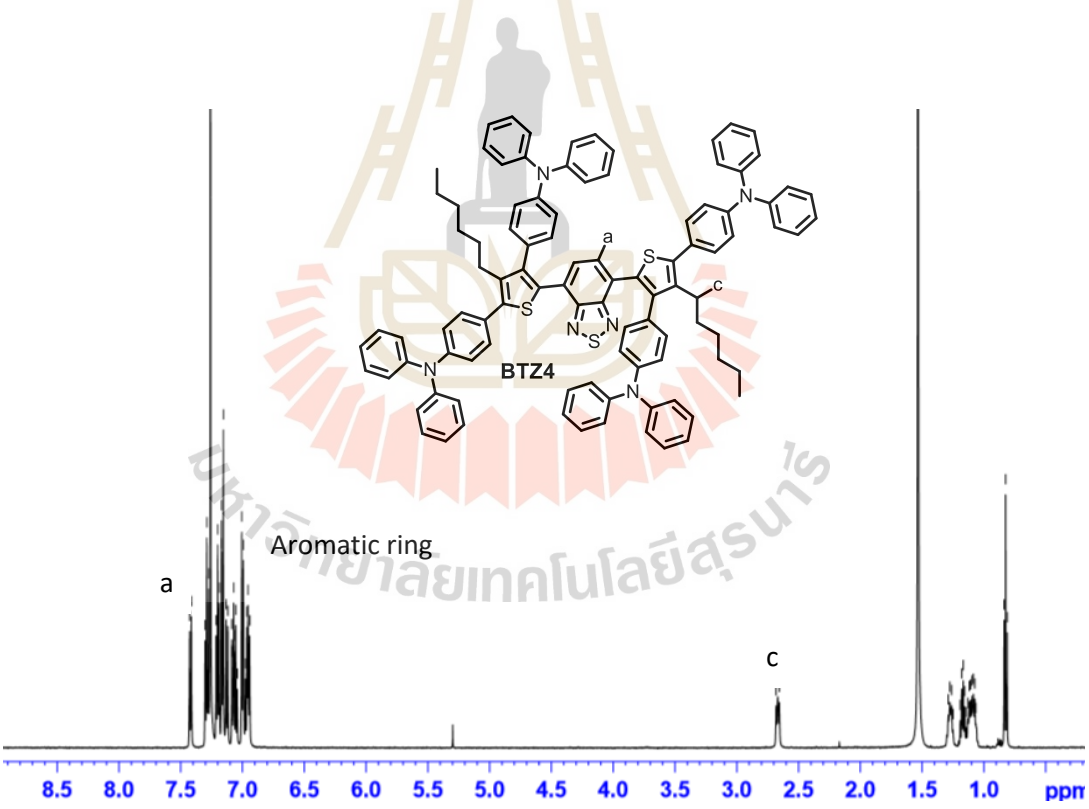

Figure 3.21 The ^{1}H-NMR spectra in $CDCl_3$ of final product **BTZ4**.

3.2.2.2 Theoretical Calculation

To gain insight into the structure-property relationships of the new compounds **BTZ1-6**, density functional theory (DFT) calculation were conducted at the TD-DFT B3LYP/6-31G(d,p) level in CH_2Cl_2. In the optimized structures of these compounds (Figure 3.22), It was clearly observed that introduction of hexly or/and triarylamine groups on 3- and 4- position of thiophene unit could enhance the distortion degree in the bis(thiophene-2-yl)-benzothiadiazole core and bulkiness of molecule. These could help suppress the formation of aggregation or π-π stacking and maintain high quantum yield in the solid state. The large dihedral angles in the range of 53 - 59° were found between thiophene and benzole thiadiazole core when the thiophene ring were substituted on 3- position (**BTZ1-2**) and disubstituted on both 3- and 4- position (**BTZ3** and **BTZ4**) such large twist angles can interrupt intramolecular extending of π-electron in the molecule, which whould result in a blue-shift in absorption and emission spectra. However, single hexyl substitution on 4-position of thiophene ring (**BTZ4** and **BTZ5**) caused much less twist of the bis(hexylthiophene-2-yl)-benzothiadiazole plane with dihedral angles in the scope of 7° - 8°.

มหาวิทยาลัยเทคโนโลยีสุรนารี

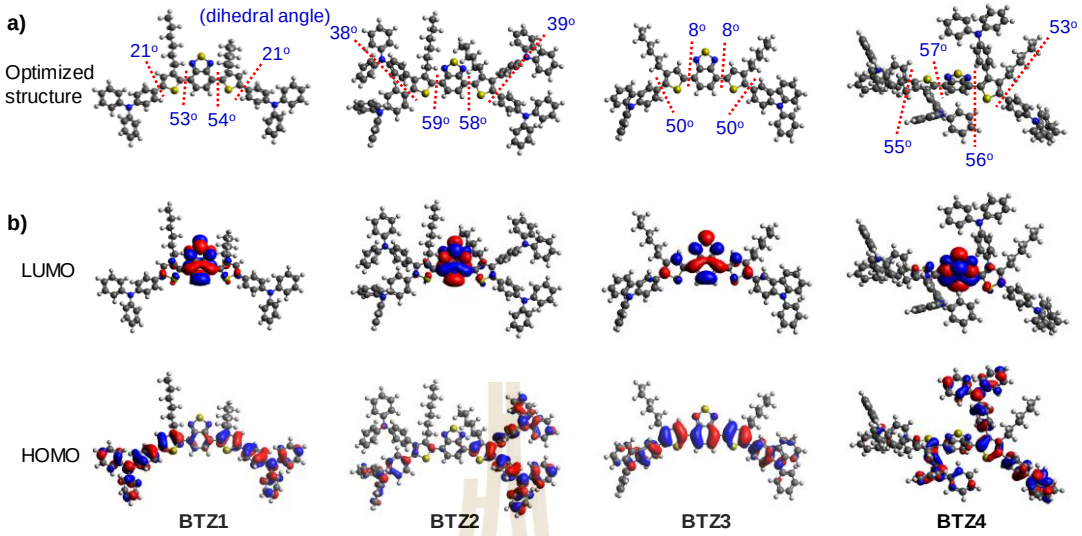

Figure 3.22 The optimized structures with dihedral angle, HOMOs and LUMOs of **BTZ1-4** calculated by TD-DFT B3LYP/6-31G(d,p) in CH_2Cl_2.

In addition, all molecules showed the moderate to large dihedral angles between the thiophene and end-capped traiarylamine planes, however this would not make much diffidence on their properties. Figure 3.22b shows the spatial distributions of HOME and LUMO for **BTZ1-4**. The LUMOs of all compound mostly locate on electron deficient benzothiadiazole unit. The HOMEs of **BTZ1-3** delocalize on the triarylamine donor and the adjacent thiophene ring with little residual on the benzothiadiazole. Besides, the HOMOs of **BTZ4** can spread over the entire π- conjugation backbone due to much smaller twist angle between the thiophene unit and benzothiadiazole plane. The HOMO and LUMO of all compounds are well separated which could contribute to ICT process.

3.2.2.3 Photophysical Properties

The UV-Vis absorption and PL spectra of **BTZ1-4** were analyzed in solution and thin film spin coated on fused silica substrates. The results are plotted in Figure 3.23a-c and the key parameters. The results are listed in Table 3.1. As shown in Figure 3.23(1a), solution UV-Vis absorption spectra exhibited two main absorption band (λ_{abs}): absorption bands at the scope of 300 - 354 nm derive from the π-π transition of the triarylamine-thiophene conjugations and the longer wavelength absorption bands at around 463 - 511 nm could be recognized as intramolecular charge transfer (ICT) transition from the triarylamine donor to benzothiadiazole core acceptor. The ICTs of **BTZ4** is more intense and red-shifted compared to those of the remaining compounds, indicating donor-acceptor interactions in these molecules are stronger than others due to more planar alignment of the bis(thiophen-2-yl)-benzothiadiazole backbone. The intensity of the ICTs can be ordered as follows: **BTZ4** > **BTZ1** ≈ **BTZ2** > **BTZ3**, which harmonizes well with the dihedral angles between benzothiadiazole core and the adjacent thiophene rings observed in the theoretical calculation. The solution PL spectra of all compounds showed featureless emission bands in red region with the maximum emission wavelengths (λpl) in the range of 641 - 672 nm. The shift in these emissions coincides well with that of the ICT absorption peaks, suggesting donor-acceptor or ICT characteristic emissions. The ICT was further confirmed by solvatochromism behaviors with the solvent polarity increased under photoexcitation. As illustrated in Figure 1b, the emission peak position (**BTZ4**) was strongly dependence on solvent polarity. The emission band

bathochromically shifted as the solvent polarity was increased from hexane to EtOH. Figure 3.23c shows the UV-Vis absorption and PL spectra of **BTZ1-4** in thin film, which have similar feature to the spectra in solution. It is notable that the emission peaks of **BTZ1-2** and **BTZ4** in the thin film compared to solution show larger red shifts (11 - 21 nm) than those of **BTZ3** (2 nm), suggesting stronger intermolecular interactions in the film state. The relatively slight red shift from the solution to the solid state of **BTZ3** and **BTZ4** undoubtedly results from their more steric molecular structure due to the substitutions on both 3- and 4- positions of the thiophene rings.

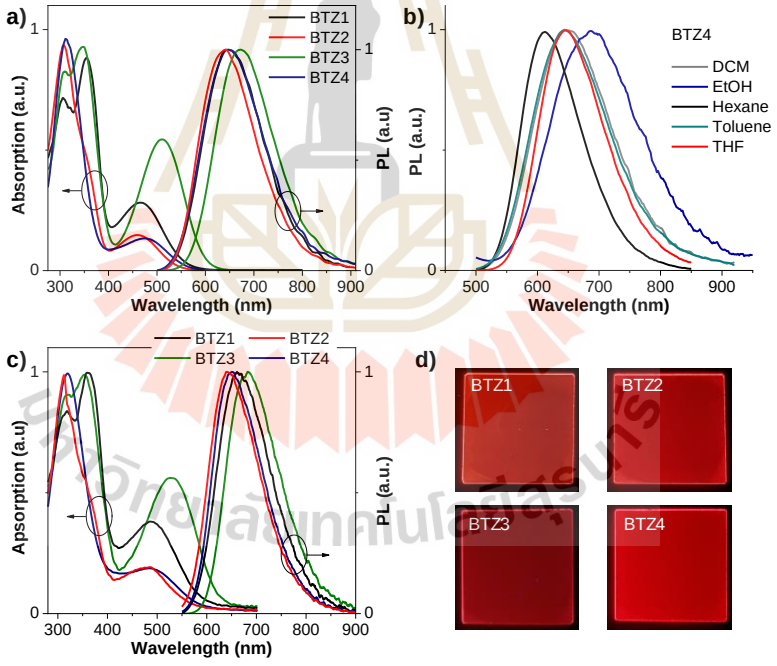

Figure 3.23 UV-vis absorption and PL spectra of **BTZ1-4** in a) CH_2Cl_2 solution and c) as thin films coated on fused silica substrates. b) PL spectra of **BTZ4** in different solvents. d) **BTZ1-4** thin films coated on fused-silica substrates exposure under UV lamp light.

The absolute PL quantum yields (PLQY) of all new compounds in CH_2Cl_2 and solid film were determined by using an integrating sphere and the results are listed in Table 3.1. **BTZ4** and **BTZ2** exhibited solution PLQYs as high as 62 and 52%, respectively, while **BTZ1**, and **BTZ3** showed moderate PLQYs of 32, and 28%, respectively. In solid film, **BTZ2** and **BTZ4** still exhibited high PLQYs in the scope of 51 - 58%, whereas those of the remaining dropped significantly to 5 - 6%. Figure 1d depicts spin-coated thin films of all compounds under UV light illumination showing visually perceivable bright red emission. High PLQYs observed in the thin films of **BTZ2** and **BTZ4** hint that they are promising candidates for red OLED emitters. Additionally, optical band-gap (E_g) of **BTZ1-4** calculated from the onset wavelengths of the thin film absorption bands were 2.21, 2.29, 1.95, and 2.21 eV, respectively (Table 3.1).

3.2.2.4 Thermal properties and morphology

Thermal properties of benzothiadiazole derivatives **BTZ1-4** were examined with TGA and DSC under N_2 flow, as shown in Figure 3.24 and summarized in Table 3.1. In the TGA measurements, all of them show high 5% weight-loss temperatures (T5d) of over 44 °C, indicating high thermal stability materials. The results by DSC (1^{st} and 2^{nd} scan) reveal that **BTZ1**, **BTZ3** and **BTZ4** have amorphous property with only endothermic base line shift corresponding to glass transition temperature (Tg) at 65 °C, 105 °C and 90 °C being detected, respectively, while **BTZ3** is crystalline with only a sharp endothermic peak assigning to melting temperature (Tm) at 198 °C being observed. The DSC traces (1^{st} heating scan) of BTZ2 display glass transition and melting peak, however the subsequent 2^{nd} heating scans exhibit only glass

transition at Tg of 81 °C and 73 °C, respectively, indicating that as prepared samples of **BTZ2** are semi crystalline and then become amorphous after annealing. It was found that the benzothiadiazole derivatives (**BTZ1-3**) hexyl substitution on 4-position of thiophene ring exhibit a higher Tg than that of their corresponding 3-hexylthiophene derivatives (**BTZ4**), and **BTZ3** and **BTZ4** are two high Tg materials in this series. These could come from the more steric structures.

มหาวิทยาลัยเทคโนโลยีสุรนารี

Table 3.1 Key physical data of the new compounds.

Compound	$\lambda_{abs}(\log\varepsilon)^a$(nm)/ $M^{-1}cm^{-1}$	λ_{abs} (nm)^b	λ_{pl} (nm)^a	λ_{pl} (nm)^b	$T_g/T_m/T_{5d}$ (^oC)^c	E_g (eV)^d	HOMO/LUMO (eV)^e	PLQY (%)^a	PLQY (%)^b
BTZ1	354(6.77), 466(6.27)	362, 489	644	665	65/ - /440	2.21	-5.40/-3.29	32	5
BTZ2	307(7.04), 460(6.23)	312, 483	641	643	105/ - /455	2.29	-5.48/-3.19	57	51
BTZ3	348(6.98), 511(6.75)	353, 532	670	681	- /198/462	1.95	-5.32/-3.37	28	6
BTZ4	312(7.06), 481(6.19)	319, 494	648	650	90/ - /470	2.21	-5.45/-3.24	62	58

[a] Measured in solution of CH_2Cl_2. [b] Measured in thin film coated on fused silica substrates.

[c] Measured by DSC (2nd scan) and TGA under N_2 flow.

[d] Estimated from absorption onset in thin film: $E_g = \lambda onset/1240$.

[e] Measured by Riken AC2 and LUMO = HOMO + E_g.

มหาวิทยาลัยเทคโนโลยีสุรนารี

The solid films of **BTZ1-4** could be prepared by solution-spin coating process. The morphology of the thin films was examined by AFM as shown in Figure 3.24. All thin films casting from toluene solution have a smooth and pinhole-free surface, suggesting good film forming ability. In case of **BTZ4**, few small spots were observed that could be due to partial crystallization of the compound in the film.

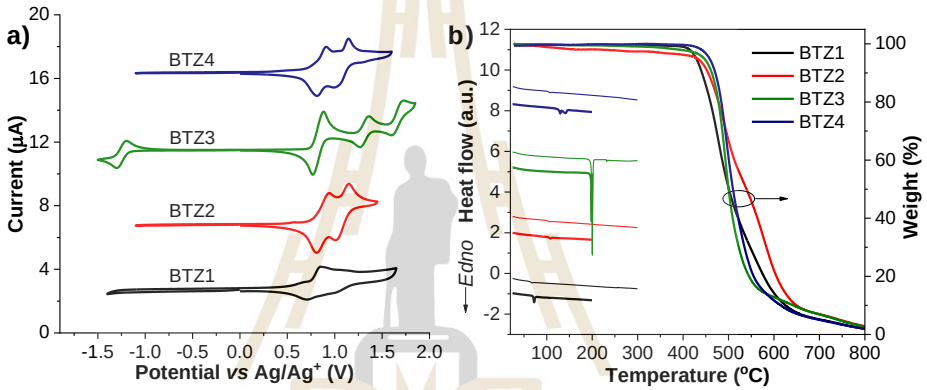

Figure 3.24 a) CV plots measured by and b) DSC (1st heating scan (thick line) and 2nd heating scan (thin line)) and TGA traces of **BTZ1-4**.

3.2.2.5 Electrochemical Properties

To explore the electrochemical properties of **BTZ1-4**, cyclic voltammetry studies were performed. As shown in Figure 3.24, CV traces of all compounds displayed well-defined multiple oxidation processes. The first oxidation wave could be assigned to the oxidation of the electron donating triarylamine moiety. CV curves of **BTZ1-2** and **BTZ3-4** showed single quasi-reversible reduction wave, which corresponds the formation of the anion radical

of the electron-poor benzothiadiazole unit. However, under this measurement conditions, on reduction wave was observed for **BTZ3** and **BTZ4**. Moreover, repeated CV scans of all compounds prove that they are electrochemically stable molecules as identical CV curves being recorded.

The HOMO energy levels of **BTZ1-4** were determined by photoelectron yield spectroscopy (Riken AC-2). The LUMO energy levels were estimated from the HOMO values and the optical band gaps (Eg) by using the equation LUMO = HOMO + Eg. The corresponding HOMO/LUMO energy levels for **BTZ1-4** were then calculated to be -5.40/-3.29 eV, -5.48/-3.19 eV, -5.32/-3.37 eV, and -5.45/ -3.24 eV, respectively (Table 1). The HOMO energy levels (-5.32 - -5. 48 eV) of these new compounds match well with the work function of commonly used PEDOT: PSS coated ITO anode (-5.20 eV), suggesting that they could be used as hole-transporting layer-free red emitters in OLEDs. Their LUMO energy levels (-3.19 - -3.37 eV) are close to the work function of the LiF: Al cathode (-3.10 eV), ensuring efficient electron injection from the cathode.

3.2.2.6 Electroluminescent performances

Based on the mentioned properties, **BTZ4** showing the highest solid PLQY was first preferred to study and optimize EL performances and the solution processed non-doped single layer OLED was fabricated with a configuration of ITO/PEDOT: PSS (40nm)/BTZ4 (60nm)/LiF (0.5nm)/AL (150 nm) (Figure 3.25). In this device, PEDOT: PSS was used as the hole injection layer (HIL) and LiF AS interlayer for enhancing the electron injection.

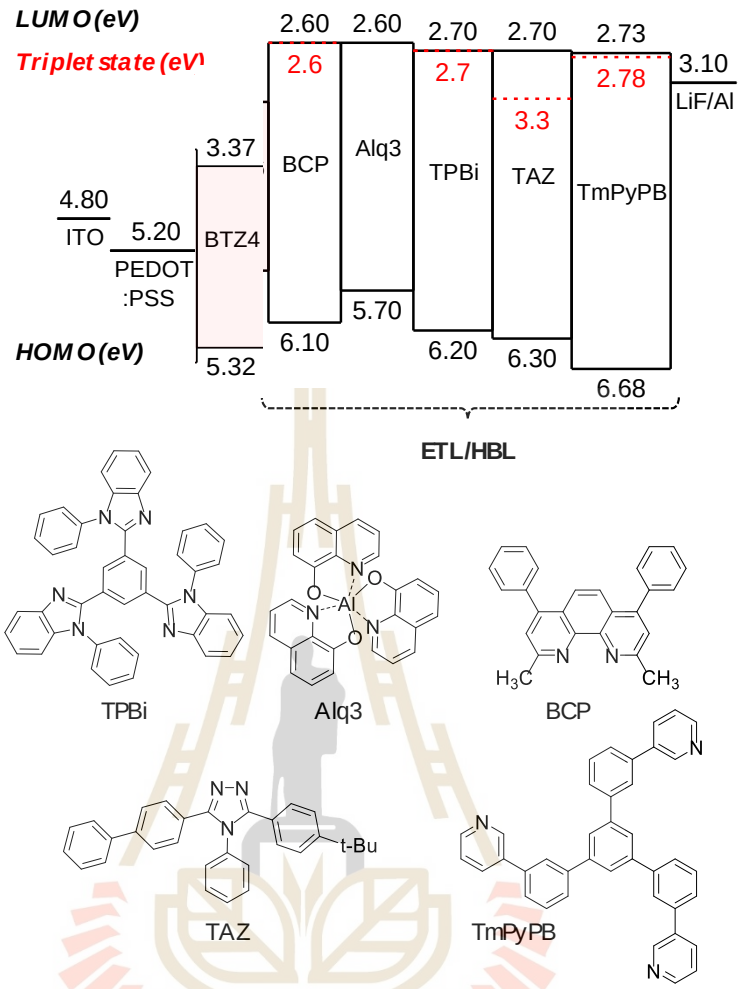

Figure 3.25 The optimize EL performances and the solution processed non-doped single layer OLED was fabricated with a configuration of ITO/ PEDOT: PSS (40nm)/BTZ4 (60nm)/LiF (0.5nm)/AL (150nm).

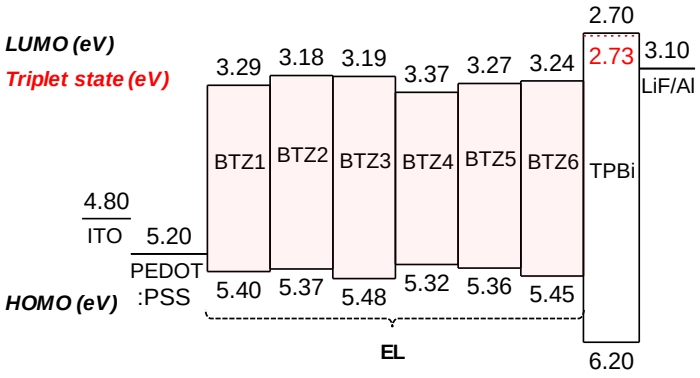

Figure 3.26 Device structures and energy levels (relative to the vacuum energy level) of the materials.

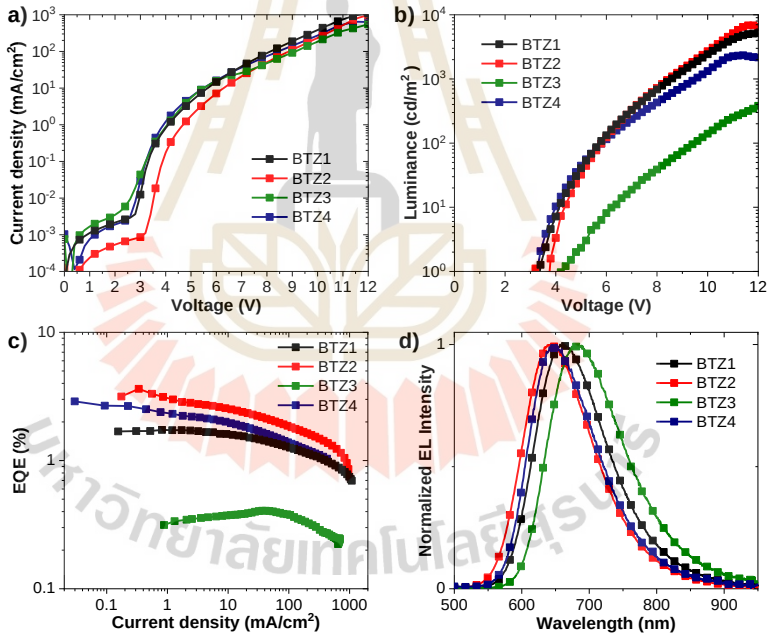

Figure 3.27 a) current density-voltage-luminance (*J-V-L*) plots, b) luminance-current density-voltage (J-V) curves the fabricated OLEDs, c) current density-external quantum efficiency (EQE) plots of the fabricated OLEDs, and d) normalized EL spectra under different applied voltages.

Table 3.2 Performance of devices fabricated with **BTZ4** as EL.

Device[a]	ETL	Von (V)	*L*max/*J*max (cd/m^2)/(mA/cm^2)	λEL (nm)	EQEmax (%) at V	CE (cd/A)[b]	CIE (x,y)
I	-	3.4	287/	652	0.07/5.2	0.03	(0.66, 0.34)
II	BCP(40 nm)	4.9	1518/	643	0.94/7.2	0.66	(0.65, 0.35)
III	BCP(10nm)/Alq3(40 nm)	3.5	2247/	643	0.94/3.4	0.48	(0.54, 0.42)
IV	BCP(20nm)/Alq3(30 nm)	5.1	1934/	644	0.57/7.0	0.34	(0.65, 0.34)
V	TAZ(40nm)	3.8	1040/	644	0.61/8.0	0.32	(0.66, 0.34)
VI	TAZ(30nm)/TPBi(10 nm)	3.8	2073/	644	0.95/6.6	0.61	(0.66, 0.34)
VII	TPBi(10 nm)/TAZ(30nm)	3.5	1449/	645	1.22/4.0	0.73	(0.66, 0.34)
VIII	TPBi(40nm)/TAZ(10nm)	3.6	1007/	649	1.49/4.2	0.75	(0.66, 0.33)
IX	TPBi(50nm)	3.3	2334/636	650	2.66/3.5	0.71	(0.65, 0.34)
X	TmPyPB(60nm)	3.1	2193/	657	1.46/6.0	0.72	(0.67, 0.33)

[a] ITO/PEDOT: PSS(40 nm)/BTZ6(60 nm)/ETL/LiF(0.5 nm):Al(150 nm).

[b] Luminous efficiency at 100 cd/m^2

มหาวิทยาลัยเทคโนโลยีสุรนารี

Table 3.3 Performance of devices fabricated with **BTZ1-4** as EL.

EL	V_{on} (V)	*L*max/*J*max (cd/m^2)/(mA/cm^2)	λ_{EL}(nm)	EQEmax (%) at V	CE (cd/A)[c]	CIE (x,y)
BTZ1[a]	3.4	5148/1086	663	1.73/4.0	0.91	(0.66, 0.33)
BTZ2[a]	3.7	6842/899	648	3.62/4.0	1.73	(0.63, 0.36)
BTZ3[a]	4.1	500/688	686	0.41/7.6	0.08	(0.68, 0.32)
BTZ4[a]	3.3	2334/636	650	2.66/3.5	0.71	(0.65, 0.34)
BTZ2[b]	3.1	2955/415	646	2.78/3.3	1.59	(0.66, 0.33)

[a] ITO/PEDOT: PSS (40 nm)/BTZ1-6(60 nm)/TPBi(50 nm)/ LiF(0.5 nm):Al(150 nm).

[b] ITO/PEDOT: PSS (40 nm)/BTZ3(60 nm)/TmPyPB(50 nm)/LiF(0.5 nm):Al(150 nm).

[c] Luminous efficiency at 100 cd/m^2.

มหาวิทยาลัยเทคโนโลยีสุรนารี

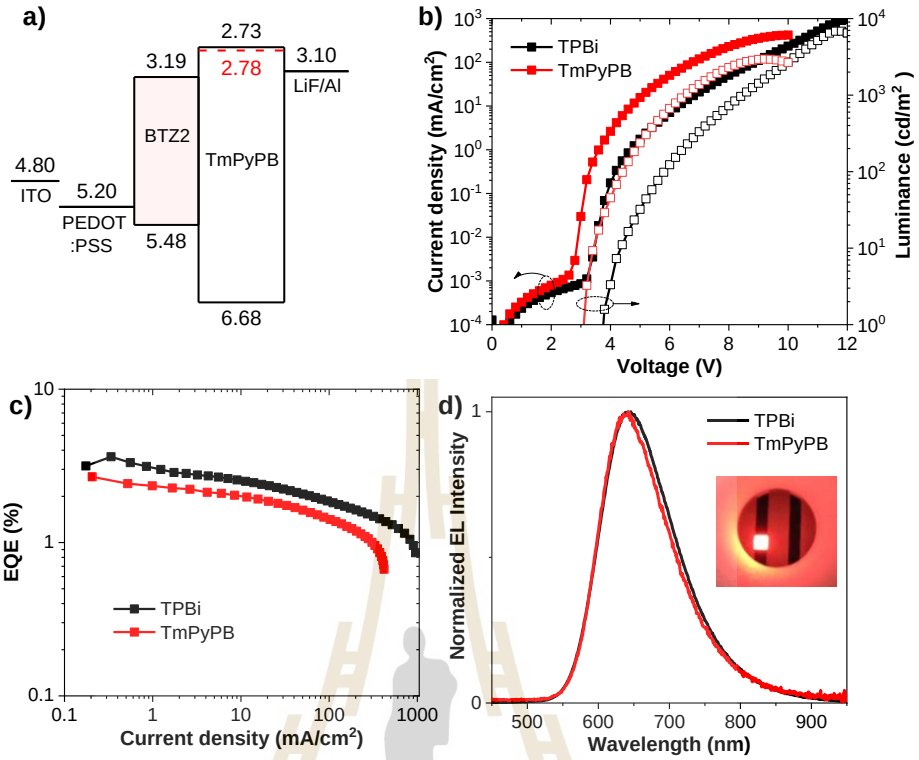

Figure 3.28 a) Device structures and energy levels (relative to the vacuum energy level) of the materials used, b) current density-voltage-luminance (*J-V-L*) plots, c) luminance efficiency-current density-external quantum efficiency (LE-J-EQE) plots of the fabricated OLEDs), and d) normalized EL spectra (Insert: photographs of the OLED devices).

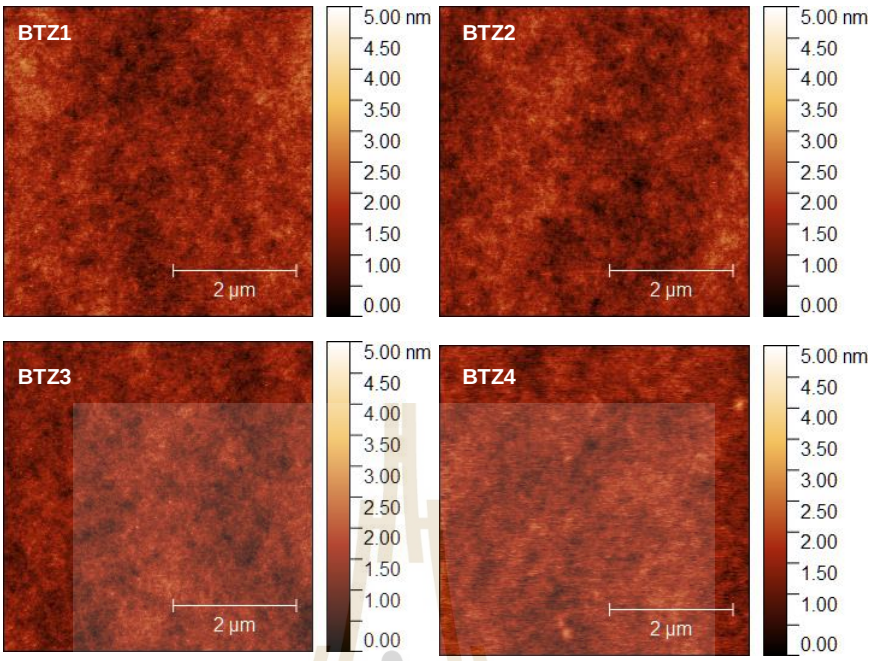

Figure 3.29 AFM images of the thin film of **BTZ1**, **BTZ2**, **BTZ3** and **BTZ4** 20wt% doped in the CBP host.

3.3 High efficiency solution-processed NIR OLEDs based on sample oligosthiophene benzothiadiazoles

3.3.1 Aim of the study

In this part, we report the synthesis NIR OLEDs based on sample molecules oligosthiophene and benzothiadiazoles. Both 4,7-positions of benzothiadiazole were occupied with hexylthiophene and (diphenylamino)phenyl group. Here, thiophene was incorporated for extended π-conjugation by adding more unit and good electron delocalize trough planar structure, while (diphenylamino)phenyl has the common hole transporting property. Two hexyl groups in **TBtz1-2** compounds were introduced at 4-position of thiophene in order to have better solubility for easier device fabrication.

Besides of this, introducing two hexyl groups could inevitably decrease the intermolecular interaction and approach higher emission efficiency in solid states. The target molecules **TBtz1** and **TBtz2** shown in Figure 3.30.

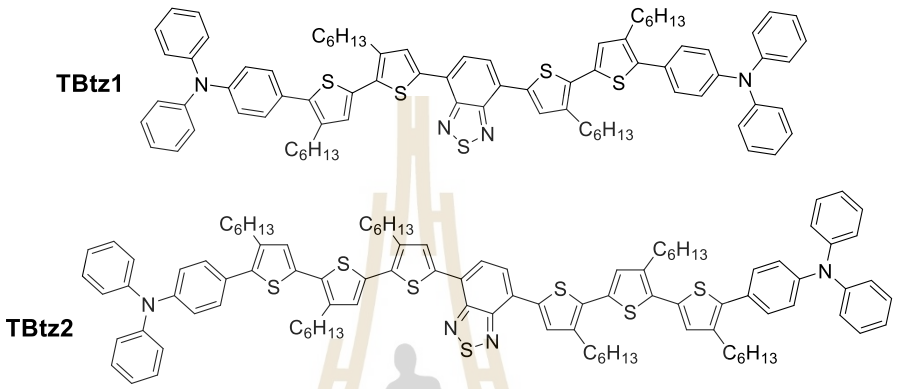

Figure 3.30 Molecular structures of oligothiophene-benzothiadiazoles **TBtz1-2**.

3.3.2 Results and discussion

3.3.2.1 Synthesis

TBtz1-2 were synthesized using a combination of Suzuki-Miyaura cross-coupling and NIS treated iodination of benzothiadiazole core follow by final coupling of the iodo intermediates with 4-(diphenylamino)phenyl)boronic acid. Their structures were confirmed by standard methods.

The intermediate **BT2T4** was prepared form Suzuki coupling between compound 6 and 4-hexylthiophene borolanes in the presence of $Pd(PPh_3)_4$ as catalyst and Na_2CO_3 as a base in THF as a solvent reflux for 24 h to give as red solids **BT2T4** in 83% yield as outlined in Figure 3.31.

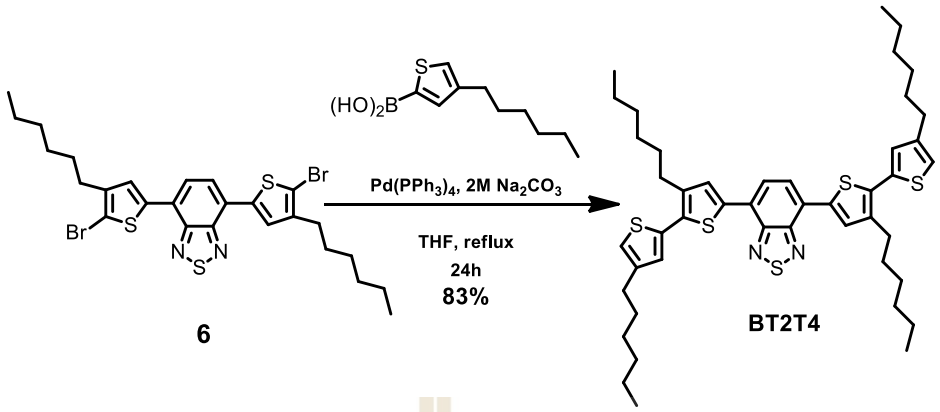

Figure 3.31 Synthesis of compound **BT2T4**.

The chemical structure of compound **BT2T4** was confirmed by ^{1}H-NMR analysis. The ^{1}H-NMR spectrum of shows high field shifted at aromatic region of the compound **BT2T4** (shown in Figure 3.32) as a singlet signal at chemical shift 7.95 ppm (2H) assigning of 2-H proton of benzothiadiazole and tri-singlet signal at chemical shift 7.78, 7.07 and 6.93 ppm (6H) assigning of 6-H proton of thiophene and two peak of low field shifted of the alkyl group as a triplet signal at chemical shift 2.83 and 2.63 ppm (8H) assigning of 4-H proton.

มหาวิทยาลัยเทคโนโลยีสุรนารี

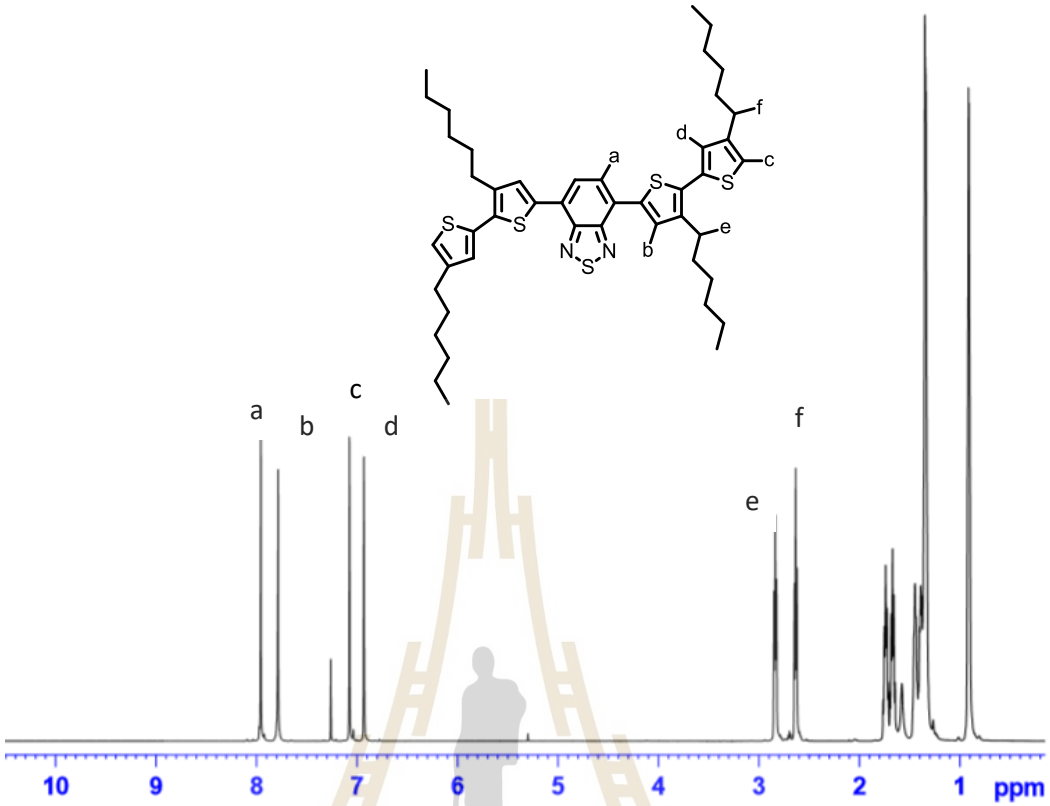

Figure 3.32 The ^{1}H-NMR spectra in $CDCl_3$ of compound **BT2T4**.

Subsequently, the intermediate compound **BT2T4-2I** was prepared form iodination of compound **BT2T4** with NIS in mixture solvent (THF: acetic acid) and obtained as red solids 84% yield as shown in Figure 3.33.

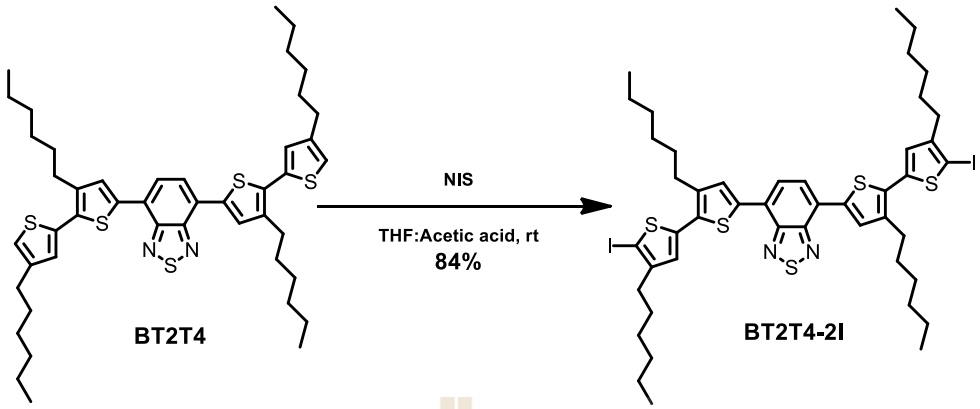

Figure 3.33 Synthesis of compound **BT2T4-2I**.

The chemical structure of compound **BT2T4-2I** was confirmed by ^{1}H-NMR analysis. The ^{1}H-NMR spectrum of shows high field shifted at aromatic region of the compound **BT2T4** (shown in Figure 3.33) as a singlet signal at chemical shift 7.94 ppm (2H) assigning of 2-H proton of benzothiadiazole and a singlet signal at chemical shift 7.81 and 6.88 ppm (2H) assigning of 2-H proton of thiophene and disappear of peak **c** position of thiophen and two peak of low field shifted of the alkyl group as a triplet signal at chemical shift 2.79 and 2.56 ppm (8H) assigning of 4-H proton.

มหาวิทยาลัยเทคโนโลยีสุรนารี

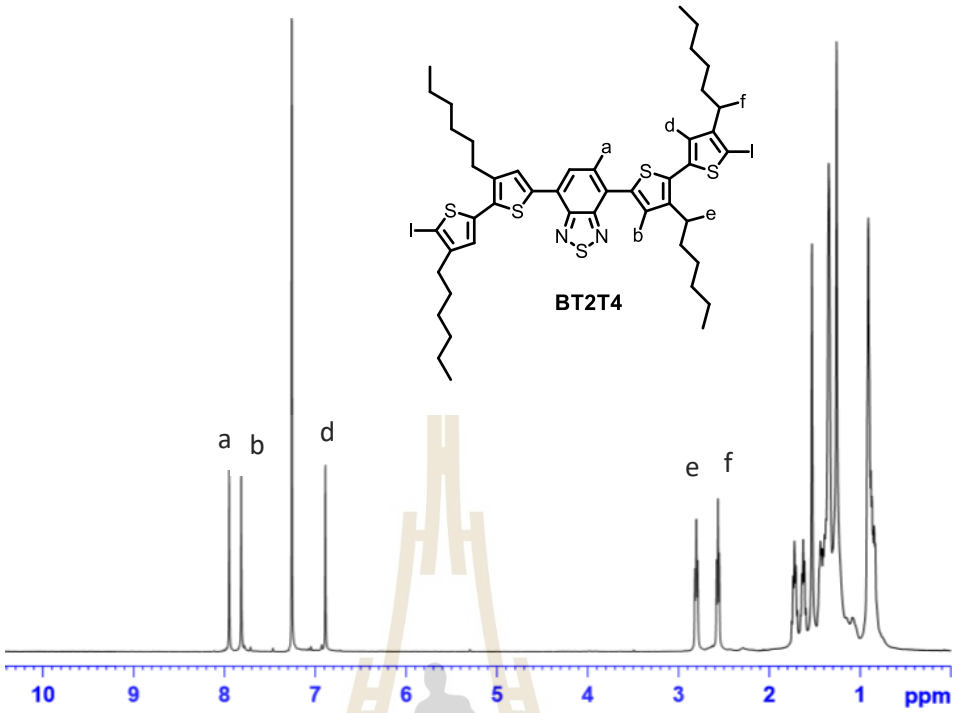

Figure 3.34 The ^{1}H-NMR spectra in $CDCl_3$ of compound **BT2T4-2I**.

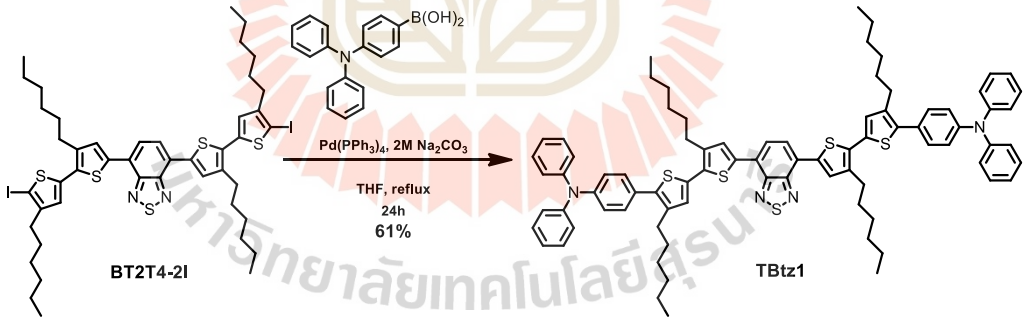

Figure 3.35 Synthesis of final product **TBtz1**.

The Suzuki cross coupling between **BT2T4-2I** and (4-(diphenylamino)phenyl) boronic acid in the presence of $Pd(PPh_3)_4$ as catalyst and Na_2CO_3 as a base in THF as a solvent reflux for 24 h to give dark red solids **TBtz1** in 61% yield as outlined in Figure 3.35.

The chemical structure of final product **TBtz1** was confirmed by ^{1}H-NMR analysis. The ^{1}H-NMR spectrum of shows high field shifted at aromatic region of the final product **TBtz1** (shown in Figure 3.35) as a singlet signal at chemical shift 8.29 ppm (2H) assigning of 2-H proton of benzothiadiazole and a single signal at chemical shift 8.18, 8.08, and 7.90 ppm (2H) assigning of 2-H proton of thiophene and a multiplet signal at chemical shift between 7.65 - 7.57 ppm assigning of 2-H proton of aromatic region of thiophene group and as shown multiplet signal at chemical shift between 7.50 - 7.43 ppm (20H) assigning of 2-H proton of (diphenylamino)phenyl group and low field shifted at alkyl region of the alkyl group as a triplet signal at chemical shift 2.82 and 2.76 ppm (8H) assigning of 4-H proton.

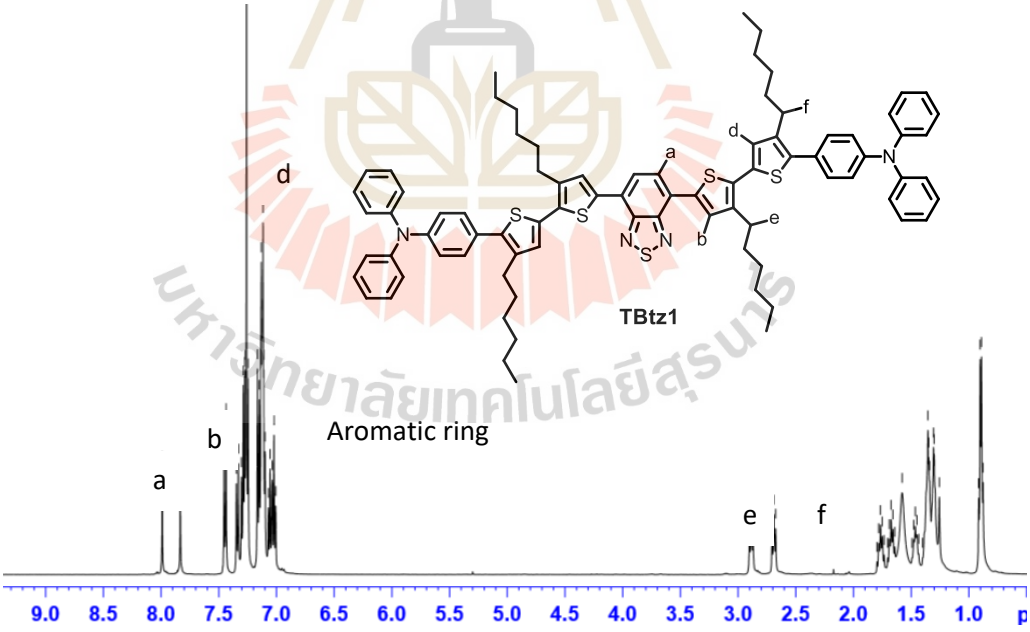

Figure 3.36 The ^{1}H-NMR spectra in $CDCl_3$ of final product **TBtz1**.

The intermediate compound **BT3T4** was accomplished by Suzuki coupling of **BT2T4-2I** with 4-hexylthiophene borolanes in the presence of $Pd(PPh_3)_4$ as catalyst and Na_2CO_3 as a base in THF as a solvent reflux for 24 h to give compound **BT3T4** as red-purple solids in 73% yield as shown in Figure 3.37.

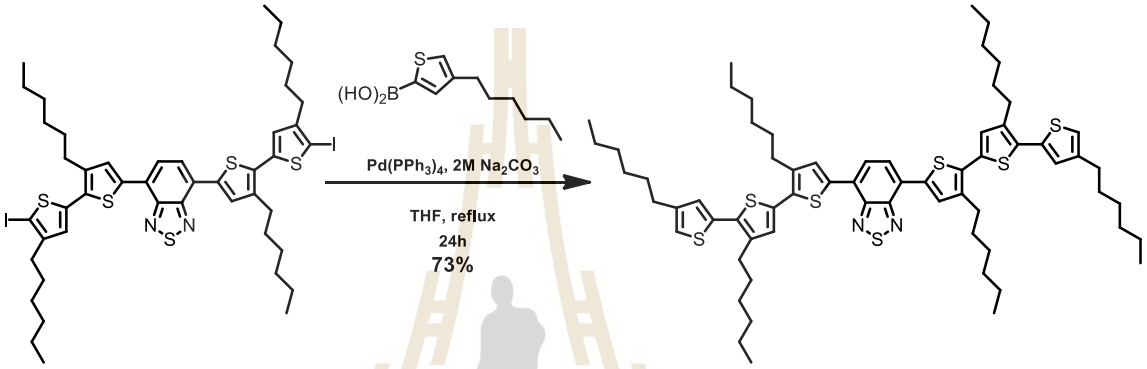

Figure 3.37 Synthesis of compound **BT3T4**.

The chemical structure of compound **BT3T4** was confirmed by ^{1}H-NMR analysis. The ^{1}H-NMR spectrum of shows high field shifted at aromatic region of the compound **BT3T4** (shown in Figure 3.38) as a singlet signal at chemical shift 7.98 ppm (2H) assigning of 2-H proton of benzothiadiazole and a single signal at chemical shift 7.83, 7.07, 6.99 and 6.91 ppm (8H) assigning of 8-H proton of thiophene and low field shifted at alkyl region of the alkyl group as a triplet signal at chemical shift 2.87, 2.77 and 2.62 ppm (6H) assigning of 6-H proton.

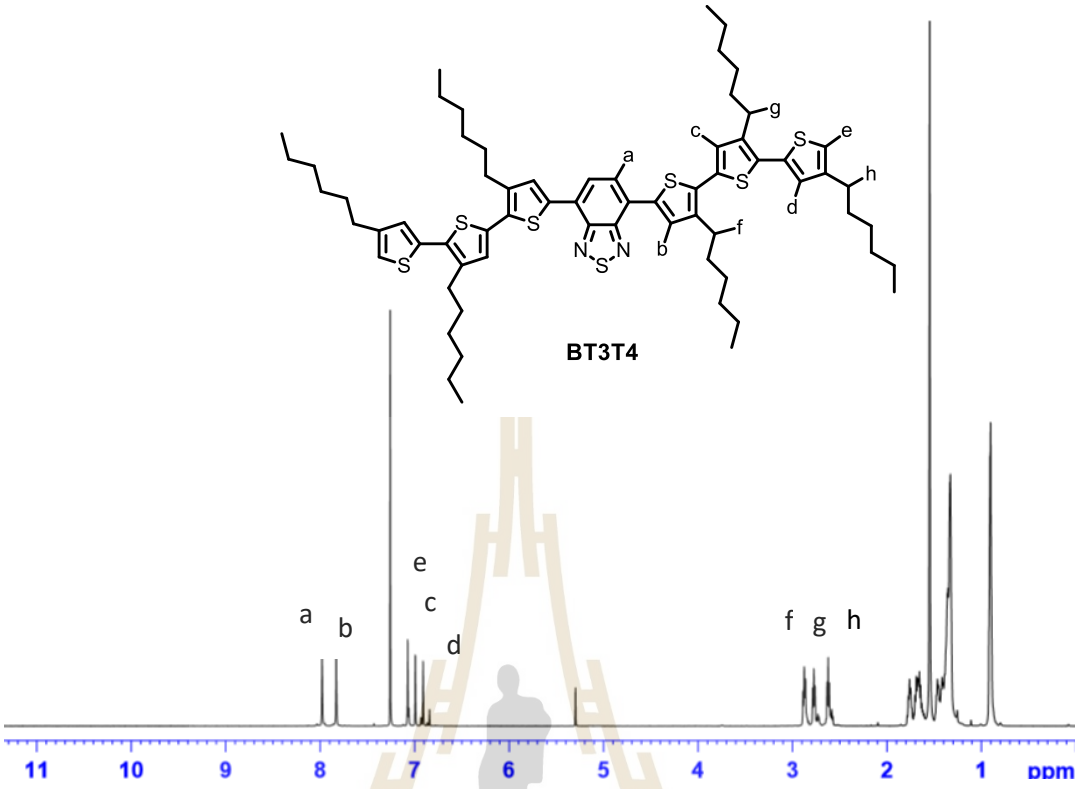

Figure 3.38 The ^{1}H-NMR spectra in $CDCl_3$ of compound **BT3T4**.

Subsequently, the intermediate compound **BT3T4-2I** was prepared form iodination of compound BT3T4 with NIS in mixture solvent (THF: acetic acid) and obtained as purple solids (**BT3T4-2I**) 71% yield as shown in Figure 3.39.

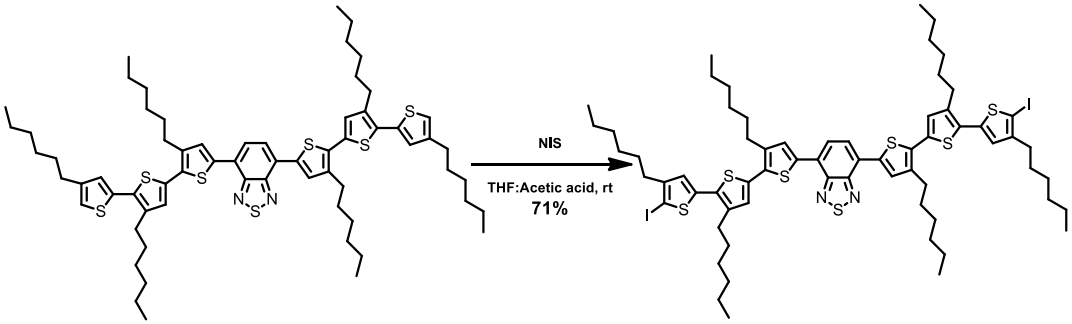

Figure 3.39 Synthesis of compound **BT3T4-2I**.

The chemical structure of compound **BT3T4-2I** was confirmed by ^{1}H-NMR analysis. The ^{1}H-NMR spectrum of shows high field shifted at aromatic region of the compound **BT3T4-2I** (shown in Figure 3.40) as a singlet signal at chemical shift 7.97, ppm (2H) assigning of 2-H proton of benzothiadiazole and a singlet signal at chemical shift 7.82, 7.06 and 6.80 ppm (6H) assigning of 6-H proton of thiophene and disappear of peak e position of thiophen and three peak of low field shifted of the alkyl group as a triplet signal at chemical shift 2.86, 2.73 and 2.55 ppm (6H) assigning of 6-H proton.

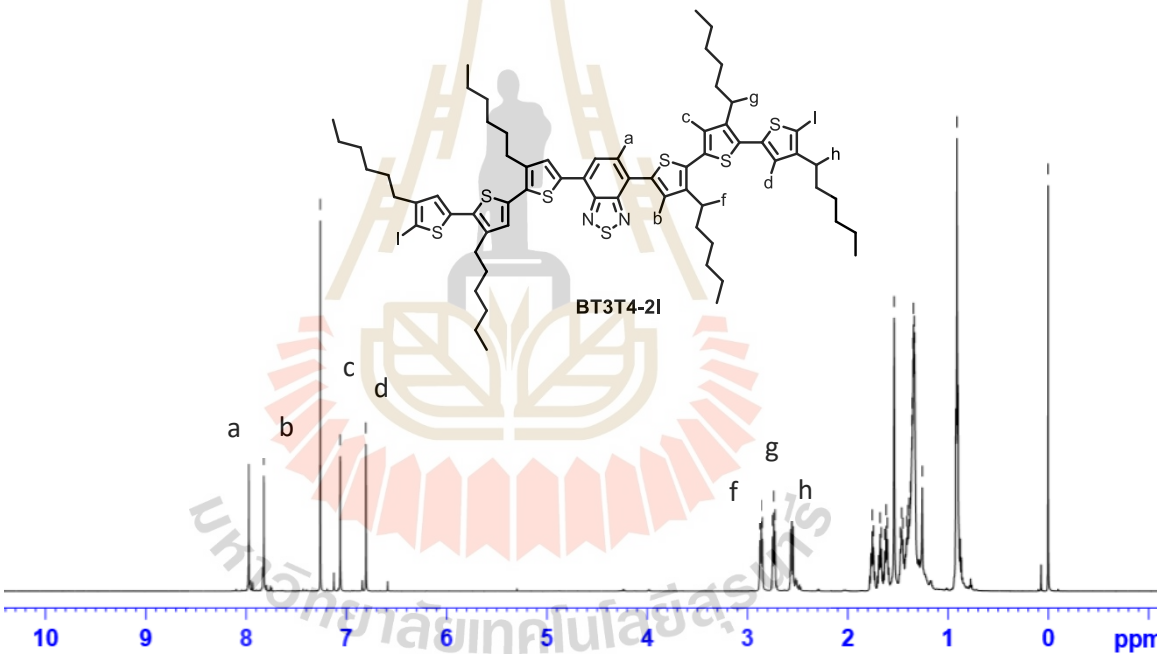

Figure 3.40 Synthesis of compound **BT3T4-2I**.

The Suzuki cross coupling between **BT3T4-2I** and (4-(diphenylamino) phenyl) boronic acid in the presence of $Pd(PPh_3)_4$ as catalyst and Na_2CO_3 as a base in THF as a solvent reflux for 24 h to give dark red solids (**TBtz2**) in 43% yield as outlined in Figure 3.43.

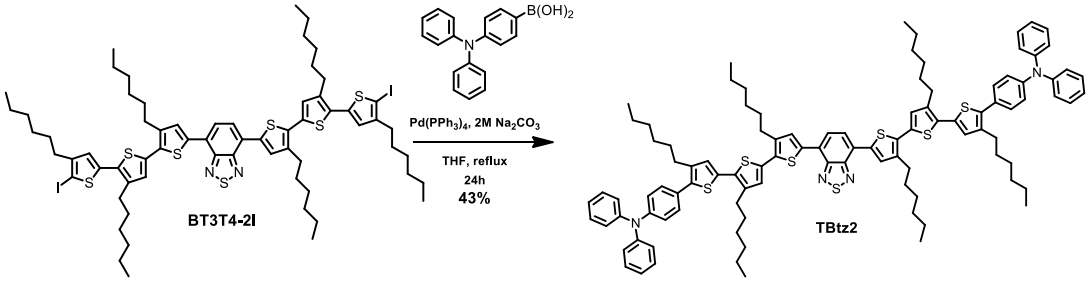

Figure 3.41 Synthesis of final product **TBtz2**.

The chemical structure of final product **TBtz2** was confirmed by ^{1}H-NMR analysis. The ^{1}H-NMR spectrum of shows high field shifted at aromatic region of the final product **TBtz2** (shown in Figure 3.41) as a double signal at chemical shift 7.42 ppm (4H) assigning of 4-H proton of benzothiadiazole and one thiophene and a triplet signal at chemical shift 7.28, and 7.20 ppm (4H) assigning of 4-H proton of thiophene and a chemical shift between 7.17 - 6.95 ppm (42H) assigning of 42-H proton of aromatic region of (diphenylamino) phenyl group and low field shifted at alkyl region of the alkyl group as a triplet signal at chemical shift 2.66 ppm (4H) and multiplet signal at chemical shift between 1.28 - 1.18 assigning of 8-H proton.

3.3.2.2 Photophysical Properties

These compounds exhibit excellent solubility in most organic solvents allowing their thin films to be fabricated by simple, cheap solution process. To fully investigate the electronical properties of **TBtz1-2**, DFT calculations of were performed at a B3LYP/6-31G(d) level in CH_2Cl_2. As depicted in Figure 3.42, the HOMOs both materials are mainly distributed over the entire π- conjugated backbone of the

oligothiophene and benzothiadiazole moieties, whereas their LUMOs are exclusively localized on the central electron deficient benzothiadiazole unit and adjacent thiophene rings. This offers clear separation of the HOMO and LUMO indicating that the HOMO-to-LUMO transition has a strong ICT character. The photophysical properties of **TBtz1-2** were analyzed in both solution and thin film spin-coated on fused silica substrates, and the results are summarized in Tables 3.4 and 3.3.

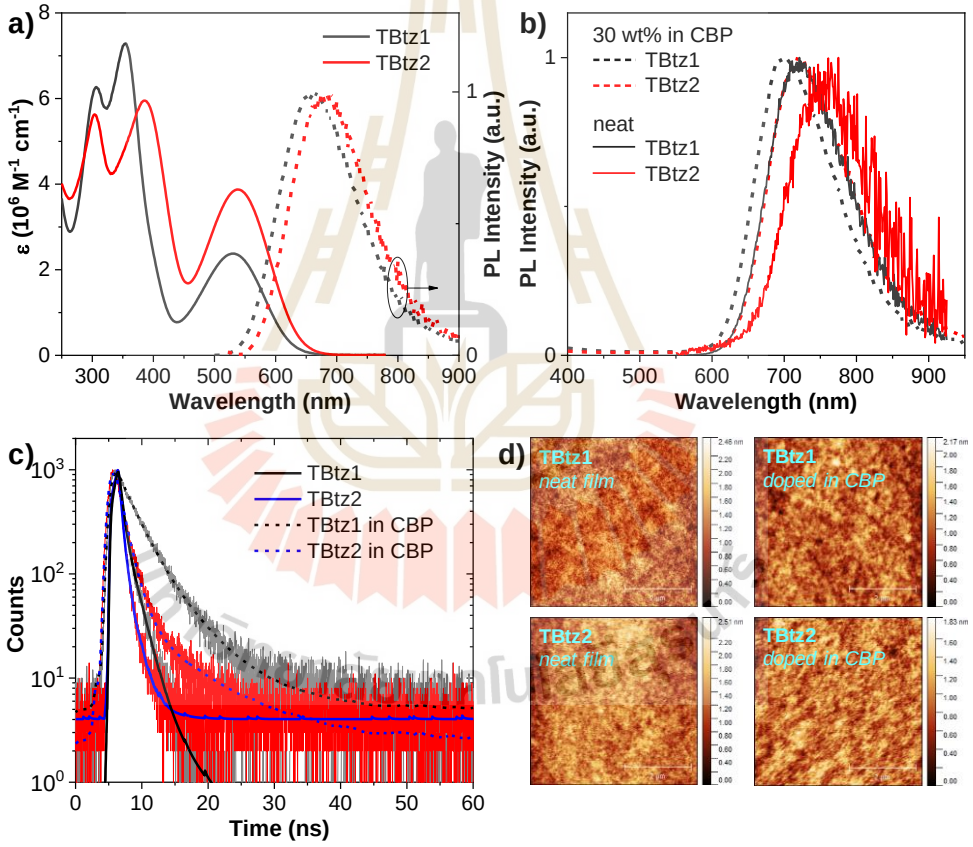

Figure 3.42 a) UV-vis absorption and PL spectra of **TBtz1-2** in CH_2Cl_2 solution. b) PL spectra and c) Transient PL spectra of thin films of neat **TBtz1-2** and 30wt% doped in CBP coated on fused silica substrates. d) AFM images of neat **TBtz1-2** and 30wt% doped in CBP spin-coated on ITO glass.

Table 3.4 Key physical data of the synthesized compounds.

Compound	λ_{abs} (nm)[a]	λ_{PL} (nm)sol[a]/film[b]	Φ_{PL} (%)[c]	T_g/T_{5d} (°C)[d]	E_g (eV)[e]	HOMO/LUMO (eV)[f]
TBtz1	530	661/720	10	114/448	1.96	5.20/3.24
TBtz2	538	686/758	5	134/463	1.93	5.05/3.12

[a] Measured in solution of CH_2Cl_2.

[b] Measured in thin film coated on fused silica substrates.

[c] Absolute PLQY evaluated using an integrating sphere.

[d] Measured by DSC and TGA under N_2 flow.

[e] Estimated from absorption onset of thin film: $E_g = 1240/\lambda_{onset}$.

[f] HOMO measured by AC2 of neat film and LUMO = HOMO + E_g.

มหาวิทยาลัยเทคโนโลยีสุรนารี

Table 3.5 Electroluminescent data of solution-processed devices fabricated with **TBtz1-2** as EL.

Device[a]	EL	Φ_{PL} (%) film[b]	τ (ns) film[c]	V_{on} (V)[d]	R_{max} (mW/sr m^2) at V	J_{max} (mA/cm^2)	λ_{EL} (nm)	%EQE @ 100 mA/cm^2	$\%EQE_{max}$ at V
I	TBtz1	0.8	1.08	5.6	2676/14.0	393	730	0.21	0.48/6.2
II	TBtz2	0.6	0.58	5.8	2590/14.0	462	770	0.31	0.26/6.2
III	TBtz1 30wt%: CBP	31	3.72	5.6	1830/20.0	182	693	0.97	1.40/6.8
IV	TBtz2 30wt%: CBP	19	2.24	5.1	4463/16.6	407	719	0.86	1.12/7.2

[a] ITO/PEDOT: PSS(40 nm)/EL(60 nm)/TPBi(50 nm)/LiF(0.5 nm): Al(150 nm).

[b] Absolute PLQY evaluated using an integrating sphere.

[c] Transient PL decay of thin films.

[d] Turn on voltage at 10 mW/sr m^2.

มหาวิทยาลัยเทคโนโลยีสุรนารี

3.3.2.3 Electroluminescent performances

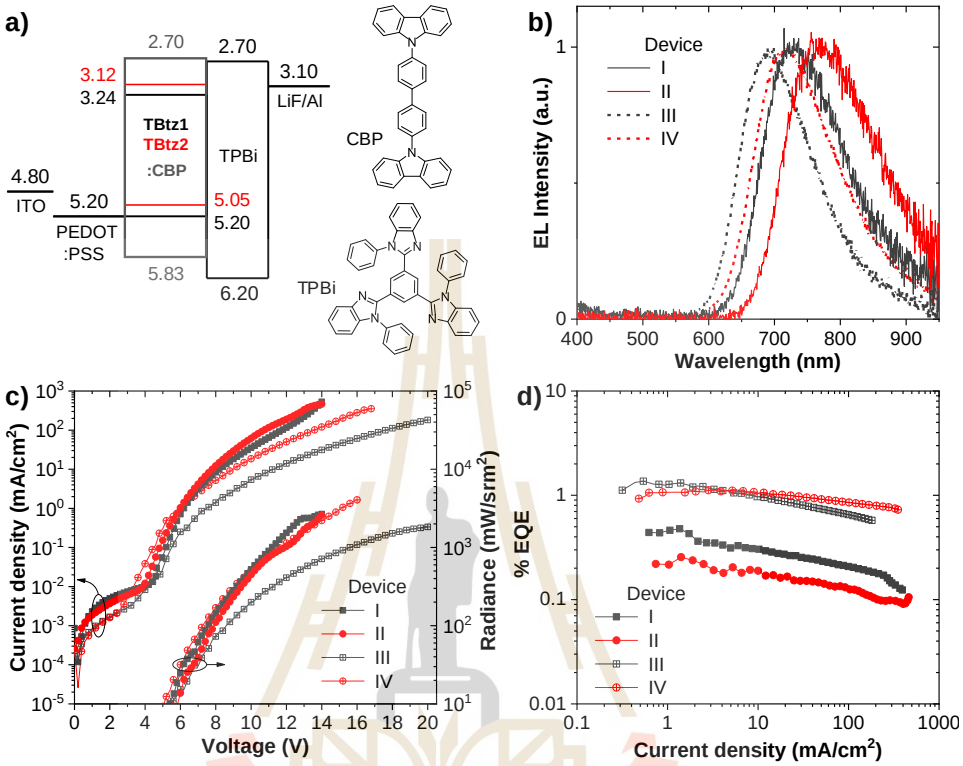

Fig. 3.43 a) Schematic energy diagram (relative to the vacuum energy level) and molecular structures of organic materials used in this study, b) Compared electroluminescence spectra, c) Current density- voltage- radiance (*J-V-R*) characteristics, and d) EQE- J characteristics of solution- processed devices I- IV fabricated with neat **TBtz1-2** and 30wt% doped in CBP as EL.

3.4 Highly fluorescent solid-state thiophene-benzothiadiazole derivatives as hole-transporting red emitters for solution processed OLEDs

3.4.1 Aim of the study

From this part, e designs new non-doped red-light emitting materials for solution processed OLEDs. Their consist of carbazole moiety was used as electron donor due to its electron donating ability and thermal properties as end-capped, Here, hexylthiophene was incorporated for extend π-conjugation and good electron delocalize trough planar structure and to have better solubility for easier device fabrication. Besides of this, two hexyl groups could inevitably decrease the intermolecular interaction and approach higher emission efficiency in solid states. Therefore, the aims of the study are following:

1. To designs and synthesize hole-transporting red emitters molecules (**CTBtz1-2** molecules shown Figure 2.46) by a combination of Bromination and Suzuki cross coupling reactions.

2. To characterize the synthesized red-light emitting materials by NMR and MALDI-TOF techniques.

3. To study the photophysical, electrochemical and thermal property of the synthesized target compound by UV-Vis, fluorescent, cyclic voltammetry and thermal gravimetric analysis technique, respectively.

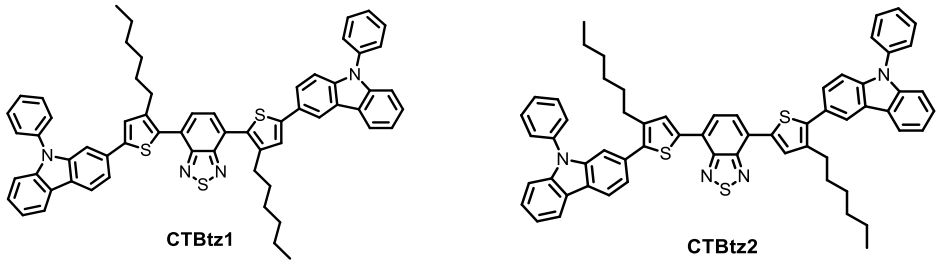

Figure 3.44 Molecular structures of oligothiophene-benzothiadiazoles **CTBtz1-2**.

3.4.2 Result and discussion

3.4.2.1 Synthesis

The synthesized strategy of hole-transporting red emitters molecules (**CTBtz1-2**) are the same as **TBtz1** and **TBtz2** which are constructing the red emitter from acceptor, followed by introducing the π-conjugation and then attached the end-capped with carbazole in the last step.

In this part, started form Suzuki cross coupling between compound **3** and (phenyl-carbazol)boronic acid, $Pd(PPh_3)_4$, as catalyst and 2M Na_2CO_3 as base in THF solvent gave purple solid (**CTBtz1**) in 73% yield. Shown in Figure 3.45.

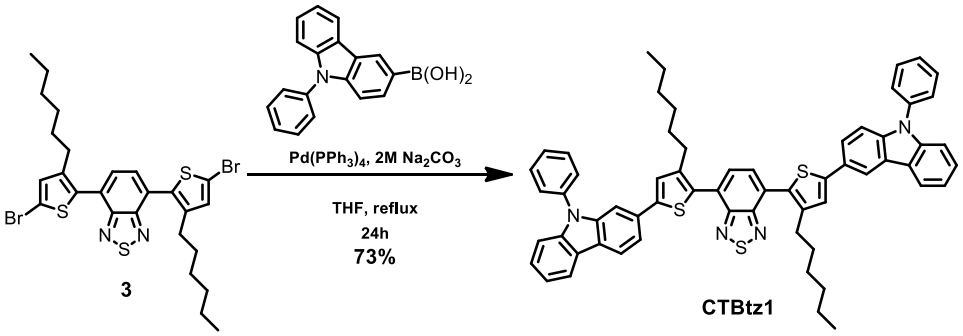

Figure 3.45 Synthesis of final product **CTBtz1**.

The chemical structure of final product **CTBtz1** was confirmed by ^{1}H-NMR analysis. The ^{1}H-NMR spectrum of shows high field shifted at aromatic region of the final product **CTBtz1** (shown in Figure 3.46) as a singlet signal at chemical shift 8.44 ppm (2H) assigning of 2-H proton of benzothiadiazole and a doublet signal at chemical shift 8.21 ppm (2H) assigning of 2-H proton of thiophene and a peak signal at chemical shift between 7.75 - 7.32 ppm (24H) assigning of 24H-proton of carbazole end-capped and low field shifted at alkyl region of the alkyl group as a triplet signal at chemical shift 2.76 ppm (4H) assigning of 4-H proton.

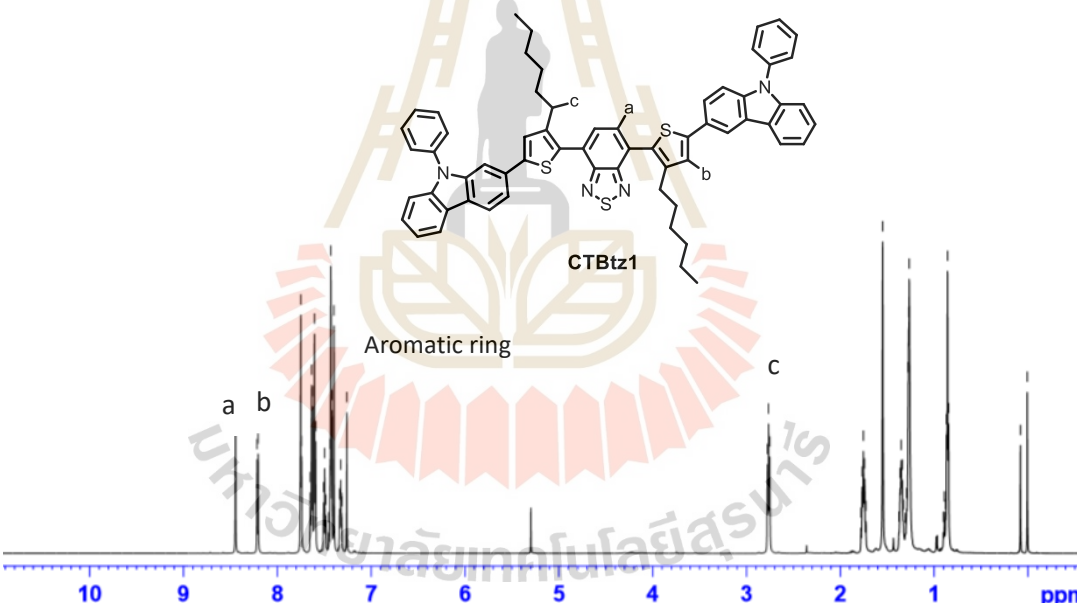

Figure 3.46 The ^{1}H-NMR spectra in $CDCl_3$ of final product **CTBtz1**.

Following, the Suzuki cross coupling between compound **6** and (phenyl-carbazol)boronic acid, $Pd(PPh_3)_4$, as catalyst and 2M Na_2CO_3 as base in THF solvent gave purple solid (**CTBtz2**) in 61% yield. Shown in Figure 3.47.

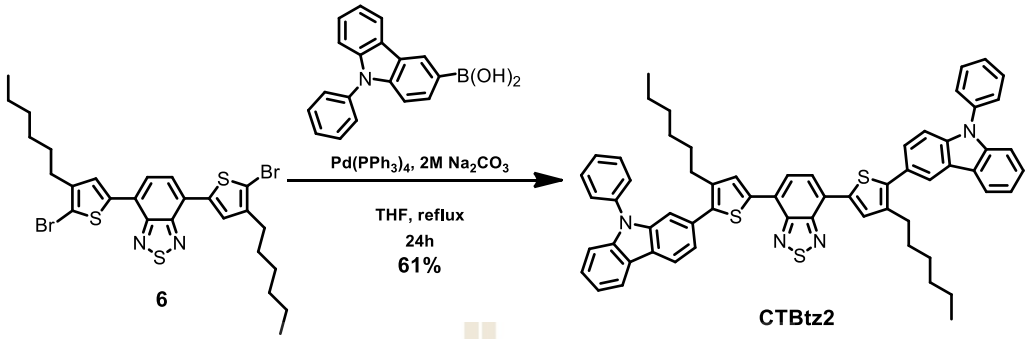

Figure 3.47 Synthesis of final product **CTBtz2**.

The chemical structure of final product **CTBtz2** was confirmed by ^{1}H-NMR analysis. The ^{1}H-NMR spectrum of shows high field shifted at aromatic region of the final product **CTBtz2** (shown in Figure 3.48) as a singlet signal at chemical shift 8.29 ppm (2H) assigning of 2-H proton of benzothiadiazole and a doublet signal at chemical shift 8.18 ppm (2H) assigning of 2-H proton of thiophene and a peak signal at chemical shift between 7.65 - 7.32 ppm (24H) assigning of 24H-proton of carbazole end-capped and low field shifted at alkyl region of the alkyl group as a triplet signal at chemical shift 2.82 ppm (4H) assigning of 4-H proton.

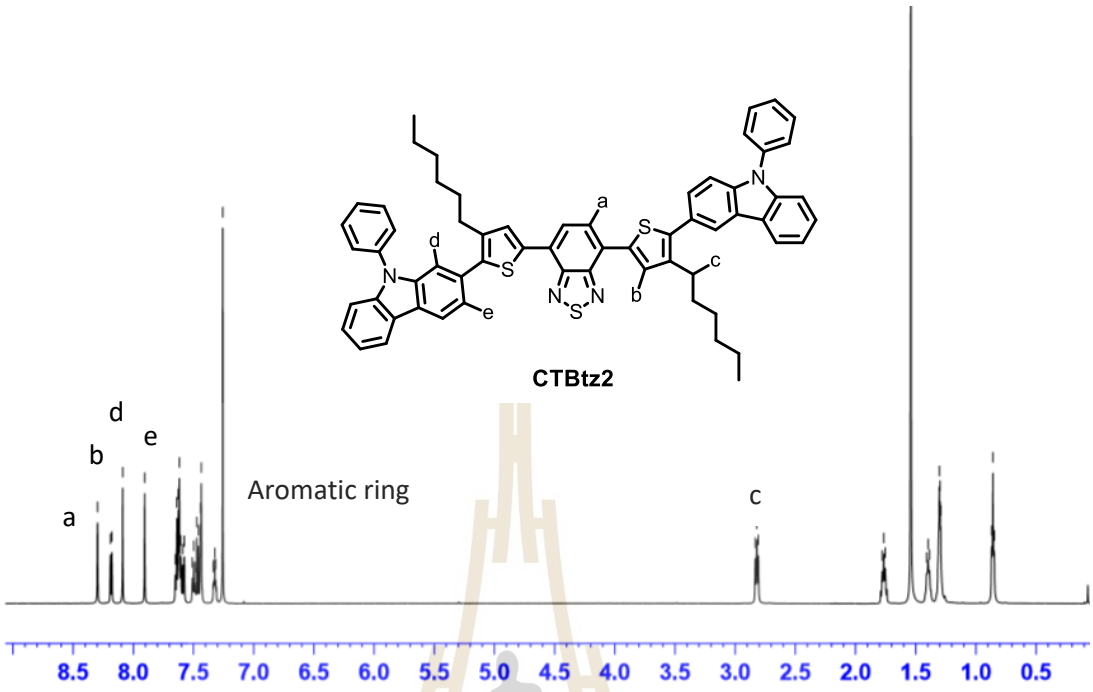

Figure 3.48 The ^{1}H-NMR spectra in $CDCl_3$ of final product **CTBtz2**.

3.4.2.2 Theoretical Calculation

To gain insight into the structure-property relationships of the new compounds **CTBtz1-2**, density functional theory (DFT) calculation were conducted at the TD-DFT B3LYP/6-31G(d,p) level in CH_2Cl_2. In the optimized structures of these compounds (Figure 3.49), It was clearly observed that introduction of hexly or/and triarylamine groups on 3- and 4- position of thiophene unit could enhance the distortion degree in the bis(thiophene-2-yl)-benzothiadiazole core and bulkiness of molecule. These could help suppress the formation of aggregation or π-π stacking and maintain high quantum yield in the solid state. The large dihedral angles in the range of 49 - 54° were found between thiophene and benzolethiadiazole core when the thiophene ring were substituted on 3- position (**CTBtz1-2**) and disubstituted on both

3- and 4- position (**CTBtz1** and **CTBtz2**) such large twist angles can interrupt intramolecular extending of π-electron in the molecule, which would result in a blue-shift in absorption and emission spectra. However, single hexyl substitution on 3-position and 4-position of thiophene ring **CTBtz1** and **CTBtz2**) caused much less twist of the bis(hexylthiophene-2-yl)-benzothiadiazole plane with dihedral angles in the scope of 7°.

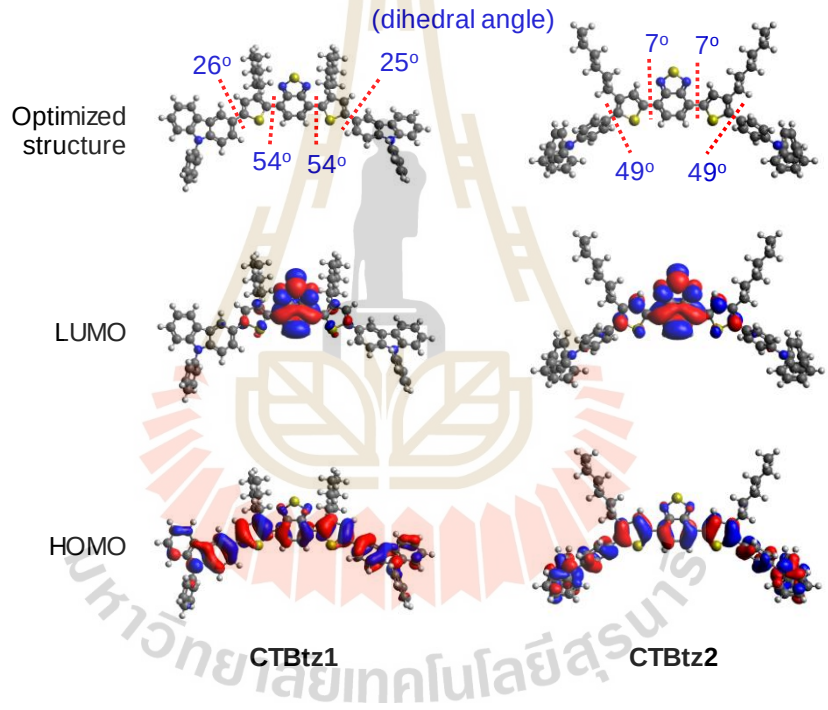

Figure 3.49 The optimized structures with dihedral angle, HOMOs and LUMOs of **CTBtz1-2** calculated by TD-DFT B3LYP/6-31G (d,p) in CH_2Cl_2.

3.4.2.3 Photophysical Properties

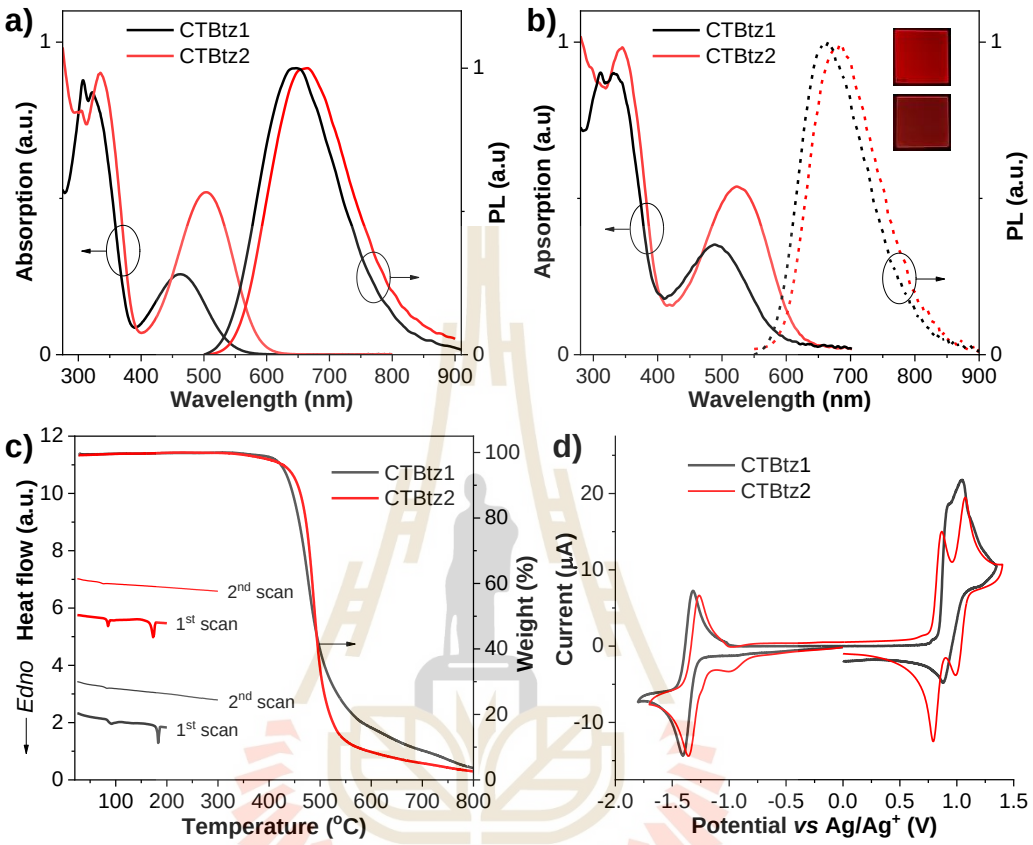

Figure 3.50 UV-vis absorption and PL spectra of **CTBtz1-2** in a) CH_2Cl_2 solution, b) as thin films coated on fused silica substrates, c) DSC (1st heating scan (thick line) and 2nd heating scan (thin line)) and TGA traces of **CTBtz1-2**, and d) CV plots measured of **CTBtz1-2**.

REFERENCES

มหาวิทยาลัยเทคโนโลยีสุรนารี

REFERENCES

Adachi, C., Tsutsui, T., and Saito, S. (1988). Organic electroluminescent device having a hole conductor as an emitting layer. **Applied Physics Letters.** 55: 1489 – 1491.

Adam, D., Schuhmacher, P., Simmerer, J., Häussling, L., Siemensmeyer, K., Etzbachi, K. H., Ringsdorf, H., and Haarer, D. (1994). "Fast photoconduction in the highly ordered columnar phase of a discotic liquid crystal. **Nature.** 371: 141 – 143.

Bardsley, J. N. (2004). International OLED technology roadmap. **IEEE Journal of Selected Topics in Quantum Electronics.** 10(3).

Baude, P. F., Ender, D. A., Haase, M. A., Kelley, T. W., Muyres, D. V., and Theiss, S. D., (2003). Pentacene-based radio-frequency identification circuitry. **Applied Physics Letters.** 82: 3964 – 3966.

Bi, X., Zuo, W., Liu, Y., Zhang, Z., Zeng, C., Xu, S., and Cao, S. (2015). Organic solution-processible electroluminescent molecular glasses for non-doped standard red OLEDs with electrically stable chromaticity. **Materials Research Bulletin.** 70: 865 – 875.

Bradley, D. C. D. (1992). Electroluminescence: a bright future for conjugated polymers. **Advanced Materials.** 4: 756 – 758.

Burroughes, J. H., Bradley, D. D. C., Brown, A. R., Marks, R. N., MacKay, K., Friend, R. H., Burns, P. L. and Holmes, A. B. (1990). Light-emitting diodes based on conjugated polymers. **Nature.** 347(6293): 539.

Chang, M. and Huang, W. (2003). Red organic electroluminescent materials. **U.S. Patent.** 6, 649, 089.

Chen, K., Zhao, H. R., Fan, Z. K., Yin, G., Chen, Q. M., Quan, Y. W., Li, S. H, and Ye, S. H. (2015). Macrospirocyclic oligomer based on triphenylamine and diphenylphosphine oxide as a bipolar host for efficient blue electro phosphorescent organic light-emitting diodes (OLEDs). **Organic Letters.** 17(6): 1413 – 1416.

Chen, Y. H., Lin, S. L., Chang, Y. C., Chen, Y. C., Lin, J. T., and Lee, R. H. (2012). Efficient non-doped blue light emitting diodes based on novel carbazole-substituted anthracene derivatives. **Organic Electronics.** 13(1): 43 – 52.

Chen, C. T. (2004). Evolution of red organic light-emitting diodes: materials and devices. **Chemistry of Materials.** 16(23): 4389 – 4400.

Chen, C. H., Tang, C. W., Shi, J., and Klubek, K. P. (2000). Recent developments in the synthesis of red dopants for Alq3 hosted electroluminescence. **Thin Solid Films.** 363: 327 – 331.

Chen, C. H., Tang, C. W., and Shi, J. (1999). Red organic electroluminescent Devices. **U.S. Patent.** 5, 935,720.

Chen, C. H., Klubek, K. P., and Shi, J. (1999). “Red organic electroluminescent materials. **U.S. Patent.** 5, 908, 581.

Cheng, Z., Li, Z., Xu, Y., Liang, J., Lin, C., Wei, J., and Wang, Y. (2019). Achieving efficient blue delayed electrofluorescence by shielding acceptors with carbazole units. ACS **Applied Materials & Interfaces.** 11(31): 28096 – 28105.

Cias, P., Slugovc, C., and Gescheidt, G. (2011). Hole transport in triphenylamine based OLED devices: from theoretical modeling to properties prediction. **The Journal of Physical Chemistry A.** 115(50): 14519 – 14525.

Cooper, M. W., Zhang, X., Zhang, Y., Jeon, S. O., Lee, H., Kim, S., Fuentes-Hernandez, C., Barlow, S., Kippelen, B., and Marder, S. R. (2018). Effect of the number and substitution pattern of carbazole donors on the singlet and triplet state energies in a series of carbazole-oxadiazole derivatives exhibiting thermally activated delayed fluorescence. **Chemistry of Materials.** 30(18): 6389 – 6399.

Craats, A. M., Warman, J. M., Fechtenkötter, A., Brand, J. D., Harbison, M. A, and Müllen, K. (1999). Record charge carrier mobility in a room-temperature discotic liquid-crystalline derivative of hexabenzo-coronene. **Advanced Materials.** 11: 1469 – 1472.

Danyliv, Y., Volyniuk, D., Bezvikonnyi, O., Hladka, I., Ivaniuk, K., Helzhynskyy, I., Stakhira, P., Tomkeviciene, A., Skhirtladze, L., and Grazulevicius, J. V. (2020). Through-space charge transfer in luminophore based on phenyl-linked carbazole- and phthalimide moieties utilized in cyan-emitting OLEDs. **Dyes and Pigments.** 172: 107833.

Deshpande, R. S., Bulovic´, V., and Forrest, S. R. (1999). White-light-emitting organic electroluminescent devices based on interlayer sequential energy transfer. **Applied Physics Letters.** 7(75): 888 – 890.

Deng, D., Yang, Y., Zhang, J., He, C., Zhang, M., Zhang, Z. G., Zhang, Z., and Li, Y. (2011). Triphenylamine-containing linear D-A-D molecules with benzothiadiazole as acceptor unit for bulk-heterojunction organic solar cell. **Organic Electronics.** 12(4): 614 – 622.

มหาวิทยาลัยเทคโนโลยีสุรนารี

Duan, L., Chin, B. D., Yang, N. C., Kim, M. H., Lee, S. T., and Chung, H. K. (2007). Multilayer blue polymer light-emitting devices with spin-coated interlayers. **Synthetic Metals.** 157: 3431.

Fechtenkotter, A., Saalwächter, K., Harbison, M. A., Müllen, K., and Spiess, H. W. (1999). Highly ordered columnar structures from hexa-peri-hexa benzocoronenes synthesis, X-ray diffraction, and solid-state heteronuclear multiple-quantum NMR investigations. **Angewandte Chemie International Edition.** 38: 3039 – 3042.

Funahashi, M. and Hanna, J. (2000). High ambipolar carrier mobility in self-organizing terthiophene derivative. **Applied Physics Letters.** 76: 2574 – 2576.

Gao, Z. J., Yeh, T. H., Xu, J. J., Lee, C. C., Chowdhury, A., Wang, B. C., Liu, S. W., and Chen, C. H. (2020). Carbazole/benzimidazole-based bipolar molecules as the hosts for phosphorescent and thermally activated delayed fluorescence emitters for efficient OLEDs. **ACS Omega.** 5(18): 10553 – 10561.

Germann, S., Jarrett, S. J., Dupureur, C. M., Rath, N. P., Gallaher, E., and Braddock-Wilking, J. (2020). Synthesis of Luminescent 2-7 Disubstituted Silafluorenes with alkynyl-carbazole, -phenanthrene, and -benzaldehyde substituents. **Journal of Organometallic Chemistry.** 927: 121514.

Gong, S., Zhao, Y., Yang, C., Zhong, C., Qin, J., and Ma, D. (2010). Tuning the photo-physical properties and energy levels by linking spacer and topology between the benzimidazole and carbazole units: bipolar host for highly efficient phosphorescent OLEDs. **The Journal of Physical Chemistry C.** 114(11): 5193 – 5198.

Hahm, S. G., Lee, T. J., Kim, D. M., Kwon, W., Ko, Y.-G., Michinobu, T., and Ree, M. (2011). Electrical memory characteristics of nitrogen-linked poly (2,7-carbazole). **The Journal of Physical Chemistry C.** 115(44): 21954 – 21962.

Han, P., Lin, C., Ma, D., Qin, A., and Tang, B. Z. (2020). Violet-blue emitters featuring aggregation-enhanced emission characteristics for nondoped OLEDs with CIEy smaller than 0.046. **ACS Applied Materials & Interfaces.** 12(41): 46366 – 46372.

Haykir, G., Aydemir, M., Han, S. H., Gumus, S., Hizal, G., Lee, J. Y., and Turksoy, F. (2018). The investigation of sky-blue emitting anthracene-carbazole derivatives: Synthesis, photophysics and OLED applications. **Organic Electronics.** 59: 319 – 329.

He, J., Liu, H., Dai, Y., Ou, X., Wang, J., Tao, S.,Zhang, X., Wang, P., and Ma, D. 2009). nonconjugated carbazoles: a series of novel host materials for highly efficient blue electrophosphorescent OLEDs. **The Journal of Physical Chemistry C.** 113(16): 6761 – 6767.

Helfrich, W. and Schneider, W. (1965). Recombination Radiation in Anthracene Crystals. **Physical Review Letters.** 14(7): 229.

Hong, M., Ravva, M. K., Winget, P., and Brédas, J. L. (2016). effect of substituents on the electronic structure and degradation process in carbazole derivatives for blue OLED host materials. **Chemistry of Materials.** 28(16): 5791 – 5798.

Huang, B., Yin, Z., Ban, X., Ma, Z., Jiang, W., Tian, W., Yang, M., Ye, S., Lin, B., and Sun, Y. (2016). Nondoped deep blue OLEDs based on Bis-(4-benzenesulfonyl-phenyl)-9-phenyl-9H-carbazoles. **Journal of Luminescence.** 172: 7 – 13.

Hung, W. Y., Chiang, P. Y., Lin, S. W., Tang, W. C., Chen, Y. T., Liu, S. H., Chou, P. T., Hung, Y. T., and Wong, K. T. (2016). Balance the carrier mobility to achieve high performance exciplex OLED using a triazine-based acceptor. **ACS Applied Materials & Interfaces.** 8(7): 4811 – 4818.

Hwang, J., Yoon, J., Kim, C. Y., Choi, S., Kang, H., Kim, J. Y., Yoon, D. W., Han, C. W., Park, S., Cho, M. J., and Choi, D. H. (2020). Structural isomers of 9-(pyridin-2-yl)-9H-carbazole in combination with 9′H-9,3':6′,9″-tercarbazole and their application to high efficiency solution processed green TADF OLEDs. **Dyes and Pigments.** 179: 108403.

Islama, A., Usmanb, K., Wattoob, A. G., Shahidb, T., Abbasb, N., Sharifc, H. M. A., Siddique, A. H., Ahmed, M., Ge, Z., and Ouyanga, X. (2019). Meta-substituted bipolar imidazole based emitter for efficient non-doped deep blue organic light emitting devices with a high electroluminescence. **Journal of Photochemistry & Photobiology A: Chemistry.** 379: 72 – 78.

Ito, S, Zakeeruddin, S. M., Humphry-Baker, R., Liska, P., Charvet, R., Comte, P., Nazeeruddin, M. K., Péchy, P., Takata, M., Miura, H., Uchida, S., and Grätzel, M. (2006). High-efficiency organic-dye-sensitized solar cells controlled by nanocrystalline-tio$_2$ electrode thickness. **Advanced Materials.** 18: 1202 – 1205.

Jang, H. J., Braveenth, R., Raagulan, K., Choi, S. Y., Park, Y. H., Oh, S, B., Bae, I. J., Kim, B. M., Wu, Q., Kim, M., and Chai, K. Y. (2020). Dibenzothiophene dioxide-benzofuro carbazole based bipolar host material for yellow and red phosphorescent OLEDs. **Dyes and Pigments.** 182: 108697.

Jayakumar, J., Wu, T. L., Huang, M. J., Huang, P. Y., Chou, T. Y., Lin, H. W., and Cheng, C. H., (2019). Pyridine-carbonitrile–carbazole-based delayed fluorescence materials with highly congested structures and excellent OLED performance. **ACS Applied Materials & Interfaces.** 11(23): 21042 – 21048.

Kelley, T. W. Baude, P. F., Gerlach, C., Ender, D. E., Muyres, D., Haase, M. A., Vogel, D. E., and Theiss, S. D. (2004). Recent progress in organic electronics: materials, devices and processes. **Chemistry of Materials.** 16(23): 4413 – 4422.

Keruckiene, R., Guzauskas, M., Narbutaitis, E., Tsiko, U., Volyniuk, D., Lee, P. H., Chen, C. H., Chiu, T. L., Lin, C. F., Lee, J. F., and Grazulevicius, J.V. (2020). Exciplex-forming derivatives of 2,7-di-tert-butyl-9,9-dimethylacridan and benzotrifluoride for efficient OLEDs. **Organic Electronics.** 78: 105576.

Kim S. J., Yadong, Z., Carlos, Z., Stephen, B., Marder, S. R., and Bernard, K. (2010). Efficient green OLED devices with an emissive layer comprised of phosphor-doped carbazole/bis-oxadiazole side-chain polymer blends. **Organic Electronics.** 12: 492 – 496.

Kim, S., Choi, H., Kim, D., Song, K., Kang, S. O., and Ko, J. (2007). Novel conjugated organic dyes containing bis-dimethyl fluoren fluorenyl amino phenyl thiophene for efficient solar cell. **Tetrahedron.** 63: 9206 – 9212.

Khrustalev, D., Yedrissov, A., Vetrova, A., and Khrustaleva, A. (2020). Synthesis of 2,7-dibromo-9H-carbazole and its N-alkylation under microwave activation conditions in a flow-type microwave reactor. **Materials Today.** Proceedings.

Kochapradist, P., Prachumrak, N., Tarsang, R., Keawin, T., Jungsuttiwong, S., Sudyoadsuk, T., and Promarak, V. (2012). Multi-triphenylamine-substituted carbazoles: synthesis characterization, properties, and applications as hole-transporting materials. **Tetrahedron Letters.** 54(28): 3683 – 3687.

Kukhta, N. A., Matulaitis, T., Volyniuk, D., Ivaniuk, K., Turyk, P., Stakhira, P., Grazulevicius, J. V., and Monkman, A. P. (2017). Deep-blue high-efficiency TTA OLED using para- and meta-conjugated cyanotriphenylbenzene and carbazole derivatives as emitter and host. **The Journal of Physical Chemistry Letters.** 8(24): 6199 – 6205.

Kumar, M., and Pereira, L. (2020). Mixed-Host Systems with a Simple Device Structure for efficient solution-processed organic light-emitting diodes of a red-orange TADF emitter. **ACS Omega.** 5(5): 2196 – 2204.

Lai, S. L., Tong, W. Y., Kui, S. C. F., Chan, M. Y., Kwok, C. C., and Che C. M. (2013). High efficiency white organic light-emitting devices incorporating yellow phosphorescent platinum (ii) complex and composite blue host. **Advanced Functional Materials.** 23(41): 5168 – 5176.

Lee, S. K., Ahn, T., Cho, N. S., Lee, J., Jung, Y. K., Lee, J. H., and Shim, H. K. (2007). Synthesis of new polyfluorene copolymers with a comonomer containing triphenylamine units and their applications in white-light-emitting diodes. **Journal of Polymer Science Part A Polymer Chemistry.** 45: 1199.

Li, G., Zheng, J., Klimes, K., Zhu, Z. Q., Wu, J., Zhu, H., and Li, J. (2019). Novel carbazole/fluorene-based host material for stable and efficient phosphorescent OLEDs. **ACS Applied Materials & Interfaces.** 11(43): 40320 - 40331.

Li, Y., Xu, Z., Zhu, X., Chen, B., Wang, Z., Xiao, B., Lam, J. W. Y., Zhao, Z., Ma, D., and Tang, B. Z. (2019). Creation of efficient blue aggregation-induced emission luminogens for high-performance nondoped blue OLEDs and hybrid white OLEDs. **ACS Applied Materials & Interfaces.** 11(19): 17592 – 17601.

Li, S. W., Yu, C. H., Ko, C. L., Chatterjee, T., Hung, W. Y., and Wong, K. T. (2018). Cyanopyrimidine–carbazole hybrid host materials for high-efficiency and low-efficiency roll-off TADF OLEDs. **ACS Applied Materials & Interfaces.** 10(15): 12930 – 12936.

Li, J., Li, Q., and Di Liu, D. (2011). Novel thieno-[3,4-b]-pyrazines cored dendrimers with carbazole dendrons: design, synthesis, and application in solution-processed red organic light-emitting diodes. **ACS Applied Materials & Interfaces.** 3(6): 2099 – 2107.

Li, Y., Wu, Y., Gardnera, S., and Ong, B. S. (2005). Novel peripherally substituted indolo[3, 2 b]carbazoles for high-mobility organic thin-film transistors. **Advanced Materials.** 17: 849 – 853.

Liang, X., Wang, K., Zhang, R., Li, K., Lu, X., Guo, K., Wang, H., Miao, Y., Xu, H., and Wang, Z. (2017). Tetra-carbazole substituted spiro[fluorene-9,9′-xanthene]-based hole-transporting materials with high thermal stability and mobility for efficient OLEDs. **Dyes and Pigments.** 139: 764 – 771.

Lin, N., Qiao, J., Duan, L., Li, H., Wang, L., and Qiu, Y. (2012). Achilles heels of phosphine oxide materials for OLEDs: chemical stability and degradation mechanism of a bipolar phosphine oxide/carbazole hybrid host material. **The Journal of Physical Chemistry C.** 116 (36): 19451 – 19457.

Liu, C. K., Chen, Y. H., Long, Y. J., Sah, P. T., Chang, W. C., Chan, L. H., Wu, J. L., Jeng, R. J., Yeh, S. C., and Chen, C. T. (2018). Bipolar 9-linked carbazole-π-dimesitylborane fluorophores for nondoped blue OLEDs and red phosphorescent OLEDs. **Dyes and Pigments.** 157: 101 – 108.

Liu, Y., Wang, Y., Li, C., Ren, Z., Ma, D., and Yan, S. (2018). Efficient thermally activated delayed fluorescence conjugated polymeric emitters with tunable nature of excited states regulated via carbazole derivatives for solution-processed OLEDs. **Macromolecules.** 51(12): 4615 – 4623.

Lovinger A. J. and Rothberg, L. J. (1996). Electrically active organic and polymeric materials for thin-film-transistor technologies. **Journal of Materials Research.** 12: 3174 – 3186.

Mallick, T., Karmakar, A., Bag, J., Sahu, S., Mishra, M., and Begum, N. A. (2020). Carbazole analog anchored fluorescent silica nanoparticle showing enhanced biocompatibility and selective sensing ability towards biomacromolecule. **Dyes and Pigments.** 173: 107994.

Ma, C., Liang, Z., Wang, X., Zhang, B., Cao, Y., Wang, L., and Qiu, Y. (2003). A novel family of red fluorescent materials for organic light-emitting diodes. **Synthetic Metals.** 138: 537 – 542.

Mao, H. T., Zang, C. X., Shan, G. G., Sun, H. Z., Xie, W. F., and Su, Z. M. (2017). Achieving high performances of nondoped oleds using carbazole and diphenylphosphoryl-functionalized Ir(III) complexes as active components. **Inorganic Chemistry.** 56(16): 9979 – 9987.

McCulloch, I., Heeney, M., Bailey, C., Genevicius, K., MacDonald, I., Shkunov, M., Sparrowe, D., Tierney, S., Wagner, R., Zhang, W., Chabinyc, M. L., Kline, R. J., McGehee, M. D., and Toney, M. F. (2006). Liquid-crystalline semiconducting polymers with high charge carrier mobility. **Nature Mater.** 5: 328 – 333.

Nasiri, S., Cekaviciute, M., Simokaitiene, J., Petrauskaite, A., Volyniuk, D., Burroughes Andruleviciene, V., Bezvikonnyi, O., and Grazulevicius, J. V. (2019). Carbazole derivatives containing one or two tetra-/triphenylethenyl units as efficient hole-transporting OLED emitters. **Dyes and Pigments.** 168: 93 – 102.

Panthi, K., Adhikari, R. M., and Kinstle, T. H. (2010). carbazole donor−carbazole linker-based compounds: preparation, photophysical properties, and formation of fluorescent nanoparticles. **The Journal of Physical Chemistry A.** 114(13): 4550 – 4557.

Patil, V. V., Lee, K. H., and Lee, J. Y. (2020). 11,11-Dimethyl-11H-indeno[1,2-b] indolo [1,2,3-jk] carbazole: A rigid chromophore with novel amalgamation strategy for long lifetime blue fluorescent organic light-emitting diodes. **Chemical Engineering Journal.** 395: 125125.

Peng, H., Wei, Z., Wu, L., and Li, X. (2020). Efficient non-doped blue fluorescent OLEDs based on bipolar phenanthroimidazole-triphenylamine derivatives. **Optical Materials.** 101: 109726.

Qing, L., Jiuyan, L., Lijun, D., Qian, W., Zhanxian, G., and Di, L. (2011). Synthesis and characterization of thieno[3,4-b]pyrazine materials for solution-processible organic red light-emitting diodes. **Chemistry Letters.** 40(4).

Qiu, X., Ying, S., Yao, J., Zhou, J., Wang, C., Wang, B., Li, Y., Xu, Y., Jiang, Q., Zhao, R., Hu, D., Ma, D., and Ma, Y. (2020). Universal host materials based on carbazole-formate derivatives for blue, green and red phosphorescent organic light-emitting diodes. **Dyes and Pigments.** 174: 108045.

Ramírez, C. L., Parise, A. R., Bertolotti, S. G., Previtali, C. M., and Arbeloa, E. M. (2020). Study on the triplet states of N-phenyl carbazoles. transient spectra and singlet oxygen generation. **Journal of Photochemistry and Photobiology A:** Chemistry. 397: 112503.

Romanov, A. S., Yang, L., Jones, S. T. E., Di, D., Morley, O. J., Drummond, B. H., Reponen, A. P. M., Linnolahti, M., Credgington, D., and Bochmann, M. (2019). Dendritic carbene metal carbazole complexes as photo-emitters for fully solution-processed OLEDs. **Chemistry of Materials.** 31: 3613 – 3623.

Sallenave, X., Bucinskas, A., Salman, S., Volyniuk, D., Bezvikonnyi, O., Mimaite, V., Grazulevicius, J. V., and Sini, G. (2018). Sensitivity of redox and optical properties of electroactive carbazole derivatives to the molecular architecture and methoxy substitutions. **The Journal of Physical Chemistry C.** 122 (18): 10138 – 10152.

Sano, M., Pope, M., and Kallmann, H. (1965). Electroluminescence and band gap in anthracene. **The Journal of Chemical Physics.** 43(8): 2920.

Serevičius, T., Skaisgiris, R., Fiodorova, I., Steckis, V., Dodonova, J., Banevičius, D., Kazlauskas, K., Juršėnas, S., and Tumkevičius, S. (2020). Achieving efficient deep-blue TADF in carbazole-pyrimidine compounds. **Organic Electronics.** 82: 105723.

Sharma, A., Saklani, D., Thomas, K. R. J., Shahnawaz, Swayamprabha, S. S., and Jou, J. H. (2020). Synthesis and characterization of multi-substituted carbazole derivatives exhibiting aggregation-induced emission for OLED applications. **Organic Electronics.** 86: 105864.

Sheats, J. R., Antoniadis, H., Hueschen, M., Leonard, W., Miller, J., Moon, R., Roitman, D., and Stocking, A. (1996). Organic electroluminescent devices. **Science.** 273: 884 – 888.

Shih, P. I., Chiang, C. L., Dixit, A. K., Chen, C. K., Yuan, M. C., Lee, R. Y., Chen, C. T., Diau, E. W. G., and Shu, C. F. (2006). novel carbazole/fluorene hybrids: host materials for blue phosphorescent OLEDs. **Organic Letters.** 8(13): 2799 – 2802.

Siddiqui, Q. T., Awasthi, A. A., Bhui, P., Muneer, M., Chandrakumar, K. R. S., Bose, S., and Agarwal, N. (2019). Thermally activated delayed fluorescence (green) in undoped film and exciplex emission (blue) in acridone–carbazole derivatives for OLEDs. **The Journal of Physical Chemistry C.**123(2): 1003 – 1014.

Sirringhaus, H., Wilson, R. J., and Friend, R. H. (2000). Mobility enhancement in conjugated polymer field-effect transistors through chain alignment in a liquid-crystalline phase **Applied Physics Letters.** 77: 406.

Su, R., Zhao, Y., Yang, F., Duan, L., Lan, J., Bin, Z., and You, J. (2021). Triazolotriazine-based thermally activated delayed fluorescence materials for highly efficient fluorescent organic light-emitting diodes (TSF-OLEDs). **Science Bulletin.** 66(5): 441 – 448.

Sundar, V. C., Zaumseil J., Podzorov, V., Menard, E., Willett, R. L., Someya, T., Gershenson, M. E., and Rogers, J. (2004). elastomeric transistor stamps: reversible probing of charge transportin organic crystals. **Science.** 303: 1644 – 1646.

มหาวิทยาลัยเทคโนโลยีสุรนารี

Tan, X. F., Wang, P. P., Lu, L., Bezvikonnyi, O., Volyniuk, D., Grazulevicius, J. V., and Zhao, Q. H. (2020). Comparative study of multi-functional luminogens with 1,3,5-triazine as the core and phenothiazine or phenoxy donors as the peripheral moieties for non-doped/doped fluorescent and red phosphorescent OLEDs. **Dyes and Pigments.** 173: 107793.

Tang, C., Chen, Y., Wang, F., Jiang, T., Hu, J., Cao, X., Zhang, L., Zhang, X. (2020). Effect of methyl-substitution on carbazole/oxadiazole donor-acceptor (D-A) type host materials for efficient solution-processed green organic light-emitting diodes. **Tetrahedron.** 76(13): 131030.

Tang, C. W., VanSlyke, S. A., and Chen, C. H. (1989). Electroluminescence of doped organic thin films. **Applied Physics Letters.** 65: 3610.

Tang, C. W. and Vanslyke, S. A. (1987). Organic electroluminescent diodes. **Applied Physics Letters.** 51(12): 913.

Tavgeniene, D., Krucaite, G., Baranauskyte, U., Wu, J. Z., Su, H. Y., Huang, C. W., Chang, C. H., and Grigalevicius, S. (2017). Phenanthro[9,10-d]imidazole based new host materials for efficient red phosphorescent OLEDs. **Dye and Pigment.** 137: 615 – 621.

Thangtong, A. Meunmart, D., Prachumrak, N., Jungsuttiwong, S., Keawin, T., Sudyoadsuka, T., and Promarak, V. (2011). Bifunctional anthracene derivatives as non-doped blue mitters and hole-transporters for electroluminescent devices. **Chemical Communications.** 47(25): 7122 – 7124

Tingting, Y., Zhang, D., Zhao, Y., Xu, H., Hua, W., Gao, Z., Qu, W., and Bingshe, X. (2020). Non-doped blue fluorescent emitting materials with donor-π-acceptor-π-donor structures based 1,2,4-triazole/carbazole derivatives. **Journal of Photochemistry and Photobiology A: Chemistry.** 400: 112707.

Tsuchiya, K., Kasuga, H., Kawakami, A., Taka, H., Kita, H., and Ogino, K. (2010). Synthesis of bipolar charge transporting block copolymers and characterization for organic light-emitting diode. **Journal of Polymer Science Part A Polymer Chemistry.** 48: 1461.

Venkateswararao, A., Thomas, K. R. J., Lee, C. P., Li, C. T., and Ho, K. C. (2014). Organic dyes containing carbazole as donor and π-linker: optical, electrochemical, and photovoltaic properties. **ACS Applied Materials & Interfaces.** 6(4): 2528 – 2539.

Wang, P., Fan, S., Liang, J., Ying, L., You, J., Wang, S., and Li, X. (2017). Carbazole-diphenylimidazole based bipolar material and its application in blue, green and red single layer OLEDs by solution processing. **Dyes and Pigments.** 142: 175 – 182.

Wang, C., Li, X., Pan, Y., Zhang, S., Yao, L., Bai, Q., Li, W., Lu, P., Yang, B., Su, S., and Ma, Y. (2016). Highly efficient nondoped green organic light-emitting diodes with combination of high photoluminescence and high exciton utilization. **ACS Applied Materials & Interfaces.** 8(5): 3041 – 3049.

Wang, Z. S., Koumura, N., Cui, Y., Takahashi, M., Sekiguchi, H., Mori, A., Kubo, T., Furube, A., and Hara, K. (2008). Hexylthiophene-functionalized carbazoled for efficient molecular photovoltaics: tuning of solar-cell performance by structural modification. **Chemistry of Materials.** 20: 3993 – 4003.

Webster, F. G. and McColgin, W. C. (1974). **U.S. Patent.** 3, 852,683.

Wong, K. T., Chen, Y. M., Lin, Y. T., Su, H. C., and Wu, C. C. (2005). Nonconjugated hybrid of carbazole and fluorene: a novel host material for highly efficient green and red phosphorescent OLEDs. **Organic Letters.** 7(24): 5361 – 5364.

Wu, C., Zhang, Y., Ma, D., and Wang, Q. (2020). Phthalonitrile-based bipolar host for efficient green to red phosphorescent and TADF **OLEDs. Dyes and Pigments.** 173: 107895.

Wu. Y., Li, Y., Gardner, S., and Ong, B. S. (2005). Indolo[3,2-b]carbazole-Based Thin-Film Transistors with High Mobility and Stability. **Journal of the American Chemical Society.** 127: 614 – 618.

Wu, C. C., Chen, C. W., Lin, C. L., and Yang, C. J. (2005). Advanced organic light-emitting devices for enhancin display performances. **Journal of Information Technology.** 1(2): 248 – 266.

Xiong, Y., Zeng, J., Chen, B., Lam, J. W. Y., Zhao, Z., Chen, S., and Tang, B. Z. (2019). New carbazole-substituted siloles for the fabrication of efficient non-doped OLEDs. **Chinese Chemical Letters.** 30(3): 592 – 596.

Yang, H., Li, Y., Zhao, Y., Yu, S., Ma, H., Qian, L., Wang, R., Yu, T., and Su, W. (2021). Four new bipolar Indolo[3,2-b] carbazole derivatives for blue OLEDs. **Dyes and Pigments.** 187: 109096.

Yang, Y., Zhou, Y., He, Q., He, C., Yang, C., Bai, F., and Li, Y. (2009). Solution-processable red-emission organic materials containing triphenylamine and benzothiodiazole units: synthesis and applications in organic light-emitting diodes. **The Journal of Physical Chemistry B.** 113(22): 7745 – 7752.

Ye, J., Chen, Z., Fung, M. K., Zheng, C., Ou, X., Zhang, X., Yuan, Y., and Lee, C. S. (2013). Carbazole/sulfone hybrid d-π-a-structured bipolar fluorophores for high-efficiency blue-violet electroluminescence. **Chemistry of Materials.** 25(13): 2630 – 2637.

Yu, F., Liu, Q., Sheng, Y., Chen, Y., Zhang, Y., Sun, Z., Zhang, C., Xia, Q., Li, H., Hang, X. C., and Huang, W. (2020). Solution-processable Csp3-annulated hosts for high-efficiency deep red phosphorescent OLEDs. **ACS Applied Materials & Interfaces.**

Yuan, W. Z., Gong, Y., Chen, S., Shen, X. Y., Lam, J. W. Y., Lu, P., Lu, Y., Wang, Z., Hu, R., Xie, N., Kwok, H. S., Zhang, Y., Sun, J. Z., and Tang, B. Z. (2012). Efficient solid emitters with aggregation-induced emission and intramolecular charge transfer characteristics: molecular design, synthesis, photophysical behaviors, and OLED application. **Chemistry of Materials.** 24(8): 1518 – 1528.

Yuan, W., Yang, H., Zhang, M., Hu, D., Wan, S., Li, Z., Shi, C., Sun, N., Tao, Y., and Huang, W. (2019). Molecular engineering on all ortho-linked carbazole/ oxadiazole hybrids toward highly-efficient thermally activated delayed fluorescence materials in OLEDs. **Chinese Chemical Letters.** 30(11): 1955 – 1958.

Zassowski, P., Ledwon, P., Kurowska, A., Herman, A. P., Lapkowski, M., Cherpak, V., Hotra, Z., Turyk, P., Ivaniuk, K., Stakhira, P., Sych, G., Volyniuk, D., and Grazulevicius, J. V. (2018). 1,3,5-Triazine and carbazole derivatives for OLED applications. **Dyes and Pigments.** 149: 804 – 811.

Zhang, T., Ye, J., Luo, A., Liu, D. (2020). Efficient deep blue emitter based on carbazole-pyrene hybrid for non-doped electroluminescent device. **Optical Materials.** 100: 109632.

Zhang, L., Bai, Y., Liu, Z., Jiang, W., Lei, T., Yang, R., Islam, A., Zhang, Y., Ouyang, X., and Ge, Z. (2017). Substituted Diindenopyrazinediones with symmetrical Polyalkyl-carbazole for high-efficiency blueish green solution-processable OLED. **Dyes and Pigments.** 142: 544 – 551.

Zhang, H., Wang, S., Li, Y., Zhang, B., Du, C., Wan, X., and Chen, Y. (2009). Synthesis, characterization, and electroluminescent properties of star shaped donor-acceptor dendrimers with carbazole dendrons as peripheral branches and heterotriangulene as central core. **Tetrahedron.** 23(65): 4455 – 4463.

Zhao, Z., Xu, X., Wang, H., Lu, P., Yu, G., and Liu, Y. (2008). Zigzag molecules from pyrene-modified carbazole oligomers: synthesis, characterization, and application in OLEDs. **The Journal of Organic Chemistry.** 73(2): 594 – 602.

Zheng, C. J., Ye, J., Lo, M. F., Fung, M. K., Ou, X. M., Zhang, X. H., and Lee, C. S. (2012). New ambipolar hosts based on carbazole and 4,5-diazafluorene units for highly efficient blue phosphorescent OLEDs with low efficiency roll-off. **Chemistry of Materials.** 24(4): 643 – 650.

มหาวิทยาลัยเทคโนโลยีสุรนารี

APPENDIX

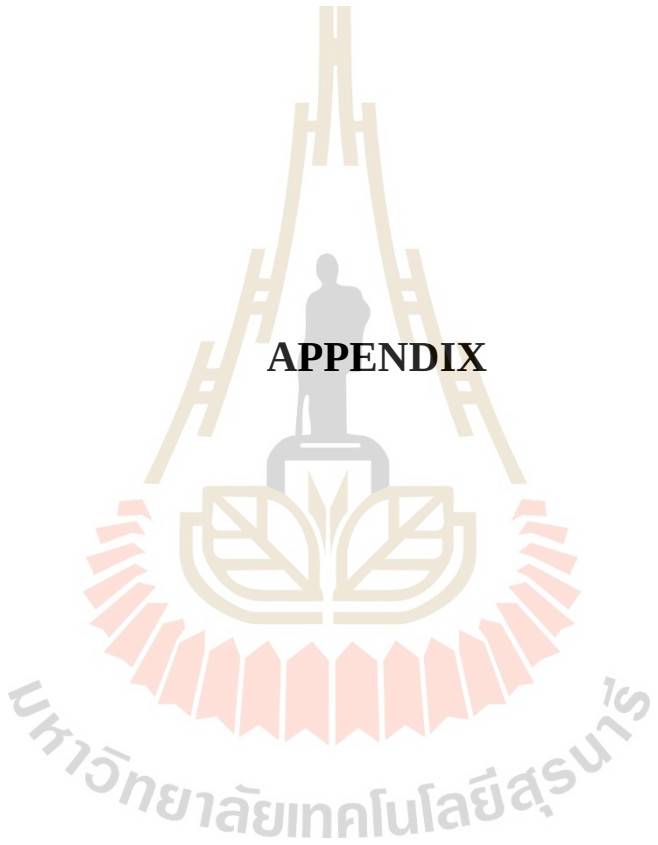

APPENDIX

NMR AND MASS SPECTRA

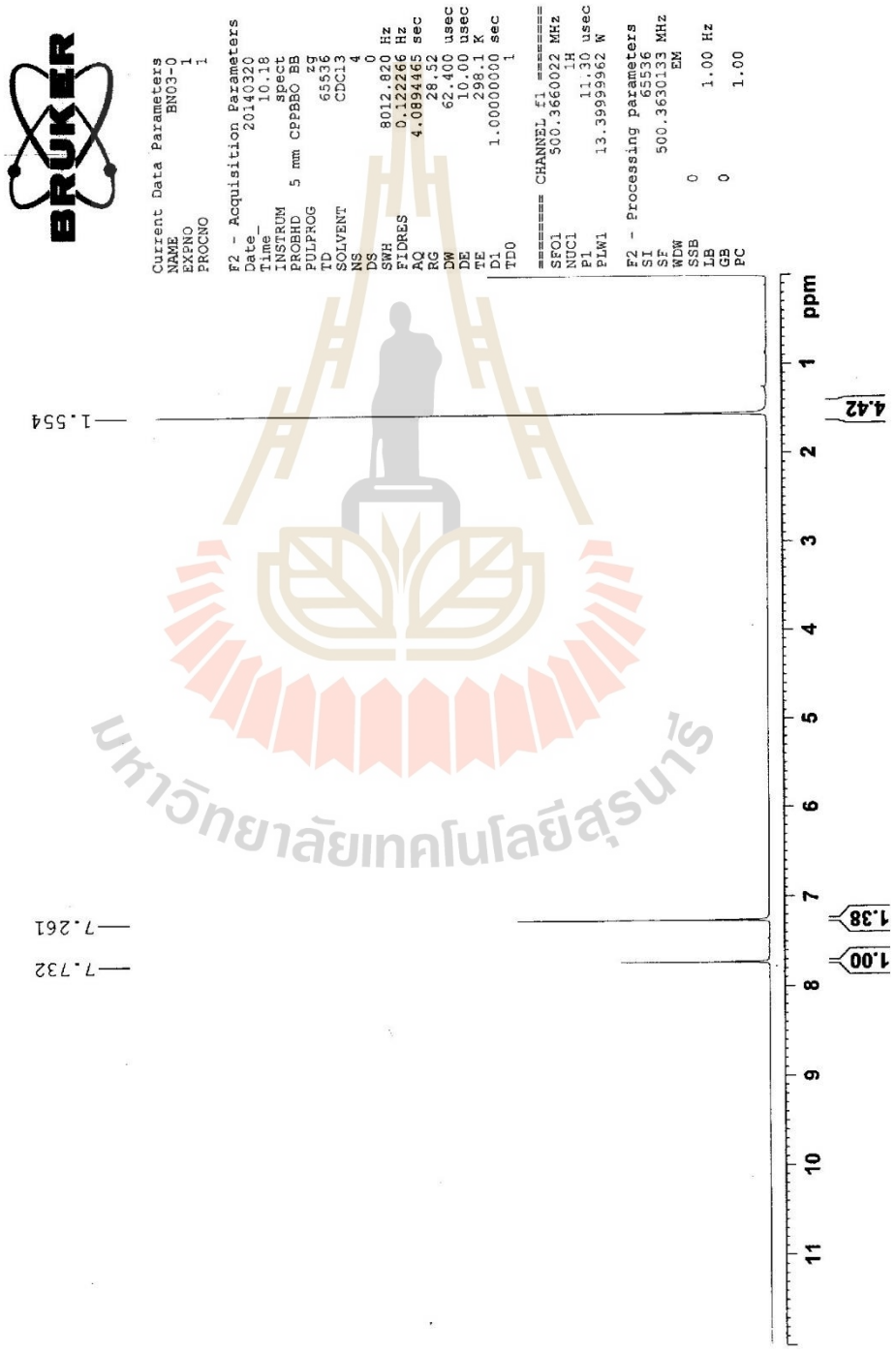

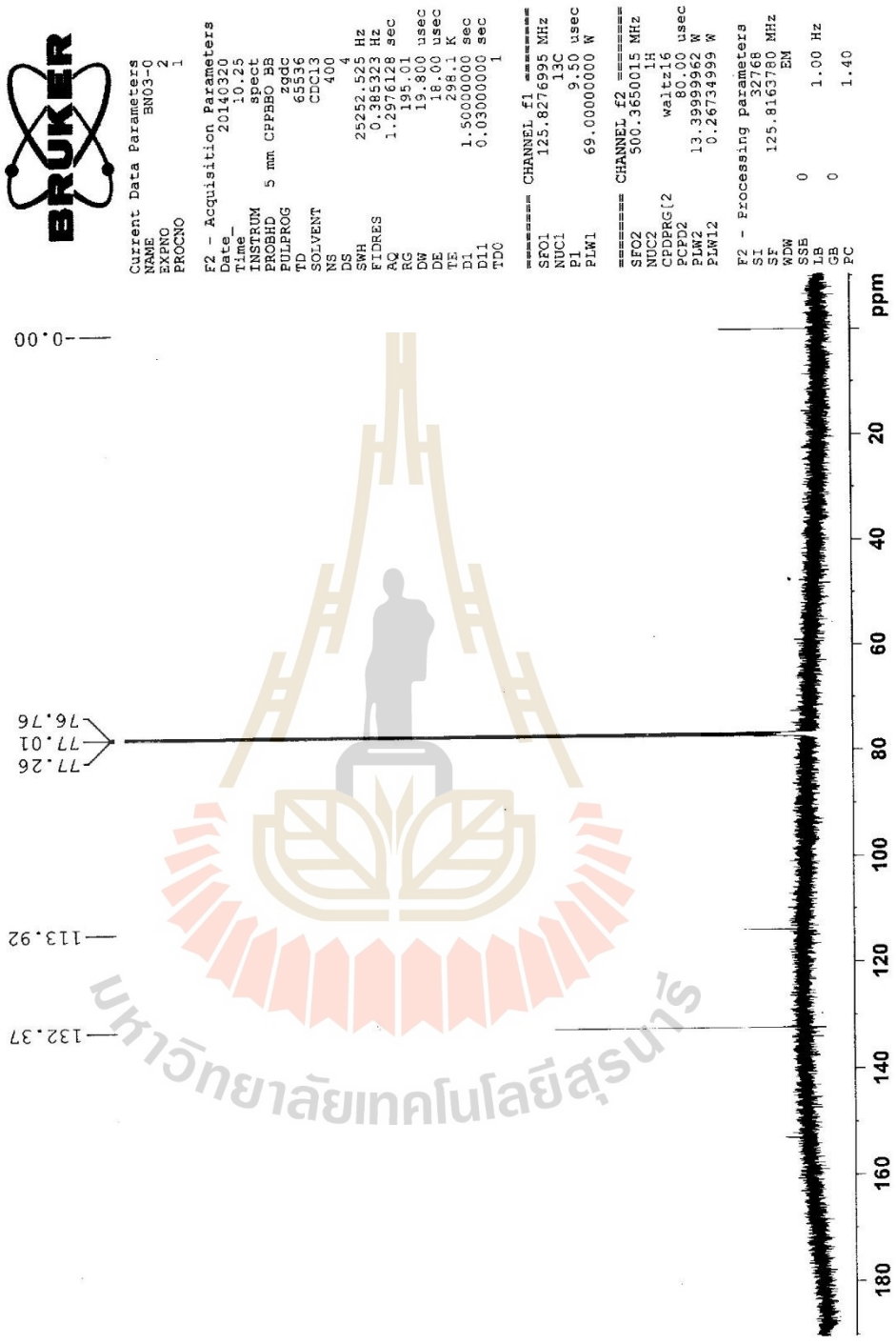
Current Data Parameters
NAME BN03-0
EXPNO 2
PROCNO 1
F2 - Acquisition Parameters
Date_ 20140320
Time_ 10.25
INSTRUM spect
PROBHD 5 mm CPPBBO BB
PULPROG zgdc
TD 65536
SOLVENT CDCl3
NS 400
DS 4
SWH 25252.525 Hz
FIDRES 0.385323 Hz
AQ 1.2976128 sec
RG 195.01
DW 19.800 usec
DE 18.00 usec
TE 298.1 K
D1 1.50000000 sec
D11 0.03000000 sec
TD0 1
======== CHANNEL f1 ========
SFO1 125.8276995 MHz
NUC1 13C
P1 9.50 usec
PLW1 69.00000000 W
======== CHANNEL f2 ========
SFO2 500.3650015 MHz
NUC2 1H
CPDPRG[2 waltz16
PCPD2 80.00 usec
PLW2 13.39999962 W
PLW12 0.26734999 W
F2 - Processing parameters
SI 32768
SF 125.8165780 MHz
WDW EM
SSB 0
LB 1.00 Hz
GB 0
PC 1.40
0.00
76.76
77.01
77.26
113.92
132.37
ppm
180
160
140
120
100
80
60
40
20

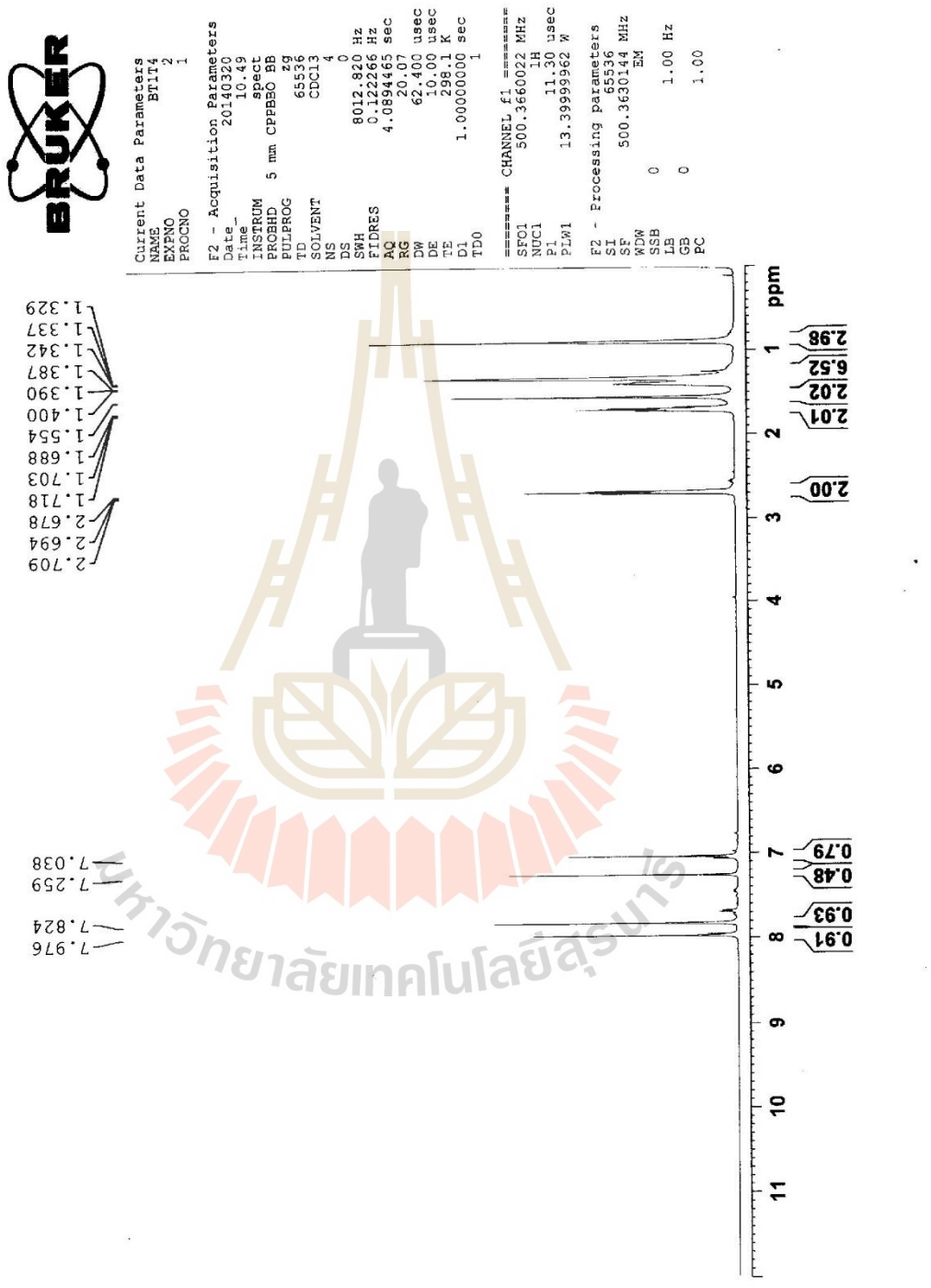

มหาวิทยาลัยเทคโนโลยีสุรนารี

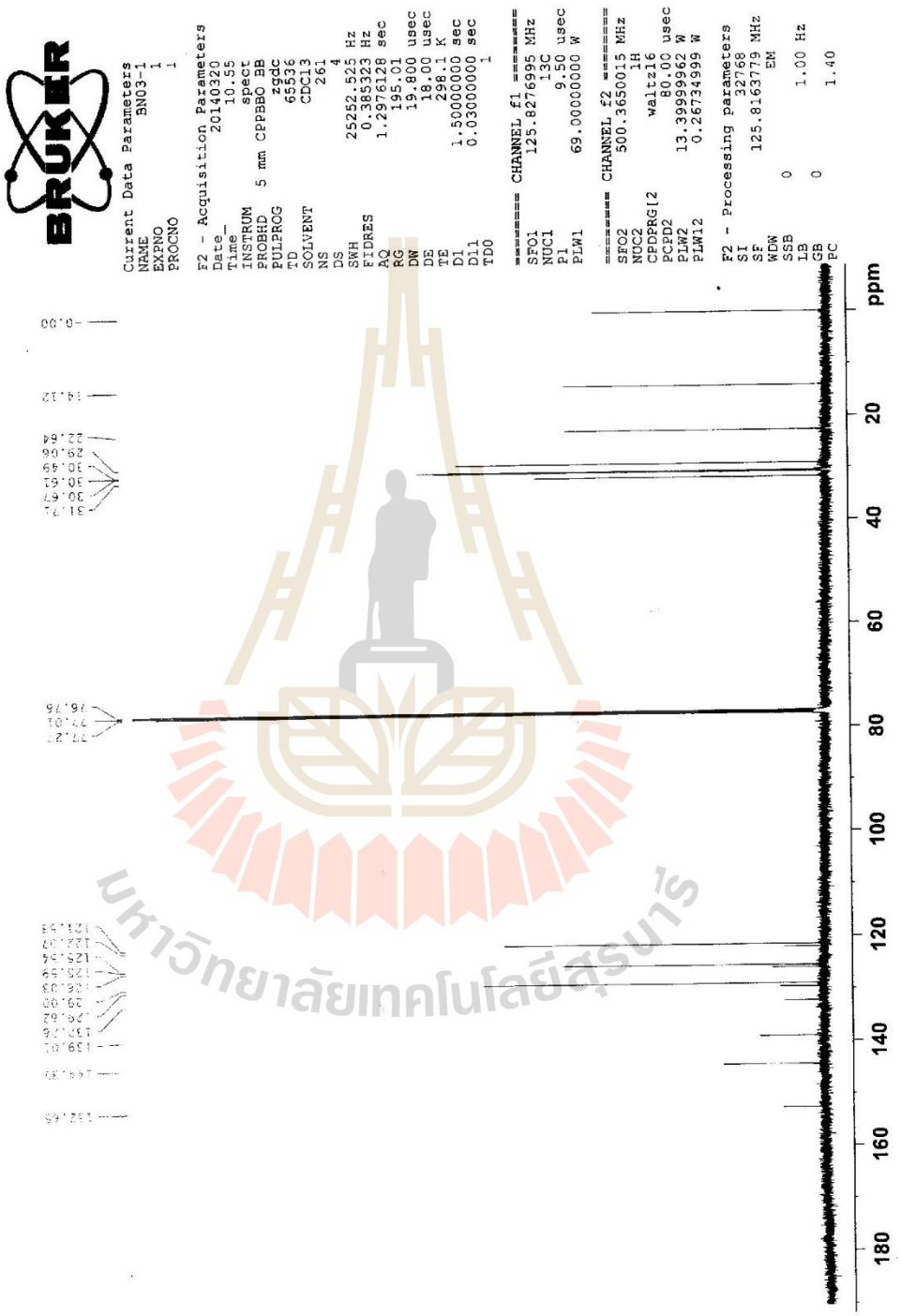

มหาวิทยาลัยเทคโนโลยีสุรนารี

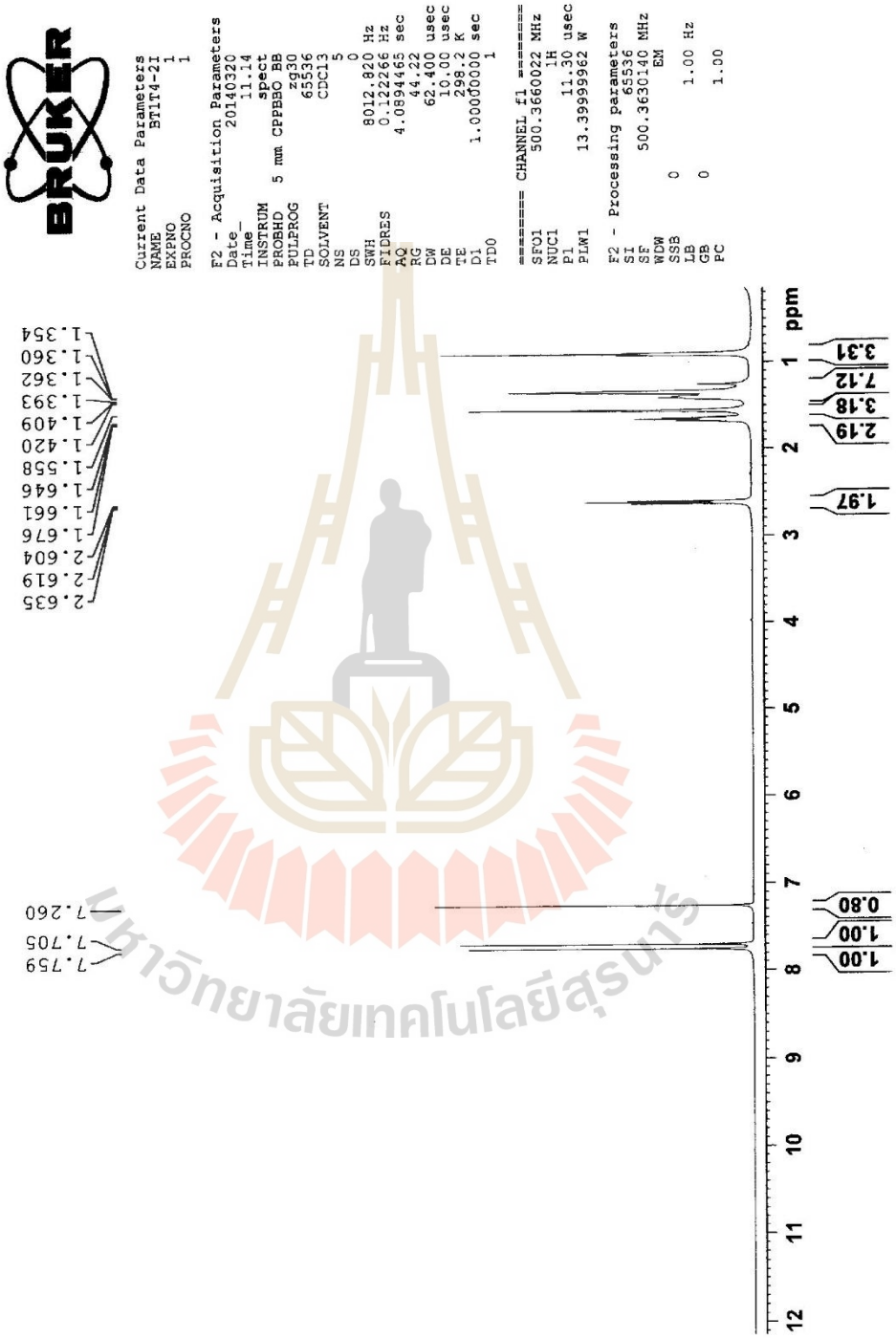
Current Data Parameters
NAME B1T4-2I
EXPNO 1
PROCNO 1
F2 - Acquisition Parameters
Date_ 20140320
Time_ 11.14
INSTRUM spect
PROBHD 5 mm CPPBBO BB
PULPROG zg30
TD 65536
SOLVENT CDCl3
NS 5
DS 0
SWH 8012.820 Hz
FIDRES 0.122266 Hz
AQ 4.0894465 sec
RG 44.22
DW 62.400 usec
DE 10.00 usec
TE 298.2 K
D1 1.00000000 sec
TD0 1
======== CHANNEL f1 ========
SFO1 500.3660022 MHz
NUC1 1H
P1 11.30 usec
PLW1 13.39999962 W
F2 - Processing parameters
SI 65536
SF 500.3630140 MHz
WDW EM
SSB 0
LB 1.00 Hz
GB 0
PC 1.00
ppm
3.31
7.12
3.18
2.19
1.97
0.80
1.00
1.00
7.759
7.705
7.260
2.635
2.619
2.604
1.676
1.661
1.646
1.558
1.420
1.409
1.393
1.362
1.360
1.354

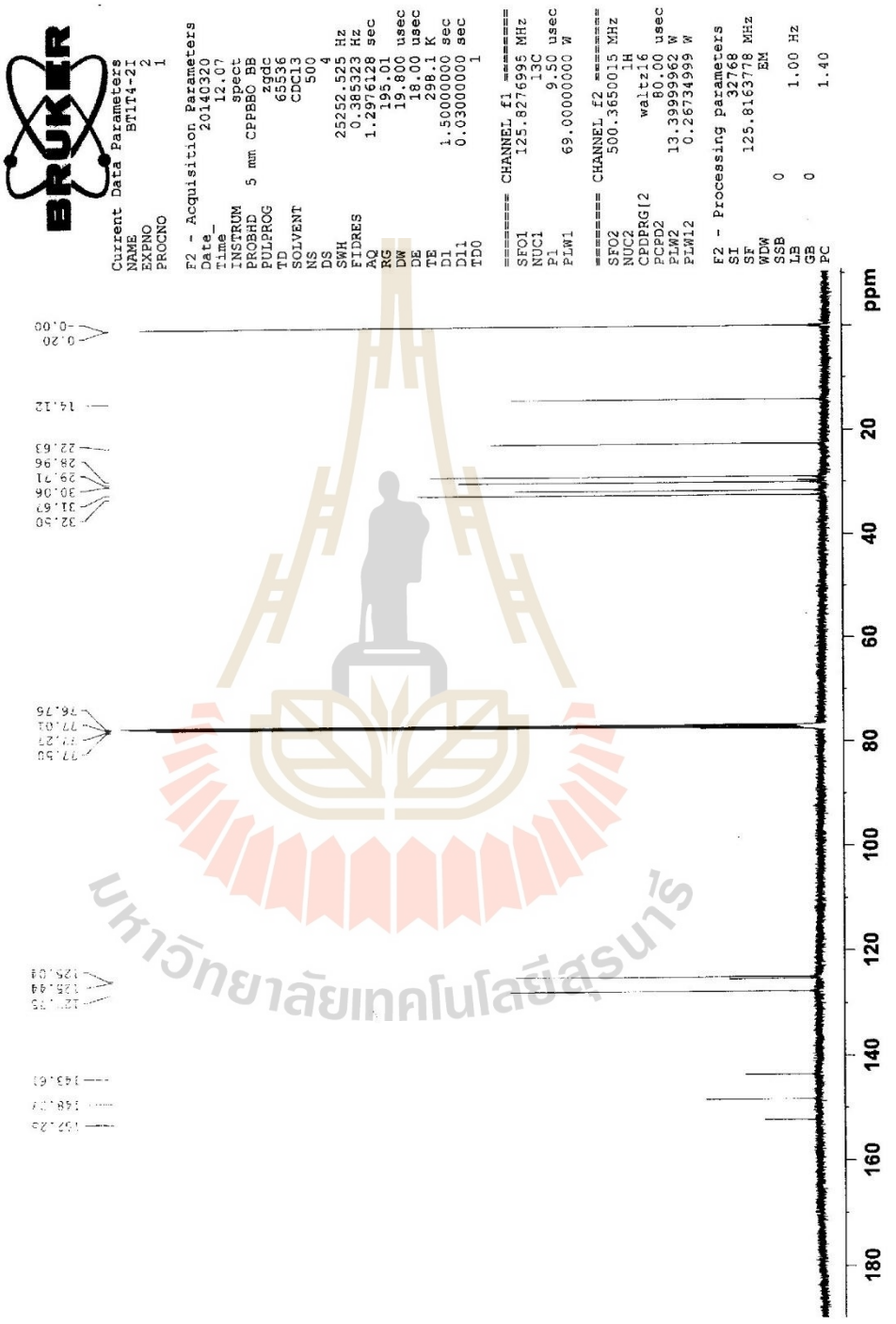
Current Data Parameters
NAME BT1T4-21
EXPNO 2
PROCNO 1
F2 - Acquisition Parameters
Date_ 20140320
Time_ 12.07
INSTRUM spect
PROBHD 5 mm CPPBBO BB
PULPROG zgdc
TD 65536
SOLVENT CDCl3
NS 500
DS 4
SWH 25252.525 Hz
FIDRES 0.385323 Hz
AQ 1.2976128 sec
RG 195.01
DW 19.800 usec
DE 18.00 usec
TE 298.1 K
D1 1.50000000 sec
D11 0.03000000 sec
TD0 1
CHANNEL f1
SFO1 125.8276995 MHz
NUC1 13C
P1 9.50 usec
PLW1 69.00000000 W
CHANNEL f2
SFO2 500.3650015 MHz
NUC2 1H
CPDPRG2 waltz16
PCPD2 80.00 usec
PLW2 13.39999962 W
PLW12 0.26734999 W
F2 - Processing parameters
SI 32768
SF 125.8163778 MHz
WDW EM
SSB 0
LB 1.00 Hz
GB 0
PC 1.40
0.20
-0.00
14.12
22.63
28.96
29.71
30.06
31.67
32.50
76.76
77.01
77.27
77.50
125.04
125.44
125.75
143.61
148.17
152.26
ppm
20
40
60
80
100
120
140
160
180

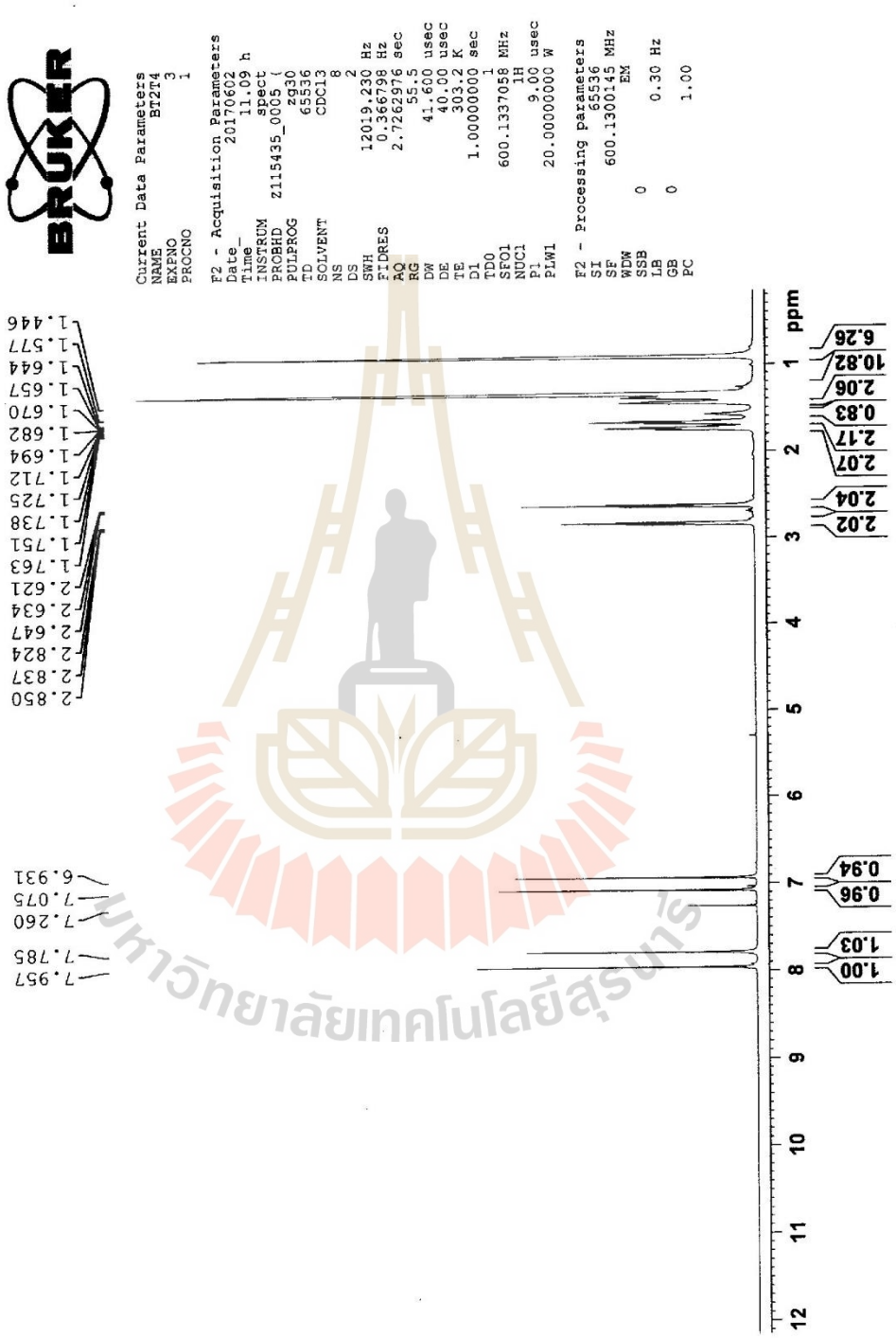

มหาวิทยาลัยเทคโนโลยีสุรนารี

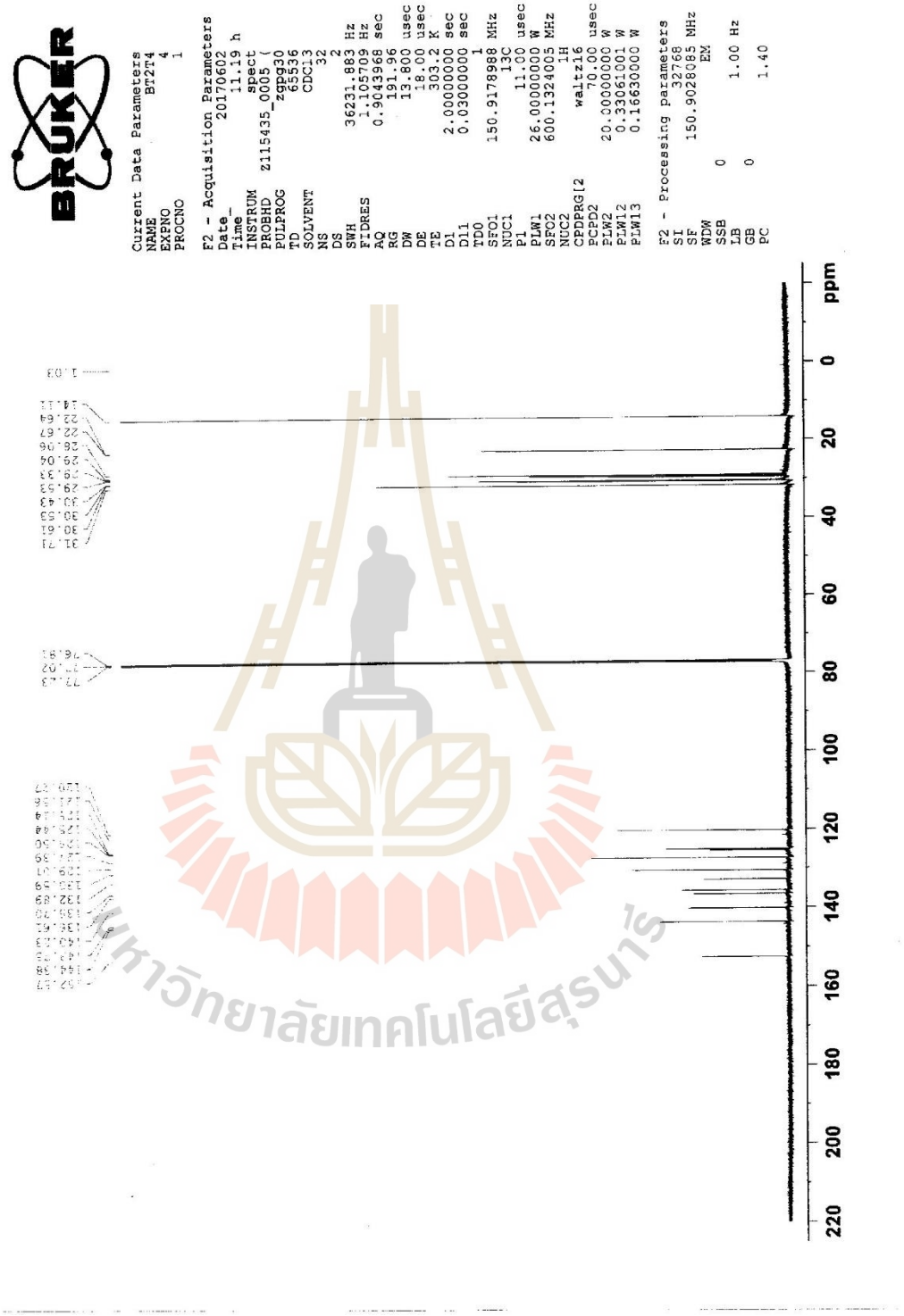
Current Data Parameters
NAME BT2T4
EXPNO 4
PROCNO 1
F2 - Acquisition Parameters
Date_ 20170602
Time 11.19 h
INSTRUM spect
PROBHD 2115435_0005 (
PULPROG zgpg30
TD 65536
SOLVENT CDCl3
NS 32
DS 2
SWH 36231.883 Hz
FIDRES 1.105709 Hz
AQ 0.9043968 sec
RG 191.96
DW 13.800 usec
DE 18.00 usec
TE 303.2 K
D1 2.00000000 sec
D11 0.03000000 sec
TD0 1
SFO1 150.9178988 MHz
NUC1 13C
P1 11.00 usec
PLW1 26.00000000 W
SFO2 600.1324005 MHz
NUC2 1H
CPDPRG[2 waltz16
PCPD2 70.00 usec
PLW2 20.00000000 W
PLW12 0.33061001 W
PLW13 0.16630000 W
F2 - Processing parameters
SI 32768
SF 150.9028085 MHz
WDW EM
SSB 0
LB 1.00 Hz
GB 0
PC 1.40
ppm
220
200
180
160
140
120
100
80
60
40
20
0

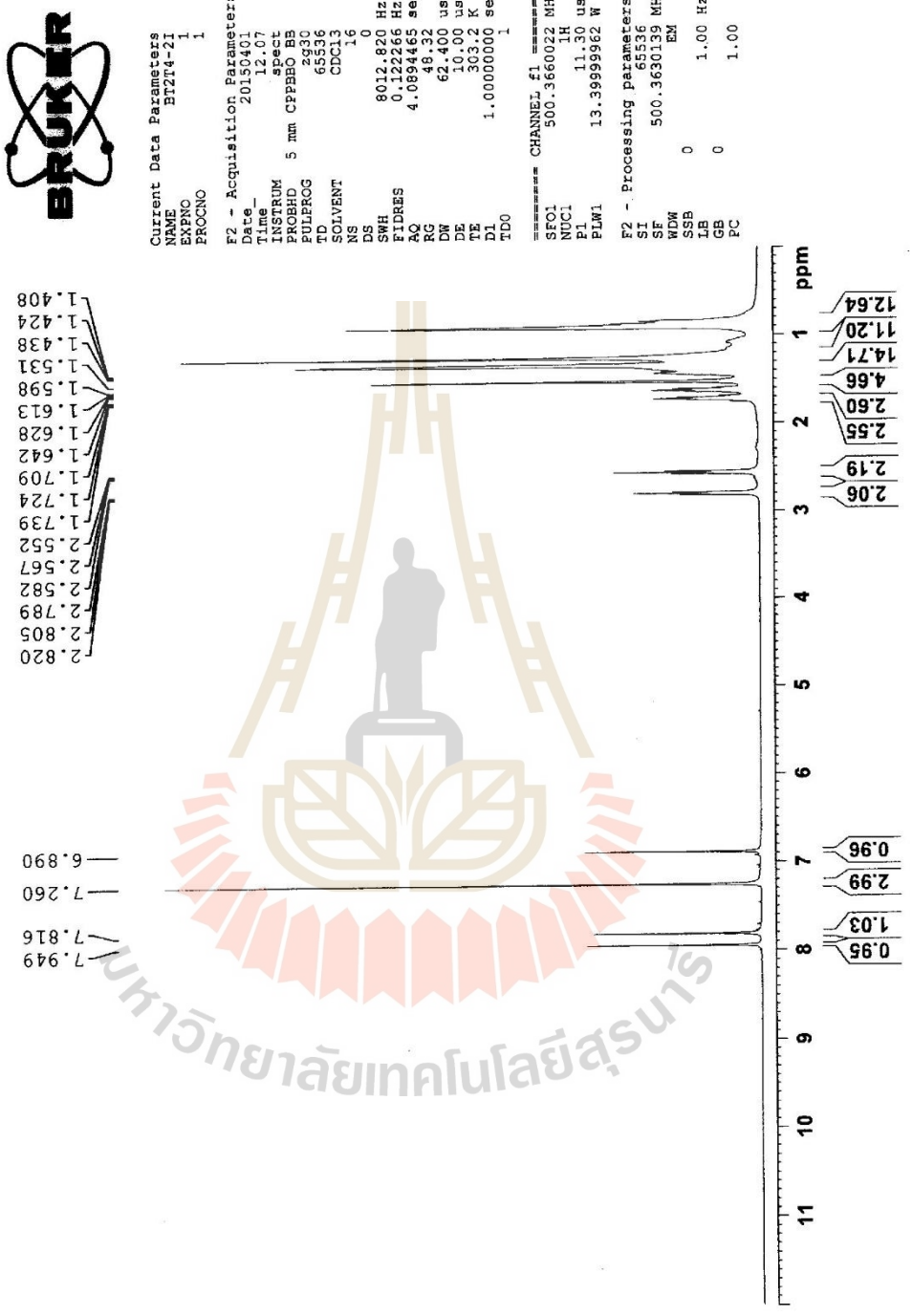
Current Data Parameters
NAME B12T4-2I
EXPNO 1
PROCNO 1
F2 - Acquisition Parameters
Date_ 20150401
Time 12.07
INSTRUM spect
PROBHD 5 mm CPPBBO BB
PULPROG zg30
TD 65536
SOLVENT CDCl3
NS 16
DS 0
SWH 8012.820 Hz
FIDRES 0.122266 Hz
AQ 4.0894465 sec
RG 48.32
DW 62.400 usec
DE 10.00 usec
TE 303.2 K
D1 1.00000000 sec
TD0 1
======== CHANNEL f1 ========
SFO1 500.3660022 MHz
NUC1 1H
P1 11.30 usec
PLW1 13.39999962 W
F2 - Processing parameters
SI 65536
SF 500.3630139 MHz
WDW EM
SSB 0
LB 1.00 Hz
GB 0
PC 1.00
ppm
12.64
11.20
14.71
4.66
2.60
2.55
2.19
2.06
0.96
2.99
1.03
0.95
1.408
1.424
1.438
1.531
1.598
1.613
1.628
1.642
1.709
1.724
1.739
2.552
2.567
2.582
2.789
2.805
2.820
6.890
7.260
7.816
7.949

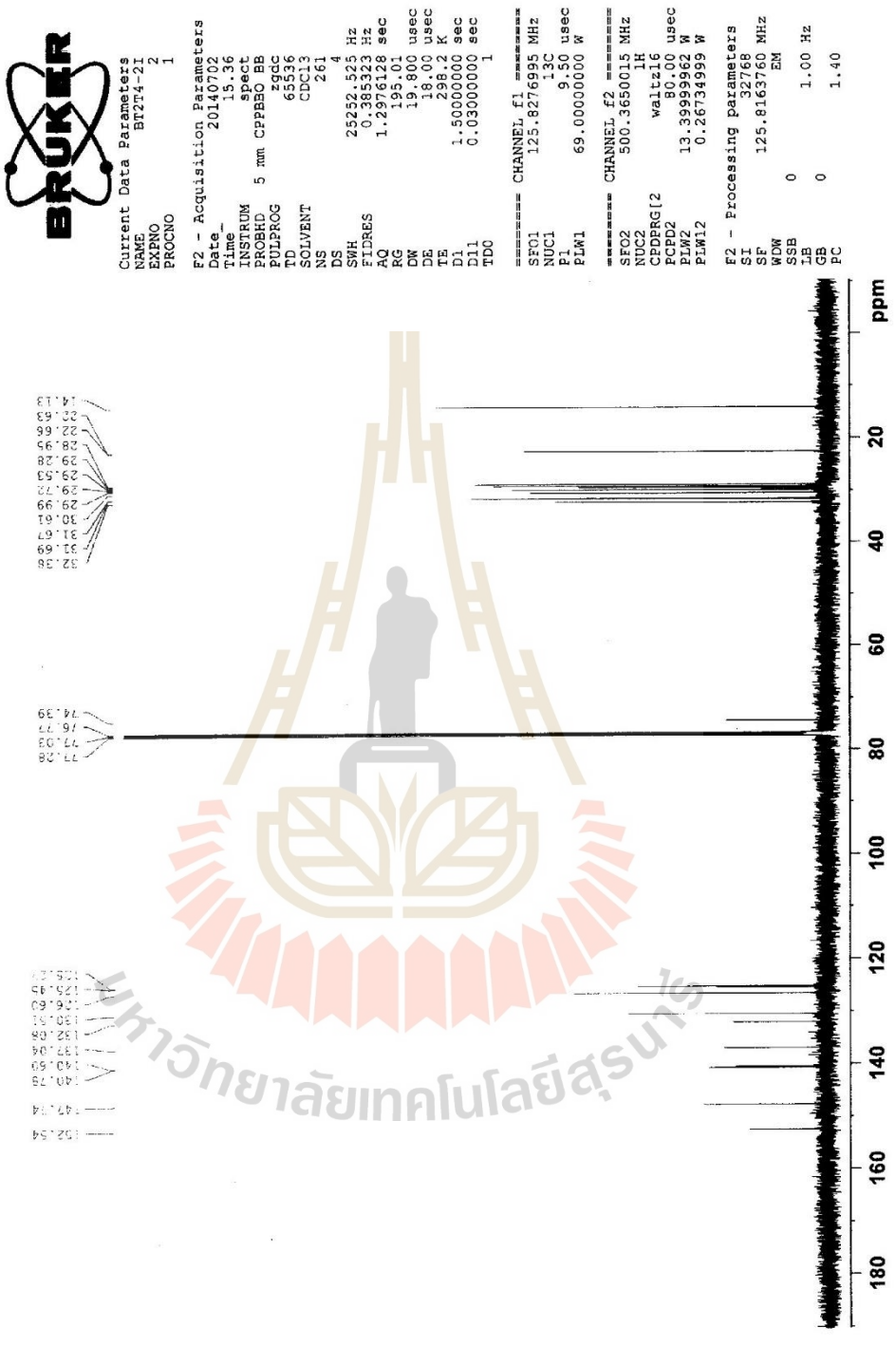
BRUKER
Current Data Parameters
NAME BT274-2I
EXPNO 2
PROCNO 1
F2 - Acquisition Parameters
Date_ 20140702
Time_ 15.36
INSTRUM spect
PROBHD 5 mm CPPBBO BB
PULPROG zgdc
TD 65536
SOLVENT CDCl3
NS 261
DS 4
SWH 25252.525 Hz
FIDRES 0.385323 Hz
AQ 1.2976128 sec
RG 195.01
DW 19.800 usec
DE 18.00 usec
TE 298.2 K
D1 1.50000000 sec
D11 0.03000000 sec
TD0 1
======== CHANNEL f1 ========
SFO1 125.8276995 MHz
NUC1 13C
P1 9.50 usec
PLW1 69.00000000 W
======== CHANNEL f2 ========
SFO2 500.3650015 MHz
NUC2 1H
CPDPRG[2 waltz16
PCPD2 80.00 usec
PLW2 13.39999962 W
PLW12 0.26734999 W
F2 - Processing parameters
SI 32768
SF 125.8163760 MHz
WDW EM
SSB 0
LB 1.00 Hz
GB 0
PC 1.40
ppm
180
160
140
120
100
80
60
40
20
14.13
22.63
22.66
28.95
29.28
29.53
29.72
29.99
30.61
31.67
31.69
32.38
74.39
76.77
77.03
77.28
102.54
147.74
140.79
140.60
137.06
132.08
130.61
126.60
125.95
125.27

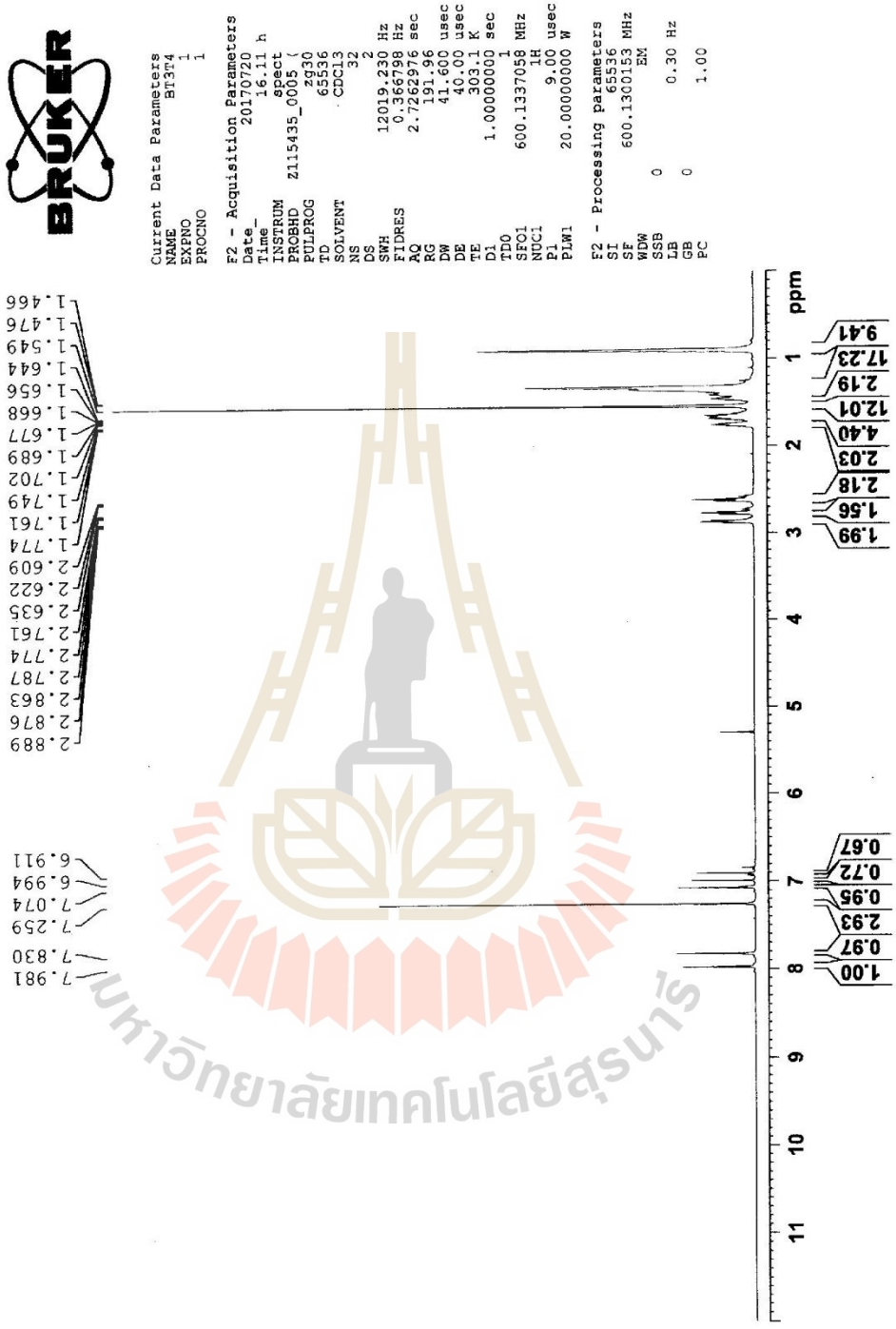

มหาวิทยาลัยเทคโนโลยีสุรนารี

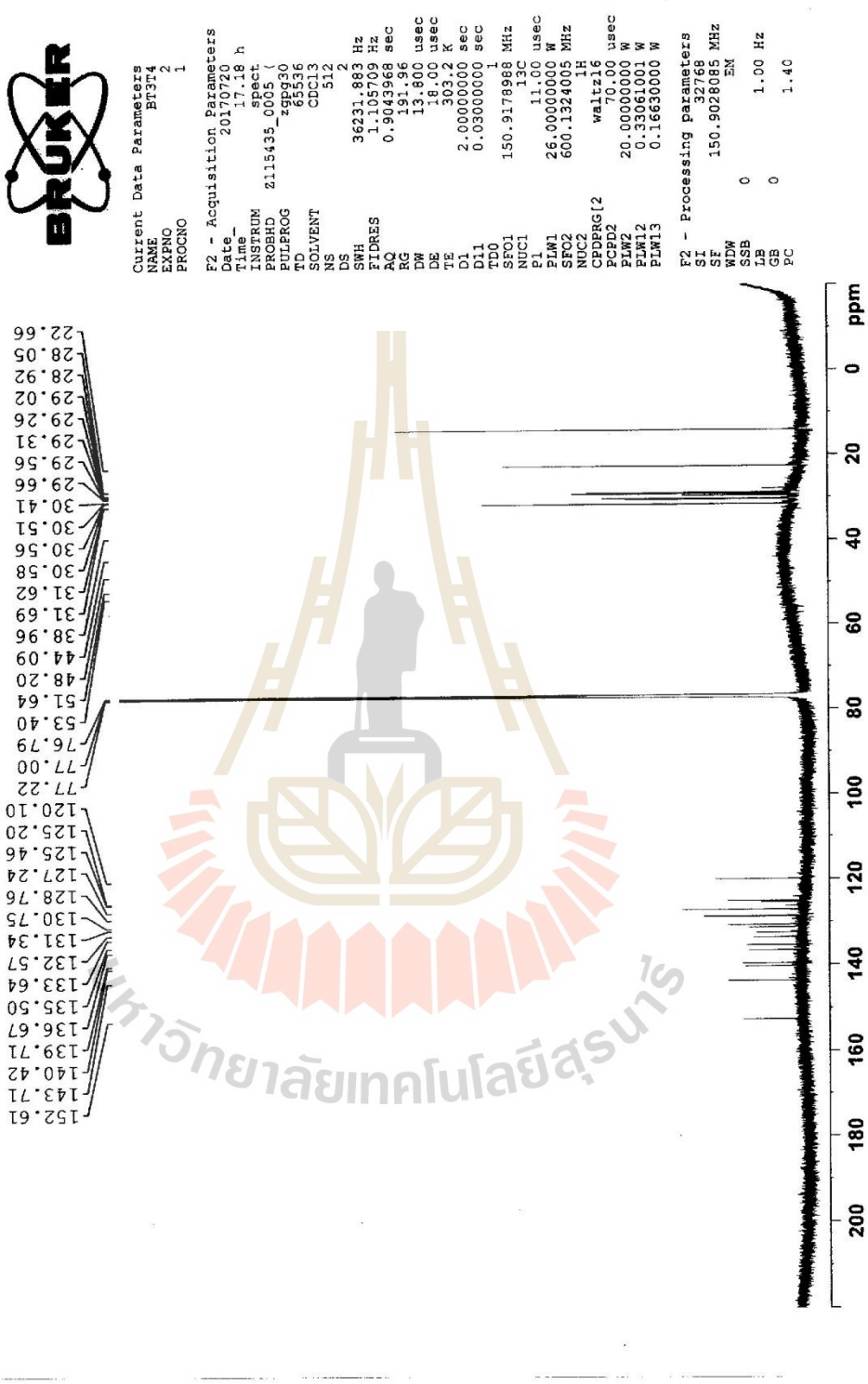
Current Data Parameters
NAME BT3T4
EXPNO 2
PROCNO 1
F2 - Acquisition Parameters
Date_ 20170720
Time 17.18 h
INSTRUM spect
PROBHD Z115435_0005 (
PULPROG zgpg30
TD 65536
SOLVENT CDCl3
NS 512
DS 2
SWH 36231.883 Hz
FIDRES 1.105709 Hz
AQ 0.9043968 sec
RG 191.96
DW 13.800 usec
DE 18.00 usec
TE 303.2 K
D1 2.00000000 sec
D11 0.03000000 sec
TD0 1
SFO1 150.9178988 MHz
NUC1 13C
P1 11.00 usec
PLW1 26.00000000 W
SFO2 600.1324005 MHz
NUC2 1H
CPDPRG[2 waltz16
PCPD2 70.00 usec
PLW2 20.00000000 W
PLW12 0.33061001 W
PLW13 0.16630000 W
F2 - Processing parameters
SI 32768
SF 150.9028085 MHz
WDW EM
SSB 0
LB 1.00 Hz
GB 0
PC 1.40
ppm
22.66
28.05
28.92
29.02
29.26
29.31
29.56
29.66
30.41
30.51
30.56
30.58
31.62
31.69
38.96
44.09
48.20
51.64
53.40
76.79
77.00
77.22
120.10
125.20
125.46
127.24
128.76
130.75
131.34
132.57
133.64
135.50
136.67
139.71
140.42
143.71
152.61

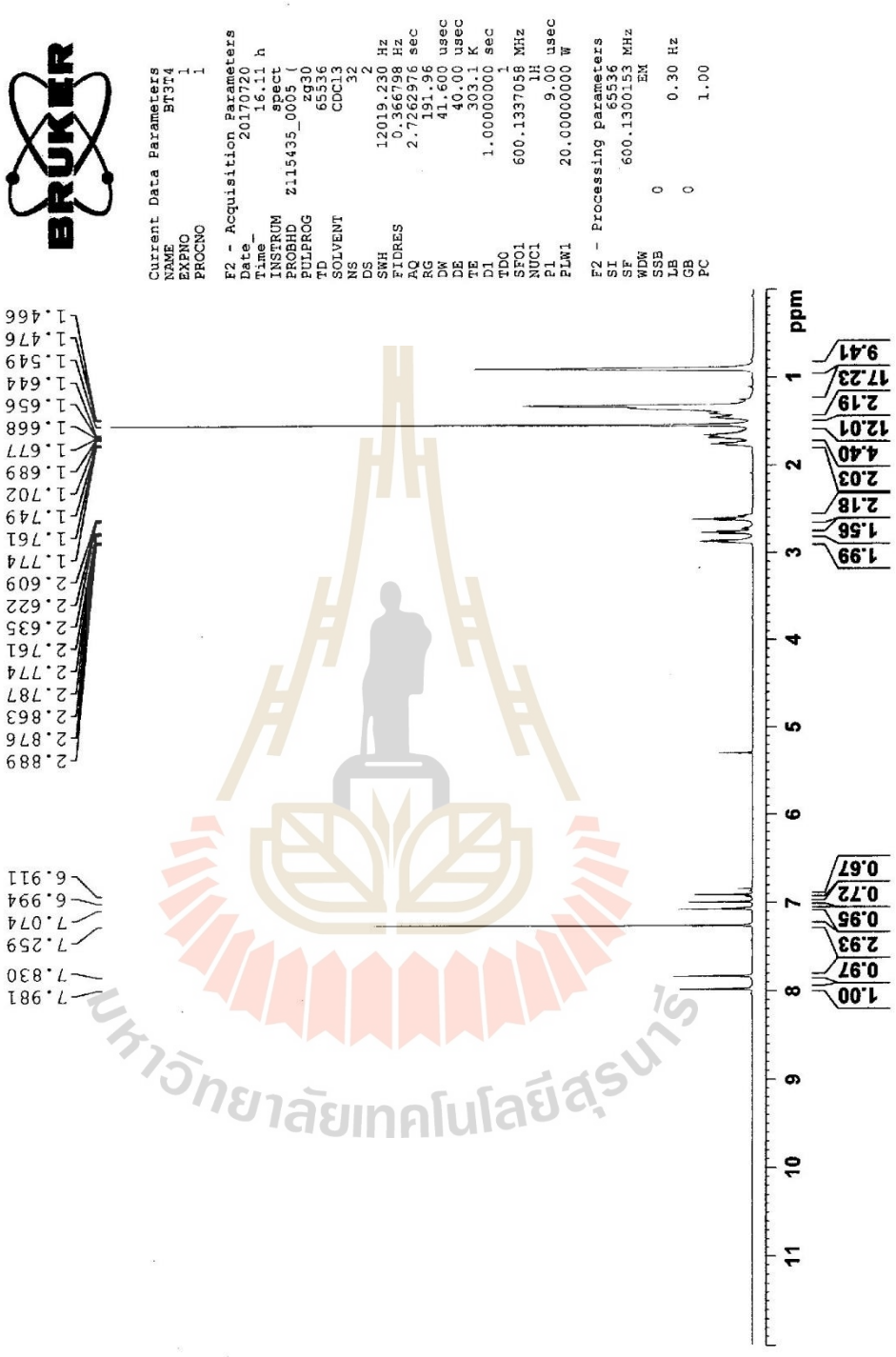

มหาวิทยาลัยเทคโนโลยีสุรนารี

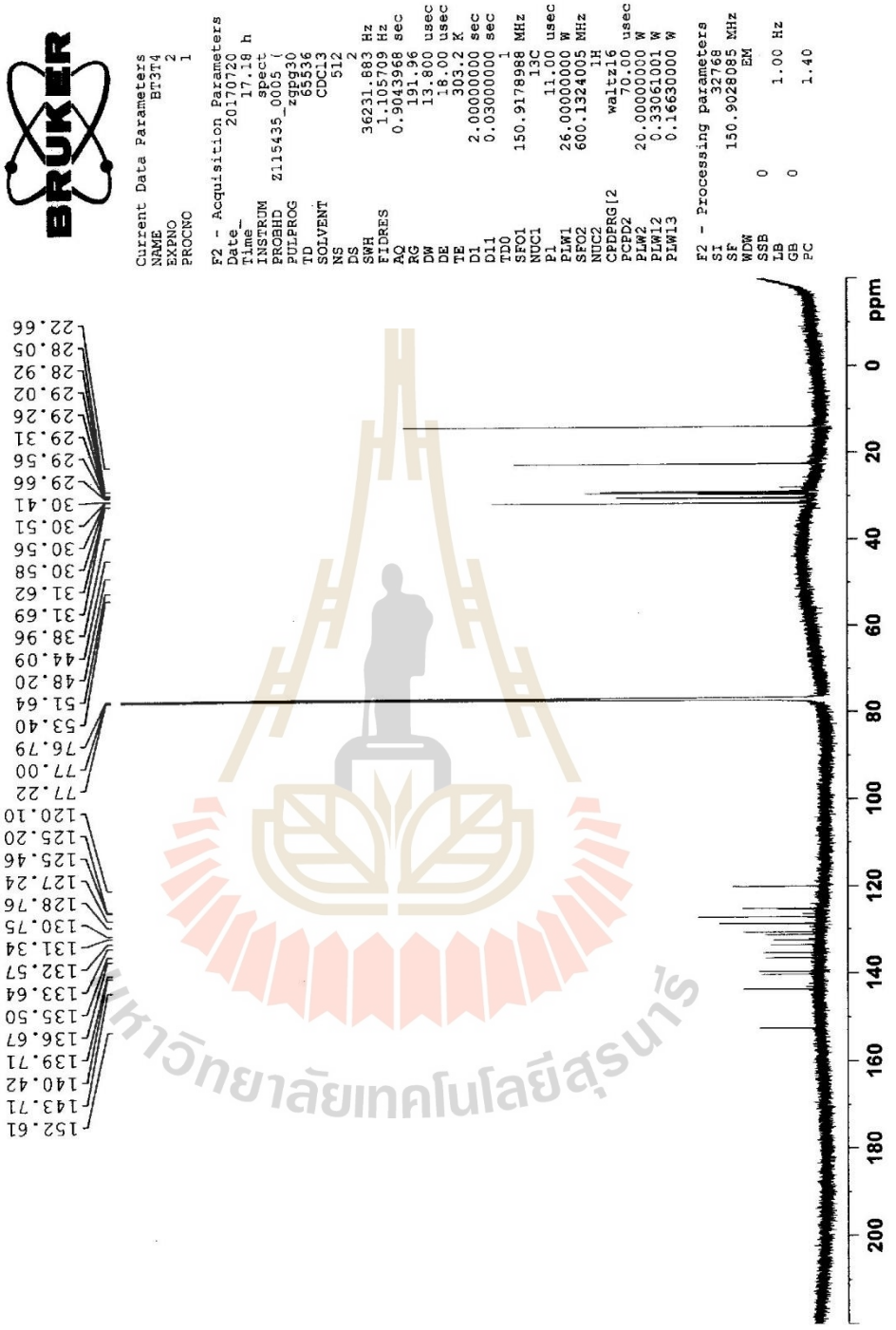
BRUKER
Current Data Parameters
NAME BT3T4
EXPNO 2
PROCNO 1
F2 - Acquisition Parameters
Date_ 20170720
Time_ 17.18 h
INSTRUM spect
PROBHD Z115435_0005 (
PULPROG zgpg30
TD 65536
SOLVENT CDCl3
NS 512
DS 2
SWH 36231.883 Hz
FIDRES 1.105709 Hz
AQ 0.9043968 sec
RG 191.96
DW 13.800 usec
DE 18.00 usec
TE 303.2 K
D1 2.00000000 sec
D11 0.03000000 sec
TD0 1
SFO1 150.9178988 MHz
NUC1 13C
P1 11.00 usec
PLW1 26.00000000 W
SFO2 600.1324005 MHz
NUC2 1H
CPDPRG[2 waltz16
PCPD2 70.00 usec
PLW2 20.00000000 W
PLW12 0.33061001 W
PLW13 0.16630000 W
F2 - Processing parameters
SI 32768
SF 150.9028085 MHz
WDW EM
SSB 0
LB 1.00 Hz
GB 0
PC 1.40
ppm
0
20
40
60
80
100
120
140
160
180
200
22.66
28.05
28.92
29.02
29.26
29.31
29.56
29.66
30.41
30.51
30.56
30.58
31.62
31.69
38.96
44.09
48.20
51.64
53.40
76.79
77.00
77.22
120.10
125.20
125.46
127.24
128.76
130.75
131.34
132.57
133.64
135.50
136.67
139.71
140.42
143.71
152.61

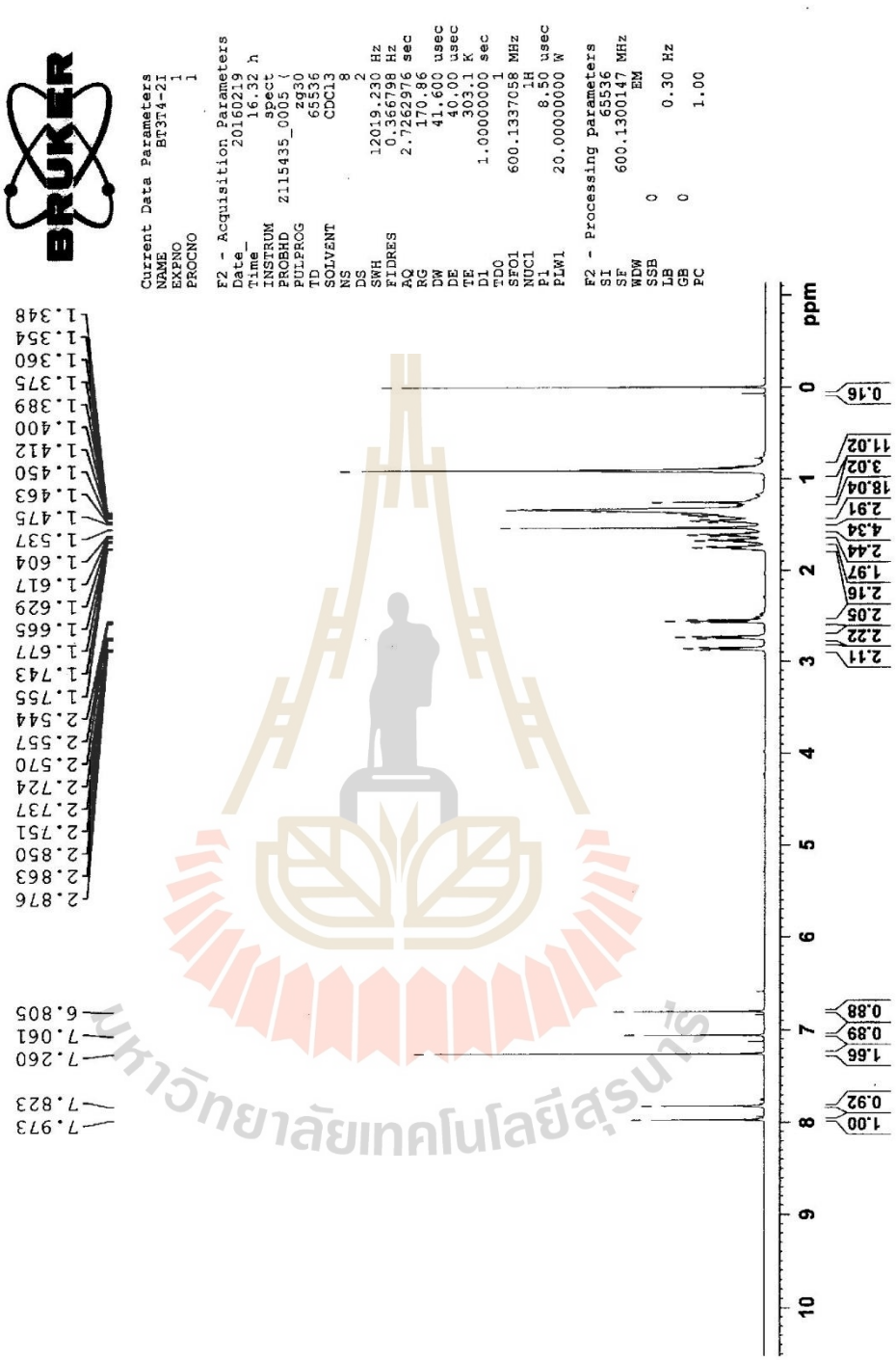
Current Data Parameters
NAME BI3T4-2I
EXPNO 1
PROCNO 1
F2 - Acquisition Parameters
Date_ 20160219
Time_ 16.32 h
INSTRUM spect
PROBHD 2115435_0005 (
PULPROG zg30
TD 65536
SOLVENT CDCl3
NS 8
DS 2
SWH 12019.230 Hz
FIDRES 0.366798 Hz
AQ 2.7262976 sec
RG 170.86
DW 41.600 usec
DE 40.00 usec
TE 303.1 K
D1 1.00000000 sec
TD0 1
SFO1 600.1337058 MHz
NUC1 1H
P1 8.50 usec
PLW1 20.00000000 W
F2 - Processing parameters
SI 65536
SF 600.1300147 MHz
WDW EM
SSB 0
LB 0.30 Hz
GB 0
PC 1.00
ppm
0.16
11.02
3.02
18.04
2.91
4.34
2.44
1.97
2.16
2.05
2.22
2.11
1.00
0.92
1.66
0.89
0.88
7.973
7.823
7.260
7.061
6.805
2.876
2.863
2.850
2.751
2.737
2.724
2.570
2.557
2.544
1.755
1.743
1.677
1.665
1.629
1.617
1.604
1.537
1.475
1.463
1.450
1.412
1.400
1.389
1.375
1.360
1.354
1.348

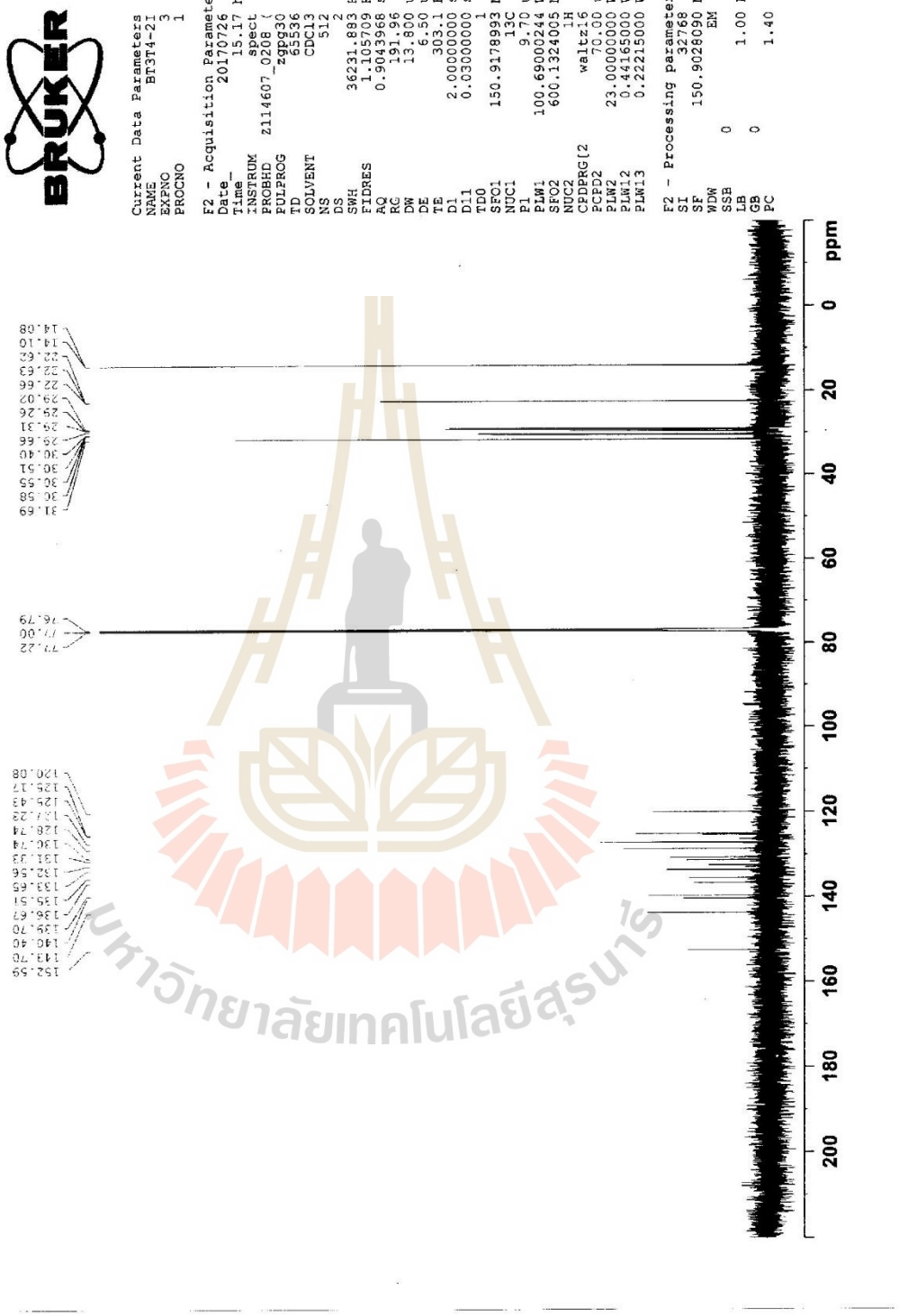
Current Data Parameters
NAME BT3T4-2I
EXPNO 3
PROCNO 1
F2 - Acquisition Parameters
Date_ 20170726
Time_ 15.17 h
INSTRUM spect
PROBHD Z114607_0208 (
PULPROG zgpg30
TD 65536
SOLVENT CDCl3
NS 512
DS 2
SWH 36231.883 Hz
FIDRES 1.105709 Hz
AQ 0.9043968 sec
RG 191.96
DW 13.800 usec
DE 6.50 usec
TE 303.1 K
D1 2.00000000 sec
D11 0.03000000 sec
TD0 1
SFO1 150.9178993 MHz
NUC1 13C
P1 9.70 usec
PLW1 100.69000244 W
SFO2 600.1324005 MHz
NUC2 1H
CPDPRG[2 waltz16
PCPD2 70.00 usec
PLW2 23.00000000 W
PLW12 0.44165000 W
PLW13 0.22215000 W
F2 - Processing parameters
SI 32768
SF 150.9028090 MHz
WDW EM
SSB 0
LB 1.00 Hz
GB 0
PC 1.40
14.08
14.10
22.62
22.63
22.66
29.02
29.26
29.31
29.66
30.40
30.51
30.55
30.58
31.69
76.79
77.00
77.22
120.08
125.17
125.43
127.23
128.74
130.74
131.33
132.56
133.65
135.51
136.67
139.70
140.40
143.70
152.59
ppm
0
20
40
60
80
100
120
140
160
180
200

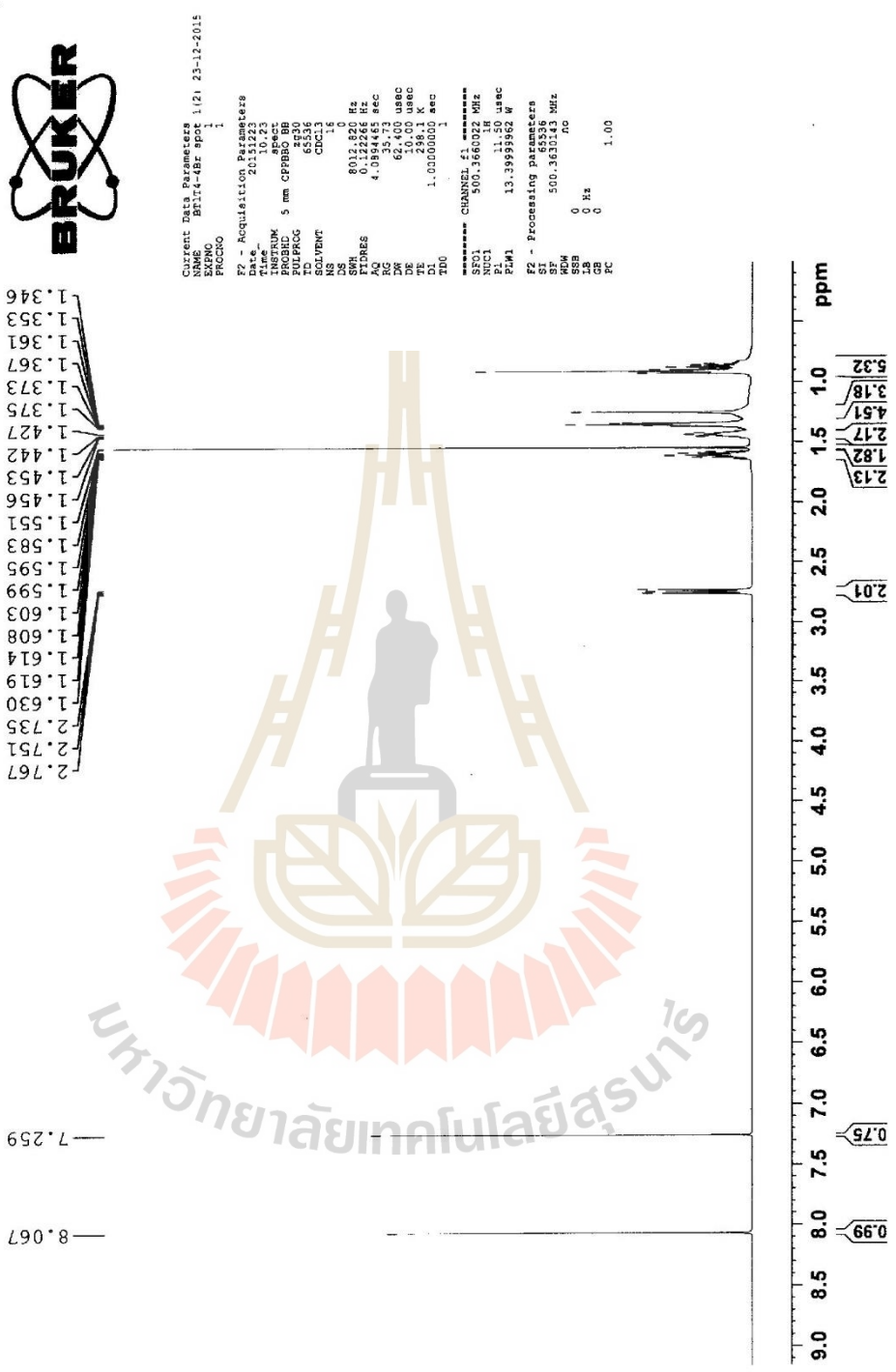

มหาวิทยาลัยเทคโนโลยีสุรนารี

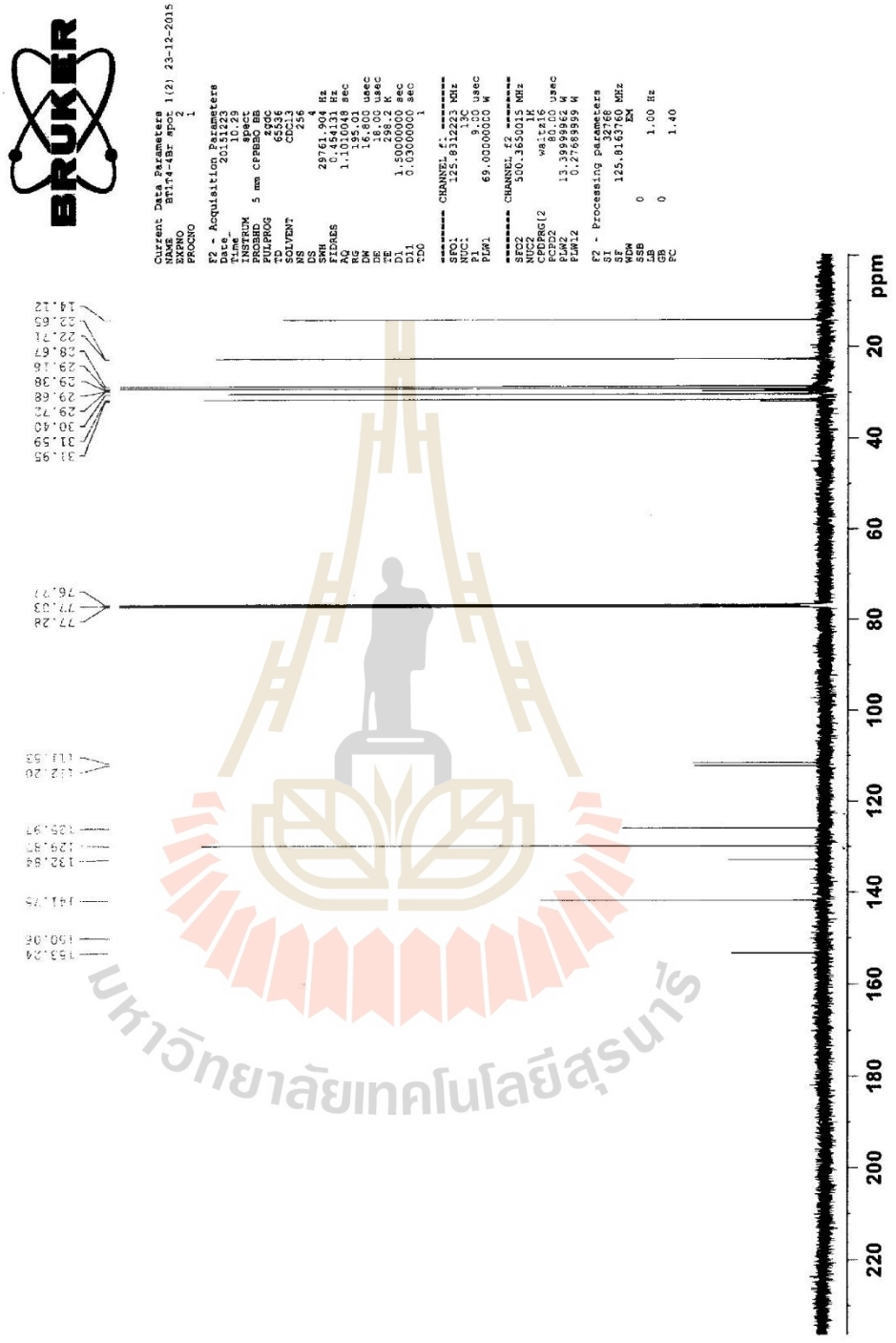
BRUKER
Current Data Parameters
NAME Br(4-Br)2
EXPNO 1(2) 23-12-2015
PROCNO 1
F2 - Acquisition Parameters
Date_ 20151223
Time 10.29
INSTRUM spect
PROBHD 5 mm CPPBBO BB
PULPROG zgpg
TD 65536
SOLVENT CDCl3
NS 256
DS 4
SWH 29761.904 Hz
FIDRES 0.454131 Hz
AQ 1.1010048 sec
RG 195.01
DW 16.800 usec
DE 18.00 usec
TE 298.2 K
D1 1.50000000 sec
D11 0.03000000 sec
TD0 1
CHANNEL f1
SFO1 125.8312223 MHz
NUC1 13C
P1 9.00 usec
PLW1 69.00000000 W
CHANNEL f2
SFO2 500.3650015 MHz
NUC2 1H
CPDPRG[2 waltz16
PCPD2 80.00 usec
PLW2 13.39999962 W
PLW12 0.27699999 W
F2 - Processing parameters
SI 32768
SF 125.0163760 MHz
WDW EM
SSB 0
LB 1.00 Hz
GB 0
PC 1.40
14.12
22.65
22.71
28.67
29.18
29.38
29.68
29.72
30.40
31.59
31.95
76.97
77.03
77.28
112.20
113.53
125.97
129.87
132.66
141.75
150.06
153.24
ppm
220
200
180
160
140
120
100
80
60
40
20

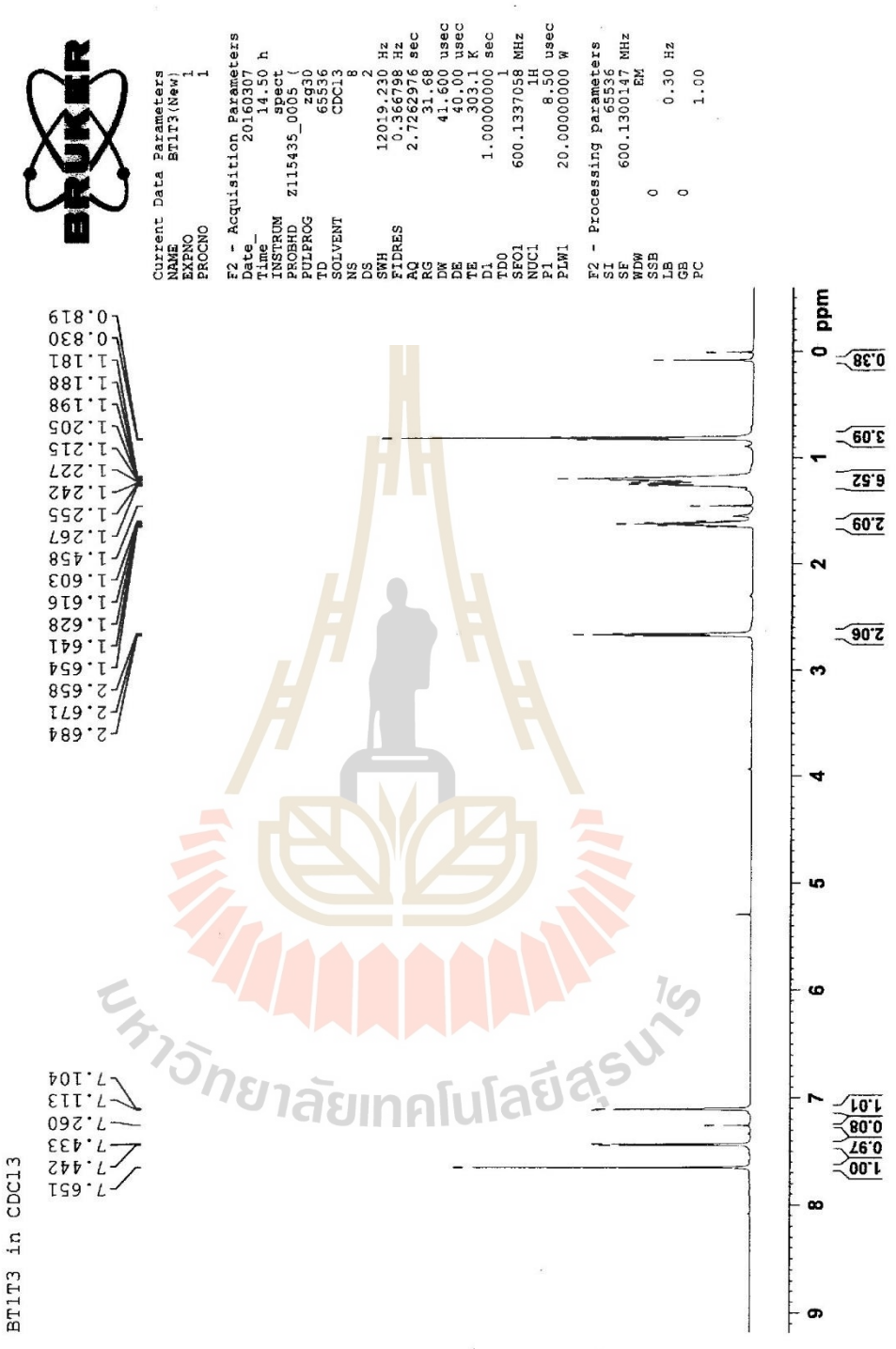
BRUKER
Current Data Parameters
NAME BT1T3(New)
EXPNO 1
PROCNO 1
F2 - Acquisition Parameters
Date_ 20160307
Time 14.50 h
INSTRUM spect
PROBHD Z115435_0005 (
PULPROG zg30
TD 65536
SOLVENT CDCl3
NS 8
DS 2
SWH 12019.230 Hz
FIDRES 0.366798 Hz
AQ 2.7262976 sec
RG 31.68
DW 41.600 usec
DE 40.00 usec
TE 303.1 K
D1 1.00000000 sec
TD0 1
SFO1 600.1337058 MHz
NUC1 1H
P1 8.50 usec
PLW1 20.00000000 W
F2 - Processing parameters
SI 65536
SF 600.1300147 MHz
WDW EM
SSB 0
LB 0.30 Hz
GB 0
PC 1.00
BT1T3 in CDCl3
0.819
0.830
1.181
1.188
1.198
1.205
1.215
1.227
1.242
1.255
1.267
1.458
1.603
1.616
1.628
1.641
1.654
2.658
2.671
2.684
7.104
7.113
7.260
7.433
7.442
7.651
0.38
3.09
6.52
2.09
2.06
1.00
0.97
0.08
1.01
ppm

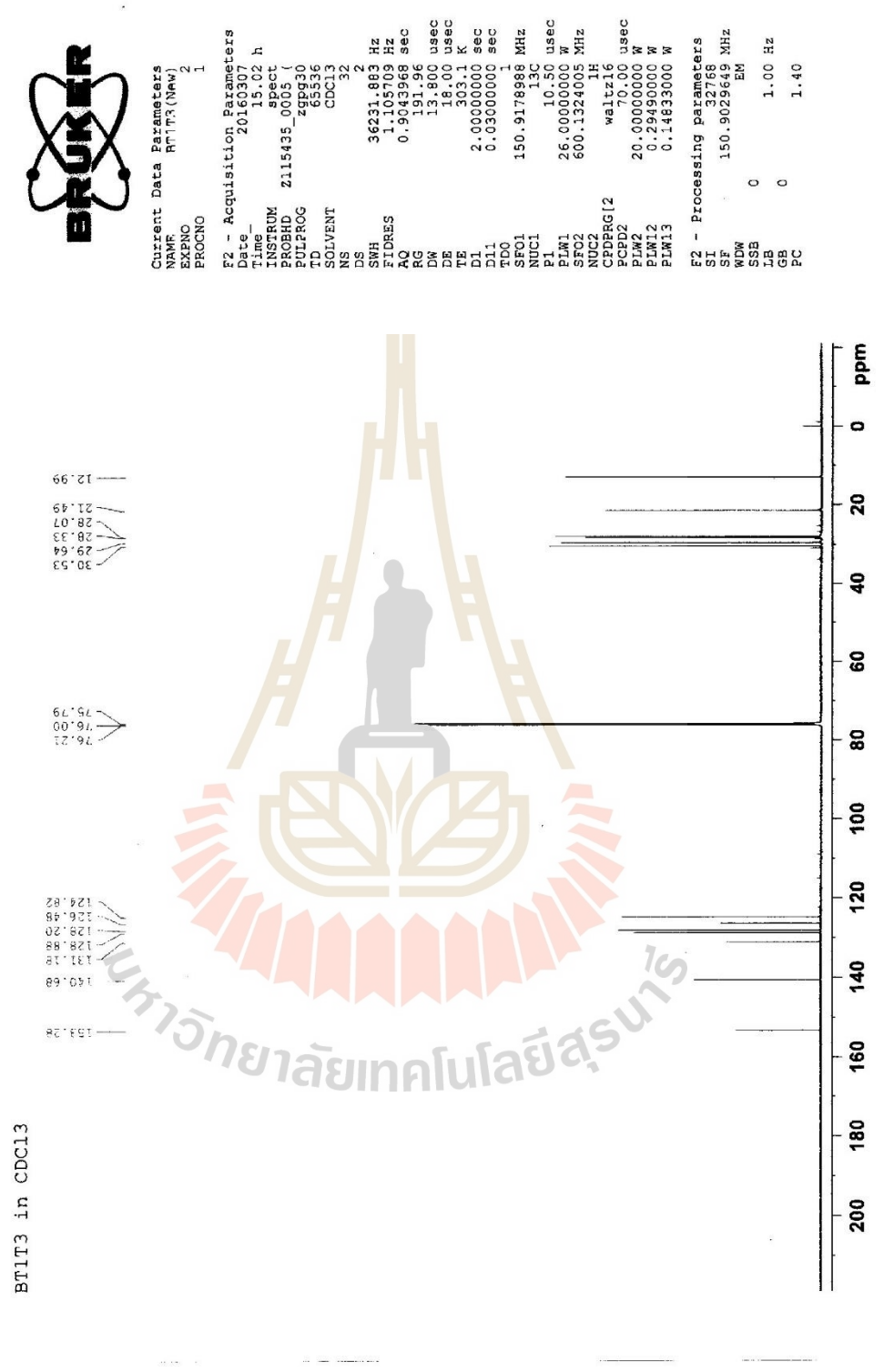
Current Data Parameters
NAME RT1T3(NMR)
EXPNO 2
PROCNO 1
F2 - Acquisition Parameters
Date_ 20160307
Time_ 15.02 h
INSTRUM spect
PROBHD 2115435_0005 (
PULPROG zgpg30
TD 65536
SOLVENT CDCl3
NS 32
DS 2
SWH 36231.883 Hz
FIDRES 1.105709 Hz
AQ 0.9043968 sec
RG 191.96
DW 13.800 usec
DE 18.00 usec
TE 303.1 K
D1 2.00000000 sec
D11 0.03000000 sec
TD0 1
SFO1 150.9178988 MHz
NUC1 13C
P1 10.50 usec
PLW1 26.00000000 W
SFO2 600.1324005 MHz
NUC2 1H
CPDPRG[2 waltz16
PCPD2 70.00 usec
PLW2 20.00000000 W
PLW12 0.29490000 W
PLW13 0.14833000 W
F2 - Processing parameters
SI 32768
SF 150.9029649 MHz
WDW EM
SSB 0
LB 1.00 Hz
GB 0
PC 1.40
BT1T3 in CDCl3
153.28
140.68
131.18
128.88
128.20
126.98
124.82
76.21
76.00
75.79
30.53
29.64
28.33
28.07
21.49
12.99
ppm

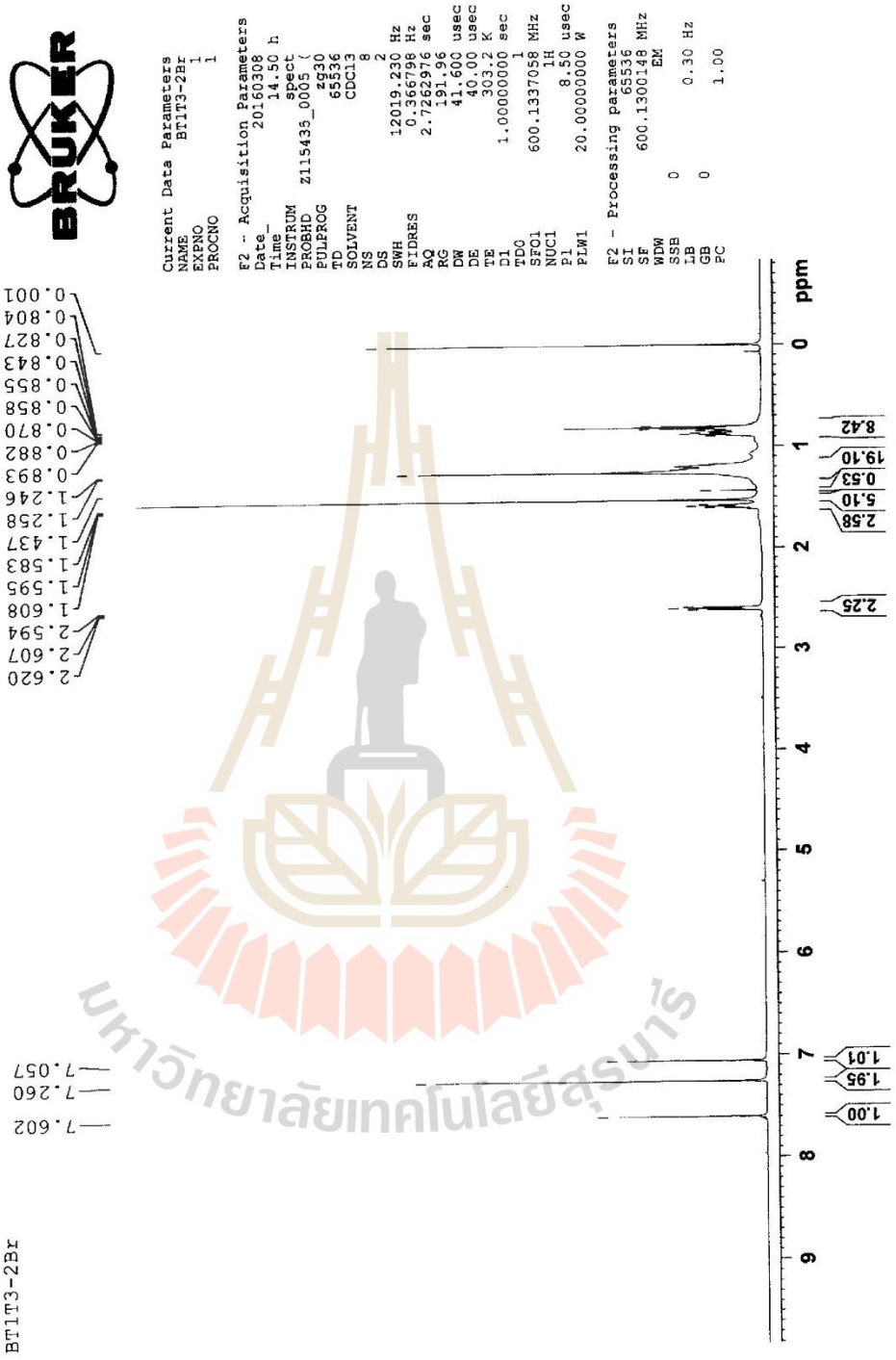

มหาวิทยาลัยเทคโนโลยีสุรนารี

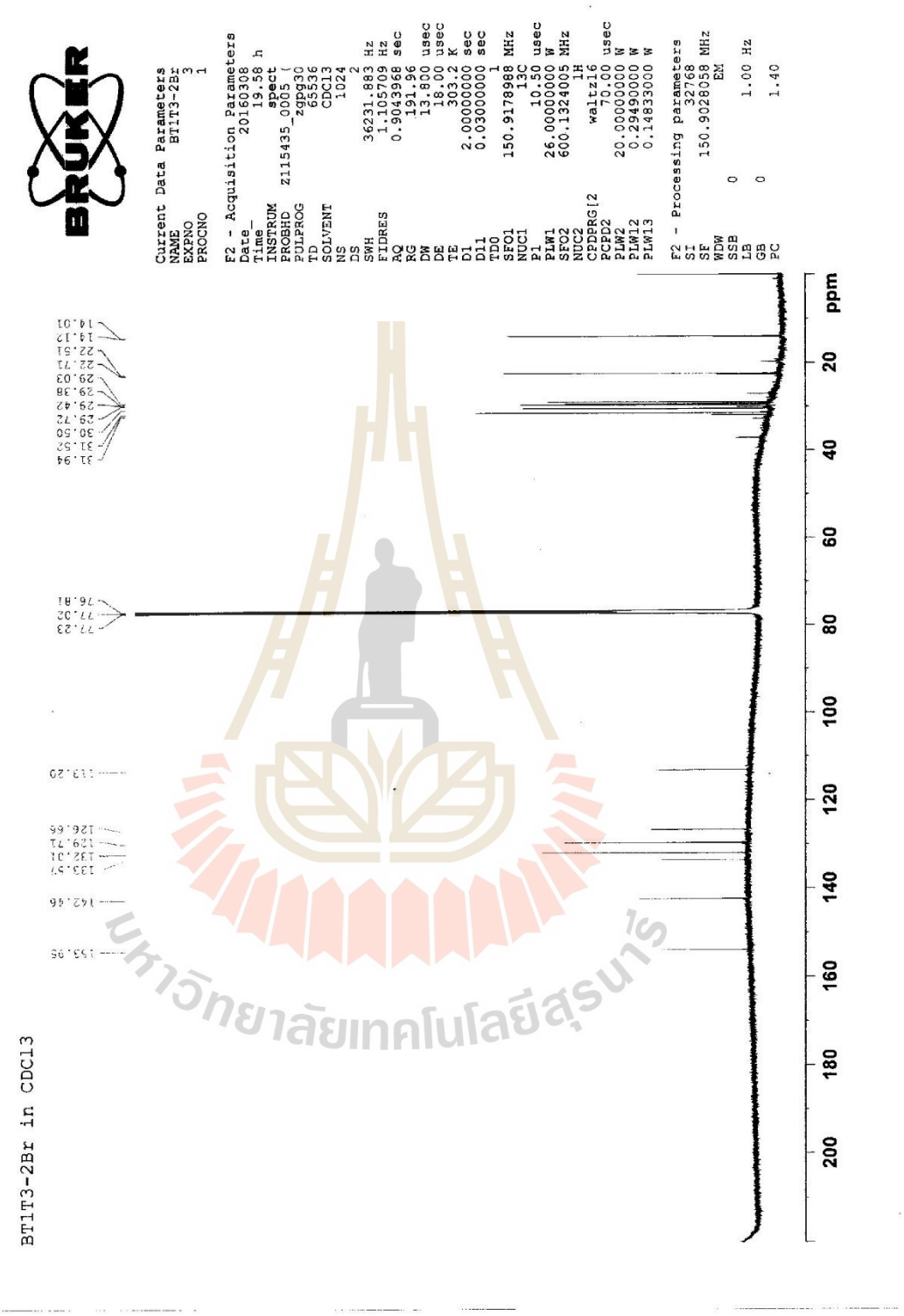
BRUKER
Current Data Parameters
NAME BT1T3-2Br
EXPNO 3
PROCNO 1
F2 - Acquisition Parameters
Date_ 20160308
Time 19.58 h
INSTRUM spect
PROBHD Z115435_0005 (
PULPROG zgpg30
TD 65536
SOLVENT CDCl3
NS 1024
DS 2
SWH 36231.883 Hz
FIDRES 1.105709 Hz
AQ 0.90439968 sec
RG 191.96
DW 13.800 usec
DE 18.00 usec
TE 303.2 K
D1 2.00000000 sec
D11 0.03000000 sec
TD0 1
SFO1 150.9178988 MHz
NUC1 13C
P1 10.50 usec
PLW1 26.00000000 W
SFO2 600.1324005 MHz
NUC2 1H
CPDPRG[2 waltz16
PCPD2 70.00 usec
PLW2 20.00000000 W
PLW12 0.29490000 W
PLW13 0.14833000 W
F2 - Processing parameters
SI 32768
SF 150.9028058 MHz
WDW EM
SSB 0
LB 1.00 Hz
GB 0
PC 1.40
14.01
19.12
22.51
22.71
29.03
29.38
29.42
29.72
30.50
31.52
31.94
76.81
77.02
77.23
113.20
126.66
129.71
132.31
135.57
142.46
153.95
BT1T3-2Br in CDCl3
ppm
200
180
160
140
120
100
80
60
40
20

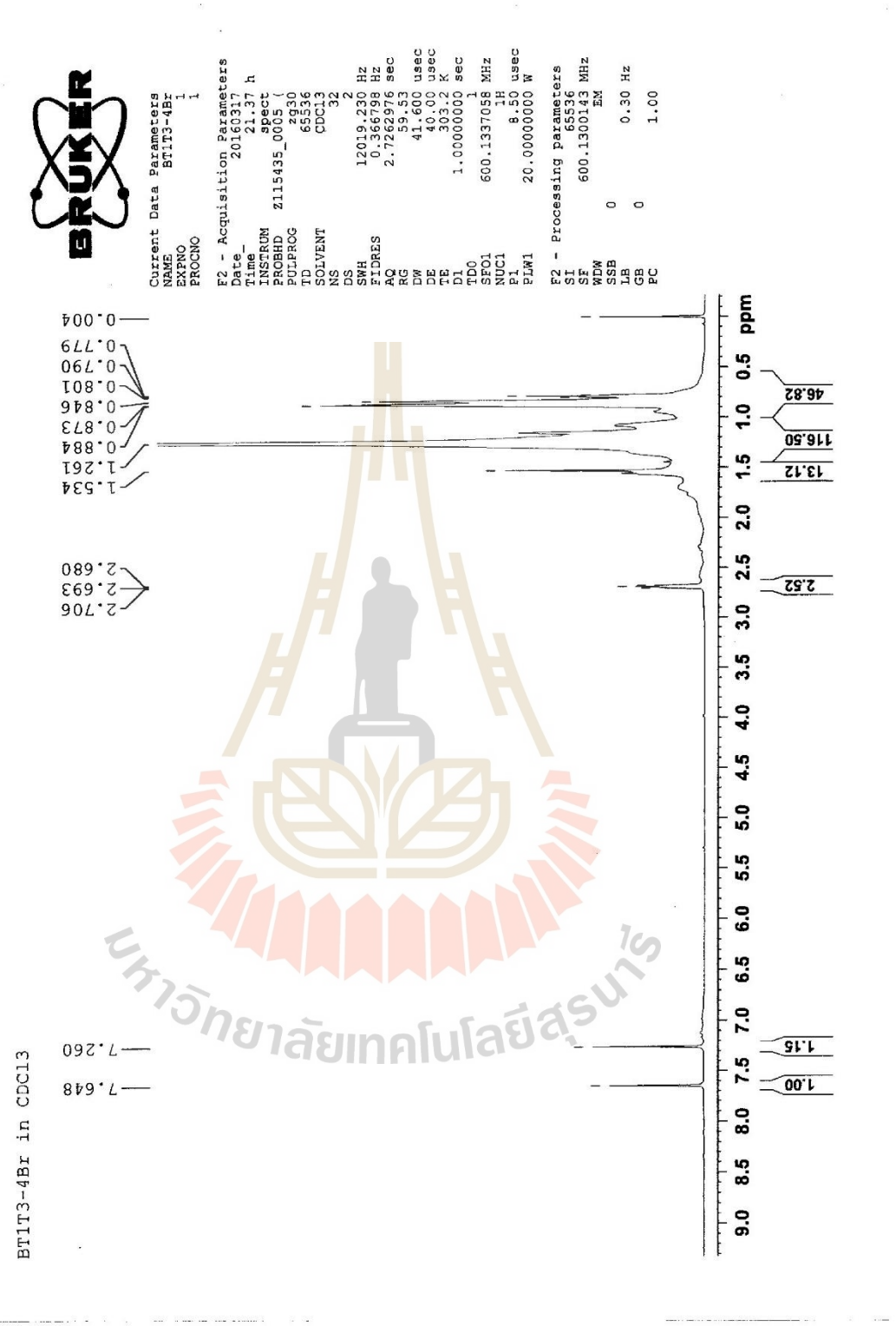
BRUKER
Current Data Parameters
NAME BT1T3-4Br
EXPNO 1
PROCNO 1
F2 - Acquisition Parameters
Date_ 20160317
Time_ 21.37 h
INSTRUM spect
PROBHD Z115435_0005 (
PULPROG zg30
TD 65536
SOLVENT CDCl3
NS 32
DS 2
SWH 12019.230 Hz
FIDRES 0.366798 Hz
AQ 2.7262976 sec
RG 59.53
DW 41.600 usec
DE 40.00 usec
TE 303.2 K
D1 1.00000000 sec
TD0 1
SFO1 600.1337058 MHz
NUC1 1H
P1 8.50 usec
PLW1 20.00000000 W
F2 - Processing parameters
SI 65536
SF 600.1300143 MHz
WDW EM
SSB 0
LB 0.30 Hz
GB 0
PC 1.00
0.004
0.779
0.790
0.801
0.846
0.873
0.884
1.261
1.534
2.680
2.693
2.706
7.260
7.648
46.82
116.50
13.12
2.52
1.15
1.00
ppm
BT1T3-4Br in CDCl3

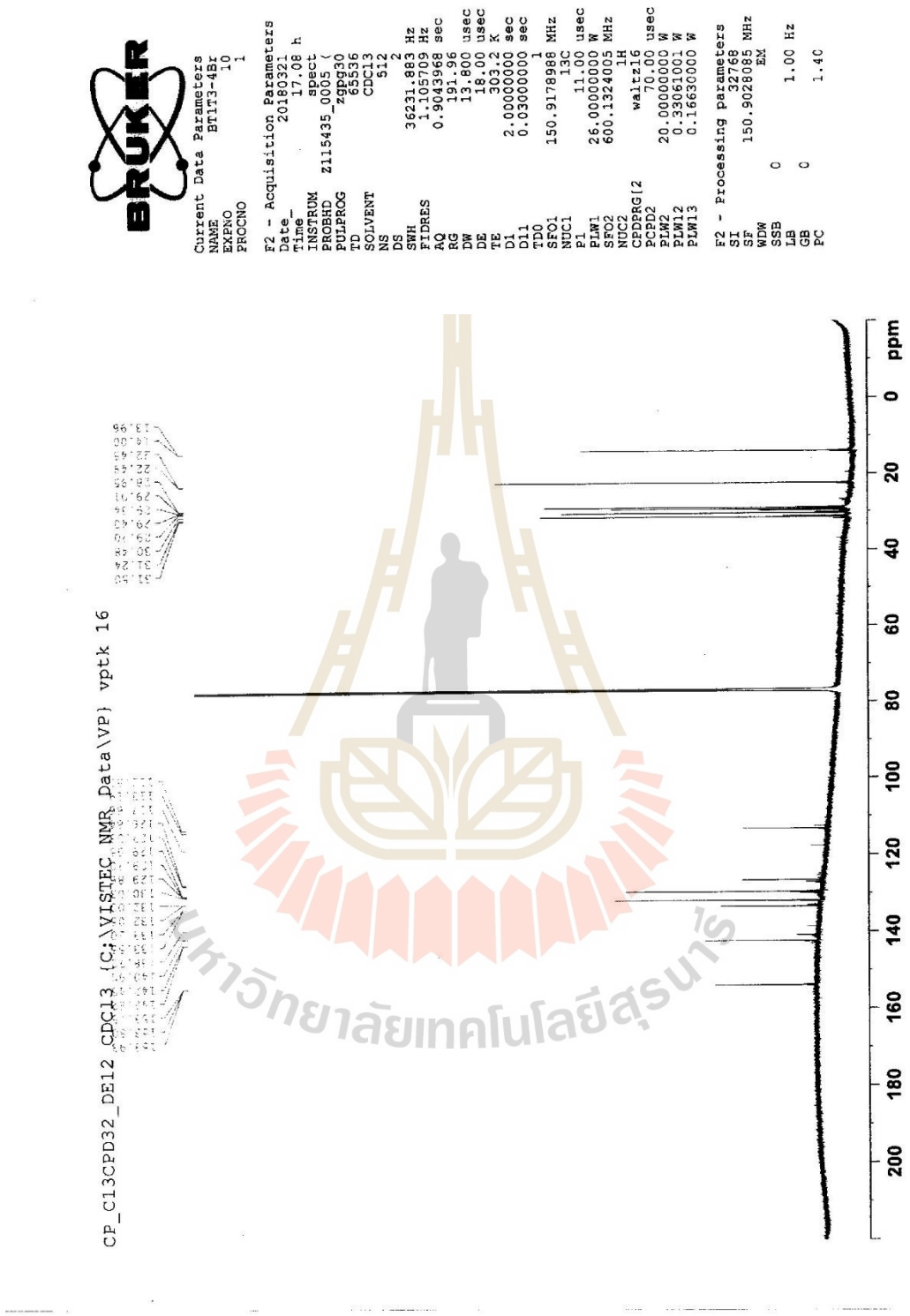
BRUKER
Current Data Parameters
NAME BT1T3-4Br
EXPNO 10
PROCNO 1
F2 - Acquisition Parameters
Date_ 20180321
Time 17.08 h
INSTRUM spect
PROBHD Z115435_0005 (
PULPROG zgpg30
TD 65536
SOLVENT CDCl3
NS 512
DS 2
SWH 36231.883 Hz
FIDRES 1.105709 Hz
AQ 0.9043968 sec
RG 191.96
DW 13.800 usec
DE 18.00 usec
TE 303.2 K
D1 2.00000000 sec
D11 0.03000000 sec
TD0 1
SFO1 150.9178988 MHz
NUC1 13C
P1 11.00 usec
PLW1 26.00000000 W
SFO2 600.1324005 MHz
NUC2 1H
CPDPRG[2 waltz16
PCPD2 70.00 usec
PLW2 20.00000000 W
PLW12 0.33061001 W
PLW13 0.16630000 W
F2 - Processing parameters
SI 32768
SF 150.9028085 MHz
WDW EM
SSB 0
LB 1.00 Hz
GB 0
PC 1.40
CP_C13CPD32_DE12 CDCl3 {C:\VISTEC NMR Data\VP} vptk 16
200
180
160
140
120
100
80
60
40
20
0
ppm

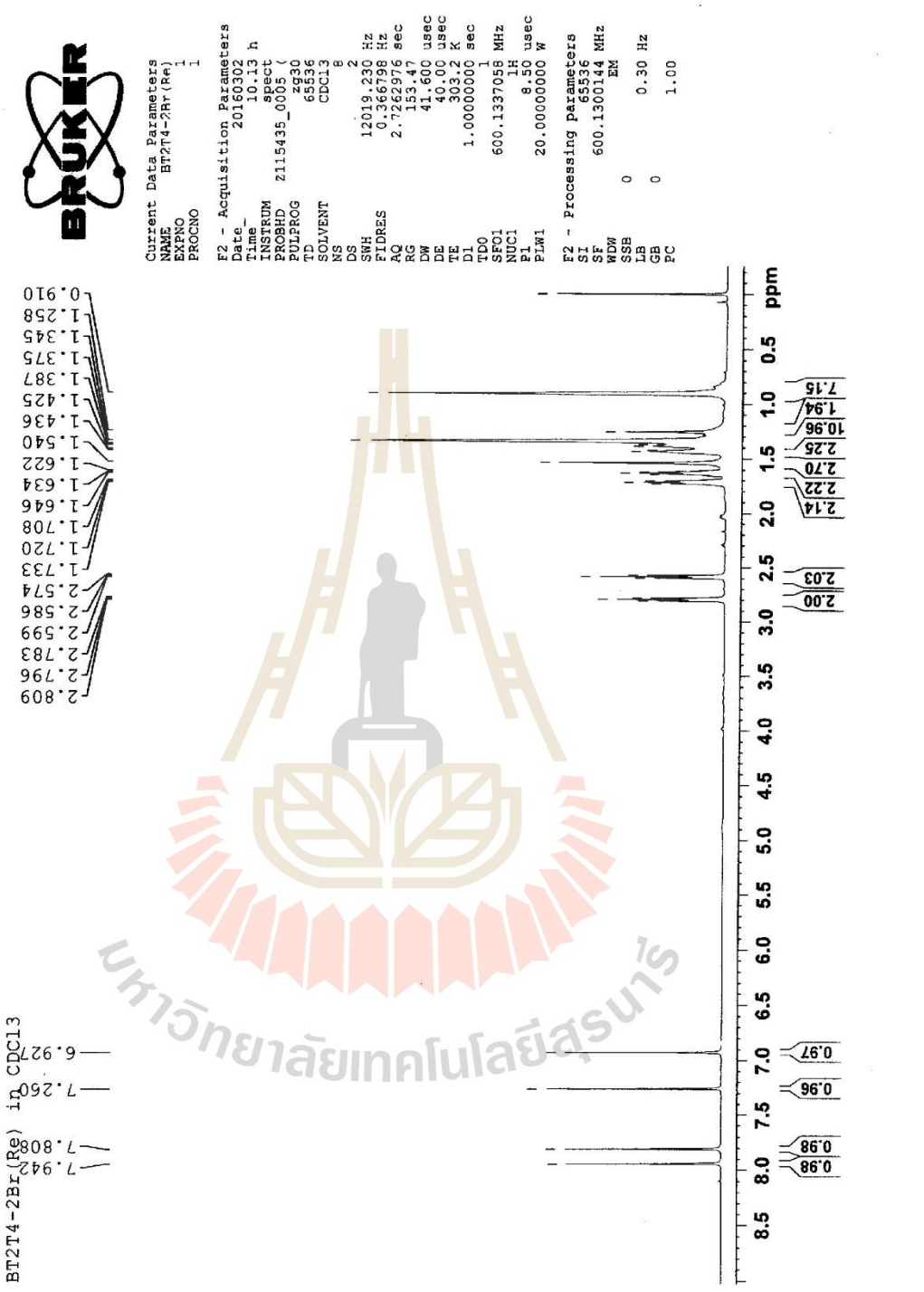

มหาวิทยาลัยเทคโนโลยีสุรนารี

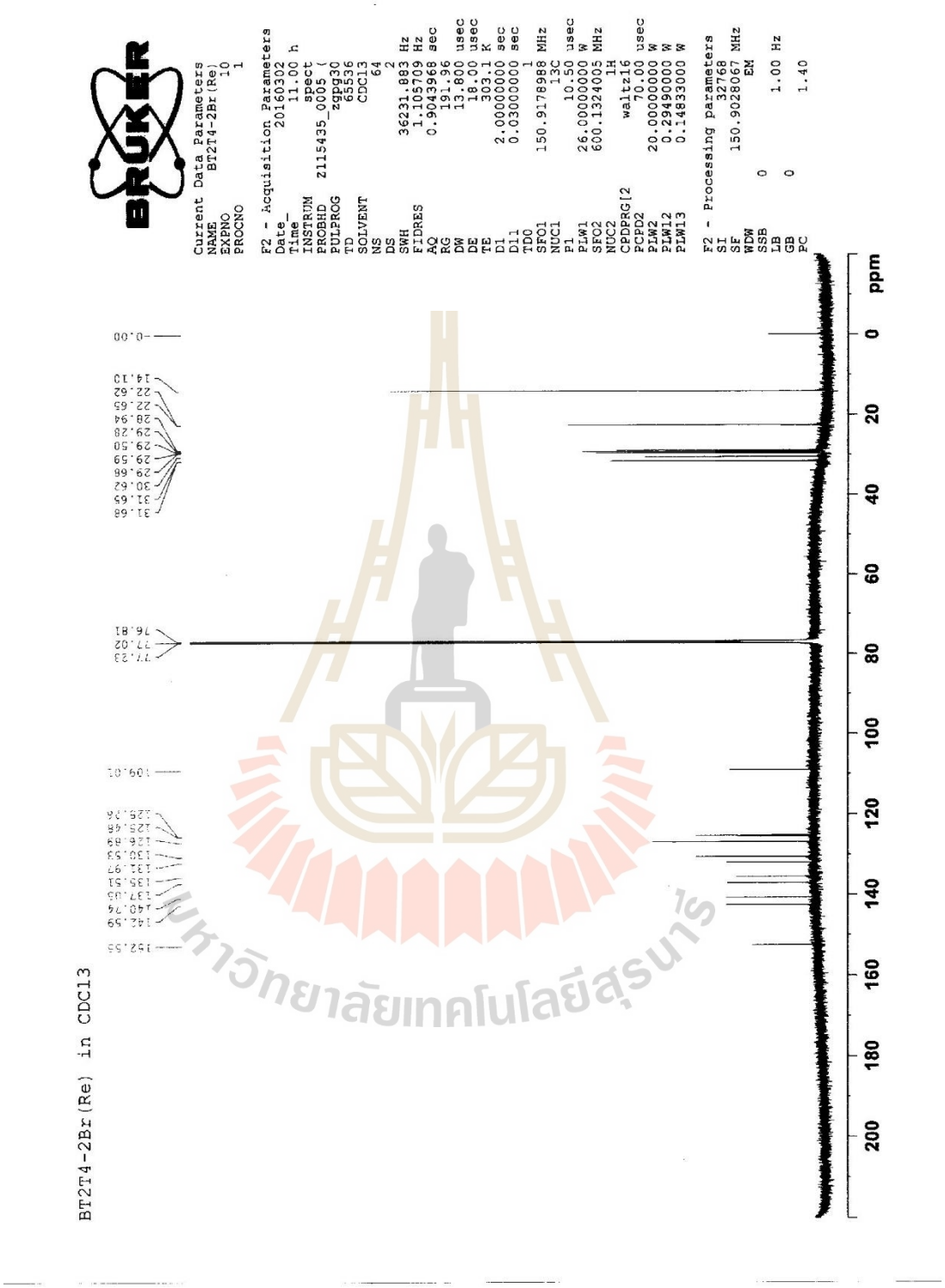
BRUKER
Current Data Parameters
NAME BT2T4-2Br(Re)
EXPNO 10
PROCNO 1
F2 - Acquisition Parameters
Date_ 20160302
Time_ 11.00 h
INSTRUM spect
PROBHD Z115435_0005 (
PULPROG zgpg30
TD 65536
SOLVENT CDCl3
NS 64
DS 2
SWH 36231.883 Hz
FIDRES 1.105709 Hz
AQ 0.9043968 sec
RG 191.96
DW 13.800 usec
DE 18.00 usec
TE 303.1 K
D1 2.00000000 sec
D11 0.03000000 sec
TD0 1
SFO1 150.9178988 MHz
NUC1 13C
P1 10.50 usec
PLW1 26.00000000 W
SFO2 600.1324005 MHz
NUC2 1H
CPDPRG[2 waltz16
PCPD2 70.00 usec
PLW2 20.00000000 W
PLW12 0.29490000 W
PLW13 0.14833000 W
F2 - Processing parameters
SI 32768
SF 150.9028067 MHz
WDW EM
SSB 0
LB 1.00 Hz
GB 0
PC 1.40
BT2T4-2Br(Re) in CDCl3
ppm

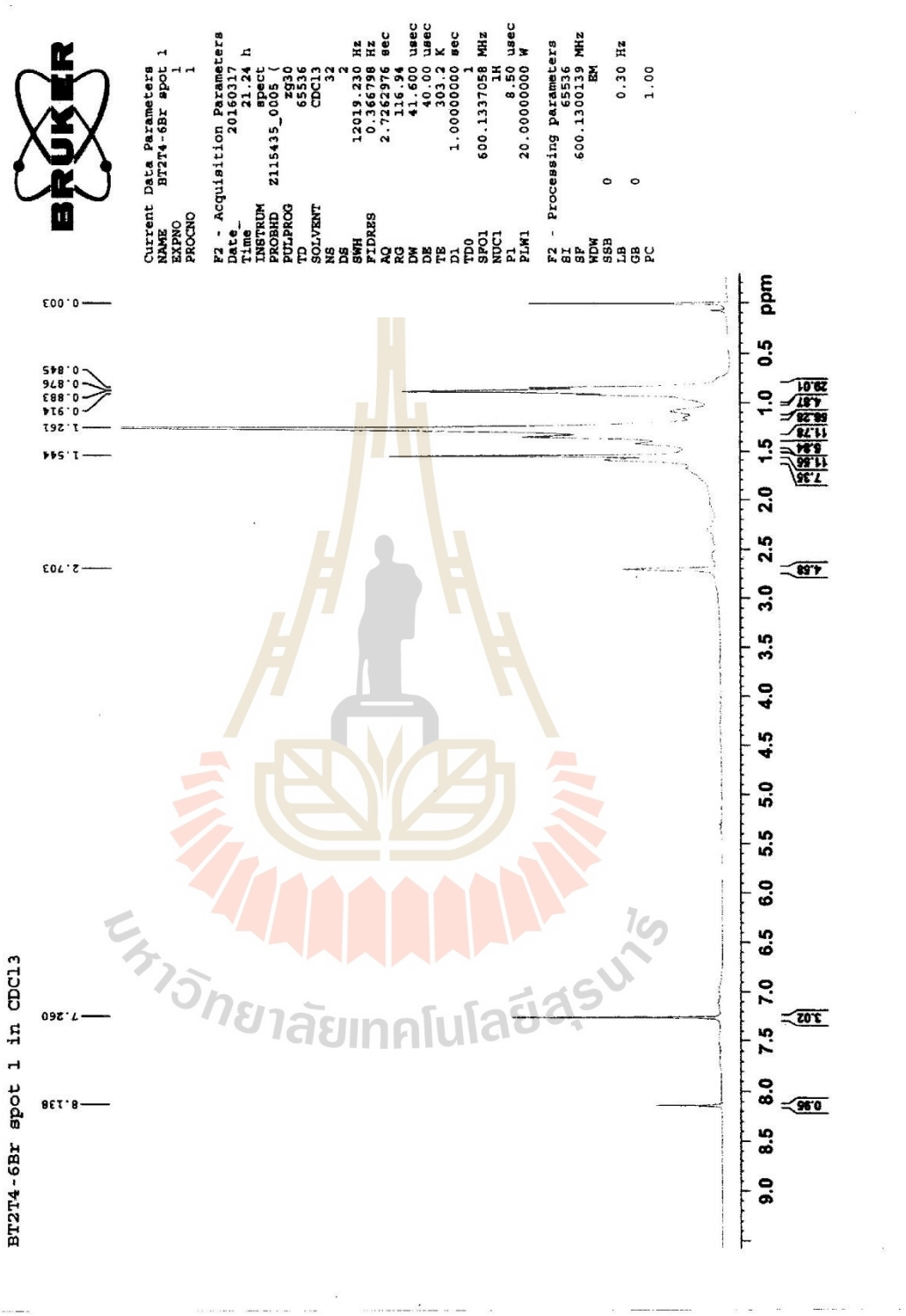
BRUKER
Current Data Parameters
NAME BT2T4-6Br spot 1
EXPNO 1
PROCNO 1
F2 - Acquisition Parameters
Date_ 20160317
Time 21.24 h
INSTRUM spect
PROBHD Z115435_0005 (
PULPROG zg30
TD 65536
SOLVENT CDCl3
NS 32
DS 2
SWH 12019.230 Hz
FIDRES 0.366798 Hz
AQ 2.7262976 sec
RG 116.94
DW 41.600 usec
DE 40.00 usec
TE 303.2 K
D1 1.00000000 sec
TD0 1
SFO1 600.1337058 MHz
NUC1 1H
P1 8.50 usec
PLW1 20.00000000 W
F2 - Processing parameters
SI 65536
SF 600.1300139 MHz
WDW EM
SSB 0
LB 0.30 Hz
GB 0
PC 1.00
BT2T4-6Br spot 1 in CDCl3
ppm

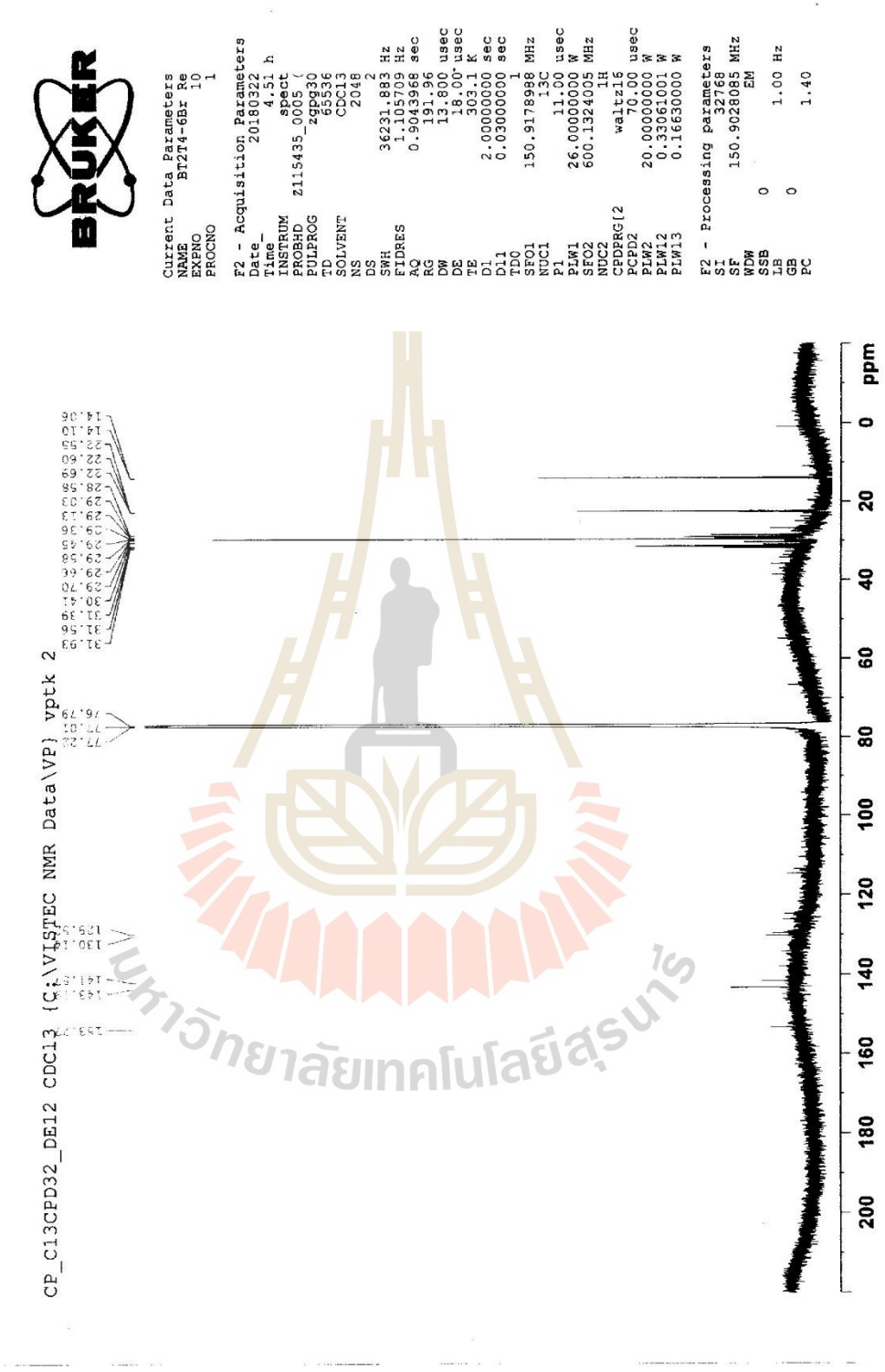
BRUKER
Current Data Parameters
NAME BT2T4-6Br Re
EXPNO 10
PROCNO 1
F2 - Acquisition Parameters
Date_ 20180322
Time 4.51 h
INSTRUM spect
PROBHD Z115435_0005 (
PULPROG zgpg30
TD 65536
SOLVENT CDCl3
NS 2048
DS 2
SWH 36231.883 Hz
FIDRES 1.105709 Hz
AQ 0.9043968 sec
RG 191.96
DW 13.800 usec
DE 18.00 usec
TE 303.1 K
D1 2.00000000 sec
D11 0.03000000 sec
TD0 1
SFO1 150.9178998 MHz
NUC1 13C
P1 11.00 usec
PLW1 26.00000000 W
SFO2 600.1324005 MHz
NUC2 1H
CPDPRG[2 waltz16
PCPD2 70.00 usec
PLW2 20.00000000 W
PLW12 0.33061001 W
PLW13 0.16630000 W
F2 - Processing parameters
SI 32768
SF 150.9028085 MHz
WDW EM
SSB 0
LB 1.00 Hz
GB 0
PC 1.40
CP_C13CPD32_DE12 CDCl3 {C:\VISTEC NMR Data\VP} vptk 2
ppm
200
180
160
140
120
100
80
60
40
20
0

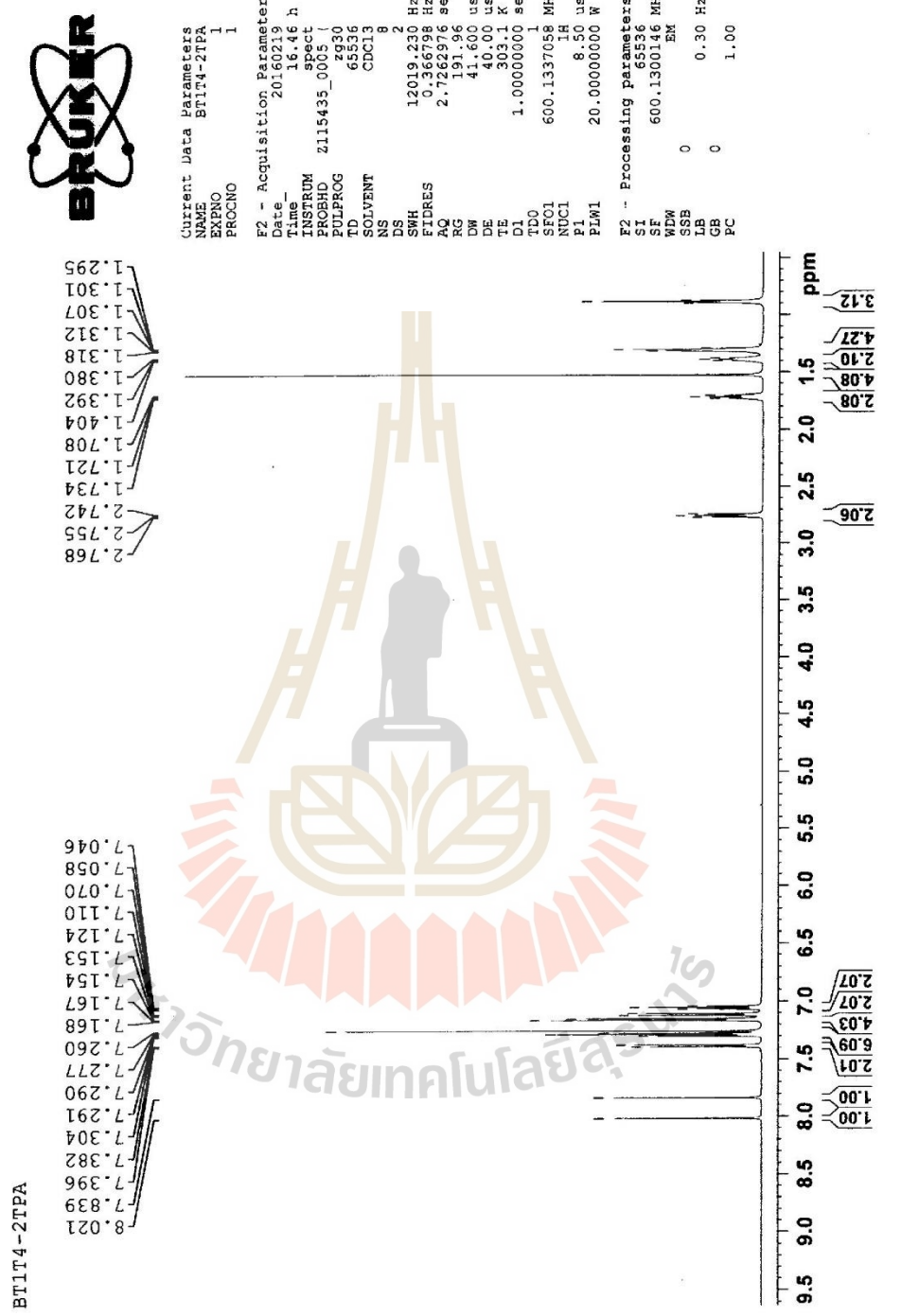
BRUKER
Current Data Parameters
NAME BT1T4-2TPA
EXPNO 1
PROCNO 1
F2 - Acquisition Parameters
Date_ 20160219
Time_ 16.46 h
INSTRUM spect
PROBHD Z115435_0005 (
PULPROG zg30
TD 65536
SOLVENT CDCl3
NS 8
DS 2
SWH 12019.230 Hz
FIDRES 0.366798 Hz
AQ 2.7262976 sec
RG 191.96
DW 41.600 usec
DE 40.00 usec
TE 303.1 K
D1 1.00000000 sec
TD0 1
SFO1 600.1337058 MHz
NUC1 1H
P1 8.50 usec
PLW1 20.00000000 W
F2 - Processing parameters
SI 65536
SF 600.1300146 MHz
WDW EM
SSB 0
LB 0.30 Hz
GB 0
PC 1.00
ppm
3.12
4.27
2.10
4.08
2.08
2.06
1.00
1.00
2.01
6.09
4.03
2.07
2.07
1.295
1.301
1.307
1.312
1.318
1.380
1.392
1.404
1.708
1.721
1.734
2.742
2.755
2.768
7.046
7.058
7.070
7.110
7.124
7.153
7.154
7.167
7.168
7.260
7.277
7.290
7.291
7.304
7.382
7.396
7.839
8.021
BT1T4-2TPA

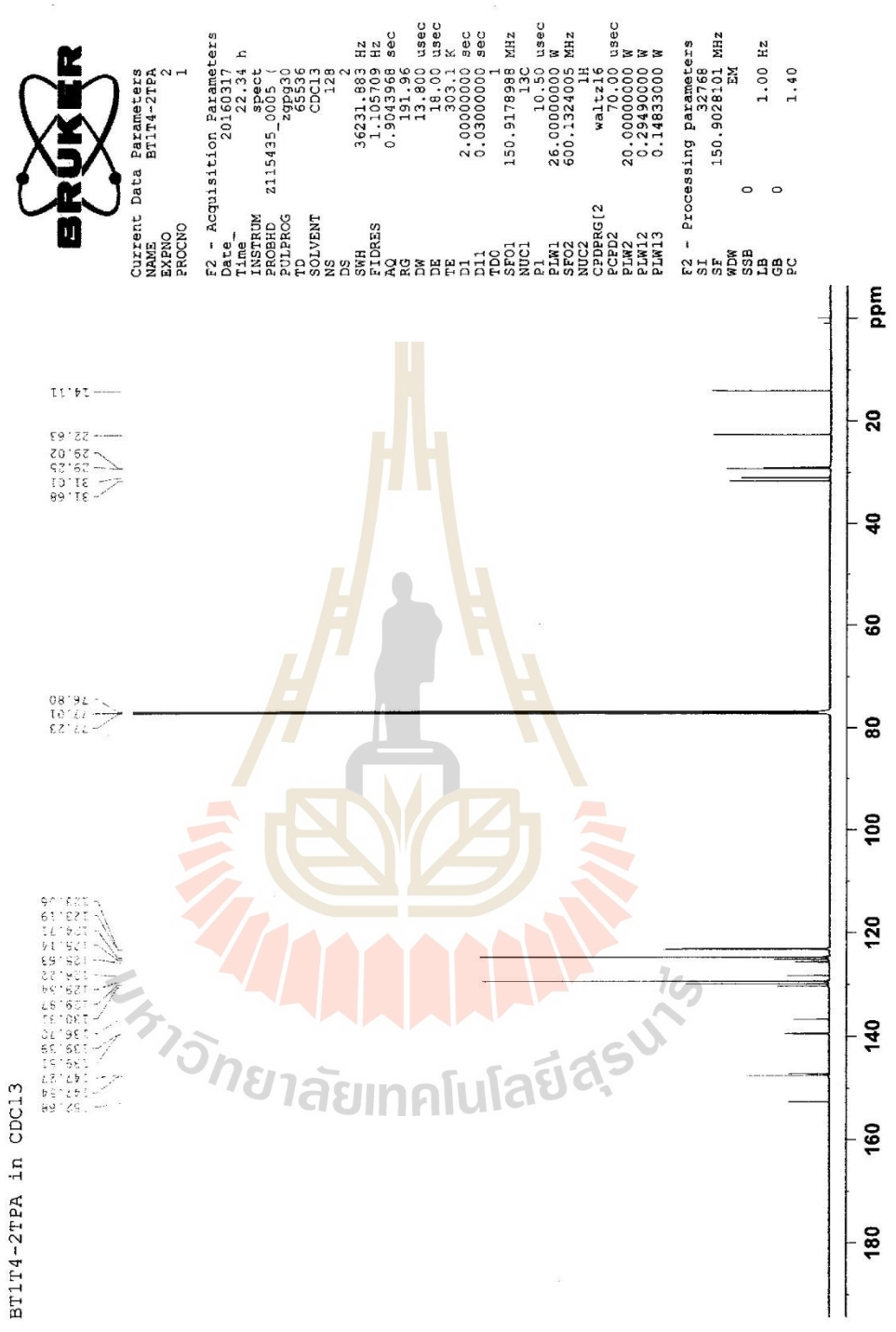
BRUKER
Current Data Parameters
NAME BT1T4-2TPA
EXPNO 2
PROCNO 1
F2 - Acquisition Parameters
Date_ 20160317
Time 22.34 h
INSTRUM spect
PROBHD 2115435_0005 (
PULPROG zgpg30
TD 65536
SOLVENT CDCl3
NS 128
DS 2
SWH 36231.883 Hz
FIDRES 1.105709 Hz
AQ 0.9043968 sec
RG 191.96
DW 13.800 usec
DE 18.00 usec
TE 303.1 K
D1 2.00000000 sec
D11 0.03000000 sec
TD0 1
SFO1 150.9178988 MHz
NUC1 13C
P1 10.50 usec
PLW1 26.00000000 W
SFO2 600.1324005 MHz
NUC2 1H
CPDPRG[2 waltz16
PCPD2 70.00 usec
PLW2 20.00000000 W
PLW12 0.29490000 W
PLW13 0.14833000 W
F2 - Processing parameters
SI 32768
SF 150.9028101 MHz
WDW EM
SSB 0
LB 1.00 Hz
GB 0
PC 1.40
BT1T4-2TPA in CDCl3
ppm
180
160
140
120
100
80
60
40
20

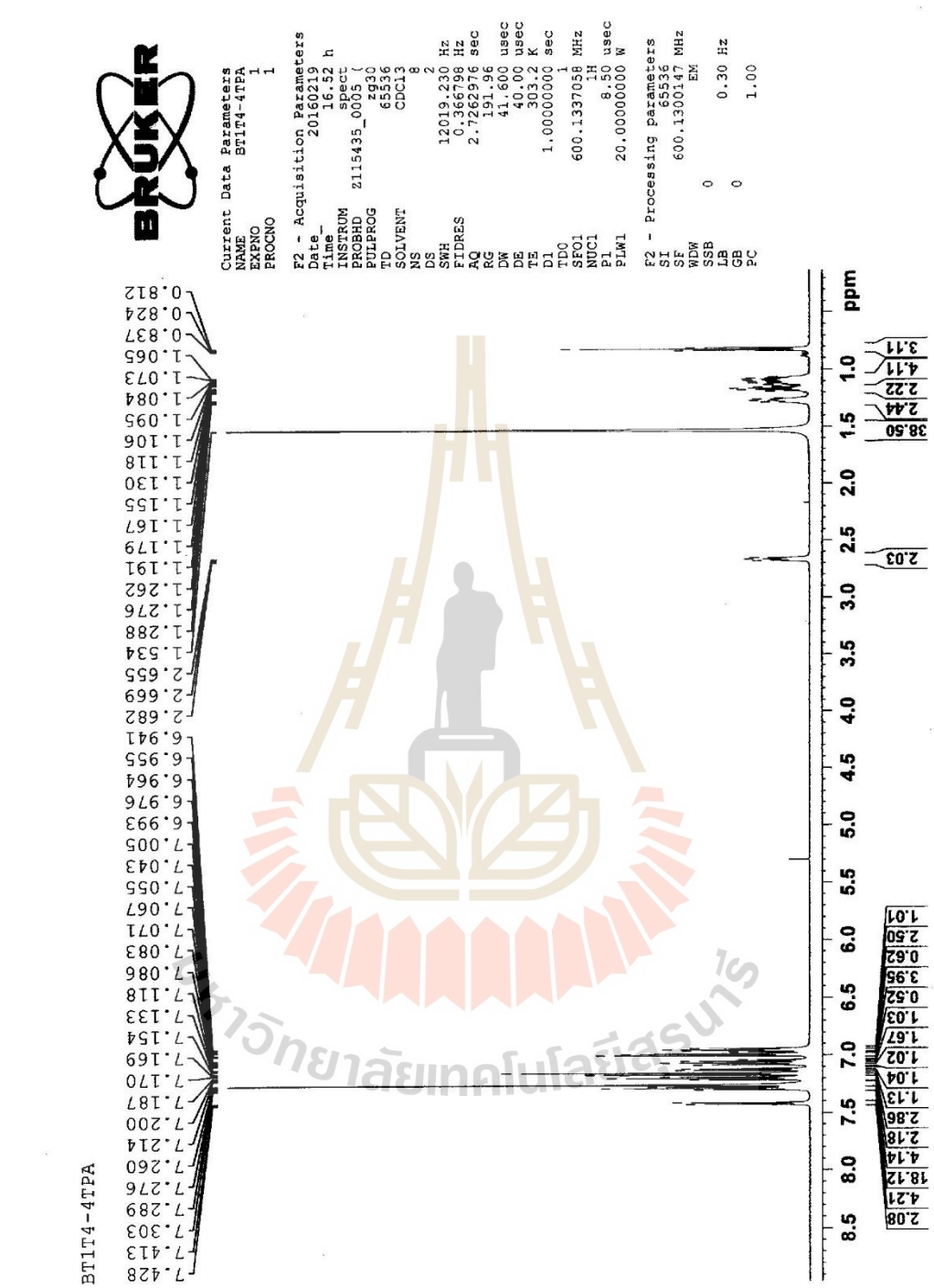
BRUKER
Current Data Parameters
NAME BT1T4-4TPA
EXPNO 1
PROCNO 1
F2 - Acquisition Parameters
Date_ 20160219
Time_ 16.52 h
INSTRUM spect
PROBHD 2115435_0005 (
PULPROG zg30
TD 65536
SOLVENT CDCl3
NS 8
DS 2
SWH 12019.230 Hz
FIDRES 0.366798 Hz
AQ 2.7262976 sec
RG 191.96
DW 41.600 usec
DE 40.00 usec
TE 303.2 K
D1 1.00000000 sec
TD0 1
SFO1 600.1337058 MHz
NUC1 1H
P1 8.50 usec
PLW1 20.00000000 W
F2 - Processing parameters
SI 65536
SF 600.1300147 MHz
WDW EM
SSB 0
LB 0.30 Hz
GB 0
PC 1.00
BT1T4-4TPA
ppm
38.50
2.44
2.22
4.11
3.11
2.03
2.08
4.21
18.12
4.14
2.18
2.86
1.13
1.04
1.02
1.67
1.03
0.52
3.95
0.62
2.50
1.01

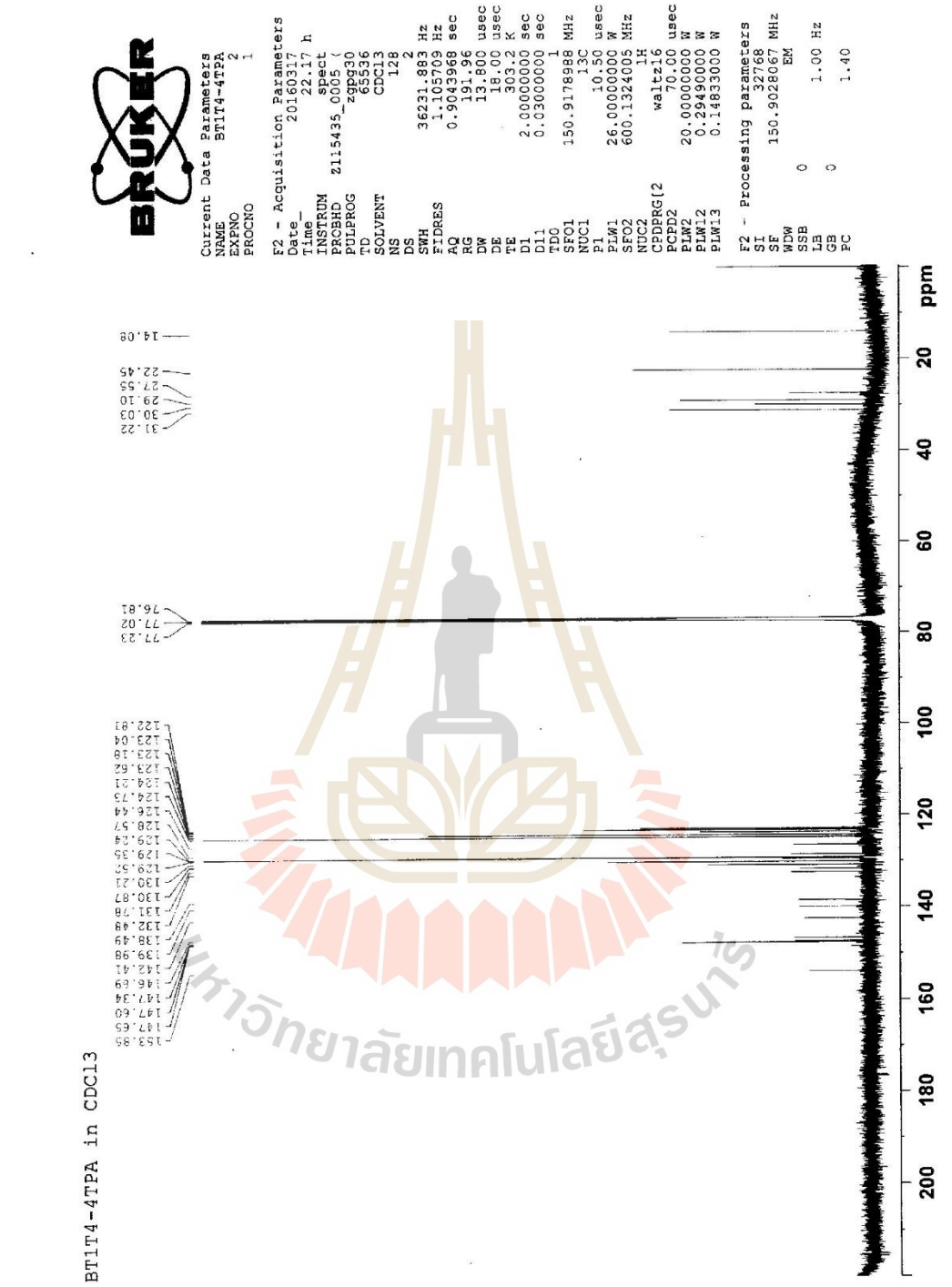
BRUKER
Current Data Parameters
NAME BT1T4-4TPA
EXPNO 2
PROCNO 1
F2 - Acquisition Parameters
Date_ 20160317
Time 22.17 h
INSTRUM spect
PROBHD 2115435_0005 (
PULPROG zgpg30
TD 65536
SOLVENT CDCl3
NS 128
DS 2
SWH 36231.883 Hz
FIDRES 1.105709 Hz
AQ 0.9043968 sec
RG 191.96
DW 13.800 usec
DE 18.00 usec
TE 303.2 K
D1 2.00000000 sec
D11 0.03000000 sec
TD0 1
SFO1 150.9178988 MHz
NUC1 13C
P1 10.50 usec
PLW1 26.00000000 W
SFO2 600.1324005 MHz
NUC2 1H
CPDPRG[2 waltz16
PCPD2 70.00 usec
PLW2 20.00000000 W
PLW12 0.29490000 W
PLW13 0.14833000 W
F2 - Processing parameters
SI 32768
SF 150.9028067 MHz
WDW EM
SSB 0
LB 1.00 Hz
GB 0
PC 1.40
BT1T4-4TPA in CDCl3
14.08
22.45
27.55
29.10
30.03
31.22
76.81
77.02
77.23
122.81
123.04
123.18
123.62
124.21
124.75
126.44
128.57
129.34
129.35
129.57
130.21
130.87
131.78
132.48
138.49
139.98
142.41
146.89
147.34
147.60
147.65
153.85
ppm
200
180
160
140
120
100
80
60
40
20

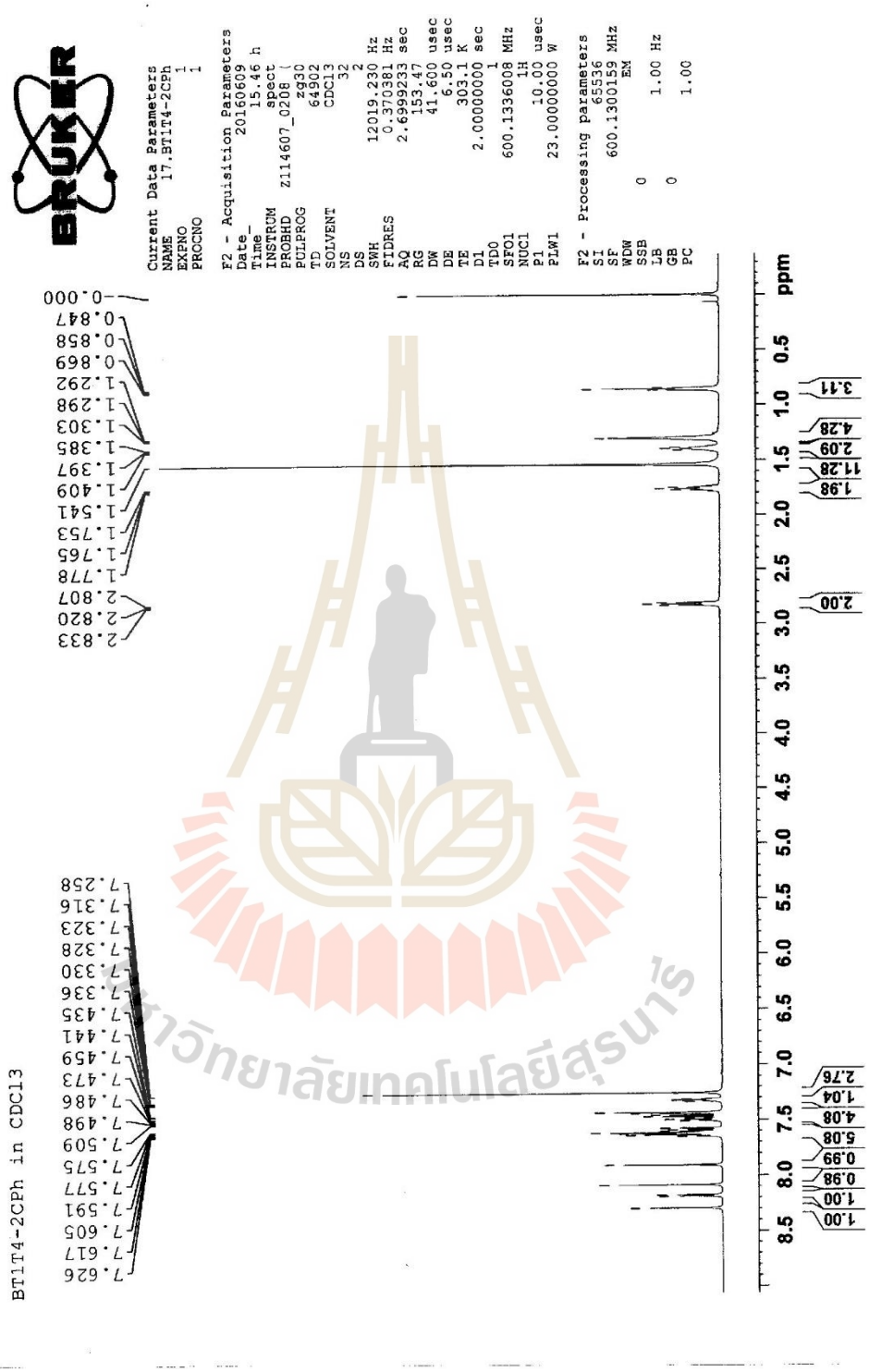
BRUKER
Current Data Parameters
NAME 17.BT1T4-2CPh
EXPNO 1
PROCNO 1
F2 - Acquisition Parameters
Date_ 20160609
Time_ 15.46 h
INSTRUM spect
PROBHD Z114607_0208 (
PULPROG zg30
TD 64902
SOLVENT CDCl3
NS 32
DS 2
SWH 12019.230 Hz
FIDRES 0.370381 Hz
AQ 2.6999233 sec
RG 153.47
DW 41.600 usec
DE 6.50 usec
TE 303.1 K
D1 2.00000000 sec
TD0 1
SFO1 600.1336008 MHz
NUC1 1H
P1 10.00 usec
PLW1 23.00000000 W
F2 - Processing parameters
SI 65536
SF 600.1300159 MHz
WDW EM
SSB 0
LB 1.00 Hz
GB 0
PC 1.00
BT1T4-2CPh in CDCl3
ppm
-0.000
0.847
0.858
0.869
1.292
1.298
1.303
1.385
1.397
1.409
1.541
1.753
1.765
1.778
2.807
2.820
2.833
7.258
7.316
7.323
7.328
7.330
7.336
7.435
7.441
7.459
7.473
7.486
7.498
7.509
7.575
7.577
7.591
7.605
7.617
7.626
3.11
4.28
2.09
11.28
1.98
2.00
2.76
1.04
4.08
5.08
0.99
0.98
1.00
1.00

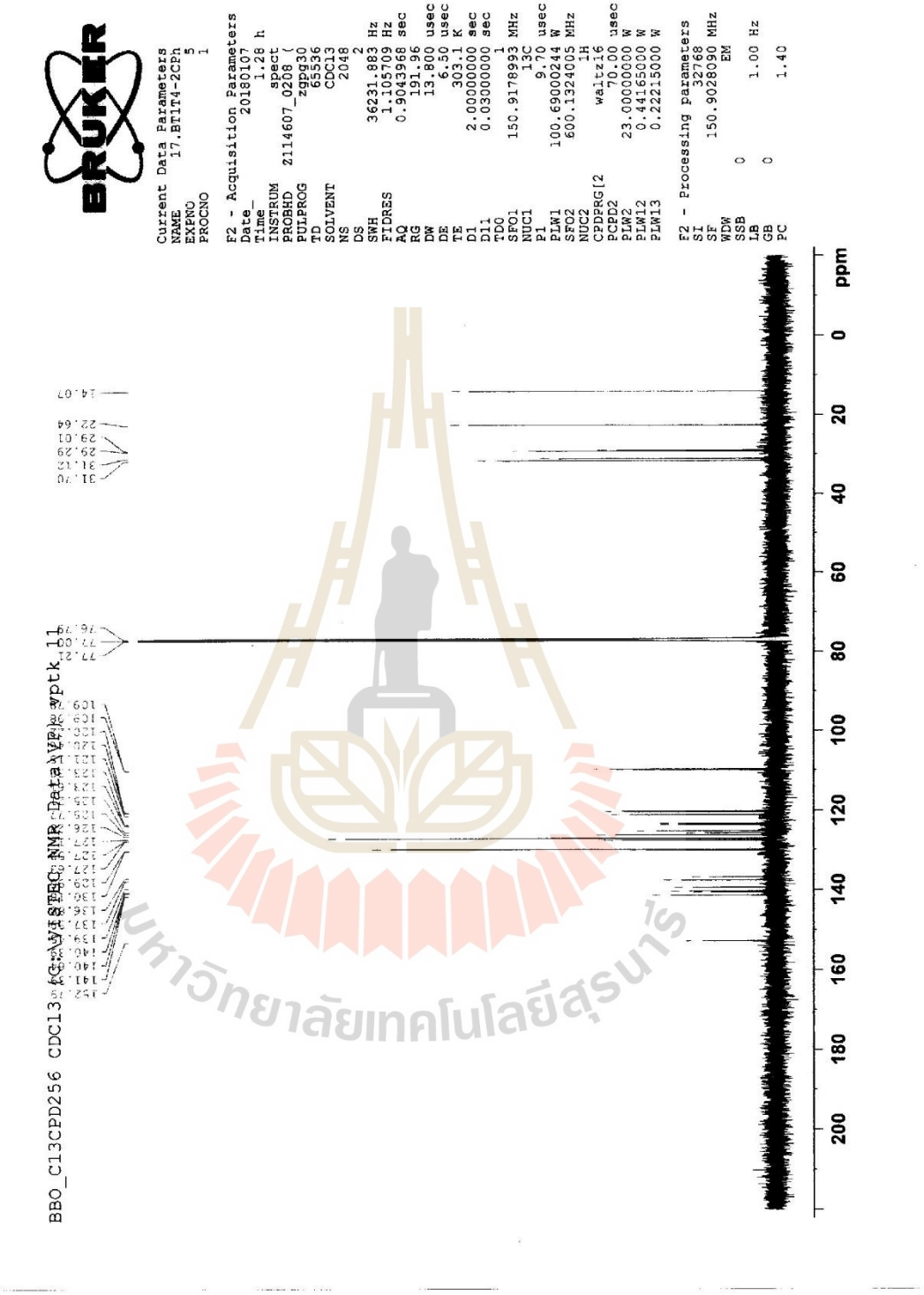
BRUKER
Current Data Parameters
NAME 17.BT1T4-2CPh
EXPNO 5
PROCNO 1
F2 - Acquisition Parameters
Date_ 20180107
Time 1.28 h
INSTRUM spect
PROBHD 2114607_0208 (
PULPROG zgpg30
TD 65536
SOLVENT CDCl3
NS 2048
DS 2
SWH 36231.883 Hz
FIDRES 1.105709 Hz
AQ 0.9043968 sec
RG 191.96
DW 13.800 usec
DE 6.50 usec
TE 303.1 K
D1 2.00000000 sec
D11 0.03000000 sec
TD0 1
SFO1 150.9178993 MHz
NUC1 13C
P1 9.70 usec
PLW1 100.69000244 W
SFO2 600.1324005 MHz
NUC2 1H
CPDPRG[2 waltz16
PCPD2 70.00 usec
PLW2 23.00000000 W
PLW12 0.44165000 W
PLW13 0.22215000 W
F2 - Processing parameters
SI 32768
SF 150.9028090 MHz
WDW EM
SSB 0
LB 1.00 Hz
GB 0
PC 1.40
BBO_C13CPD256 CDC13
ppm

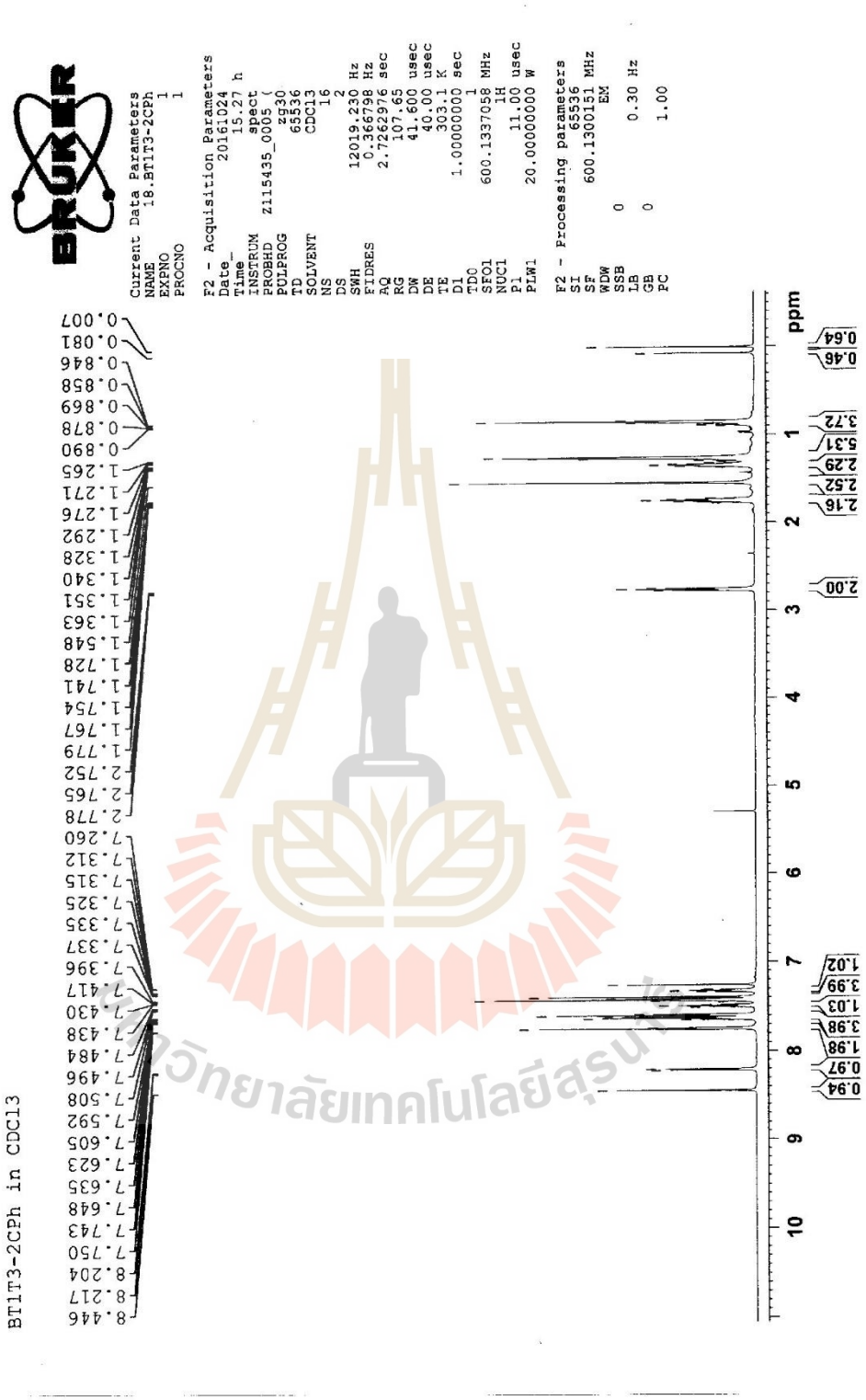
BRUKER
Current Data Parameters
NAME 18.BT1T3-2CPh
EXPNO 1
PROCNO 1
F2 - Acquisition Parameters
Date_ 20161024
Time_ 15.27 h
INSTRUM spect
PROBHD 21154435_0005 (
PULPROG zg30
TD 65536
SOLVENT CDCl3
NS 16
DS 2
SWH 12019.230 Hz
FIDRES 0.366798 Hz
AQ 2.7262976 sec
RG 107.65
DW 41.600 usec
DE 40.00 usec
TE 303.1 K
D1 1.00000000 sec
TD0 1
SFO1 600.1337058 MHz
NUC1 1H
P1 11.00 usec
PLW1 20.00000000 W
F2 - Processing parameters
SI 65536
SF 600.1300151 MHz
WDW EM
SSB 0
LB 0.30 Hz
GB 0
PC 1.00
BT1T3-2CPh in CDCl3
ppm
0.64
0.46
3.72
5.31
2.29
2.52
2.16
2.00
1.02
3.99
1.03
3.98
1.98
0.97
0.94

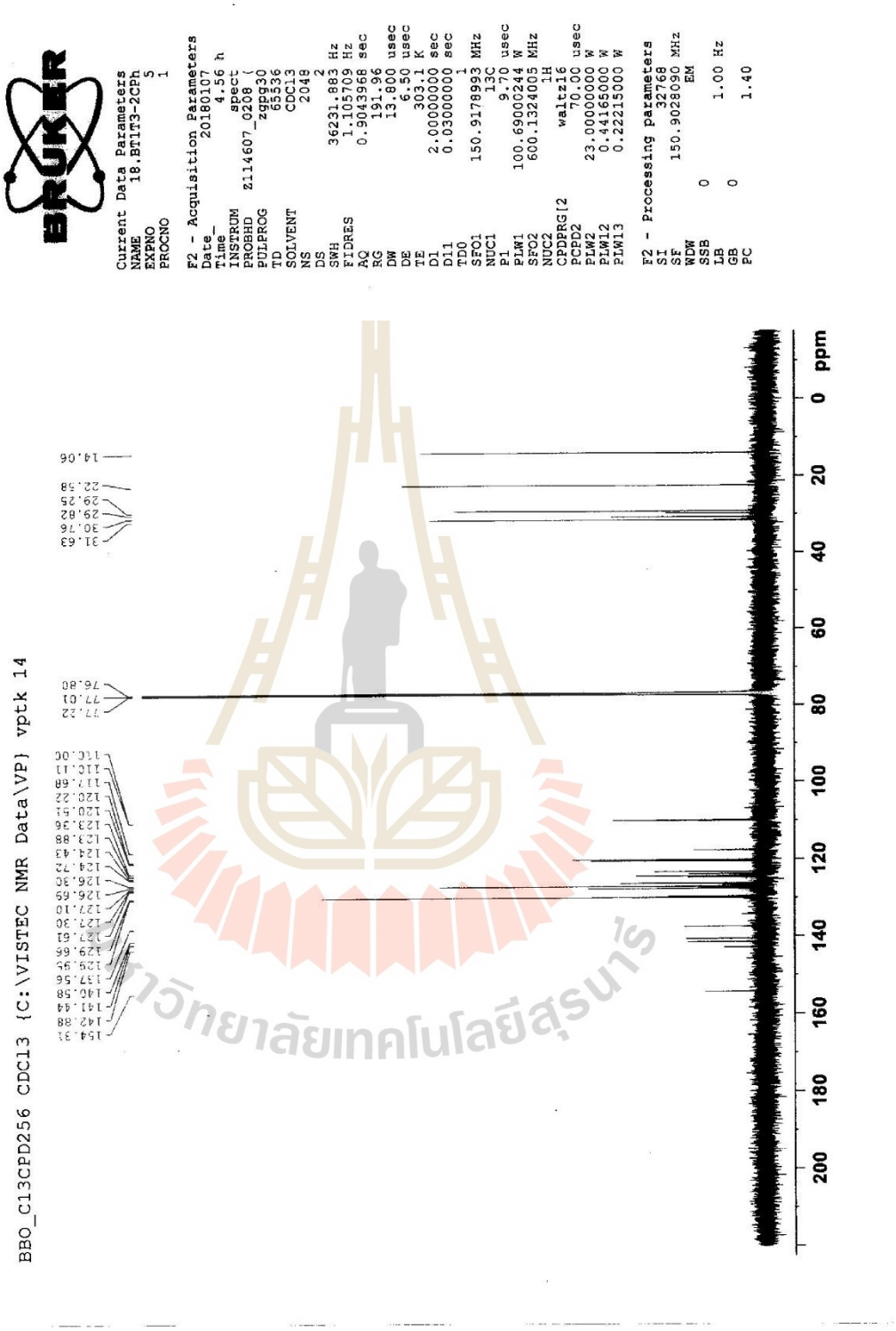
BRUKER
Current Data Parameters
NAME 18.BT1F3-2CPh
EXPNO 5
PROCNO 1
F2 - Acquisition Parameters
Date_ 20180107
Time_ 4.56 h
INSTRUM spect
PROBHD z114607_0208 (
PULPROG zgpg30
TD 65536
SOLVENT CDCl3
NS 2048
DS 2
SWH 36231.883 Hz
FIDRES 1.105709 Hz
AQ 0.9043968 sec
RG 191.96
DW 13.800 usec
DE 6.50 usec
TE 303.1 K
D1 2.00000000 sec
D11 0.03000000 sec
TD0 1
SFO1 150.9178993 MHz
NUC1 13C
P1 9.70 usec
PLW1 100.69000244 W
SFO2 600.1324005 MHz
NUC2 1H
CPDPRG[2 waltz16
PCPD2 70.00 usec
PLW2 23.00000000 W
PLW12 0.44165000 W
PLW13 0.22215000 W
F2 - Processing parameters
SI 32768
SF 150.9028090 MHz
WDW EM
SSB 0
LB 1.00 Hz
GB 0
PC 1.40
BBO_C13CPD256 CDCl3 {C:\VISTEC NMR Data\VP} vptk 14
14.06
22.58
29.25
29.82
30.76
31.63
76.80
77.01
77.22
110.00
110.11
117.68
120.22
120.51
123.36
123.88
124.43
124.72
126.36
126.65
127.10
127.30
127.61
129.66
129.95
137.56
140.58
141.44
142.88
154.31
200
180
160
140
120
100
80
60
40
20
0
ppm

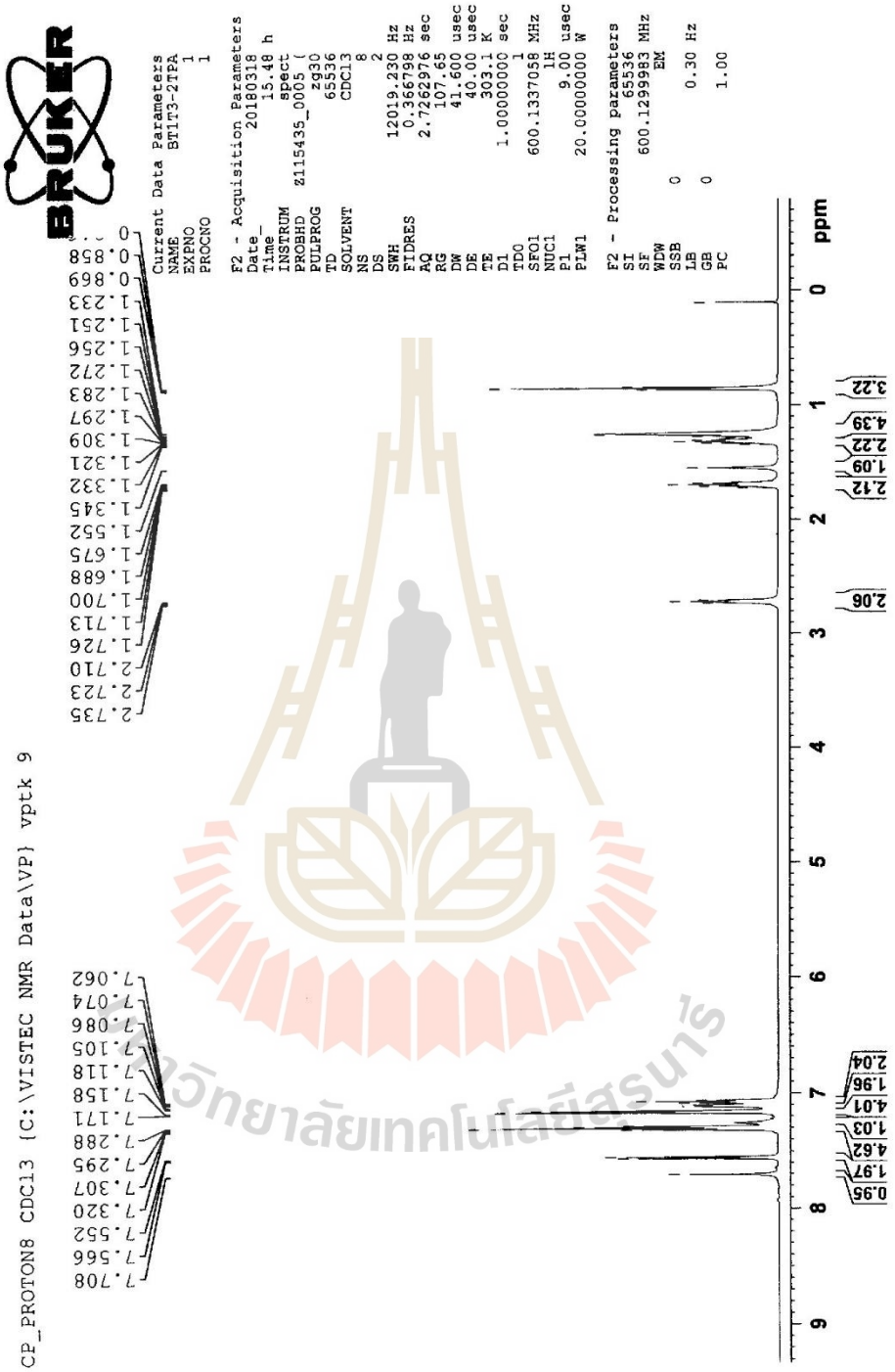
CP_PROTON8 CDC13 (C:\VISTEC NMR Data\VP) vptk 9
Current Data Parameters
NAME BTIT3-2TPA
EXPNO 1
PROCNO 1
F2 - Acquisition Parameters
Date_ 20180318
Time 15.48 h
INSTRUM spect
PROBHD z115435_0005 (
PULPROG zg30
TD 65536
SOLVENT CDCl3
NS 8
DS 2
SWH 12019.230 Hz
FIDRES 0.366798 Hz
AQ 2.7262976 sec
RG 107.65
DW 41.600 usec
DE 40.00 usec
TE 303.1 K
D1 1.00000000 sec
TD0 1
SFO1 600.1337058 MHz
NUC1 1H
P1 9.00 usec
PLW1 20.00000000 W
F2 - Processing parameters
SI 65536
SF 600.1299983 MHz
WDW EM
SSB 0
LB 0.30 Hz
GB 0
PC 1.00
ppm
3.22
4.39
2.22
1.09
2.12
2.06
0.95
1.97
4.62
1.03
4.01
1.96
2.04

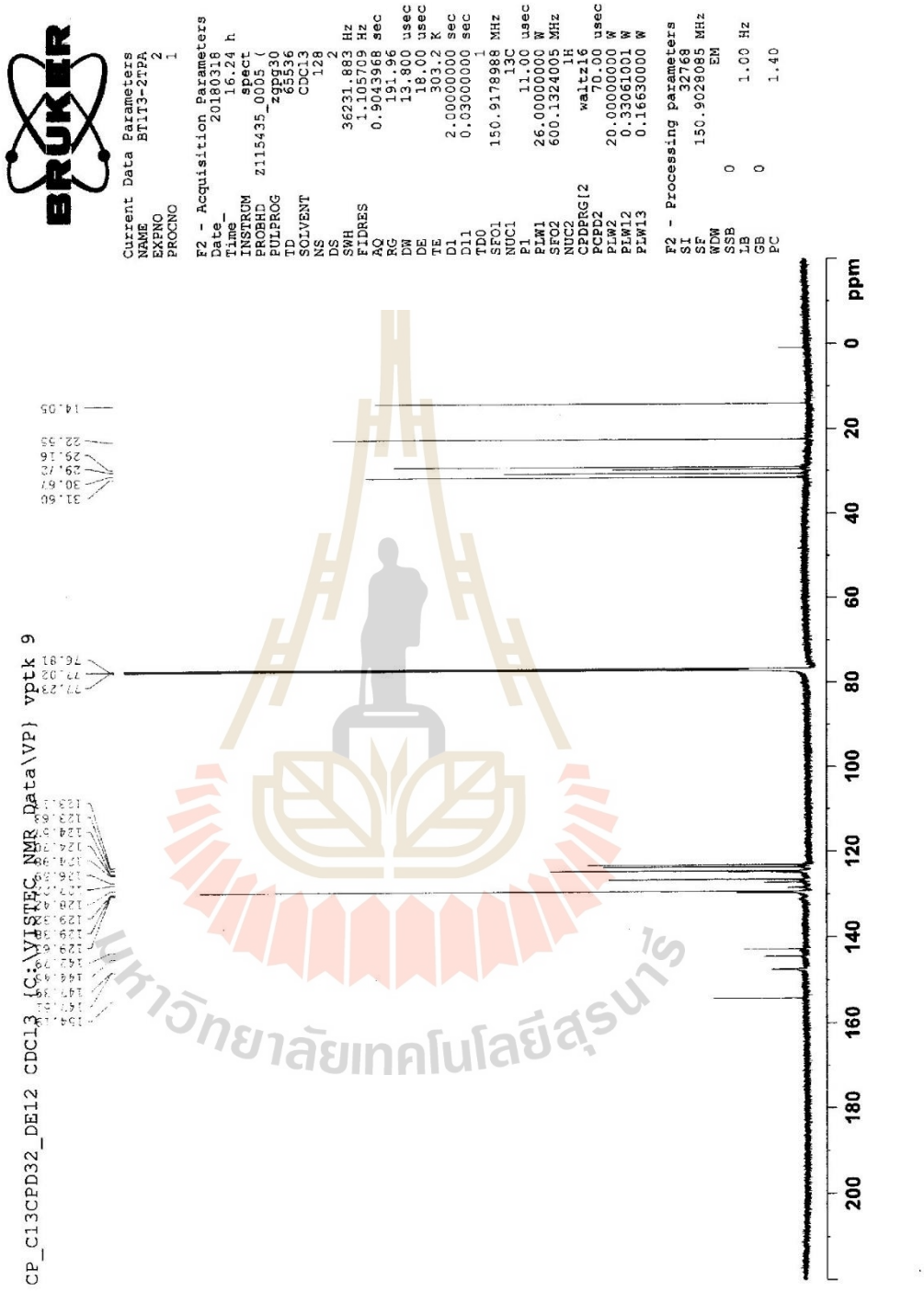
CP_C13CPD32_DE12 CDC13 {C:\VISTEC_NMR_Data\VP} vptk 9
Current Data Parameters
NAME BT1T3-2TPA
EXPNO 2
PROCNO 1
F2 - Acquisition Parameters
Date_ 20180318
Time 16.24 h
INSTRUM spect
PROBHD 2115435_0005 (
PULPROG zgpg30
TD 65536
SOLVENT CDCl3
NS 128
DS 2
SWH 36231.883 Hz
FIDRES 1.105709 Hz
AQ 0.9043968 sec
RG 191.96
DW 13.800 usec
DE 18.00 usec
TE 303.2 K
D1 2.00000000 sec
D11 0.03000000 sec
TD0 1
SFO1 150.9178988 MHz
NUC1 13C
P1 11.00 usec
PLW1 26.00000000 W
SFO2 600.1324005 MHz
NUC2 1H
CPDPRG[2 waltz16
PCPD2 70.00 usec
PLW2 20.00000000 W
PLW12 0.33061001 W
PLW13 0.16630000 W
F2 - Processing parameters
SI 32768
SF 150.9028085 MHz
WDW EM
SSB 0
LB 1.00 Hz
GB 0
PC 1.40
14.05
22.55
29.16
29.72
30.67
31.60
76.81
77.02
77.23
ppm

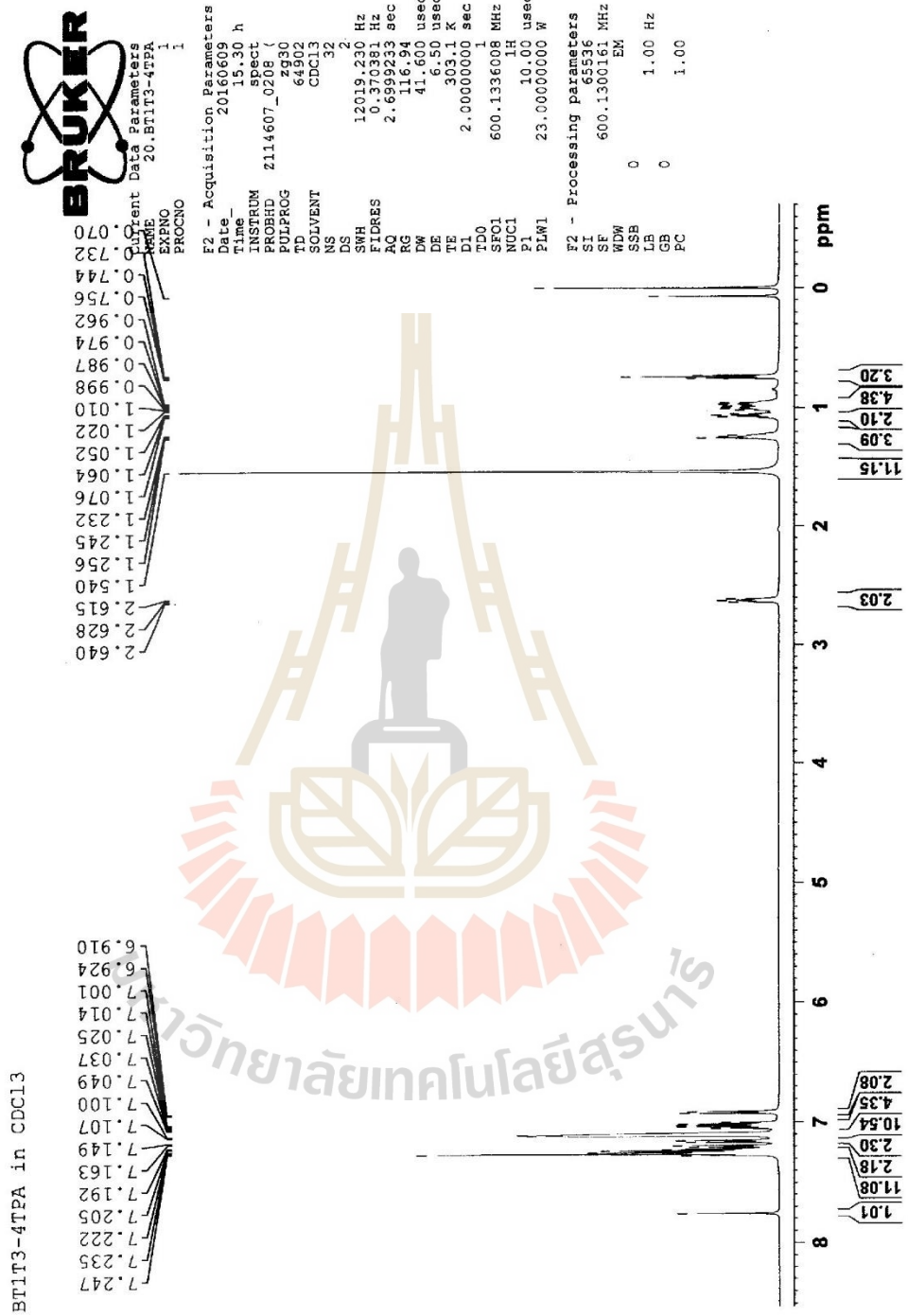
BT1T3-4TPA in CDC13
Current Data Parameters
NAME 20.BT1T3-4TPA
EXPNO 1
PROCNO 1
F2 - Acquisition Parameters
Date_ 20160609
Time_ 15.30 h
INSTRUM spect
PROBHD Z114607_0208 (
PULPROG zg30
TD 64902
SOLVENT CDCl3
NS 32
DS 2
SWH 12019.230 Hz
FIDRES 0.370381 Hz
AQ 2.69999233 sec
RG 116.94
DW 41.600 usec
DE 6.50 usec
TE 303.1 K
D1 2.00000000 sec
TD0 1
SFO1 600.1336008 MHz
NUC1 1H
P1 10.00 usec
PLW1 23.00000000 W
F2 - Processing parameters
SI 65536
SF 600.1300161 MHz
WDW EM
SSB 0
LB 1.00 Hz
GB 0
PC 1.00
ppm
3.20
4.38
2.10
3.09
11.15
2.03
1.01
11.08
2.18
2.30
10.54
4.35
2.08

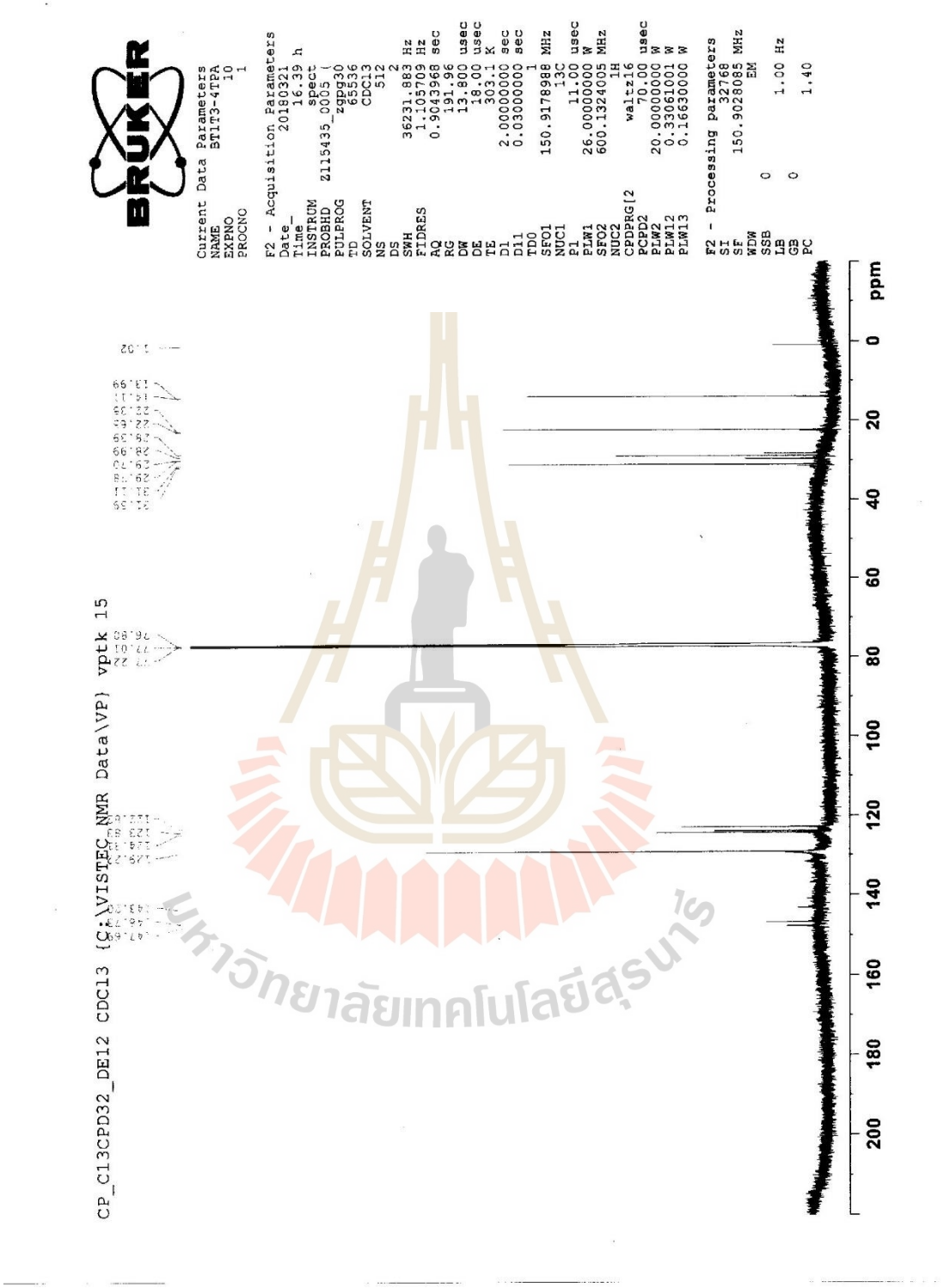
CP_C13CPD32_DE12 CDC13 {C:\VISTEC_NMR Data\VP} vptk 15
Current Data Parameters
NAME BTIT3-4TPA
EXPNO 10
PROCNO 1
F2 - Acquisition Parameters
Date_ 20180321
Time_ 16.39 h
INSTRUM spect
PROBHD Z115435_0005 (
PULPROG zgpg30
TD 65536
SOLVENT CDCl3
NS 512
DS 2
SWH 36231.883 Hz
FIDRES 1.105709 Hz
AQ 0.9043968 sec
RG 191.96
DW 13.800 usec
DE 18.00 usec
TE 303.1 K
D1 2.00000000 sec
D11 0.03000000 sec
TD0 1
SFO1 150.9178988 MHz
NUC1 13C
P1 11.00 usec
PLW1 26.00000000 W
SFO2 600.1324005 MHz
NUC2 1H
CPDPRG[2 waltz16
PCPD2 70.00 usec
PLW2 20.00000000 W
PLW12 0.33061001 W
PLW13 0.16630000 W
F2 - Processing parameters
SI 32768
SF 150.9028085 MHz
WDW EM
SSB 0
LB 1.00 Hz
GB 0
PC 1.40
200
180
160
140
120
100
80
60
40
20
0
ppm

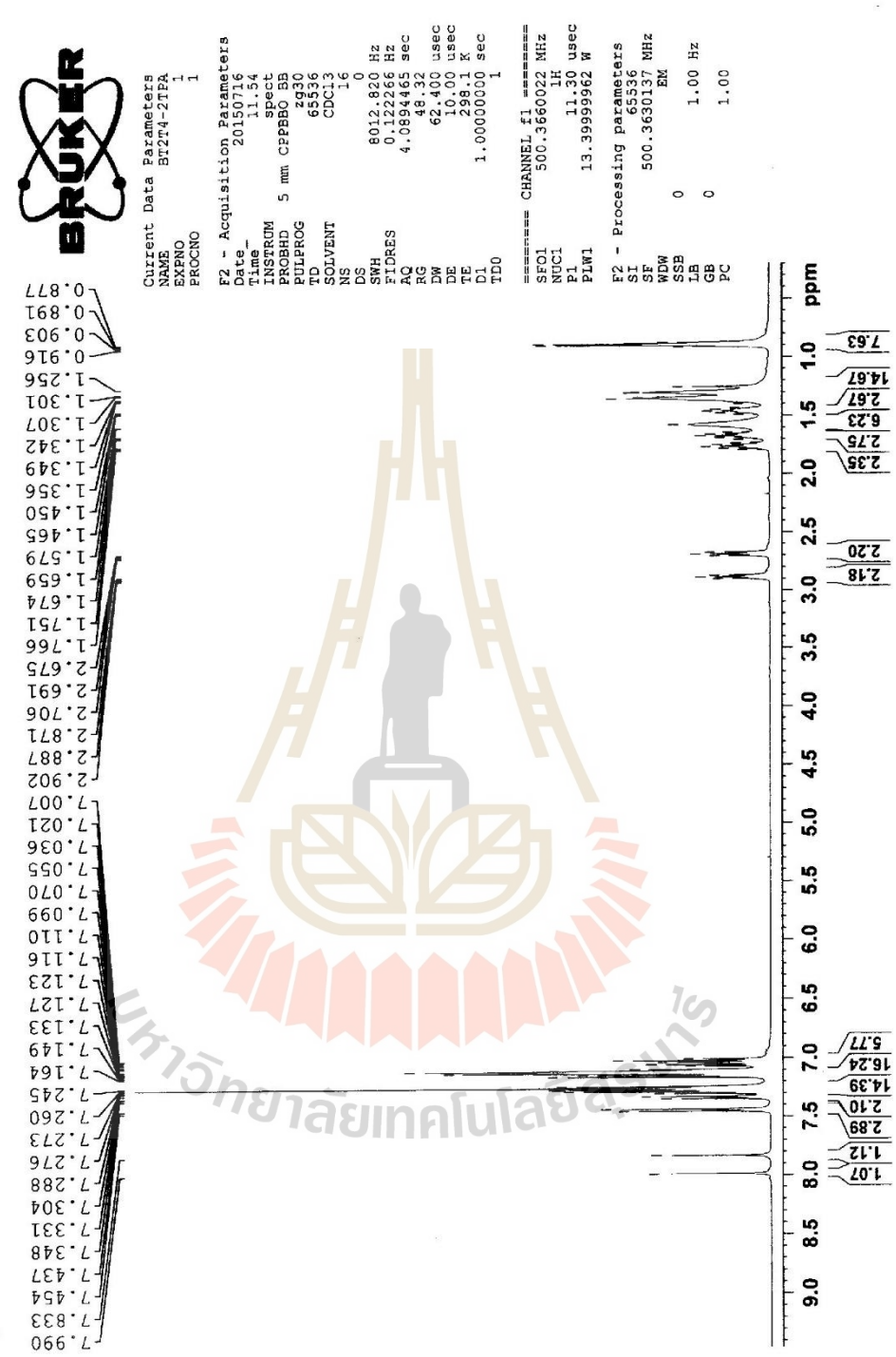
BRUKER
Current Data Parameters
NAME BT2T4-2TPA
EXPNO 1
PROCNO 1
F2 - Acquisition Parameters
Date_ 20150716
Time_ 11.54
INSTRUM spect
PROBHD 5 mm CPPBBO BB
PULPROG zg30
TD 65536
SOLVENT CDCl3
NS 16
DS 0
SWH 8012.820 Hz
FIDRES 0.122266 Hz
AQ 4.0894465 sec
RG 48.32
DW 62.400 usec
DE 10.00 usec
TE 298.1 K
D1 1.00000000 sec
TD0 1
======== CHANNEL f1 ========
SFO1 500.3660022 MHz
NUC1 1H
P1 11.30 usec
PLW1 13.39999962 W
F2 - Processing parameters
SI 65536
SF 500.3630137 MHz
WDW EM
SSB 0
LB 1.00 Hz
GB 0
PC 1.00
ppm
7.63
14.67
2.67
6.23
2.75
2.35
2.20
2.18
5.77
16.24
14.39
2.10
2.89
1.12
1.07

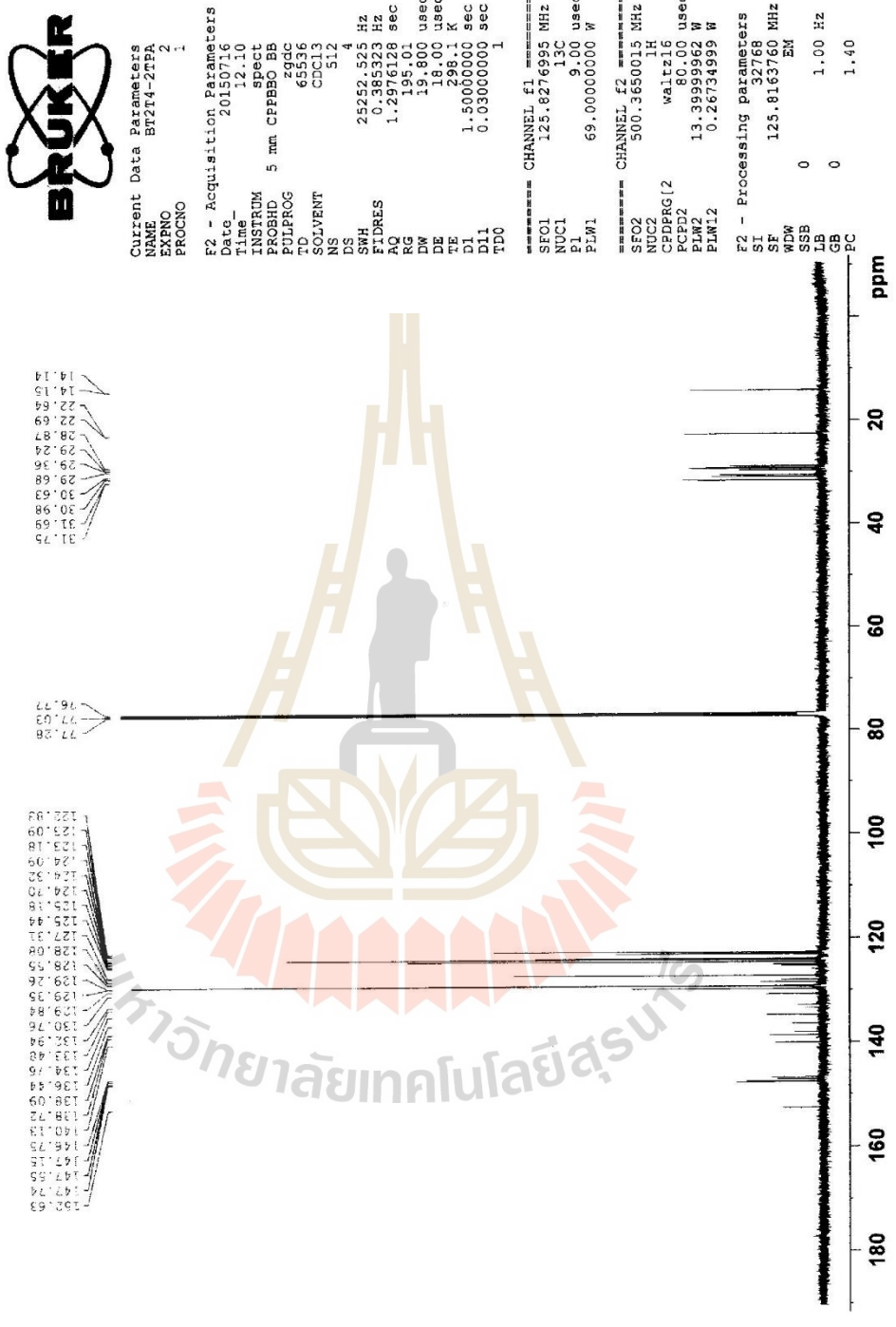
Current Data Parameters
NAME BT2T4-2TPA
EXPNO 2
PROCNO 1
F2 - Acquisition Parameters
Date_ 20150716
Time_ 12.10
INSTRUM spect
PROBHD 5 mm CPPBBO BB
PULPROG zgdc
TD 65536
SOLVENT CDCl3
NS 512
DS 4
SWH 25252.525 Hz
FIDRES 0.385323 Hz
AQ 1.2976128 sec
RG 195.01
DW 19.800 usec
DE 18.00 usec
TE 298.1 K
D1 1.50000000 sec
D11 0.03000000 sec
TD0 1
======== CHANNEL f1 ========
SFO1 125.8276995 MHz
NUC1 13C
P1 9.00 usec
PLW1 69.00000000 W
======== CHANNEL f2 ========
SFO2 500.3650015 MHz
NUC2 1H
CPDPRG[2 waltz16
PCPD2 80.00 usec
PLW2 13.39999962 W
PLW12 0.26734999 W
F2 - Processing parameters
SI 32768
SF 125.8163760 MHz
WDW EM
SSB 0
LB 1.00 Hz
GB 0
PC 1.40
ppm

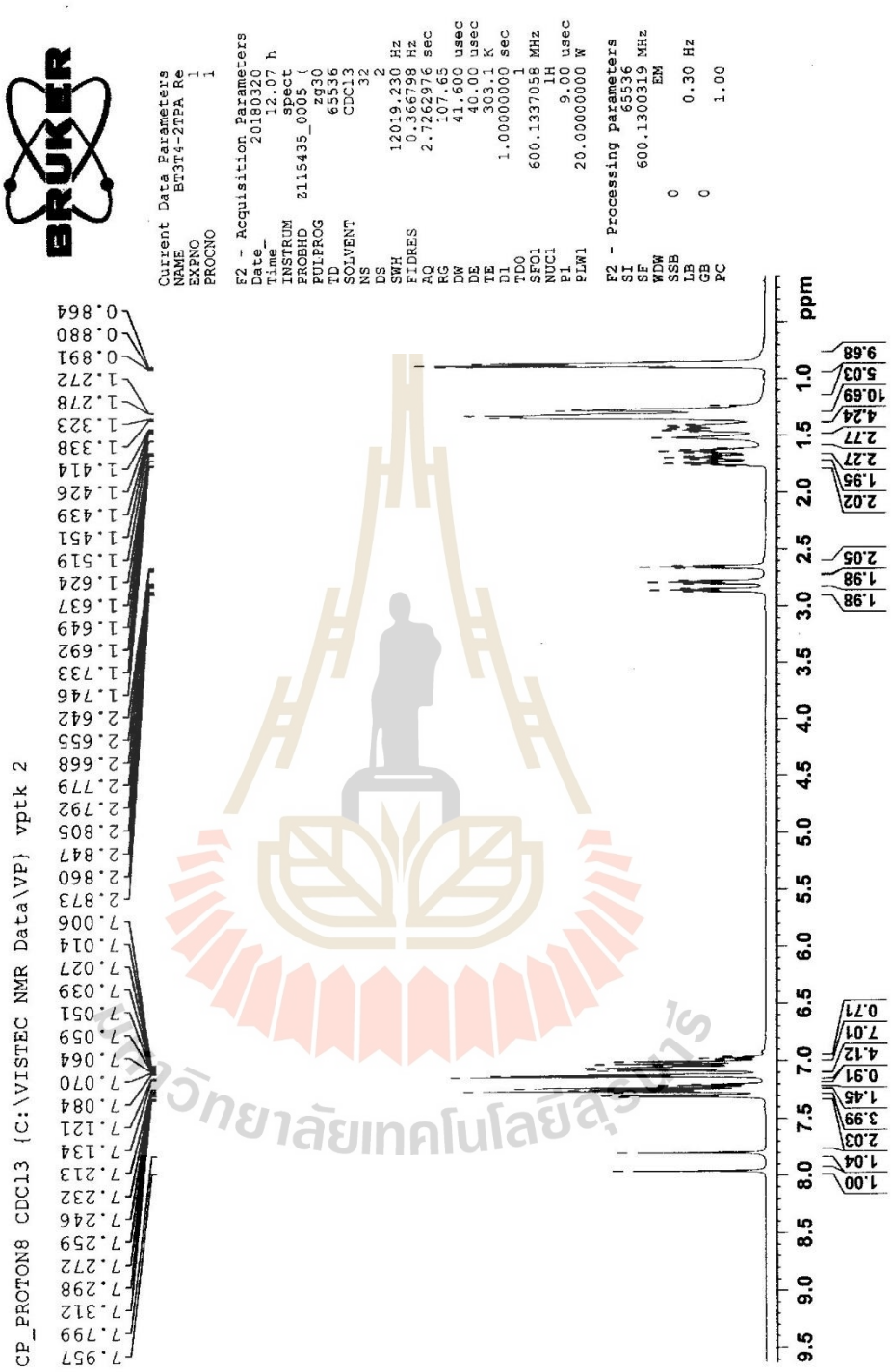
CP_PROTON8 CDC13 {C:\VISTEC NMR Data\VP} vptk 2
Current Data Parameters
NAME BT3T4-2TPA Re
EXPNO 1
PROCNO 1
F2 - Acquisition Parameters
Date_ 20180320
Time 12.07 h
INSTRUM spect
PROBHD Z115435_0005 (
PULPROG zg30
TD 65536
SOLVENT CDC13
NS 32
DS 2
SWH 12019.230 Hz
FIDRES 0.366798 Hz
AQ 2.7262976 sec
RG 107.65
DW 41.600 usec
DE 40.00 usec
TE 303.1 K
D1 1.00000000 sec
TD0 1
SFO1 600.1337058 MHz
NUC1 1H
P1 9.00 usec
PLW1 20.00000000 W
F2 - Processing parameters
SI 65536
SF 600.1300319 MHz
WDW EM
SSB 0
LB 0.30 Hz
GB 0
PC 1.00
ppm
9.68
5.03
10.69
4.24
2.77
2.27
1.95
2.02
2.05
1.98
1.98
0.71
7.01
4.12
0.91
1.45
3.99
2.03
1.04
1.00

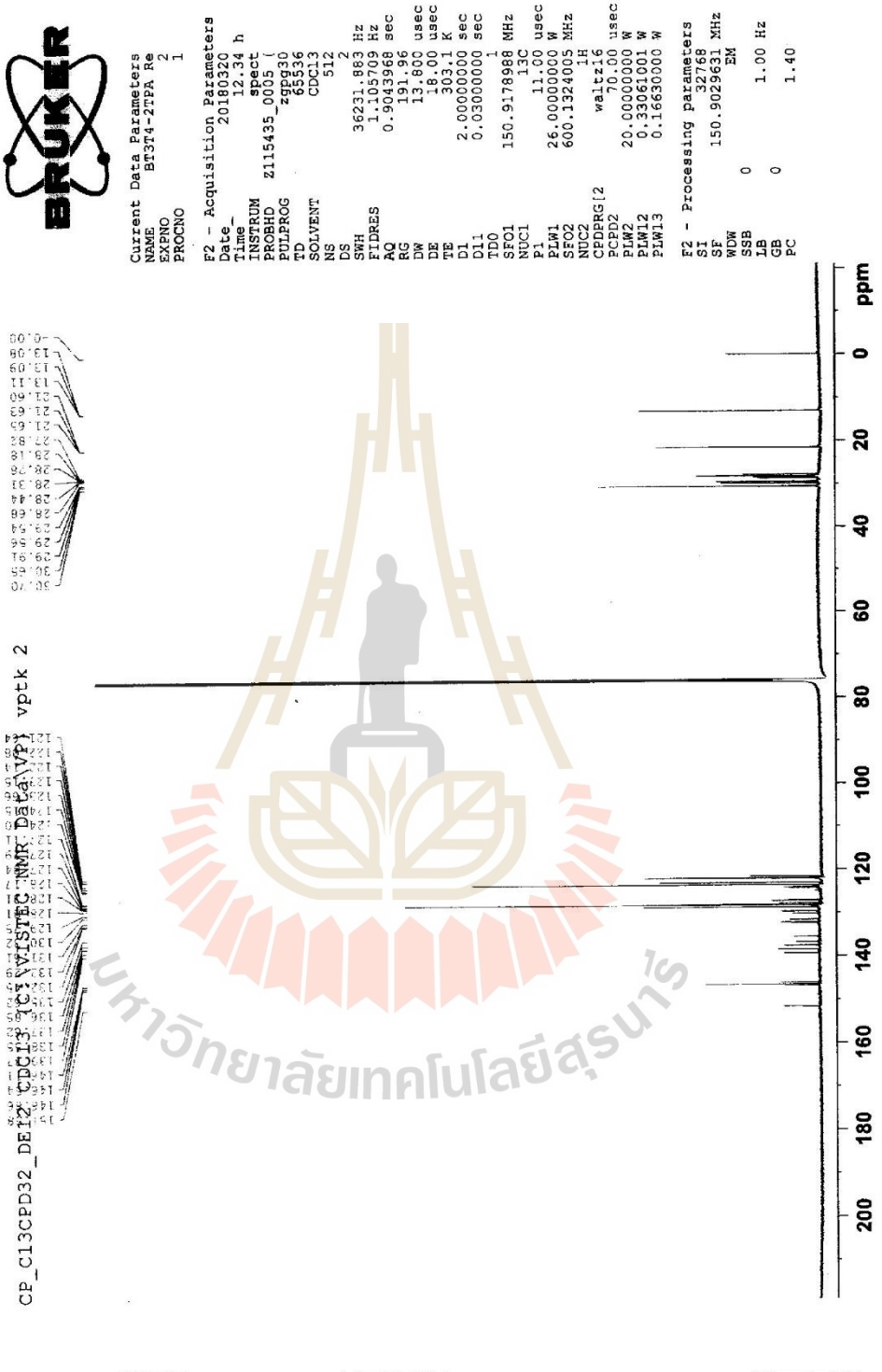
BRUKER
Current Data Parameters
NAME BT3T4-2TPA Re
EXPNO 2
PROCNO 1
F2 - Acquisition Parameters
Date_ 20180320
Time 12.34 h
INSTRUM spect
PROBHD Z115435_0005 (
PULPROG zgpg30
TD 65536
SOLVENT CDCl3
NS 512
DS 2
SWH 36231.883 Hz
FIDRES 1.105709 Hz
AQ 0.9043968 sec
RG 191.96
DW 13.800 usec
DE 10.00 usec
TE 303.1 K
D1 2.00000000 sec
D11 0.03000000 sec
TD0 1
SFO1 150.9178988 MHz
NUC1 13C
P1 11.00 usec
PLW1 26.00000000 W
SFO2 600.1324005 MHz
NUC2 1H
CPDPRG[2 waltz16
PCPD2 70.00 usec
PLW2 20.00000000 W
PLW12 0.33061001 W
PLW13 0.16630000 W
F2 - Processing parameters
SI 32768
SF 150.9029631 MHz
WDW EM
SSB 0
LB 1.00 Hz
GB 0
PC 1.40
CP_C13CPD32_DEPT_CDCl3_VISTEC_NMR Data\VP1 vptk 2
200
180
160
140
120
100
80
60
40
20
0
ppm

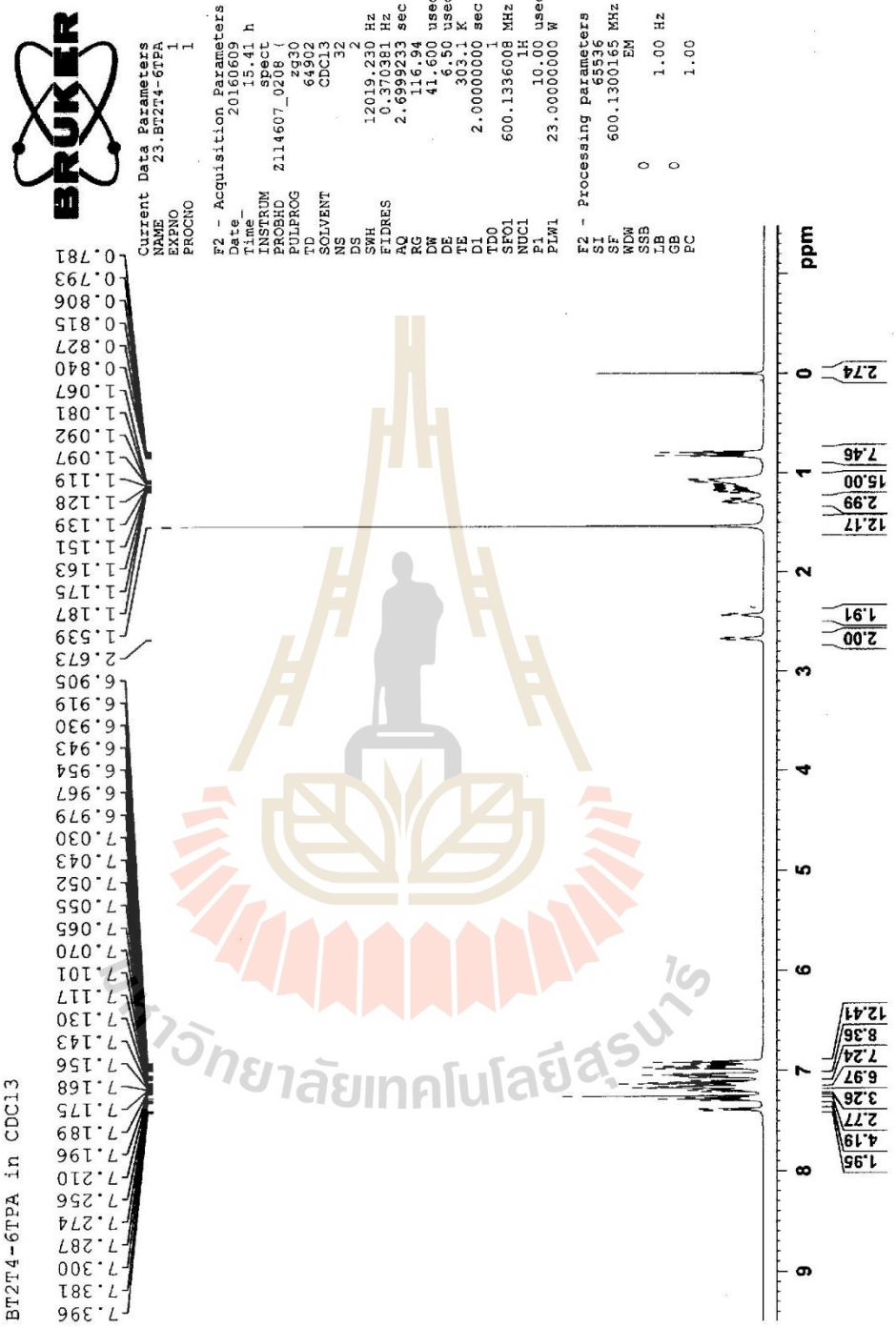
BRUKER
Current Data Parameters
NAME 23.Bt2T4-6TPA
EXPNO 1
PROCNO 1
F2 - Acquisition Parameters
Date_ 20160609
Time_ 15.41 h
INSTRUM spect
PROBHD Z114607_0208 (
PULPROG zg30
TD 64902
SOLVENT CDCl3
NS 32
DS 2
SWH 12019.230 Hz
FIDRES 0.370381 Hz
AQ 2.6999233 sec
RG 116.94
DW 41.600 usec
DE 6.50 usec
TE 303.1 K
D1 2.00000000 sec
TD0 1
SFO1 600.1336008 MHz
NUC1 1H
P1 10.00 usec
PLW1 23.00000000 W
F2 - Processing parameters
SI 65536
SF 600.1300165 MHz
WDW EM
SSB 0
LB 1.00 Hz
GB 0
PC 1.00
BT2T4-6TPA in CDCl3
ppm
2.74
7.46
15.00
2.99
12.17
1.91
2.00
1.95
4.19
2.77
3.26
6.97
7.24
8.36
12.41

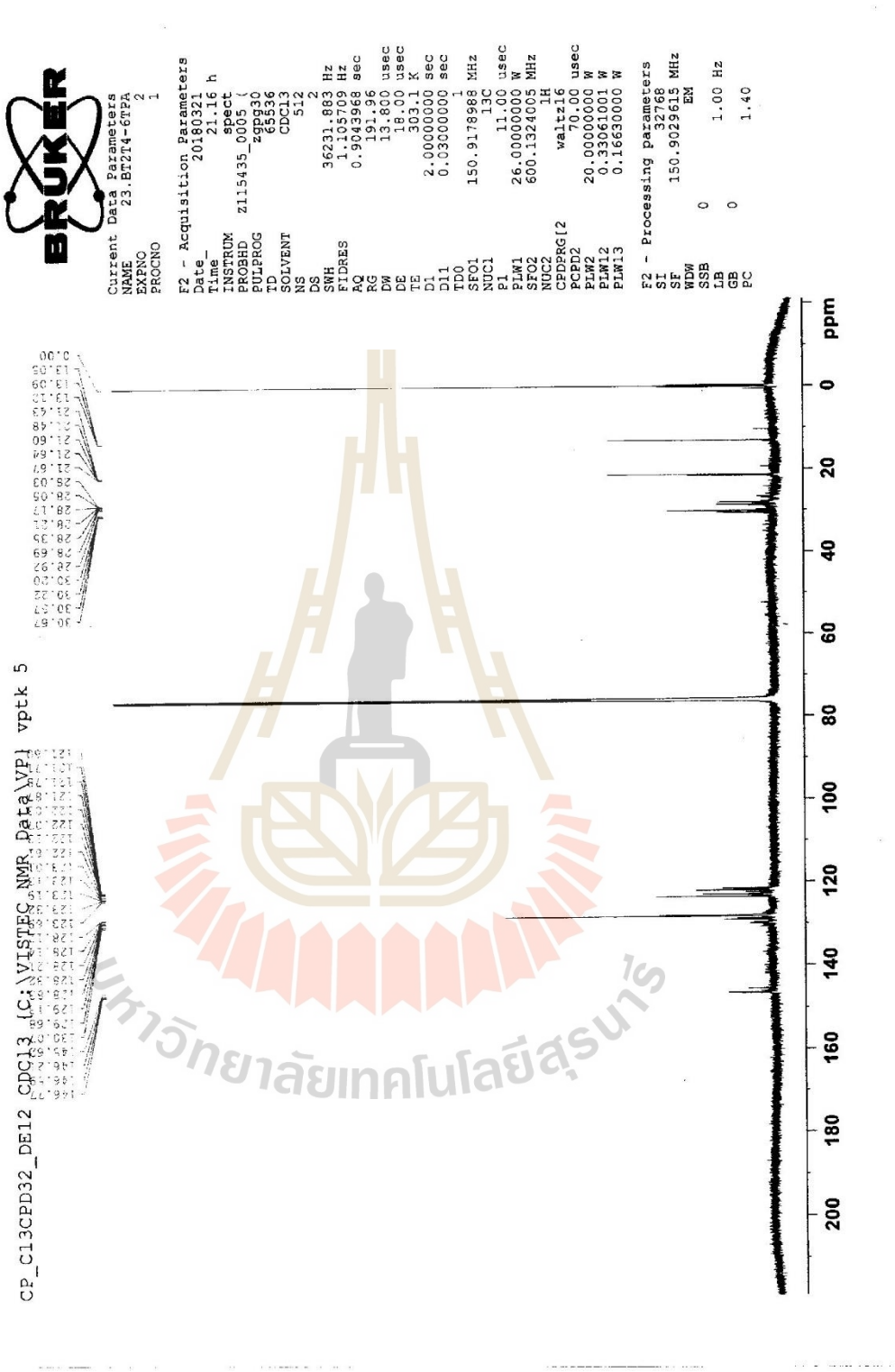
CP_C13CPD32_DE12 CDCl3 (C:\VISTEC_NMR_Data\VP) vptk 5
Current Data Parameters
NAME 23.BT2T4-6TPA
EXPNO 2
PROCNO 1
F2 - Acquisition Parameters
Date_ 20180321
Time_ 21.16 h
INSTRUM spect
PROBHD z115435_0005 (
PULPROG zgpg30
TD 65536
SOLVENT CDCl3
NS 512
DS 2
SWH 36231.883 Hz
FIDRES 1.105709 Hz
AQ 0.9043968 sec
RG 191.96
DW 13.800 usec
DE 18.00 usec
TE 303.1 K
D1 2.00000000 sec
D11 0.03000000 sec
TD0 1
SFO1 150.9178988 MHz
NUC1 13C
P1 11.00 usec
PLW1 26.00000000 W
SFO2 600.1324005 MHz
NUC2 1H
CPDPRG[2 waltz16
PCPD2 70.00 usec
PLW2 20.00000000 W
PLW12 0.33061001 W
PLW13 0.16630000 W
F2 - Processing parameters
SI 32768
SF 150.9029615 MHz
WDW EM
SSB 0
LB 1.00 Hz
GB 0
PC 1.40
ppm
200
180
160
140
120
100
80
60
40
20
0

D:\Data\MSE\POSD\Ball\BT1T4\0_M17\1\1SRef

MALDI-TOF-MS Report

Frontier Research Center, Vidyasirimedhi Institute of Science and Technology

Comment 1 m/z = 468.1728

Comment 2

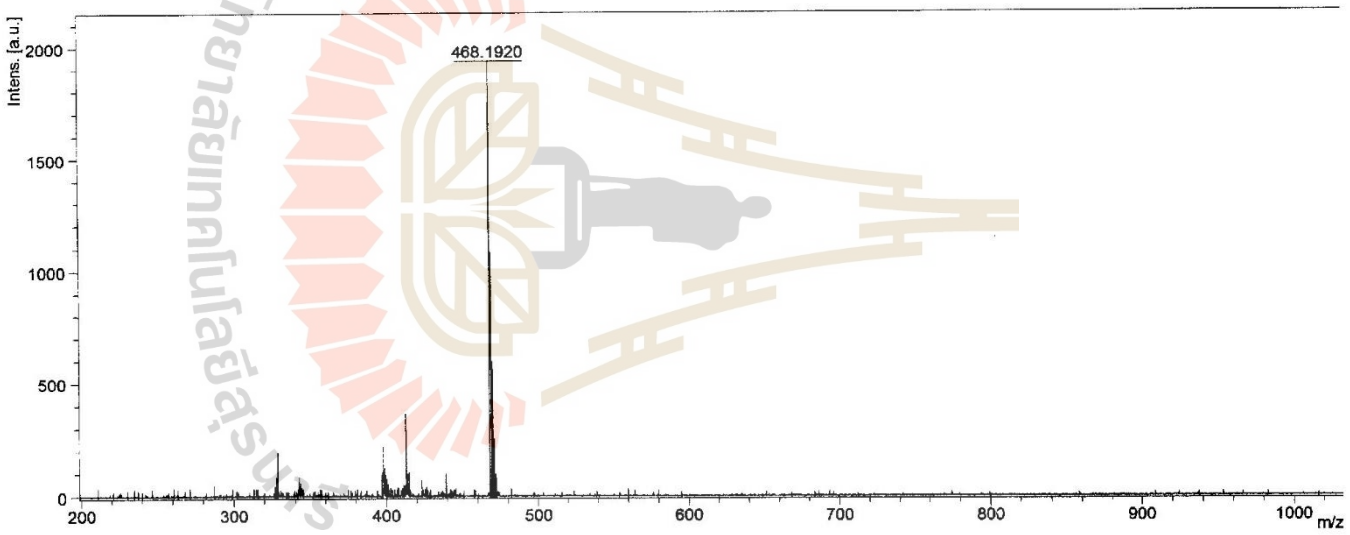

m/z	S/N	Quality Fac.	Res.	Intens.	Area
468.1920				1891	

Bruker Autoflex Speed

Printout: 16/1/2018 2:03:39 PM

D:\Data\MSE\POSD\Ball\BT1T4-2I\0_I16\1\1SRef

MALDI-TOF-MS Report

Frontier Research Center, Vidyasirimedhi Institute of Science and Technology

Comment 1 m/z = 719.9660

Comment 2

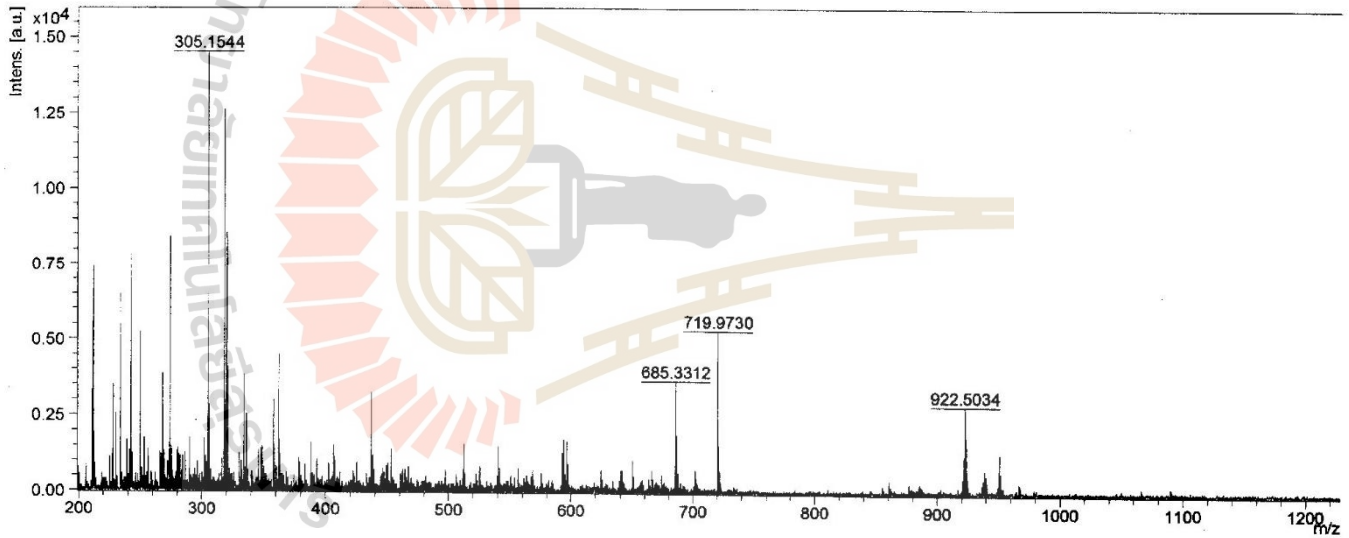

m/z	S/N	Quality Fac.	Res.	Intens.	Area
305.1544				14472	
685.3312				3590	
719.9730				4002	
922.5034				1357	

Bruker Autoflex Speed

Printout: 16/1/2018 2:08:42 PM

D:\Data\MSE\POSD\Ball\BT2T4\0_E7\1\1SRef

MALDI-TOF-MS Report

Frontier Research Center, Vidyasirimedhi Institute of Science and Technology

Comment 1 m/z = 800.3360

Comment 2

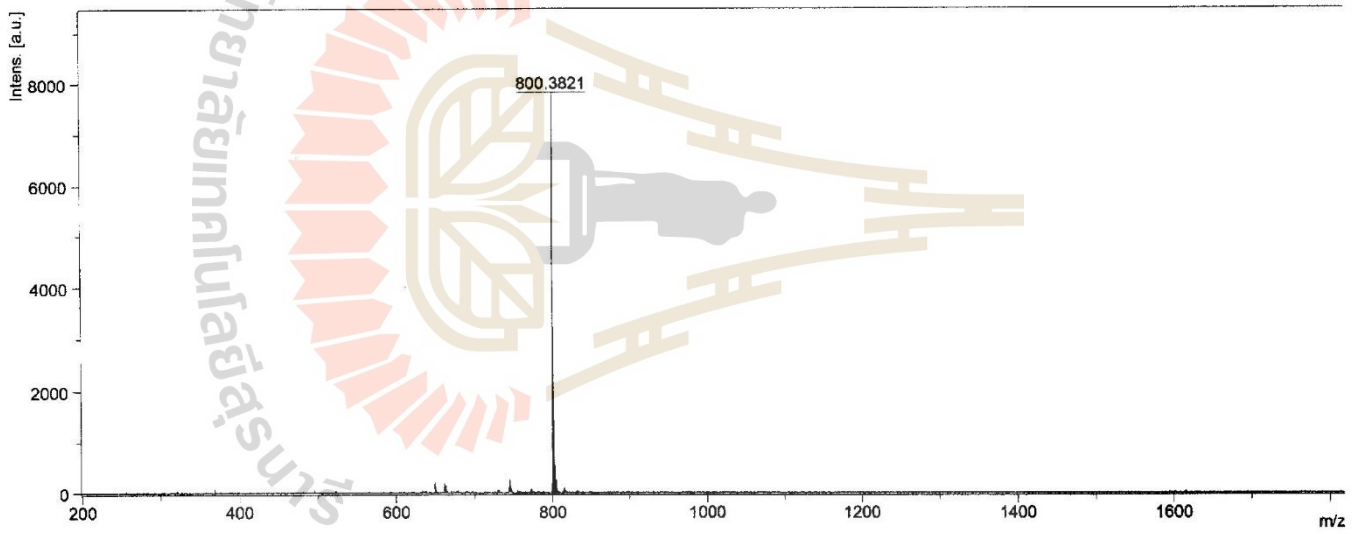

m/z	S/N	Quality Fac.	Res.	Intens.	Area
800.3821				7578	

Bruker Autoflex Speed Printout: 16/1/2018 2:14:32 PM

ลิขสิทธิ์มหาวิทยาลัยเชียงใหม่

D:\Data\MSE\POSD\Ball\BT2T4-2I\0_M12\1\1SRef

MALDI-TOF-MS Report

Frontier Research Center, Vidyasirimedhi Institute of Science and Technology

Comment 1 m/z = 1052.1293

Comment 2

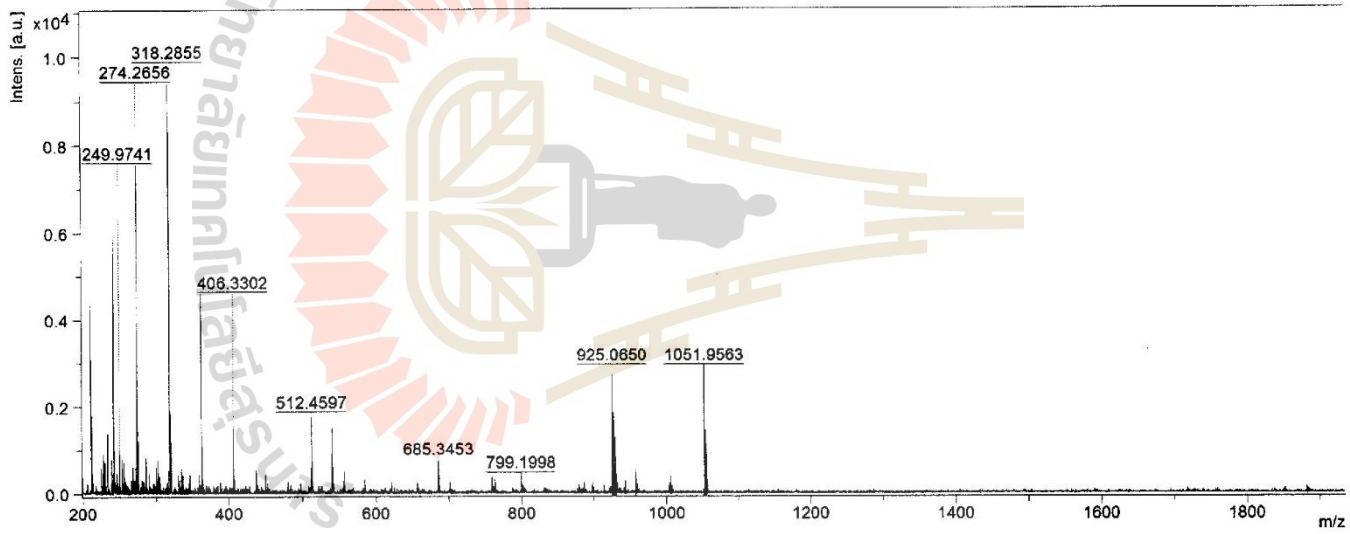

m/z	S/N	Quality Fac.	Res.	Intens.	Area
211.1632	40	2397	1598	4588	724
212.0110	23	3635	1632	2817	442
227.9794	9	211	1656	964	173
230.2169	7	368	1607	774	135
233.9993	12	2353	1798	1404	226
239.2004	7	42.3	1869	819	127
242.2679	55	4147	1713	6163	1061

D:\Data\MSE\POSD\Ball\BT2T4-2I\0_M12\1\1SRef

m/z	S/N	Quality Fac.	Res.	Intens.	Area
249.9741	9	1059	1902	1035	170
253.2168	7	59.2	1845	838	141
256.2466	7	74.0	1540	775	161
268.1940	6	40.4	1830	706	128
274.2656	72	5953	1914	8084	1436
286.2654	8	411	2083	860	149
302.2823	7	63.8	2143	749	134
318.2855	94	20433	2000	9853	1991
320.2392	9	755	2233	944	173
362.3153	47	5188	2270	4732	983
406.3302	15	1084	2465	1445	318
512.4597	25	598	2826	1829	469
540.4834	24	4855	2806	1541	426
556.4798	8	579	3137	496	129
685.3453	14	2844	3316	787	255
759.0303	7	302	3302	376	142
799.1998	8	252	3269	438	194
925.0650	53	629	3774	2906	1282
927.0674	24	390	3947	1301	553
929.0730	21	298	3848	1153	504
957.0306	10	338	3845	553	254
1005.9853	7	683	4082	361	168
1051.9563	56	1643	3879	2838	1487
1053.8885	21	430	4188	1026	504

Bruker Autoflex Speed

Printout: 16/1/2018 2:19:17 PM

D:\Data\MSE\POSD\Ball\BT3T4\0_O13\1\1SRef

MALDI-TOF-MS Report

Frontier Research Center, Vidyasirimedhi Institute of Science and Technology

Comment 1 m/z = 1132.4992

Comment 2

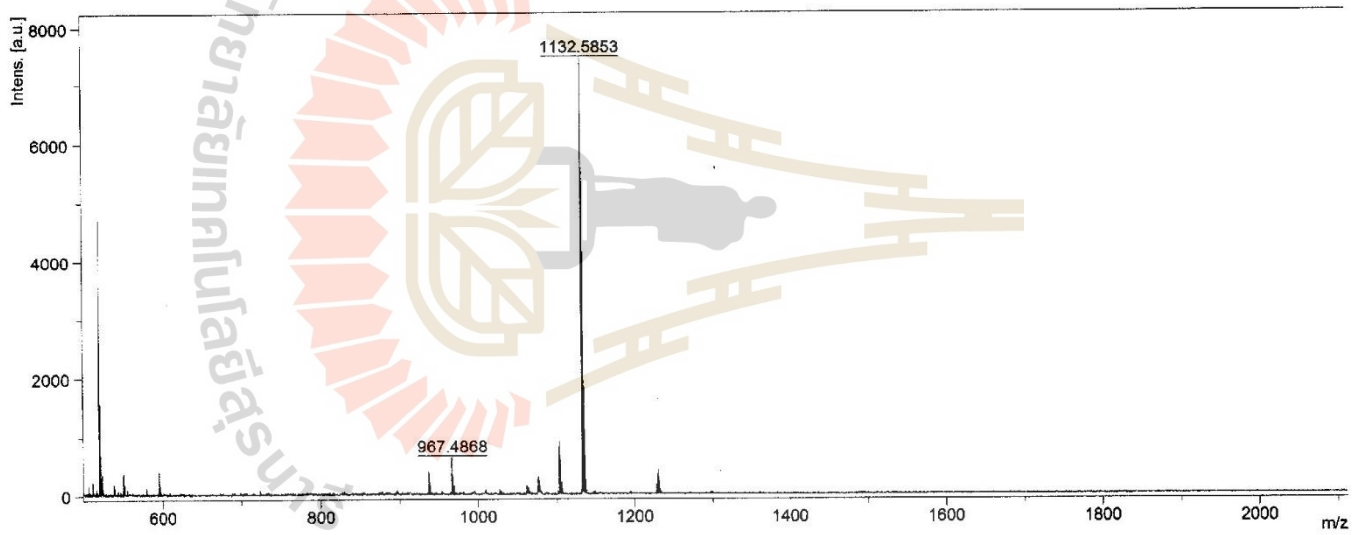

m/z	S/N	Quality Fac.	Res.	Intens.	Area
967.4868				368	
1132.5853				7448	

Bruker Autoflex Speed

Printout: 16/1/2018 2:26:47 PM

D:\Data\MSE\POSD\Ball\BT3T4-2I\0_L2\1\1SRef

MALDI-TOF-MS Report

Frontier Research Center, Vidyasirimedhi Institute of Science and Technology

Comment 1 MW=1384.2925

Comment 2

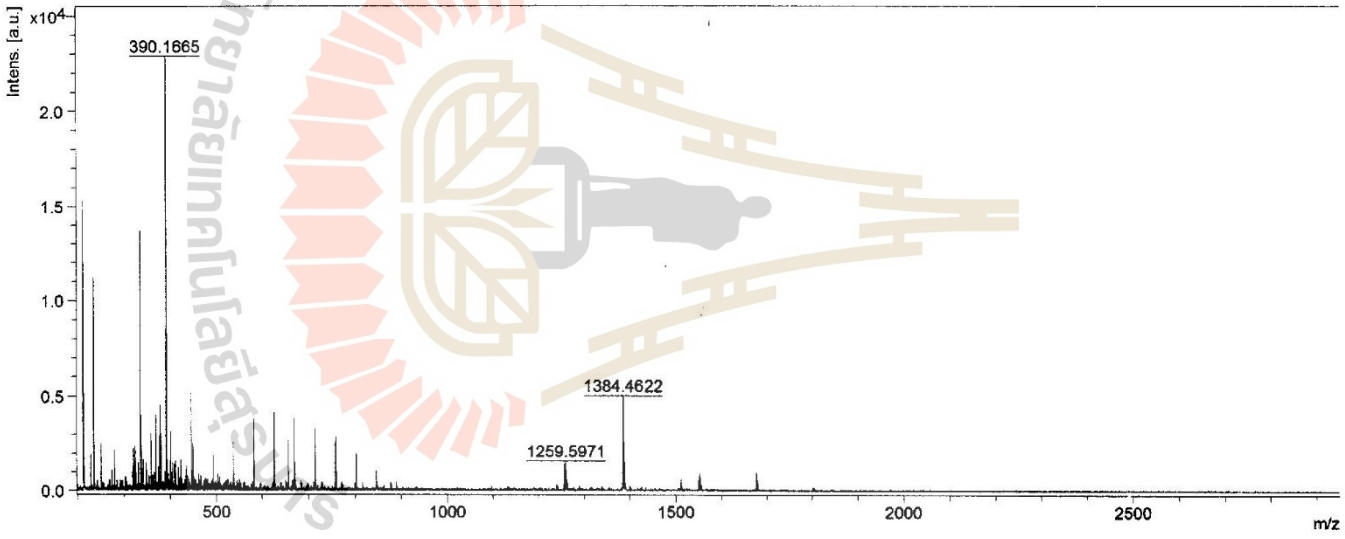

m/z	S/N	Quality Fac.	Res.	Intens.	Area
390.1665				529	
1259.5971				1090	
1384.4622				4880	

Bruker Autoflex Speed Printout: 16/1/2018 2:29:05 PM

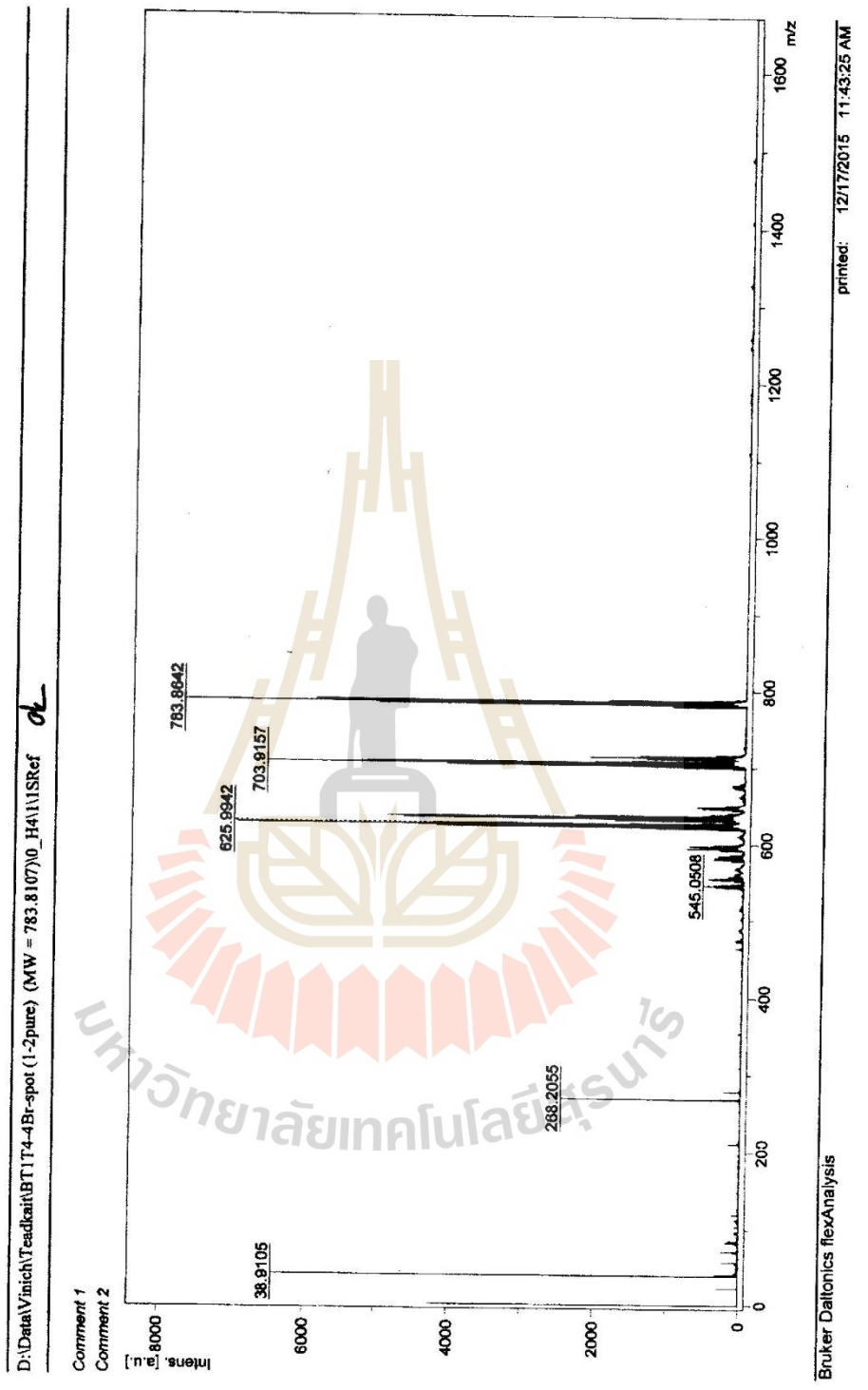

มหาวิทยาลัยเทคโนโลยีสุรนารี

D:\Data\MSE\POSD\Ball\BT1T3 Ref\0_K22\1\1SRef

MALDI-TOF-MS Report

Frontier Research Center, Vidyasirimedhi Institute of Science and Technology

Comment 1 MW=468.1728

Comment 2

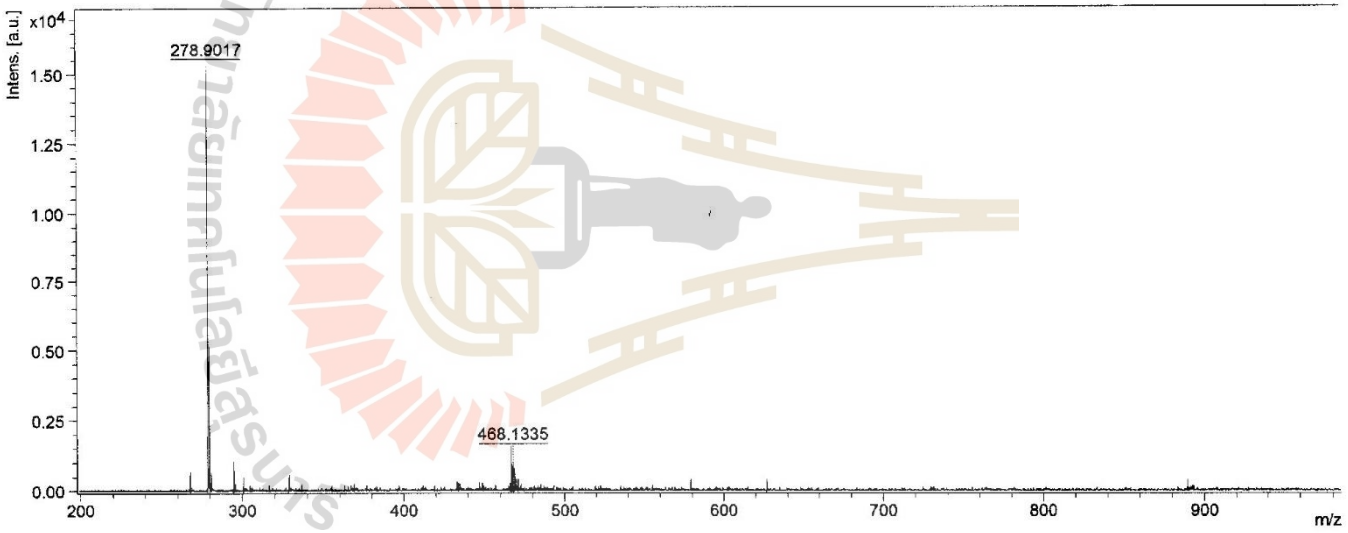

m/z	S/N	Quality Fac.	Res.	Intens.	Area
278.9017				15488	
468.1335				971	

Bruker Autoflex Speed Printout: 16/1/2018 1:53:38 PM

D:\Data\MSE\POSD\Ball\BT1T3-2Br\0_G18\1\1SRef

MALDI-TOF-MS Report

Frontier Research Center, Vidyasirimedhi Institute of Science and Technology

Comment 1 m/z = 625.9917

Comment 2

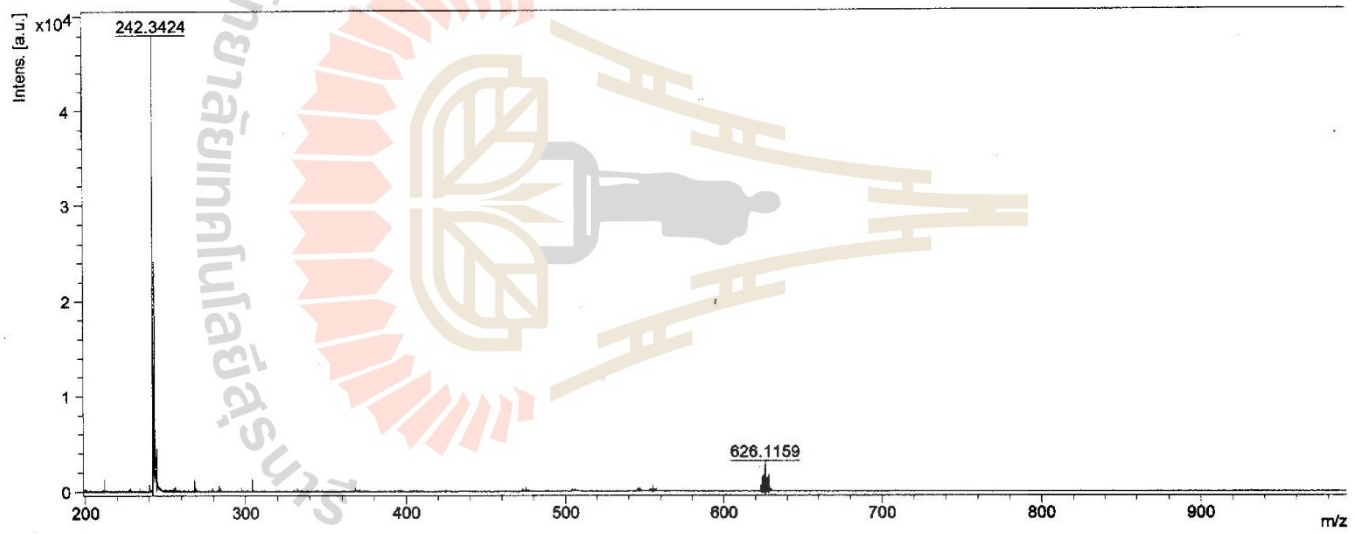

m/z	S/N	Quality Fac.	Res.	Intens.	Area
626.1159				2980	
242.3424				47831	

Bruker Autoflex Speed

Printout: 22/3/2018 12:02:30 AM

Display Report

Analysis Info

Analysis Name	D:\Data\VISTEC Data QTOF\Vinich\Terdkiat\BT1T3-4Br.d	Acquisition Date	3/10/2016 2:50:50 PM
Method	DEFAULT.m	Operator	VISTEC_Scientist
Sample Name	BT1T3-4Br	Instrument	compact 8255754.20068
Comment			

Acquisition Parameter

Source Type	APCI	Ion Polarity	Positive	Set Nebulizer	2.0 Bar
Focus	Not active	Set Capillary	4500 V	Set Dry Heater	220 °C
Scan Begin	200 m/z	Set End Plate Offset	-500 V	Set Dry Gas	3.5 l/min
Scan End	1000 m/z	Set Charging Voltage	2000 V	Set Divert Valve	Source
		Set Corona	4000 nA	Set APCI Heater	370 °C

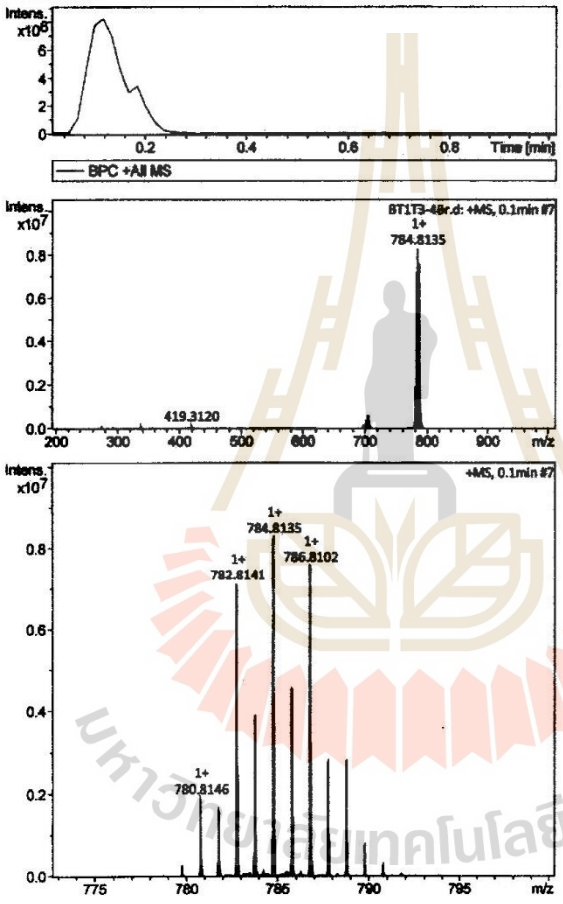

#	m/z	I
1	275.1615	93756
2	338.3385	130089
3	419.3120	162200
4	696.7196	95418
5	700.7171	148401
6	702.7153	108114
7	702.9016	217561
8	703.8971	273673
9	704.9018	609575
10	705.8981	391555
11	706.9006	636310
12	707.8991	264309
13	708.8985	269815
14	709.8998	80459
15	779.8068	292785
16	780.8146	1918085
17	781.8095	1656863
18	782.8141	7136164
19	783.4858	83400
20	783.8110	3886246
21	784.2921	110875
22	784.8135	8282732
23	785.4857	94414
24	785.8112	4577898
25	786.2938	123278
26	786.8102	7582181
27	787.8101	2842633
28	788.8069	2836808
29	789.8080	810015
30	790.8047	334580

มหาวิทยาลัยเทคโนโลยีสุรนารี

MALDI-TOF-MS Report

Frontier Research Center, Vidyasirimedhi Institute of Science and Technology

Comment 1 m/z = 958.1550

Comment 2

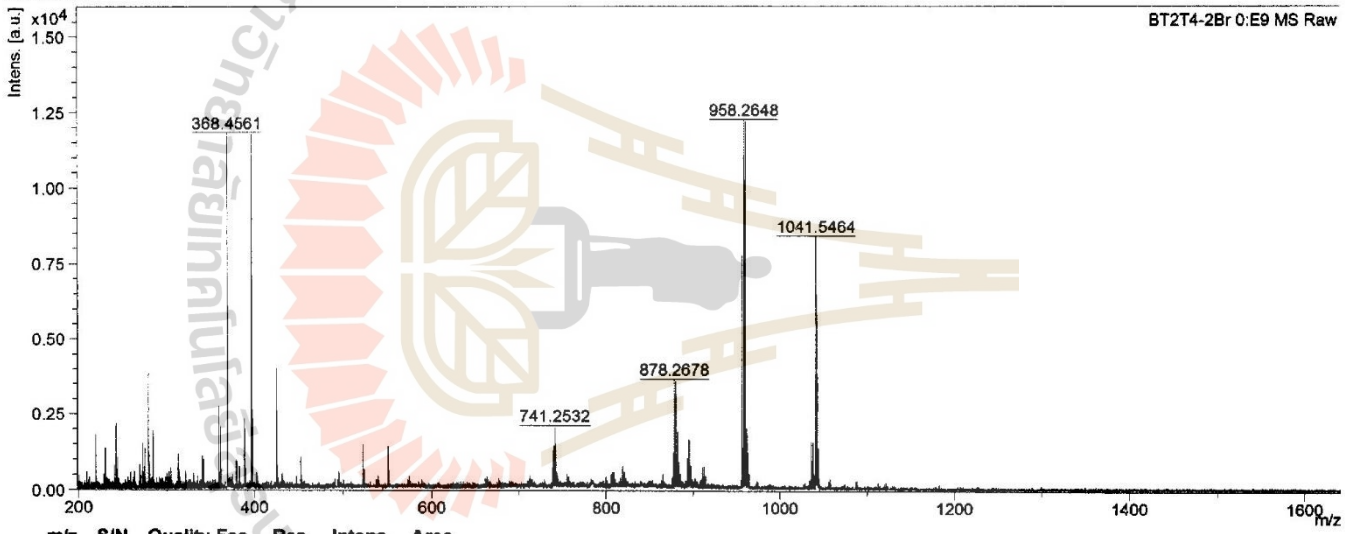

m/z	S/N	Quality Fac.	Res.	Intens.	Area
368.4561				11652	
958.2648				10885	
1041.5464				8360	
741.2532				2063	
878.2678				1230	

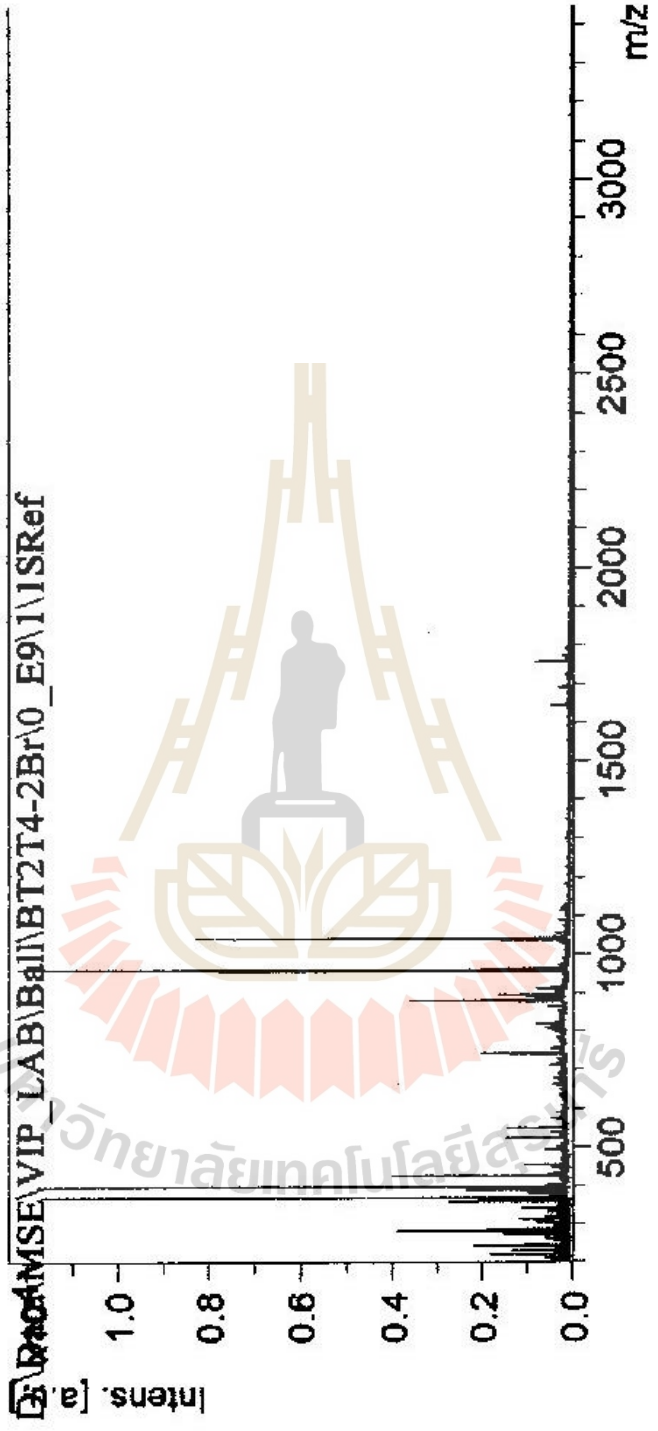
Intens. [a.u.]
1.0
0.8
0.6
0.4
0.2
0.0
500
1000
1500
2000
2500
3000
m/z

Q-ToF MS Report | Frontier Research Center@VISTEC

Analysis Info

Analysis Name	D:\Data\VISTEC Data QTOF\Vinich\Terdkiat\BT2T4-4BrRUN2.d - Copy	Acquisition Date	3/10/2016 11:21:07 PM
Method	DEFAULT.m	Operator	VISTEC_Scientist
Sample Name	BT2T4 -	Instrument	compact 8255754.20068
Comment			

Acquisition Parameter

Source Type	APCI	Ion Polarity	Positive	Set Nebulizer	2.0 Bar
Focus	Not active	Set Capillary	4500 V	Set Dry Heater	220 °C
Scan Begin	200 m/z	Set End Plate Offset	-500 V	Set Dry Gas	3.5 l/min
Scan End	1400 m/z	Set Charging Voltage	2000 V	Set Divert Valve	Source
		Set Corona	4000 nA	Set APCI Heater	370 °C

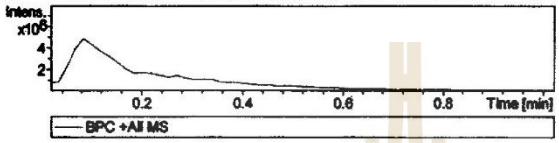

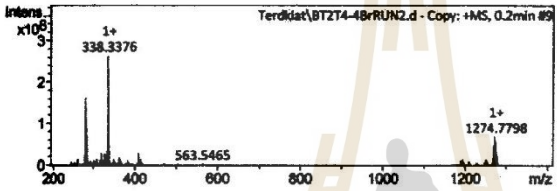

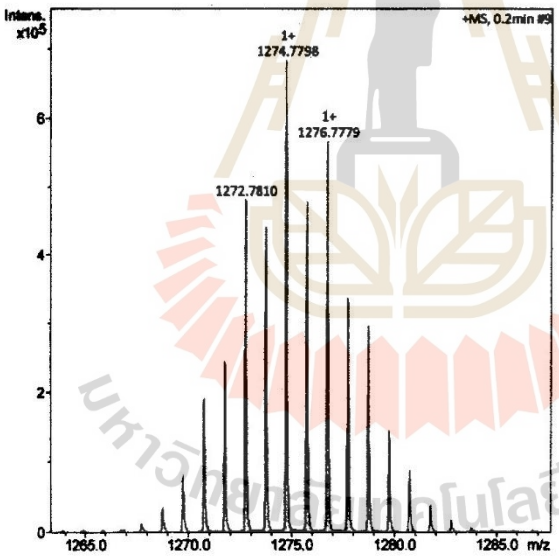

#	m/z	I
1	1193.8630	141841
2	1195.8624	157072
3	1197.8616	101722
4	1252.8766	136428
5	1253.8744	113454
6	1254.8751	148035
7	1270.7817	192719
8	1271.7772	246182
9	1272.7810	481201
10	1273.7781	442876
11	1274.7798	683718
12	1275.7780	479018
13	1276.7779	566381
14	1277.7766	338294
15	1278.7763	296908
16	1279.7758	146688

BT

D:\Data\MSE\POSD\Ball\BT1T4-2TPA\0_I1\1\1SRef

MALDI-TOF-MS Report

Frontier Research Center, Vidyasirimedhi Institute of Science and Technology

Comment 1 m/z = 954.3824

Comment 2

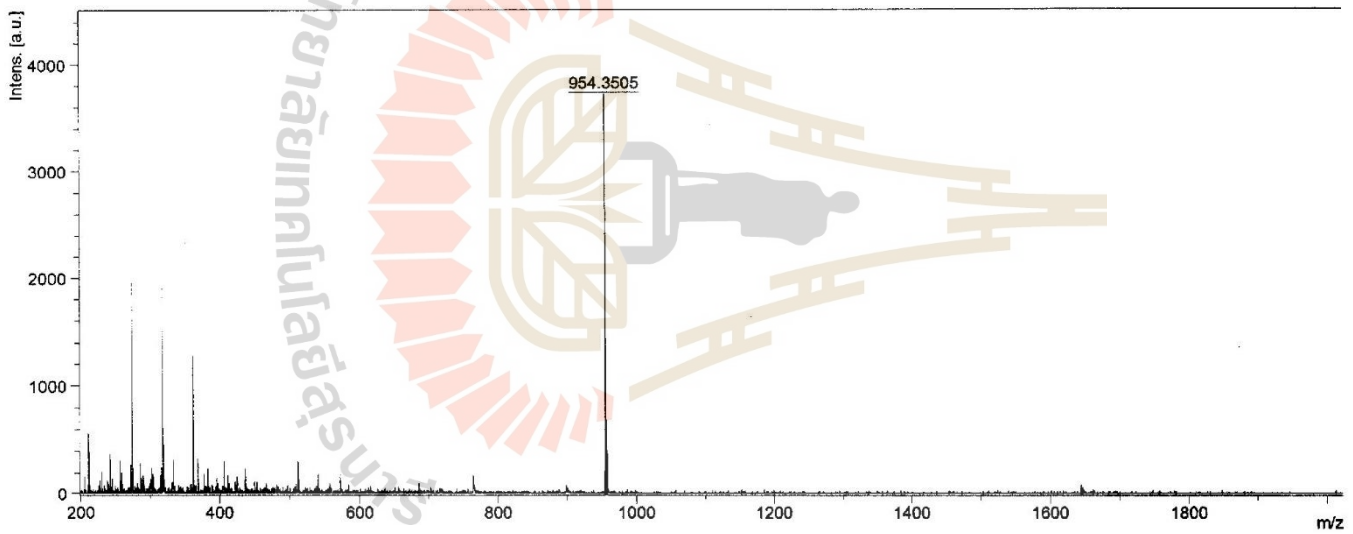

m/z	S/N	Quality Fac.	Res.	Intens.	Area
954.3505				3602	

Bruker Autoflex Speed

Printout: 16/1/2018 2:10:14 PM

D:\Data\MSE\POSD\Ball\BT1T4-4TPA\0_N6\1\1SRef

MALDI-TOF-MS Report

Frontier Research Center, Vidyasirimedhi Institute of Science and Technology

Comment 1 (MW=1441.5953)
Comment 2

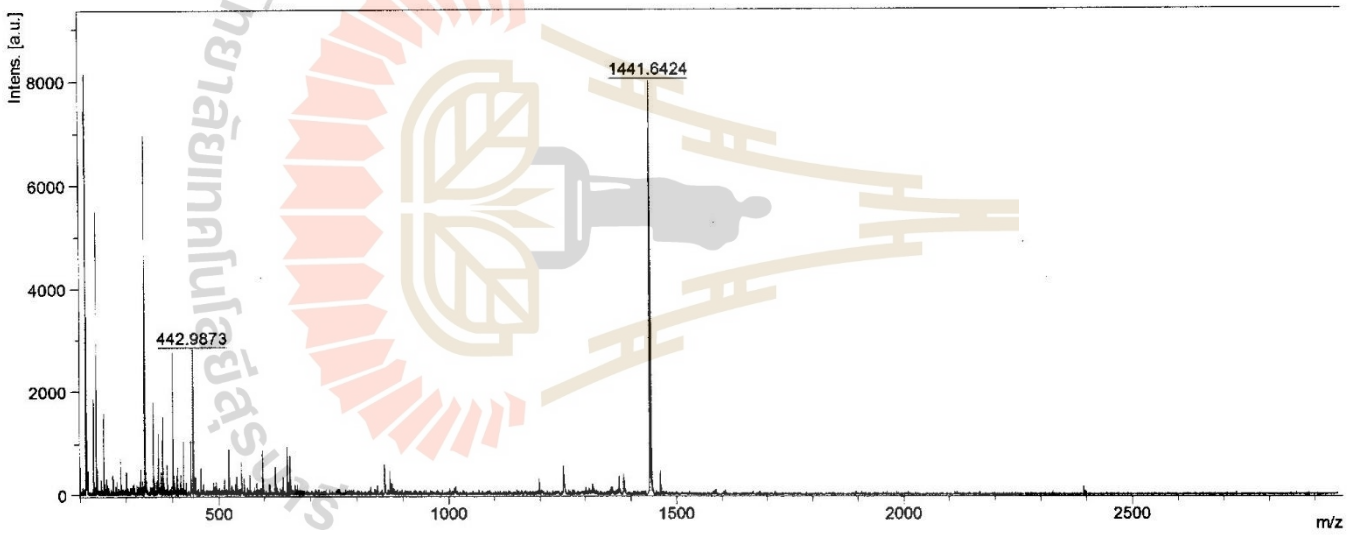

m/z	S/N	Quality Fac.	Res.	Intens.	Area
442.9873				102	
1441.6424				5378	

Bruker Autoflex Speed

Printout: 16/1/2018 2:12:24 PM

D:\Data\MSE\POSD\Ball\BT1T4-2CPh\0_M3\1\1SRef

MALDI-TOF-MS Report

Frontier Research Center, Vidyasirimedhi Institute of Science and Technology

Comment 1 m/z = 950.3511

Comment 2

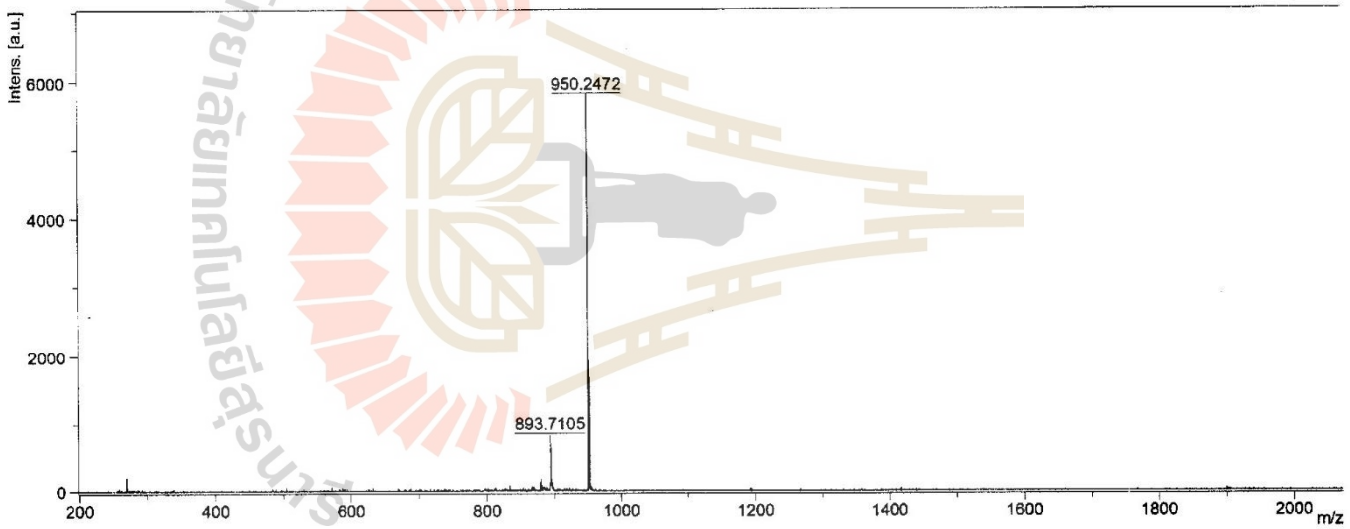

m/z	S/N	Quality Fac.	Res.	Intens.	Area
893.7105				838	
950.2472				5759	

Bruker Autoflex Speed

Printout: 16/1/2018 2:07:04 PM

D:\Data\MSE\POSD\Ball\BT1T3-2CPh\0_D20\1\1SRef

MALDI-TOF-MS Report

Frontier Research Center, Vidyasirimedhi Institute of Science and Technology

Comment 1 m/z = 950.3511

Comment 2

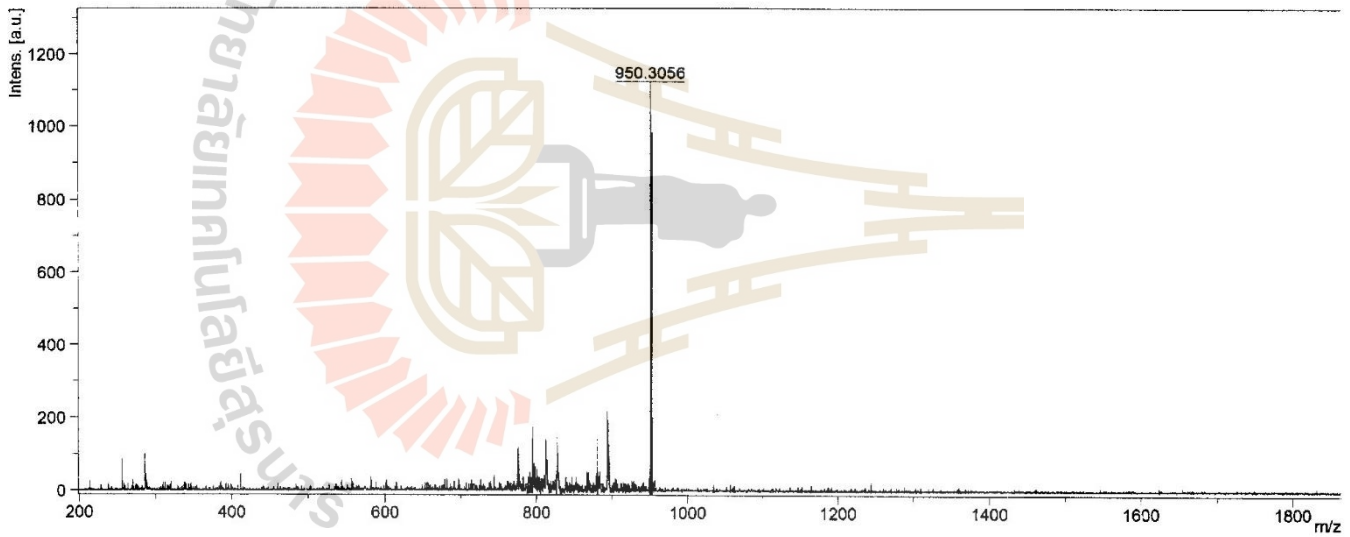

m/z	S/N	Quality Fac.	Res.	Intens.	Area
950.3056				1104	

Bruker Autoflex Speed

Printout: 16/1/2018 1:56:38 PM

D:\Data\MSE\POSD\Ball\BT1T3-2TPA\0_I13\1\1SRef

MALDI-TOF-MS Report

Frontier Research Center, Vidyasirimedhi Institute of Science and Technology

Comment 1 m/z = 954.3824

Comment 2

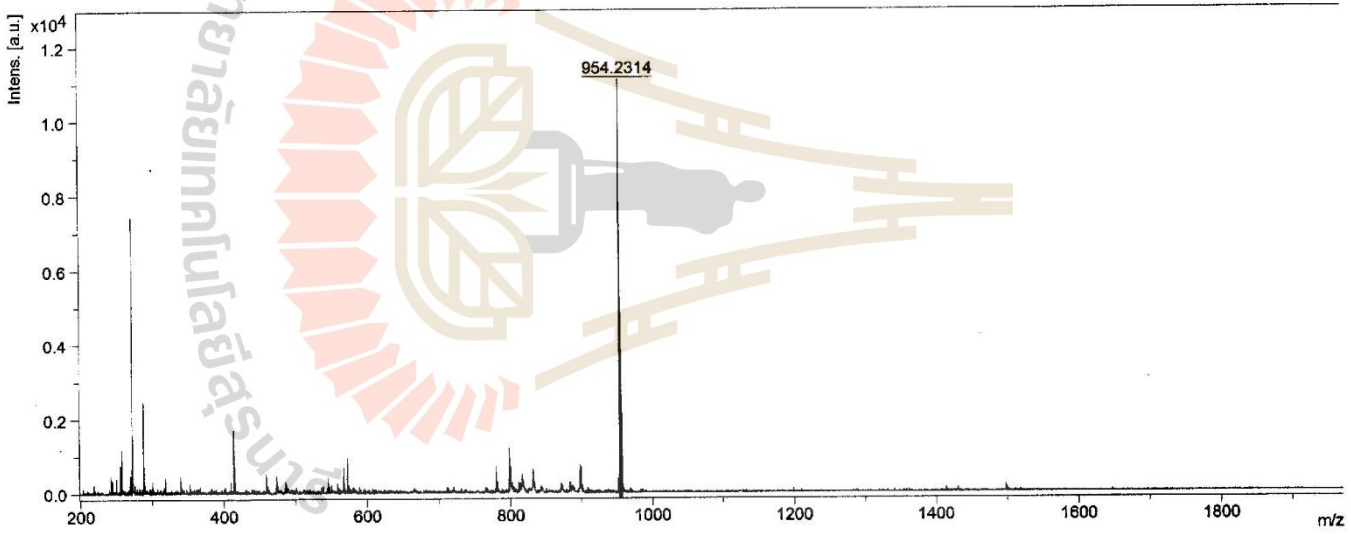

m/z	S/N	Quality Fac.	Res.	Intens.	Area
954.2314				11115	

Bruker Autoflex Speed

Printout: 16/1/2018 1:58:27 PM

ศูนย์วิทยทรัพยากร
จุฬาลงกรณ์มหาวิทยาลัย

D:\Data\MSE\POSD\Ball\BT1T3-4TPA\0_M5\1\1SRef

MALDI-TOF-MS Report

Frontier Research Center, Vidyasirimedhi Institute of Science and Technology

Comment 1 m/z =1441.5953

Comment 2

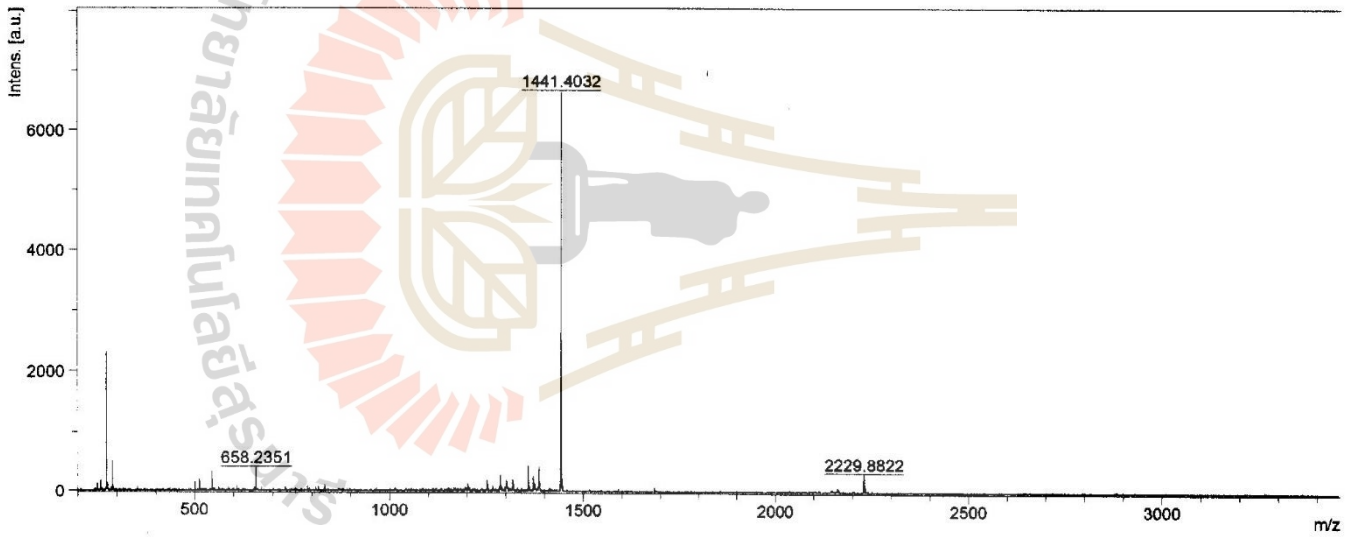

m/z	S/N	Quality Fac.	Res.	Intens.	Area
658.2351				174	
1441.4032				6608	
2229.8822				285	

Bruker Autoflex Speed

Printout: 16/1/2018 2:02:13 PM

D:\Data\MSE\POSD\Ball\BT2T4-2TPA\0_M13\1\1SRef

MALDI-TOF-MS Report

Frontier Research Center, Vidyasirimedhi Institute of Science and Technology

Comment 1 m/z = 1286.5456

Comment 2

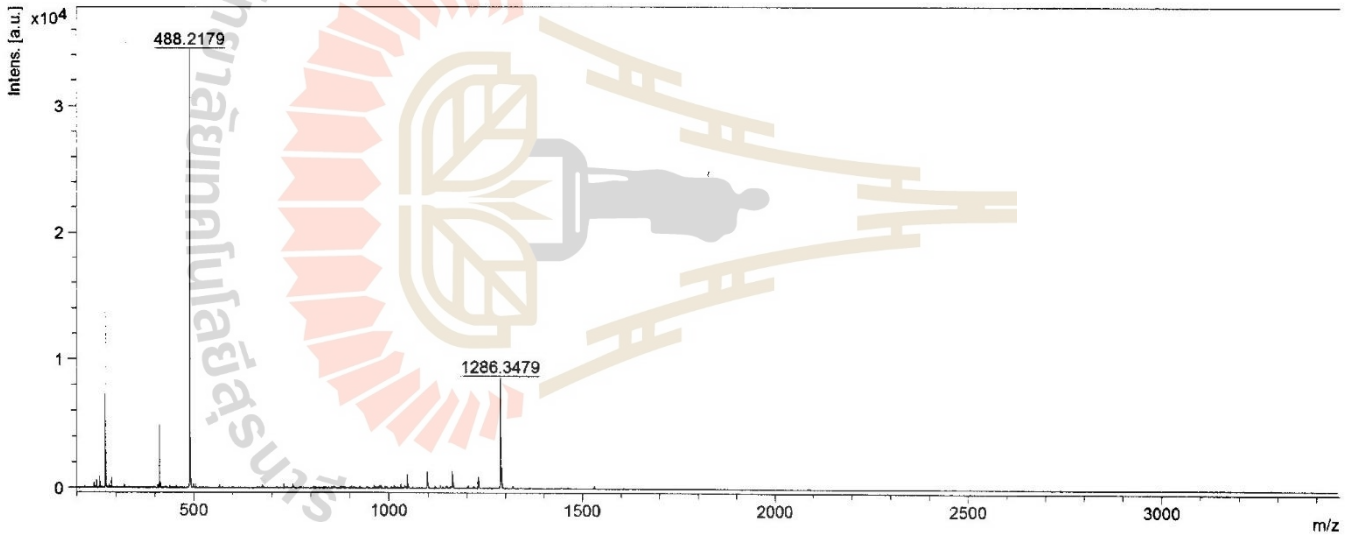

m/z	S/N	Quality Fac.	Res.	Intens.	Area
488.2179				34395	
1286.3479				8415	

Bruker Autoflex Speed

Printout: 16/1/2018 2:20:36 PM

D:\Data\MSE\POSD\Ball\BT3T4-2TPA\0_K9\1\1SRef

MALDI-TOF-MS Report

Frontier Research Center, Vidyasirimedhi Institute of Science and Technology

Comment 1 m/z = 1619.7122

Comment 2

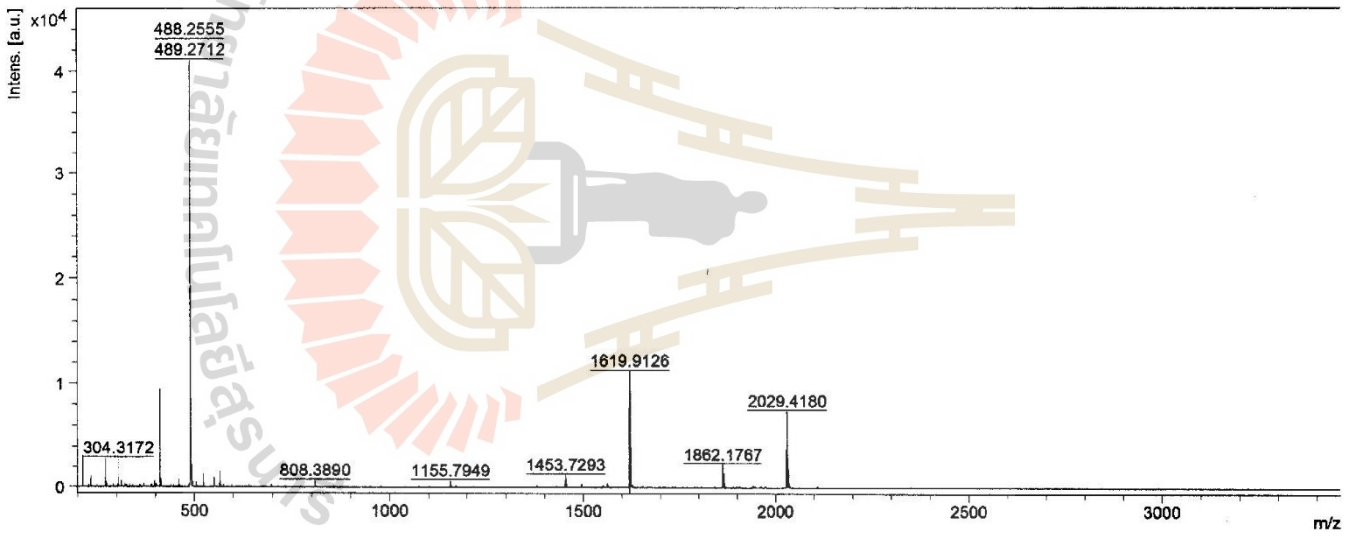

m/z	S/N	Quality Fac.	Res.	Intens.	Area
212.0238	58	6519	1552	3228	536
234.0134	22	5857	1742	1274	208
272.1394	51	2665	1876	3082	553
304.3172	13	17725	1893	1011	205
312.1649	9	396	2029	657	133
411.2220	91	15422	2386	9855	2274
412.2222	20	574	2239	2283	563

D:\Data\MSE\POSD\Ball\BT3T4-2TPA\0_K9\1\1SRef

m/z	S/N	Quality Fac.	Res.	Intens.	Area
459.3558	8	591	2413	777	205
488.2555	415	2111	1677	42930	20200
489.2712	255	6099	2288	27500	8252
490.2852	93	543	2150	10208	3502
491.4399	73	1195	3227	8974	2224
522.6205	13	3111	2627	1320	374
550.6505	10	753	2751	1049	304
565.2898	17	4364	2922	1705	480
697.4551	7	48.4	3099	292	104
808.3890	20	982	3728	617	227
1155.7949	19	351	4190	614	350
1453.7293	10	197	4861	945	693
1617.8906	39	33.9	9840	5579	2914
1619.9126	103	1731	5059	10539	9147
1621.8533	36	548	5181	3849	3293
1862.1767	16	815	5500	2095	2214
2029.4180	58	350	5639	4896	5569
2033.3880	6	74.7	5144	558	707

Bruker Autoflex Speed

Printout: 16/1/2018 2:31:12 PM

D:\Data\MSE\POSD\Ball\BT2T4-6TPA\0_M16\1\1SRef

MALDI-TOF-MS Report

Frontier Research Center, Vidyasirimedhi Institute of Science and Technology

Comment 1 m/z = 2259.9682

Comment 2

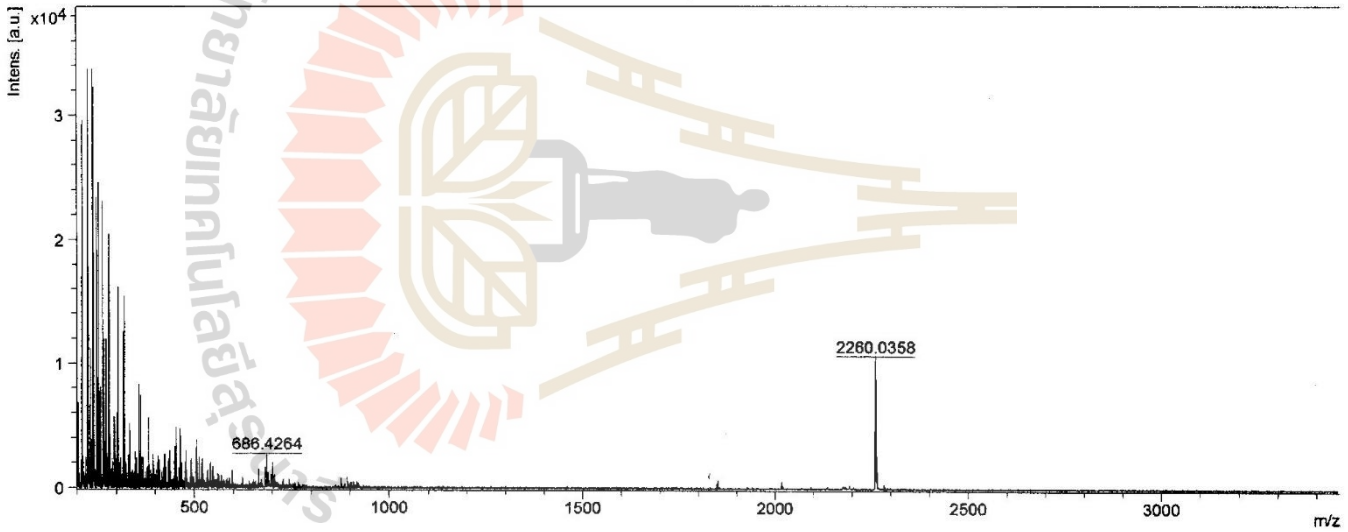

m/z	S/N	Quality Fac.	Res.	Intens.	Area
686.4264				1436	
2260.0358				10359	

Bruker Autoflex Speed

Printout: 16/1/2018 2:24:41 PM

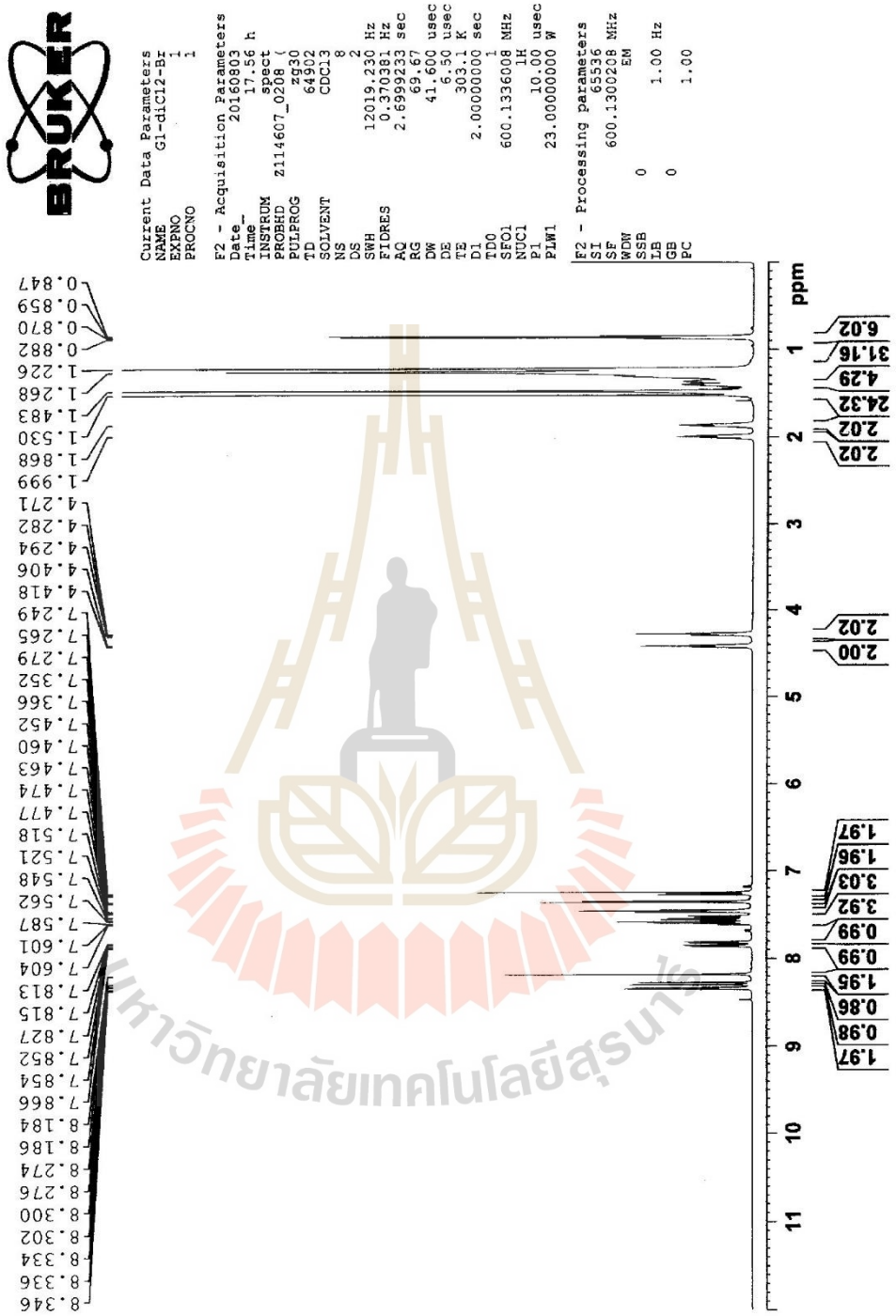
Current Data Parameters
NAME G1-diC12-Br
EXPNO 1
PROCNO 1
F2 - Acquisition Parameters
Date_ 20160803
Time 17.56 h
INSTRUM spect
PROBHD Z114607_0208 (
PULPROG zg30
TD 64902
SOLVENT CDCl3
NS 8
DS 2
SWH 12019.230 Hz
FIDRES 0.3703381 Hz
AQ 2.6999233 sec
RG 69.67
DW 41.600 usec
DE 6.50 usec
TE 303.1 K
D1 2.00000000 sec
TD0 1
SFO1 600.1336008 MHz
NUC1 1H
P1 10.00 usec
PLW1 23.00000000 W
F2 - Processing parameters
SI 65536
SF 600.1300208 MHz
WDW EM
SSB 0
LB 1.00 Hz
GB 0
PC 1.00
ppm
6.02
31.16
4.29
24.32
2.02
2.02
2.02
2.00
1.97
1.96
3.03
3.92
0.99
0.99
1.95
0.86
0.98
1.97

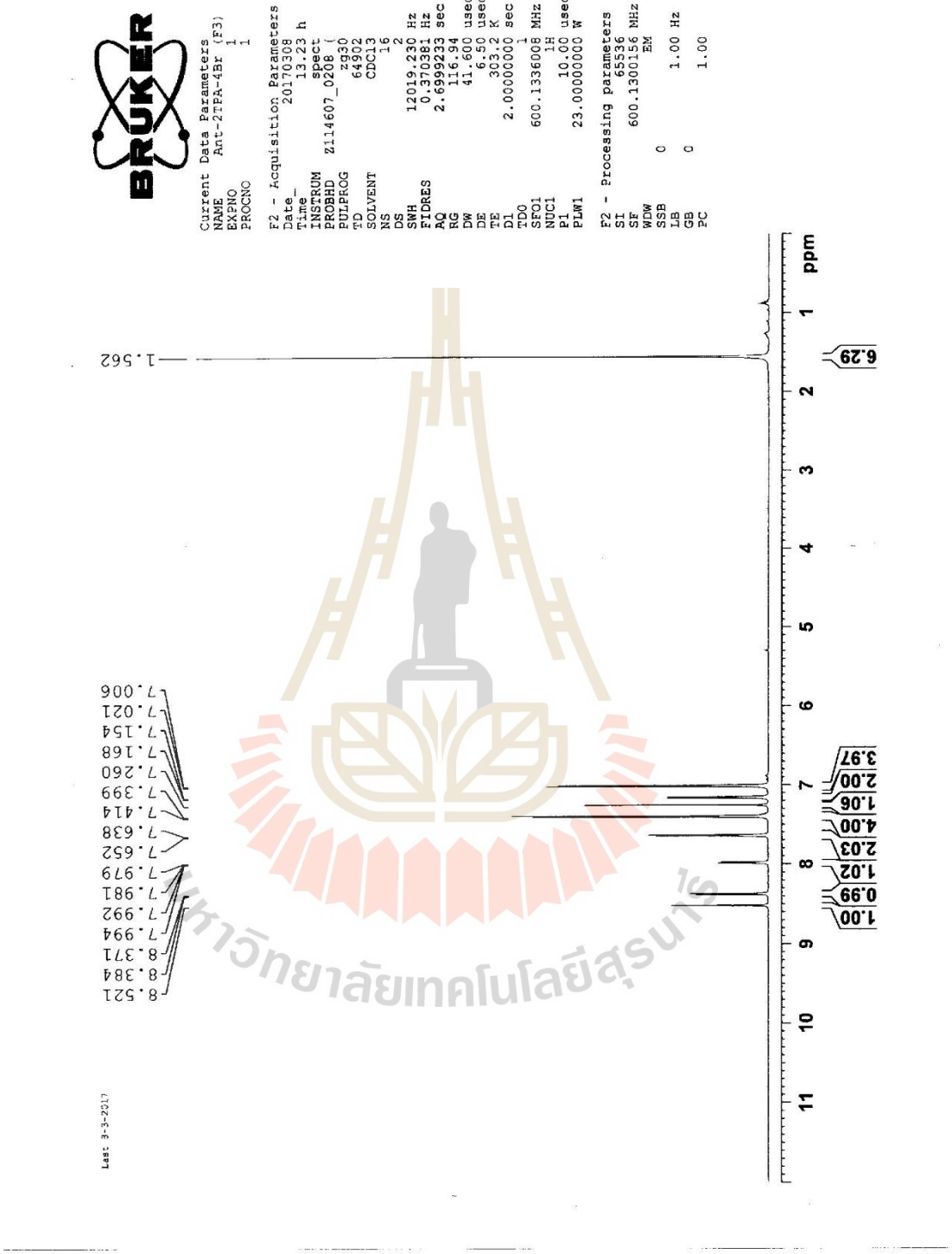
BRUKER
Current Data Parameters
NAME Ant-2TPA-4Br (F3)
EXPNO 1
PROCNO 1
F2 - Acquisition Parameters
Date_ 20170308
Time 13.23 h
INSTRUM spect
PROBHD Z114607_0208 (
PULPROG zg30
TD 64902
SOLVENT CDCl3
NS 16
DS 2
SWH 12019.230 Hz
FIDRES 0.370381 Hz
AQ 2.6999233 sec
RG 116.94
DW 41.600 usec
DE 6.50 usec
TE 303.2 K
D1 2.00000000 sec
TD0 1
SFO1 600.1336008 MHz
NUC1 1H
P1 10.00 usec
PLW1 23.00000000 W
F2 - Processing parameters
SI 65536
SF 600.1300156 MHz
WDW EM
SSB 0
LB 1.00 Hz
GB 0
PC 1.00
1.562
8.521
8.384
8.371
7.994
7.992
7.981
7.979
7.652
7.638
7.414
7.399
7.260
7.168
7.154
7.021
7.006
6.29
1.00
0.99
1.02
2.03
4.00
1.06
2.00
3.97
ppm
Last: 3-3-2017

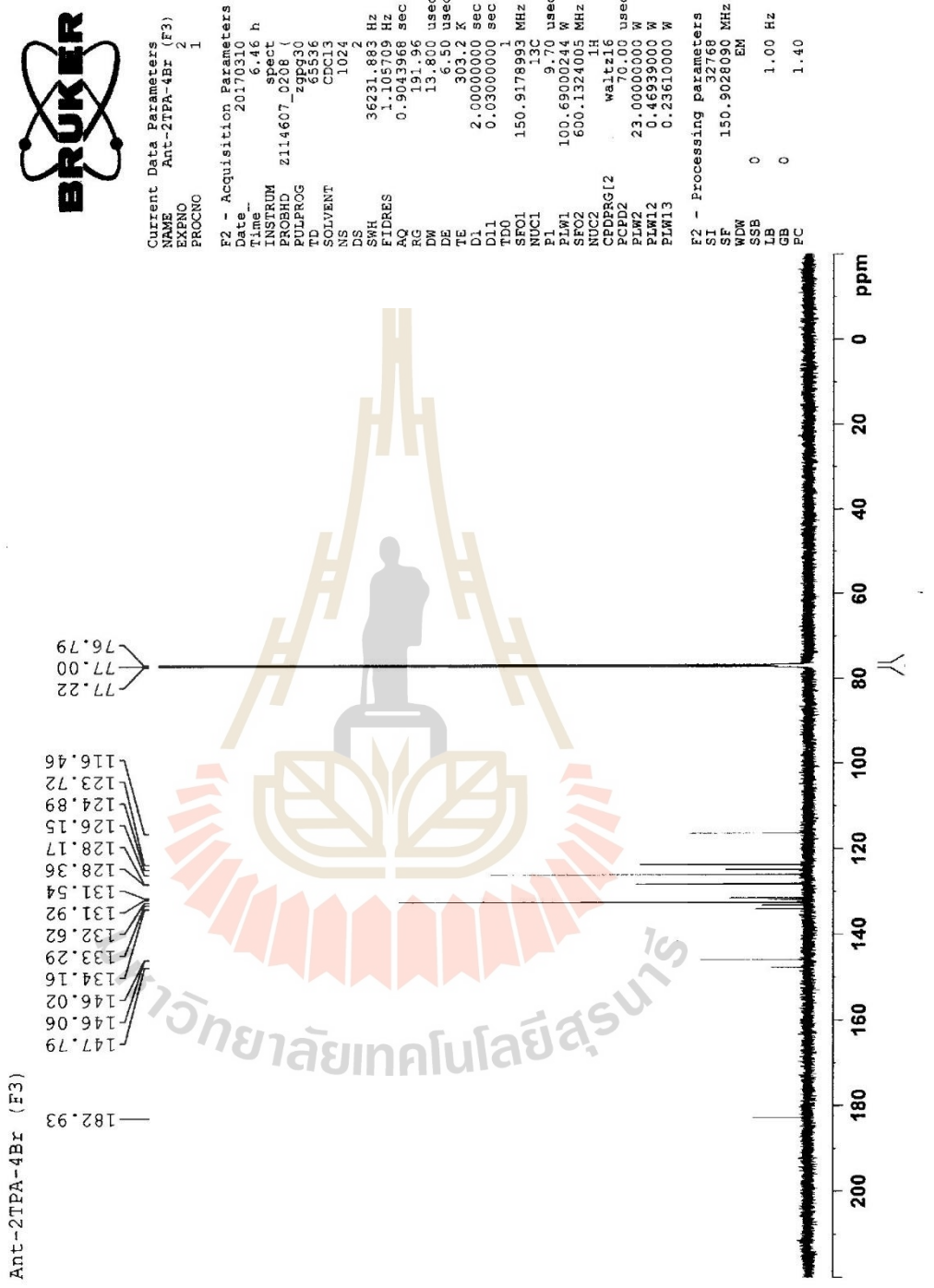
Current Data Parameters
NAME Ant-2TPA-4Br (F3)
EXPNO 2
PROCNO 1
F2 - Acquisition Parameters
Date_ 20170310
Time 6.46 h
INSTRUM spect
PROBHD Z114607_0208 (
PULPROG zgpg30
TD 65536
SOLVENT CDCl3
NS 1024
DS 2
SWH 36231.883 Hz
FIDRES 1.105709 Hz
AQ 0.9043968 sec
RG 191.96
DW 13.800 usec
DE 6.50 usec
TE 303.2 K
D1 2.00000000 sec
D11 0.03000000 sec
TD0 1
SFO1 150.9178993 MHz
NUC1 13C
P1 9.70 usec
PLW1 100.69000244 W
SFO2 600.1324005 MHz
NUC2 1H
CPDPRG[2 waltz16
PCPD2 70.00 usec
PLW2 23.00000000 W
PLW12 0.46939000 W
PLW13 0.23610000 W
F2 - Processing parameters
SI 32768
SF 150.9028090 MHz
WDW EM
SSB 0
LB 1.00 Hz
GB 0
PC 1.40
Ant-2TPA-4Br (F3)
182.93
147.79
146.06
146.02
134.16
133.29
132.62
131.92
131.54
128.36
128.17
126.15
124.89
123.72
116.46
77.22
77.00
76.79
ppm

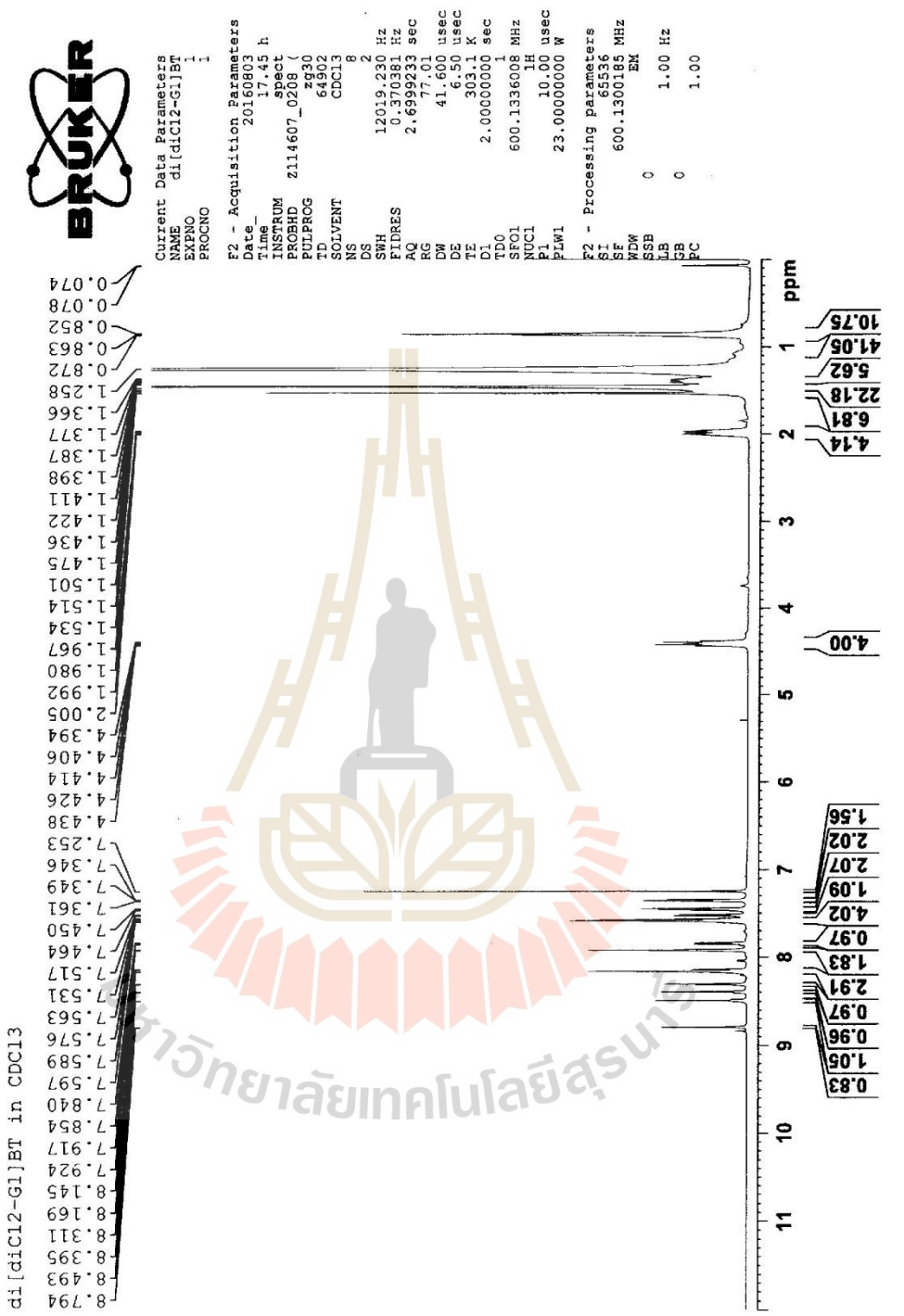
di[diC12-G1]BT in CDC13
Current Data Parameters
NAME di[diC12-G1]BT
EXPNO 1
PROCNO 1
F2 - Acquisition Parameters
Date_ 20160803
Time 17.45 h
INSTRUM spect
PROBHD Z114607_0208 (
PULPROG zg30
TD 64902
SOLVENT CDCl3
NS 8
DS 2
SWH 12019.230 Hz
FIDRES 0.370381 Hz
AQ 2.6999233 sec
RG 77.01
DW 41.600 usec
DE 6.50 usec
TE 303.1 K
D1 2.00000000 sec
TD0 1
SFO1 600.1336008 MHz
NUC1 1H
P1 10.00 usec
PLW1 23.00000000 W
F2 - Processing parameters
SI 65536
SF 600.1300185 MHz
WDW EM
SSB 0
LB 1.00 Hz
GB 0
PC 1.00
ppm
10.75
41.05
5.62
22.18
6.81
4.14
4.00
0.83
1.05
0.96
0.97
2.91
1.83
0.97
4.02
1.09
2.07
2.02
1.56

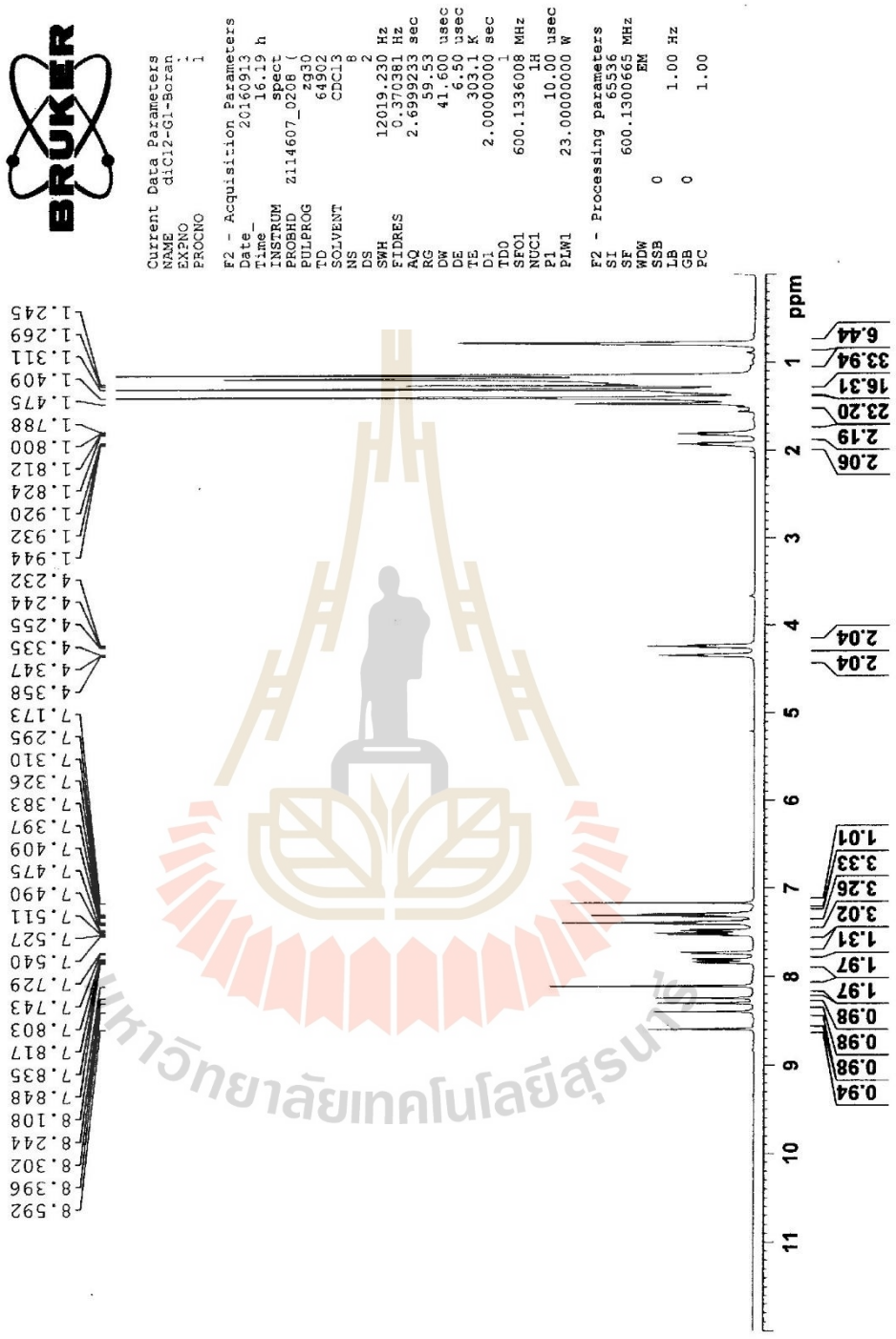
Current Data Parameters
NAME dic12-Gl-Boran
EXPNO 1
PROCNO 1
F2 - Acquisition Parameters
Date_ 20160913
Time_ 16.19 h
INSTRUM spect
PROBHD z114607_0208 (
PULPROG zg30
TD 64902
SOLVENT CDCl3
NS 8
DS 2
SWH 12019.230 Hz
FIDRES 0.370381 Hz
AQ 2.6999233 sec
RG 59.53
DW 41.600 usec
DE 6.50 usec
TE 303.1 K
D1 2.00000000 sec
TD0 1
SFO1 600.1336008 MHz
NUC1 1H
P1 10.00 usec
PLW1 23.00000000 W
F2 - Processing parameters
SI 65536
SF 600.1300665 MHz
WDW EM
SSB 0
LB 1.00 Hz
GB 0
PC 1.00
ppm
6.44
33.94
16.31
23.20
2.19
2.06
2.04
2.04
1.01
3.33
3.26
3.02
1.31
1.97
1.97
0.98
0.98
0.98
0.94
1.245
1.269
1.311
1.409
1.475
1.788
1.800
1.812
1.824
1.920
1.932
1.944
4.232
4.244
4.255
4.335
4.347
4.358
7.173
7.295
7.310
7.326
7.383
7.397
7.409
7.475
7.490
7.511
7.527
7.540
7.729
7.743
7.803
7.817
7.835
7.848
8.108
8.244
8.302
8.396
8.592

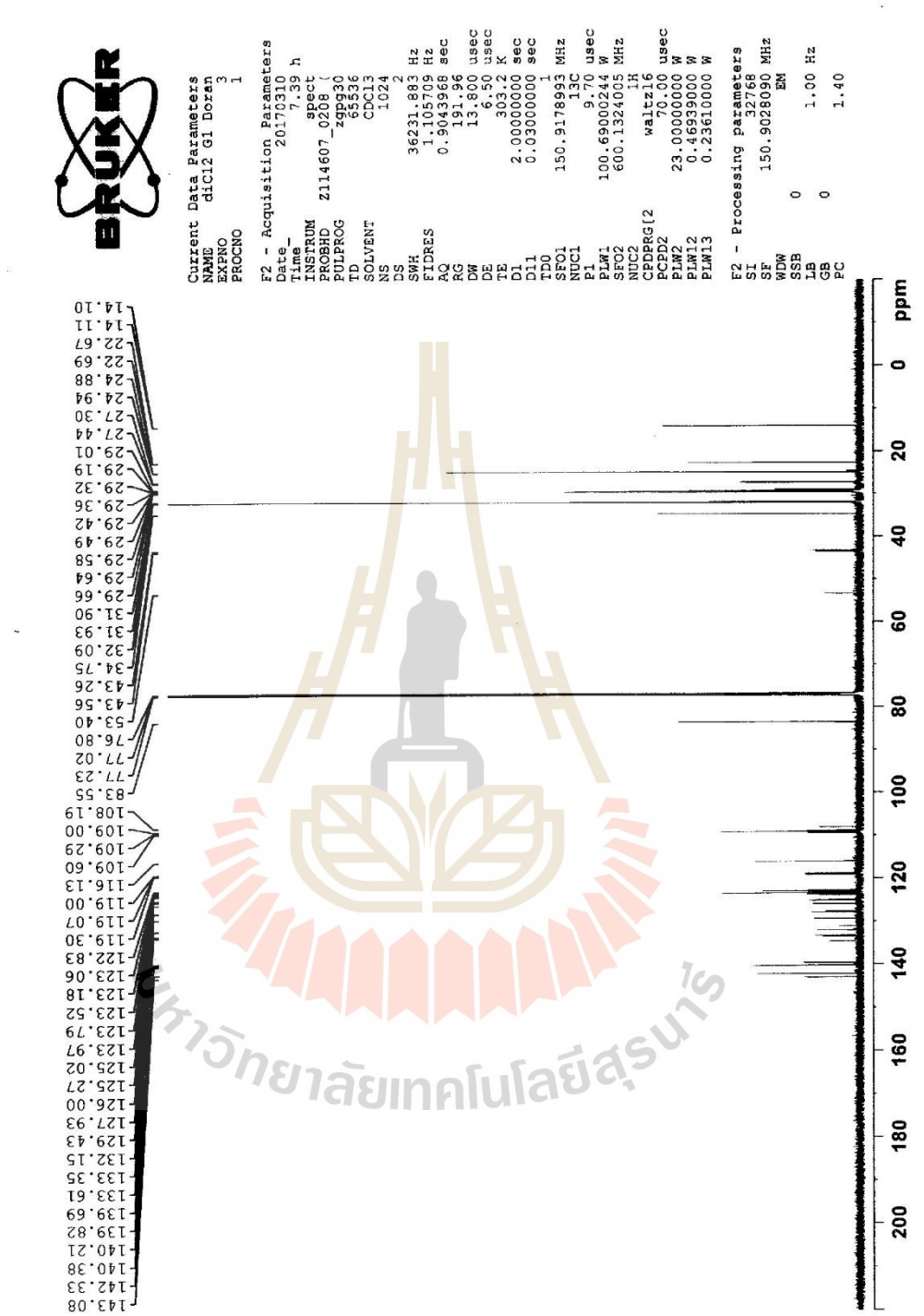
Current Data Parameters
NAME dic12 G1 Doran
EXPNO 3
PROCNO 1
F2 - Acquisition Parameters
Date_ 20170310
Time 7.39 h
INSTRUM spect
PROBHD Z114607_0208 (
PULPROG zgpg30
TD 65536
SOLVENT CDCl3
NS 1024
DS 2
SWH 36231.883 Hz
FIDRES 1.105709 Hz
AQ 0.9043968 sec
RG 191.96
DW 13.800 usec
DE 6.50 usec
TE 303.2 K
D1 2.00000000 sec
D11 0.03000000 sec
TD0 1
SFO1 150.9178993 MHz
NUC1 13C
P1 9.70 usec
PLW1 100.69000244 W
SFO2 600.1324005 MHz
NUC2 1H
CPDPRG[2 waltz16
PCPD2 70.00 usec
PLW2 23.00000000 W
PLW12 0.46939000 W
PLW13 0.23610000 W
F2 - Processing parameters
SI 32768
SF 150.9028090 MHz
WDW EM
SSB 0
LB 1.00 Hz
GB 0
PC 1.40
ppm
0
20
40
60
80
100
120
140
160
180
200
14.10
14.11
22.67
22.69
24.88
24.94
27.30
27.44
29.01
29.19
29.32
29.36
29.42
29.49
29.58
29.64
29.66
31.90
31.93
32.09
34.75
43.26
43.56
53.40
76.80
77.02
77.23
83.55
108.19
109.00
109.29
109.60
116.13
119.00
119.07
119.30
122.83
123.06
123.18
123.52
123.79
123.97
125.02
125.27
126.00
127.93
129.43
132.15
133.35
133.61
139.69
139.82
140.21
140.38
142.33
143.08

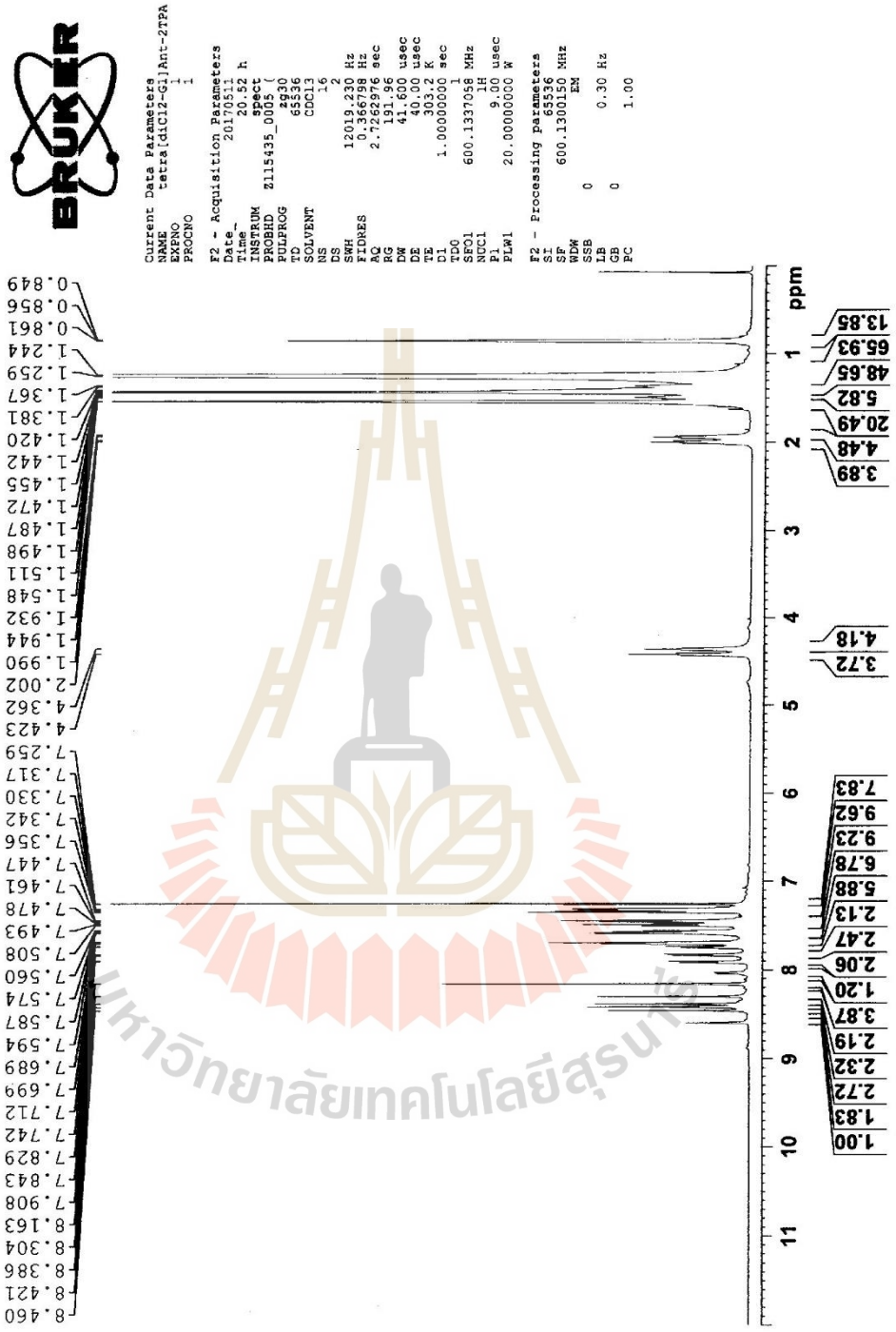
Current Data Parameters
NAME tetra[diC12-G1]Ant-2TPA
EXPNO 1
PROCNO 1
F2 - Acquisition Parameters
Date_ 20170511
Time 20.52 h
INSTRUM spect
PROBHD 2115435_0005 (
PULPROG zg30
TD 65536
SOLVENT CDCl3
NS 16
DS 2
SWH 12019.230 Hz
FIDRES 0.366798 Hz
AQ 2.7262976 sec
RG 191.96
DW 41.600 usec
DE 40.00 usec
TE 303.2 K
D1 1.00000000 sec
TD0 1
SFO1 600.1337058 MHz
NUC1 1H
P1 9.00 usec
PLW1 20.00000000 W
F2 - Processing parameters
SI 65536
SF 600.1300150 MHz
WDW EM
SSB 0
LB 0.30 Hz
GB 0
PC 1.00
ppm
13.85
65.93
48.65
5.82
20.49
4.48
3.89
4.18
3.72
1.00
1.83
2.72
2.32
2.19
3.87
1.20
2.06
2.47
2.13
5.88
6.78
9.23
9.62
7.83
0.849
0.856
0.861
1.244
1.259
1.367
1.381
1.420
1.442
1.455
1.472
1.487
1.498
1.511
1.548
1.932
1.944
1.990
2.002
4.362
4.423
7.259
7.317
7.330
7.342
7.356
7.447
7.461
7.478
7.493
7.508
7.560
7.574
7.587
7.594
7.689
7.699
7.712
7.742
7.829
7.843
7.908
8.163
8.304
8.386
8.421
8.460

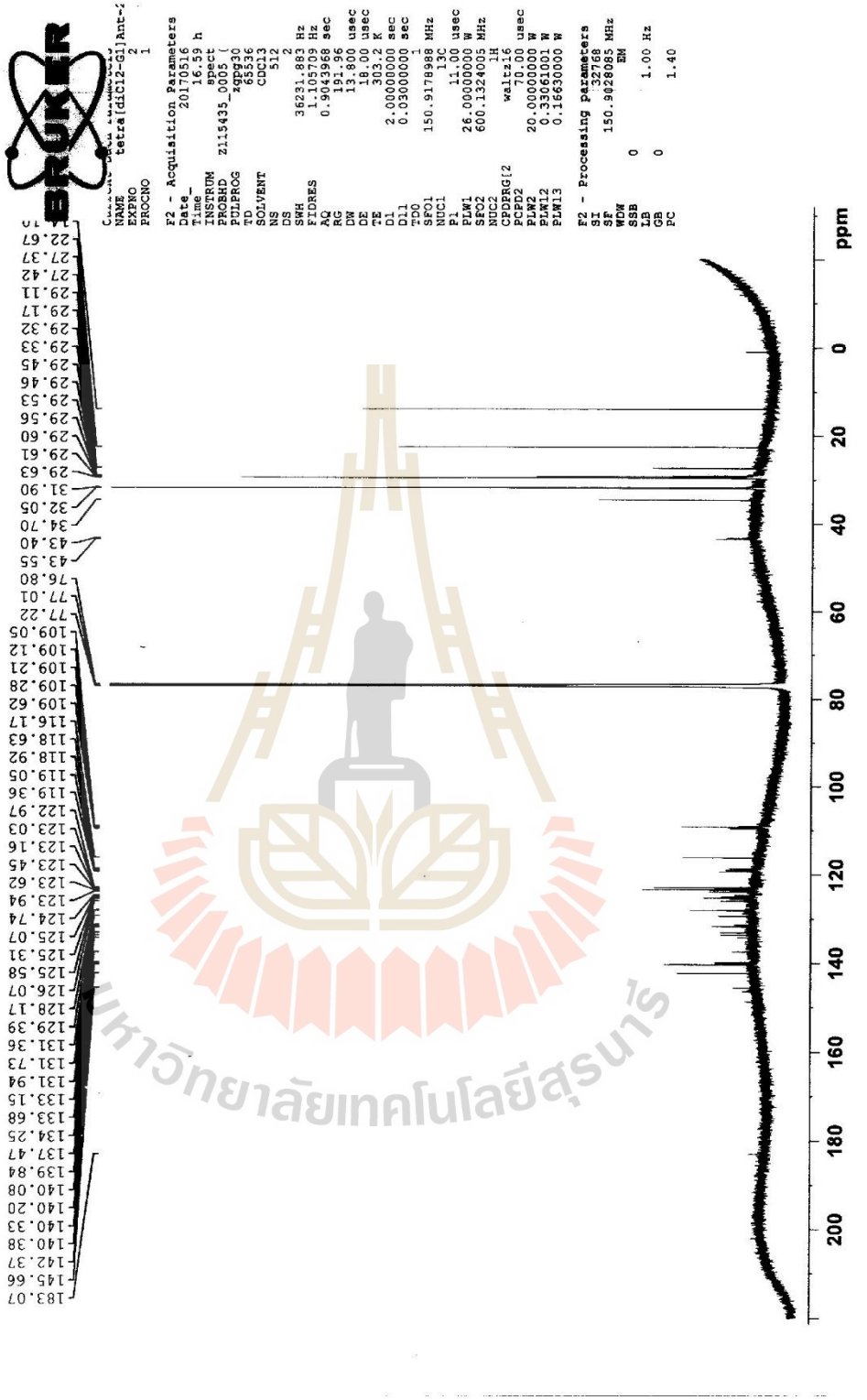

มหาวิทยาลัยเทคโนโลยีสุรนารี

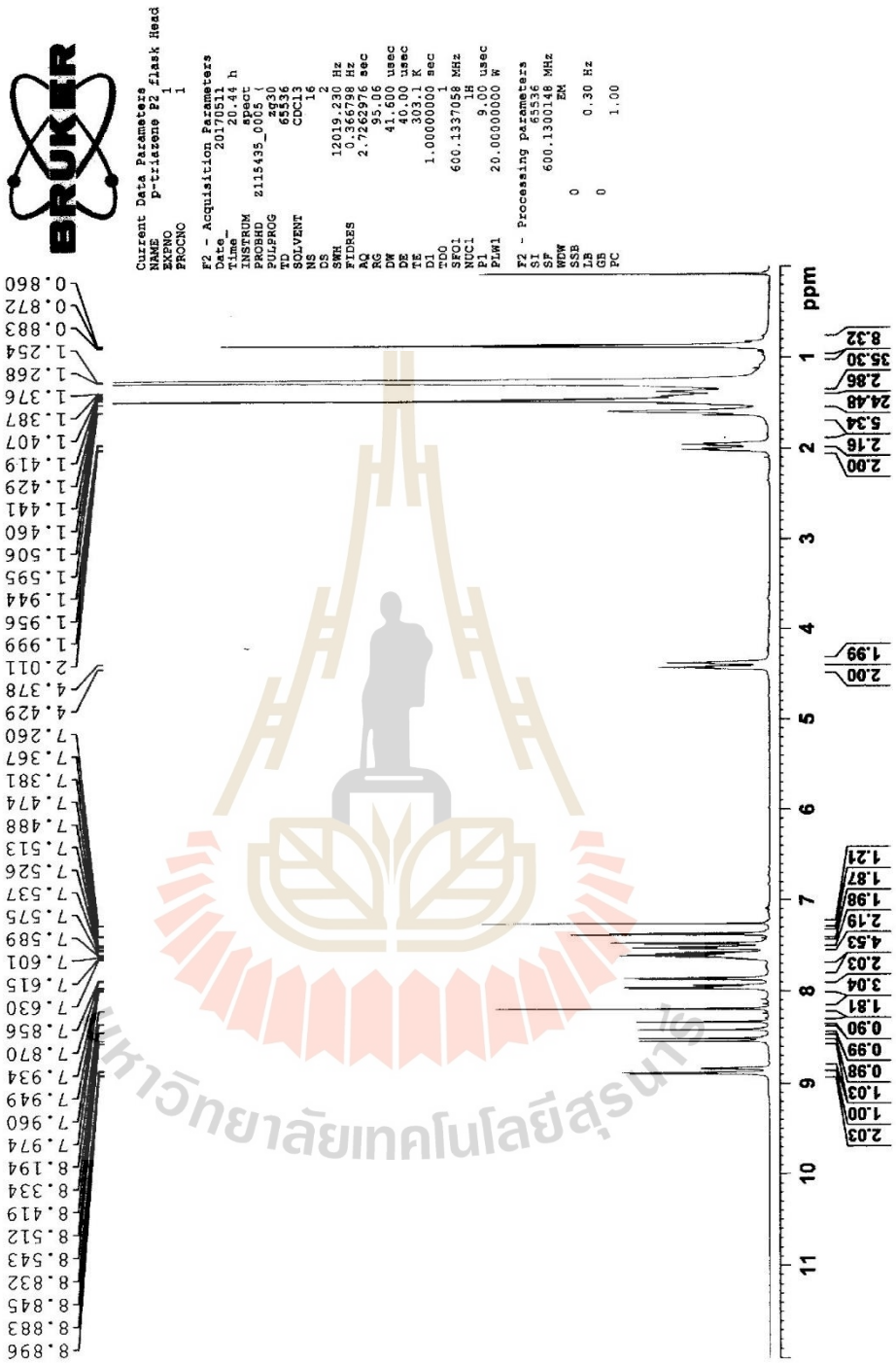

มหาวิทยาลัยเทคโนโลยีสุรนารี

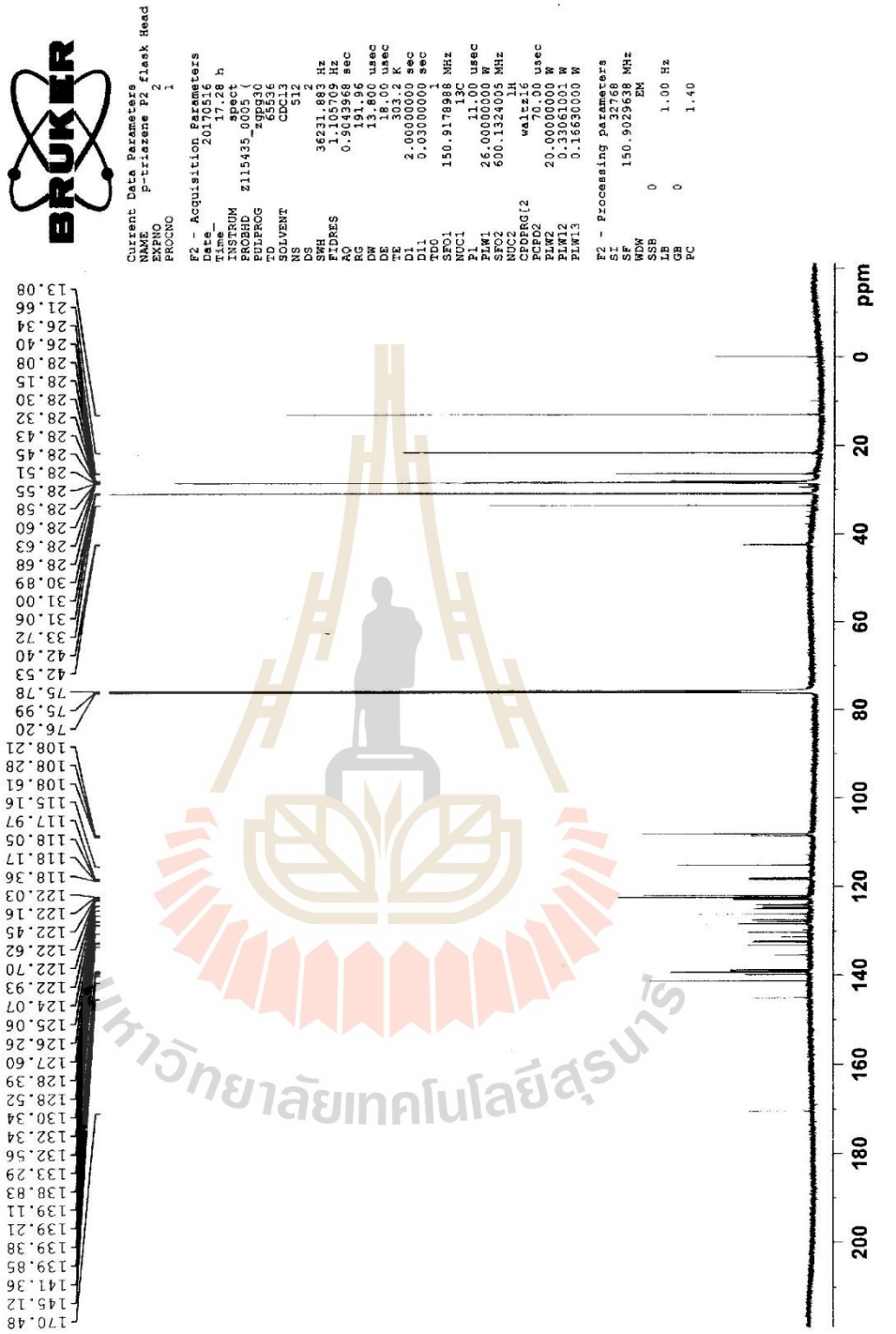

มหาวิทยาลัยเทคโนโลยีสุรนารี

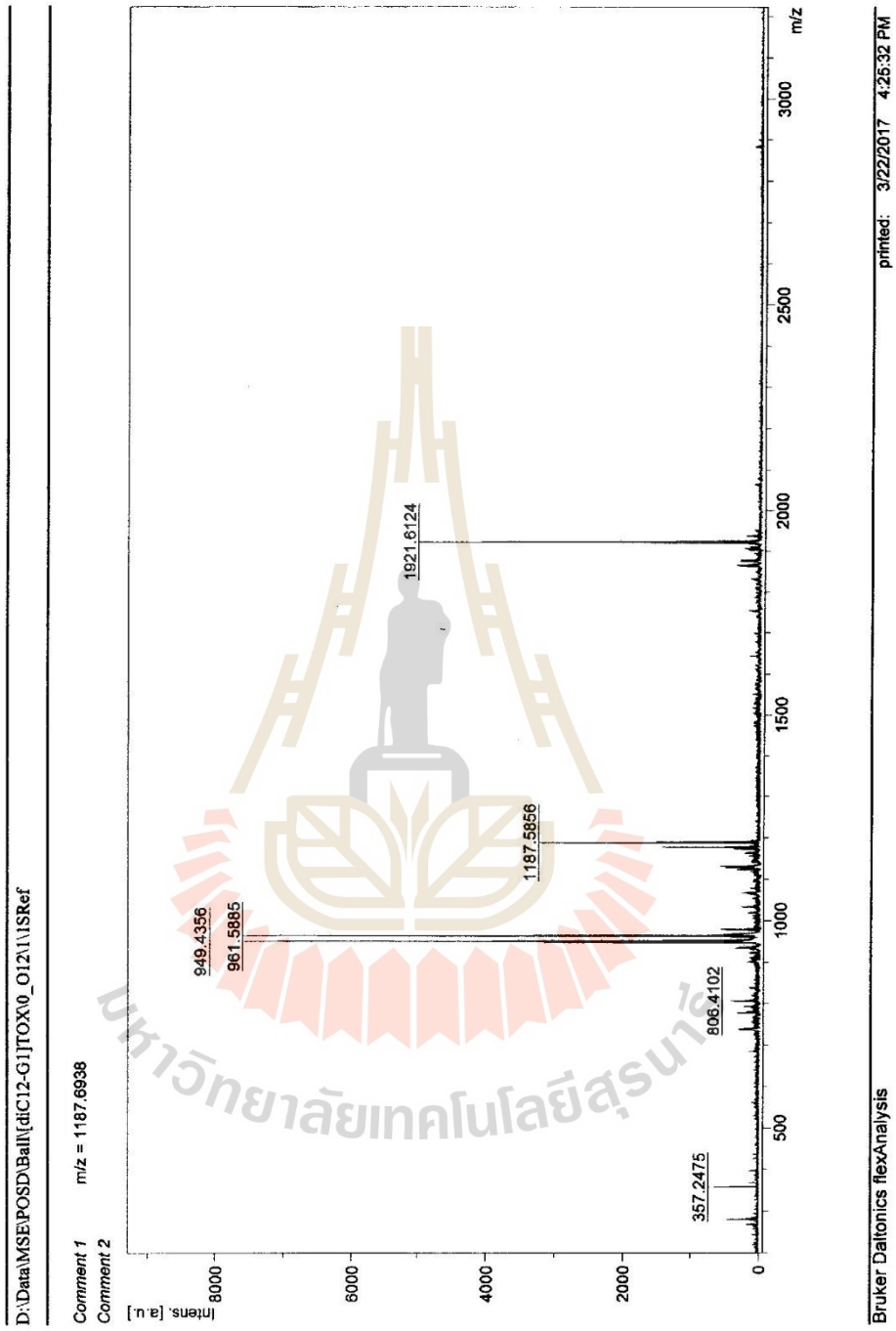
D:\Data\MSE\POSD\Ball\[diC12-G1]TOX\0_O12\1\1SRef
Comment 1 m/z = 1187.6938
Comment 2
Intens. [a.u.]
8000
6000
4000
2000
0
500
1000
1500
2000
2500
3000
m/z
949.4356
961.5885
1187.5856
1921.6124
357.2475
806.4102
Bruker Daltonics flexAnalysis
printed: 3/22/2017 4:26:32 PM

D:\Data\MSE\POSD\Ball\BT1T4-3CPh\0_P12\1\1SRef

MALDI-TOF-MS Report

Frontier Research Center, Vidyasirimedhi Institute of Science and Technology

Comment 1 m/z= 1191.4402 [3side]

Comment 2

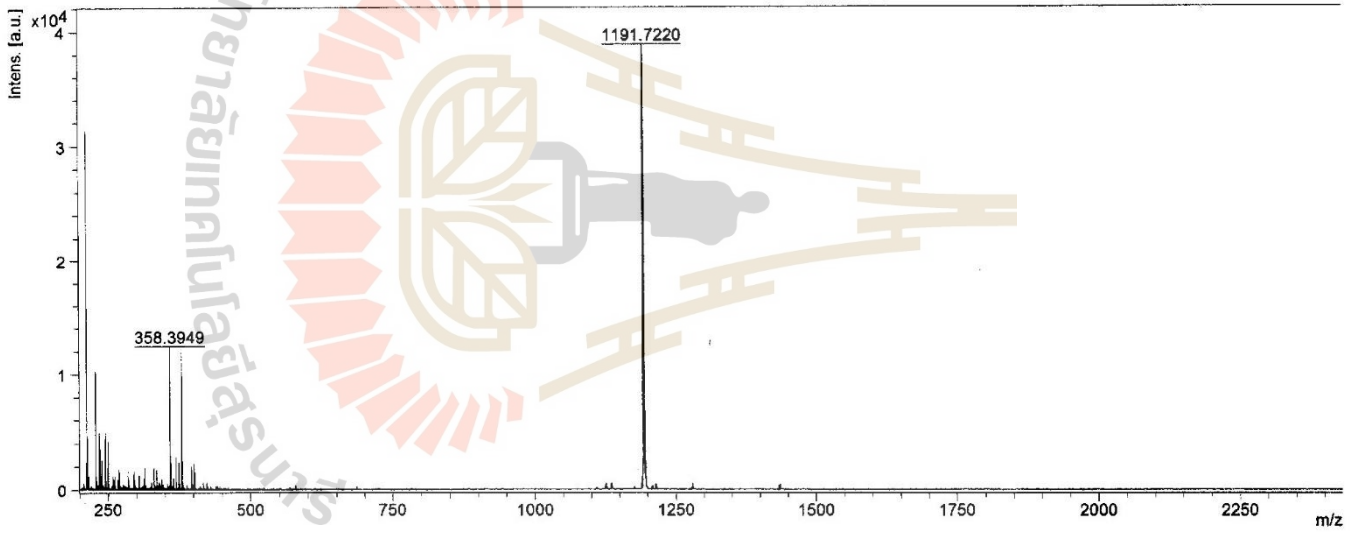

m/z	S/N	Quality Fac.	Res.	Intens.	Area
1191.7220				36812	
358.3949				12271	

Bruker Autoflex Speed Printout: 19/3/2018 3:26:52 PM

มหาวิทยาลัยวิทยาศาสตร์และเทคโนโลยีวิทยาสิริเมธี

D:\Data\MSE\POSD\Ball\BT1T4-4CPh\0_P14\1\1SRef

MALDI-TOF-MS Report

Frontier Research Center, Vidyasirimedhi Institute of Science and Technology

Comment 1 m/z= 1433.5327 [4side]

Comment 2

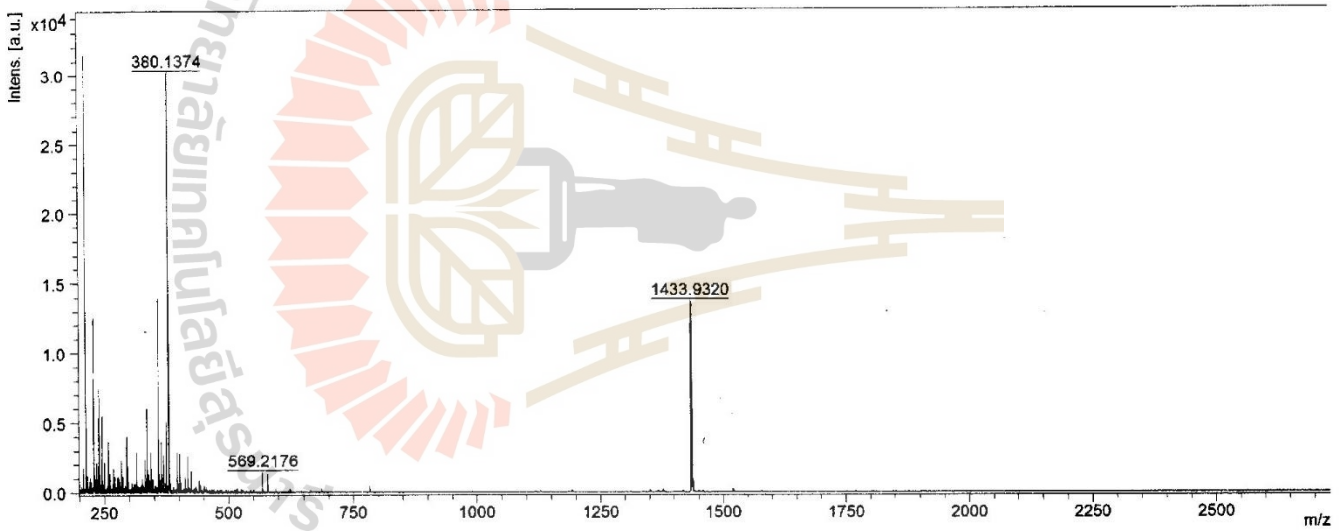

m/z	S/N	Quality Fac.	Res.	Intens.	Area
1433.9320				13671	
569.2176				422	
380.1374				11530	

Bruker Autoflex Speed Printout: 19/3/2018 3:28:51 PM

D:\Data\MSE\POSD\Ball\di[diC12-G1]BT1T4\0_O17\1\1SRef

Comment 1 m/z = 2356.5248

Comment 2

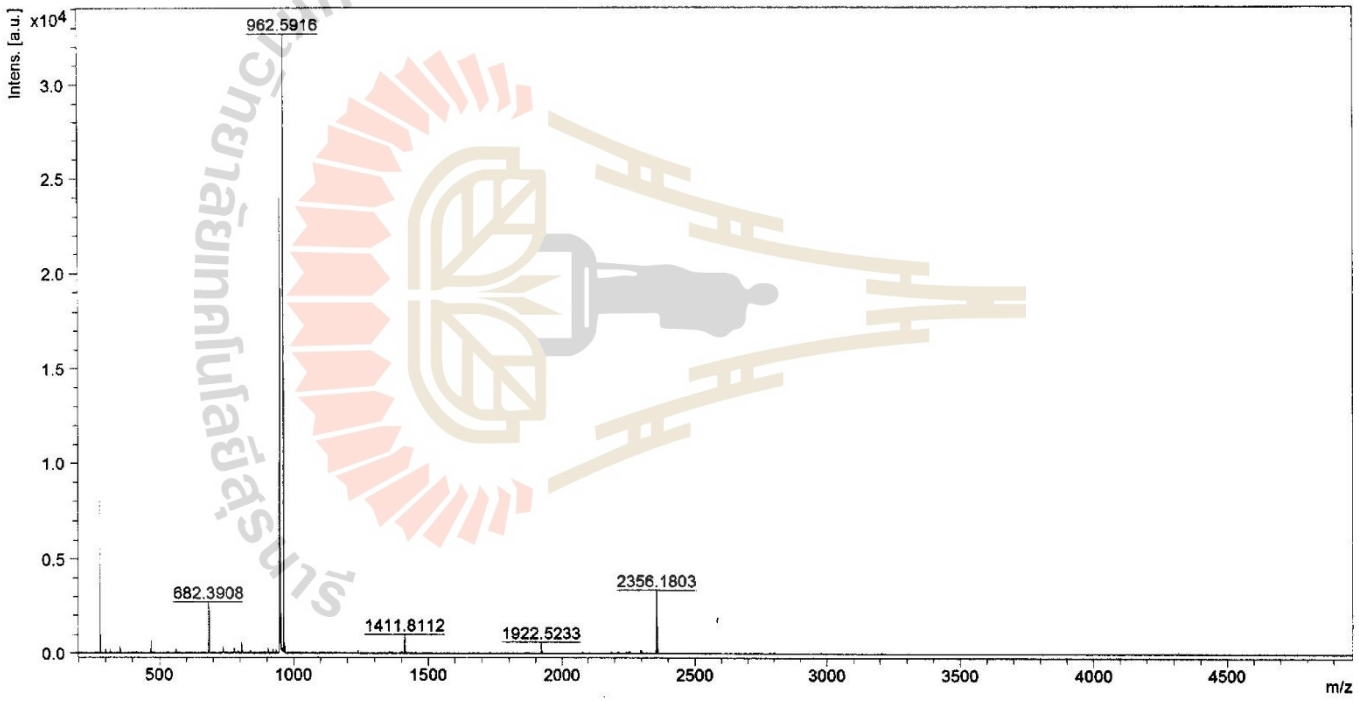

Bruker Daltonics flexAnalysis printed: 3/22/2017 4:40:16 PM

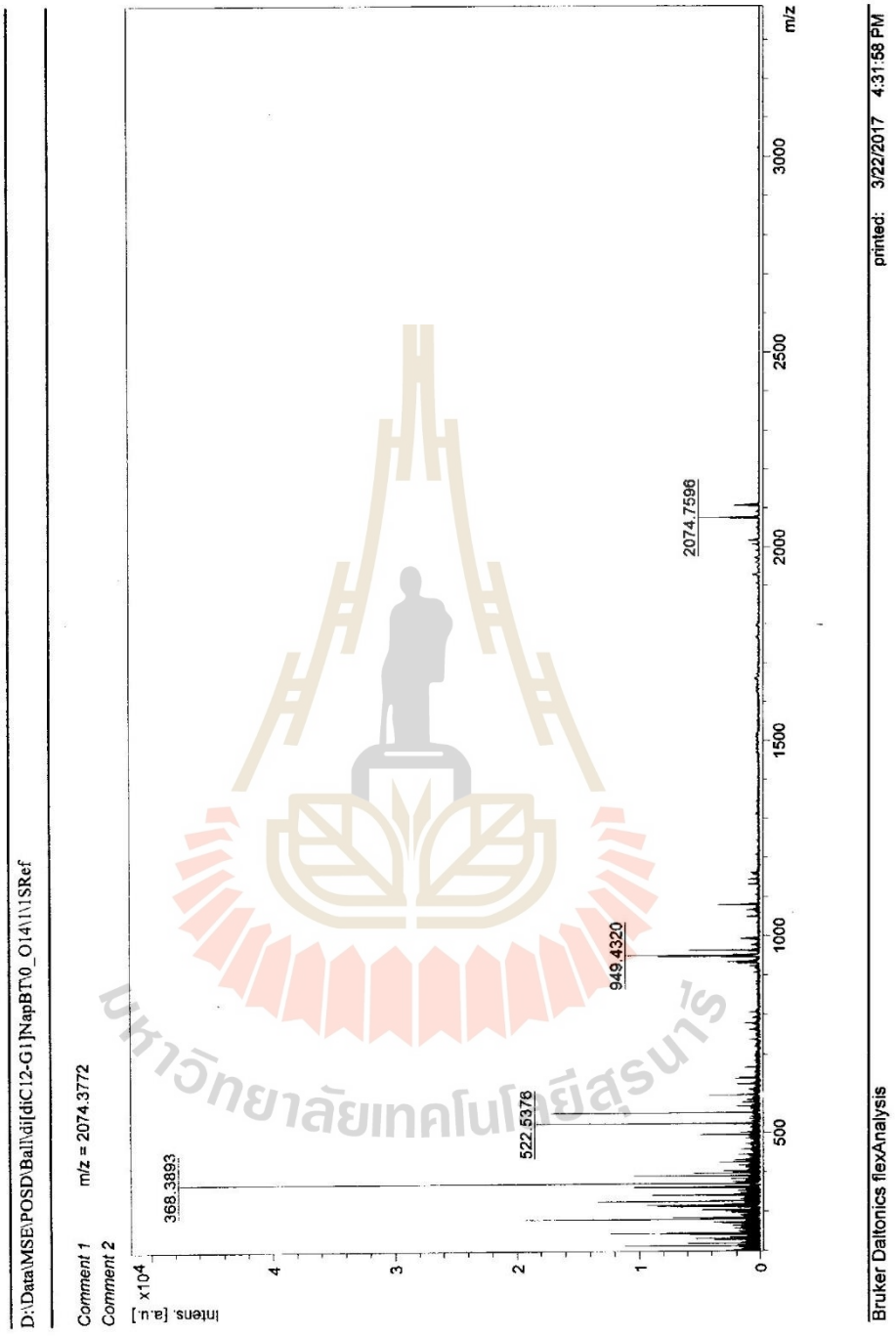
D:\Data\MSE\POSD\Ball\di[diC12-G1]NapBT\0_O14\1\1\SRef
Comment 1 m/z = 2074.3772
Comment 2
Intens. [a.u.]
x10^4
4
3
2
1
0
368.3893
522.5376
949.4320
2074.7596
500
1000
1500
2000
2500
3000
m/z
Bruker Daltonics flexAnalysis
printed: 3/22/2017 4:31:58 PM

D:\Data\MSE\POSD\Ball\di[diC12-G1]TPA-TOX\0_O10\1\1SRef

Comment 1 m/z = 2375.4763

Comment 2

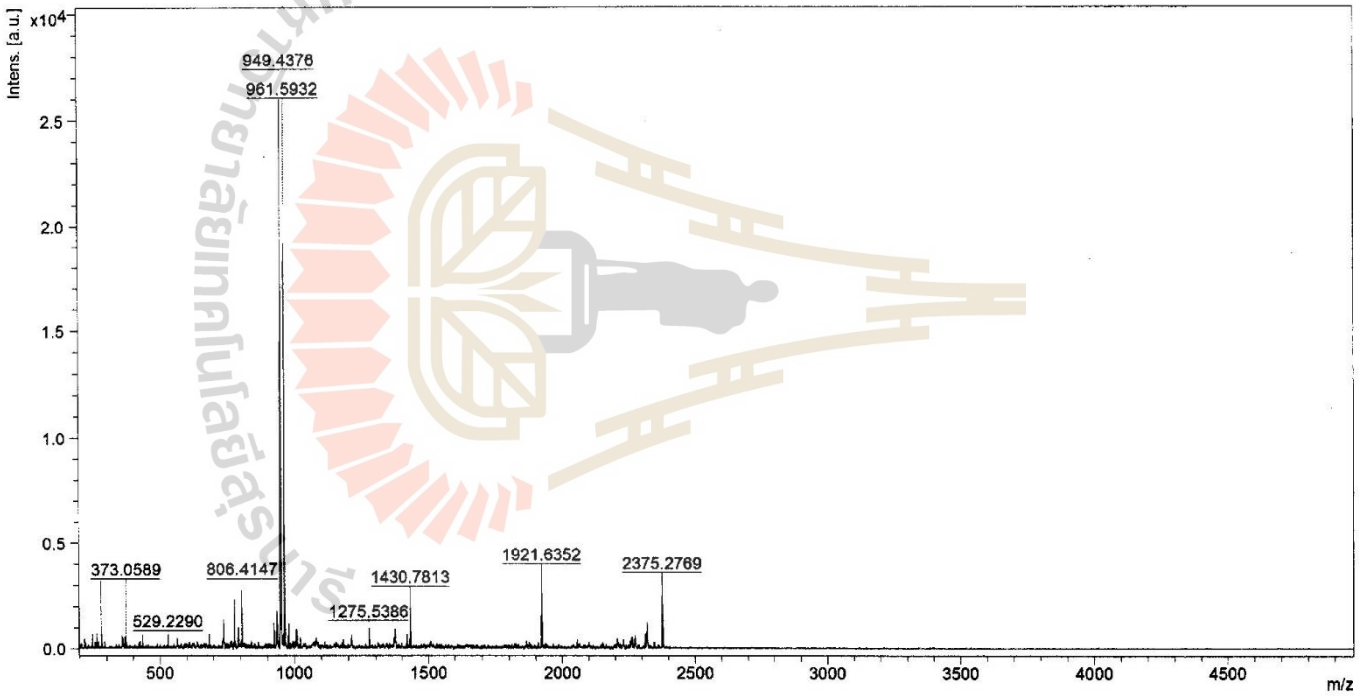

Bruker Daltonics flexAnalysis printed: 3/22/2017 4:21:30 PM

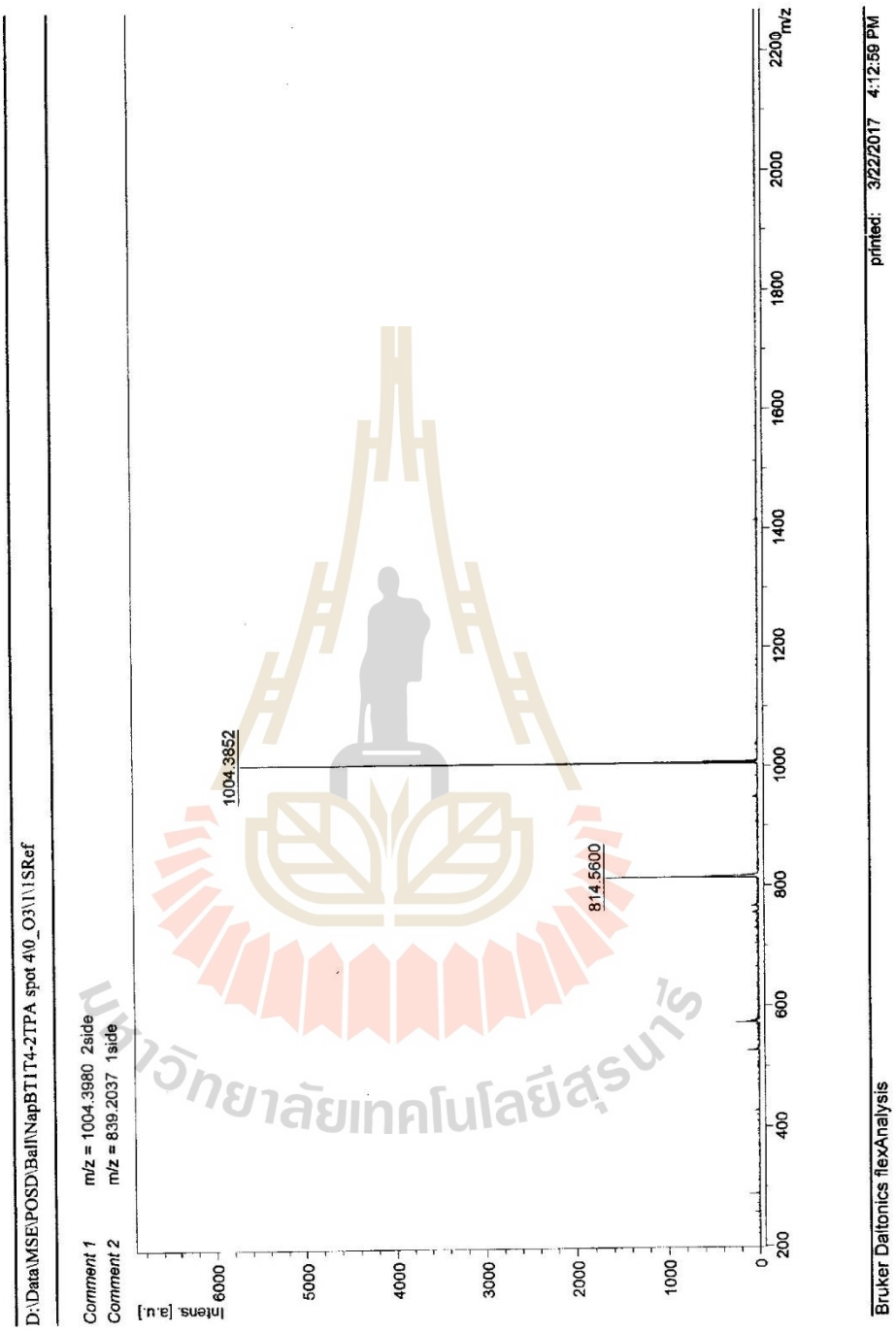
D:\Data\MSE\POSD\Ball\NapBT1T4-2TPA spot 4\0_O3\1\1\SRef
Comment 1 m/z = 1004.3980 2side
Comment 2 m/z = 839.2037 1side
Intens. [a.u.]
6000
5000
4000
3000
2000
1000
0
1004.3852
814.5600
200
400
600
800
1000
1200
1400
1600
1800
2000
2200
m/z
Bruker Daltonics flexAnalysis
printed: 3/22/2017 4:12:59 PM

D:\Data\MSE\POSD\Ball\tetra[diC12-G1]Ant-2TPA [F1]\0_P23\1\1SRef

Comment 1 m/z = 4471.9695

Comment 2

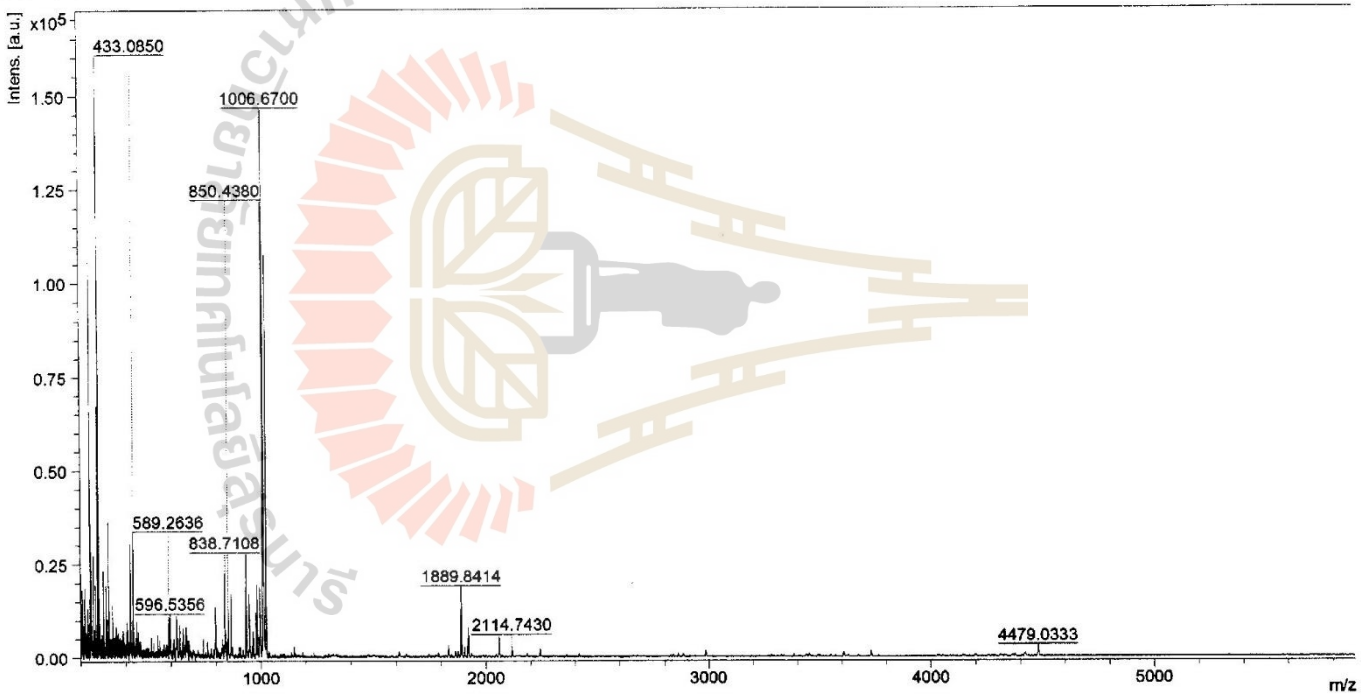

Bruker Daltonics flexAnalysis printed: 3/22/2017 5:00:09 PM

D:\Data\MSE\POSD\Ball\tri[diC12-G1]triazene\0_O16\1\1SRef

Comment 1 m/z = 3142.1564

Comment 2

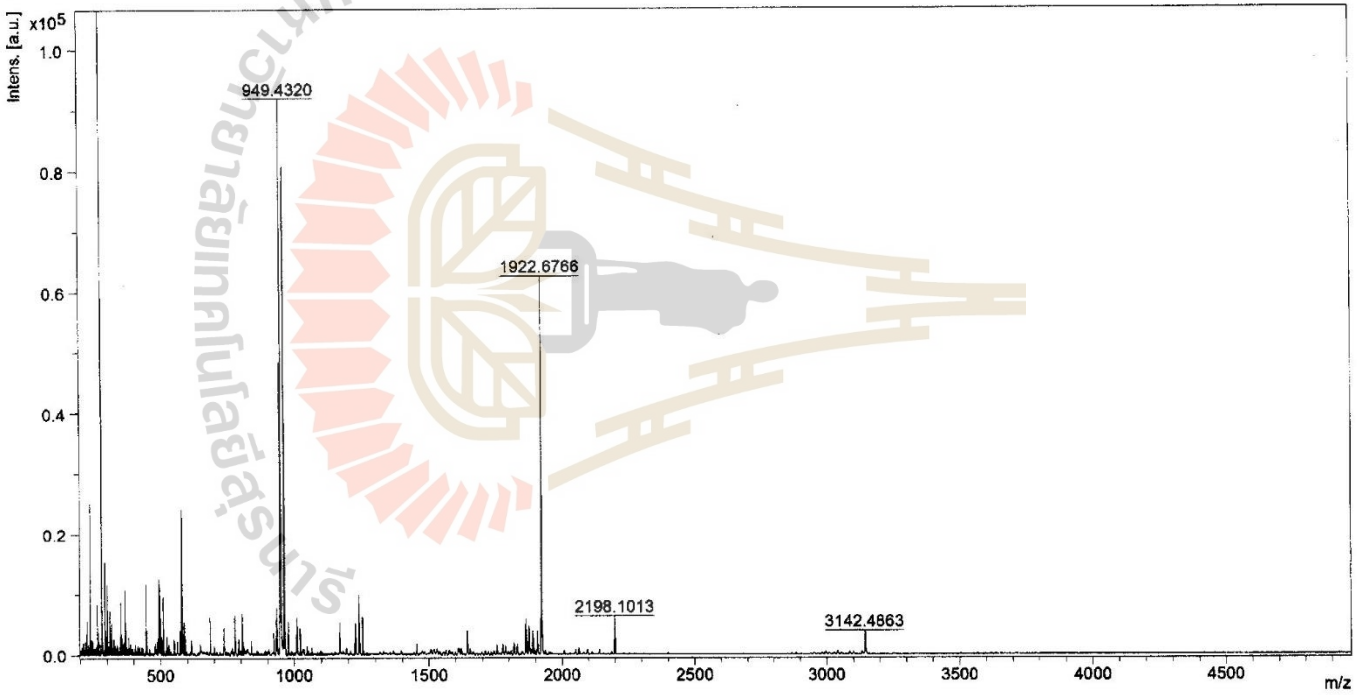

Bruker Daltonics flexAnalysis printed: 3/22/2017 4:36:22 PM

มหาวิทยาลัยเชียงใหม่

CURRICULUM VITAE

Name	Mr.TEADKAIT KAEWPUANG
Born	28 July 1982, Sisaket, Thailand
Education	
2008 - 2009	Bachelor of Science Chemistry, Ubon Ratchathani Rajabhat University, Thailand.
2009 - 2011	Master of Science Chemistry, Ubon Ratchathani University, Thailand.
2013 - 2018	Doctor of Philosophy Candidate (Chemistry) at Suranaree University of Technology, Thailand.

มหาวิทยาลัยเทคโนโลยีสุรนารี